University of Nottingham

UK | CHINA | MALAYSIA

Acquired Carbapenem Resistance in Enterobacteria from UK Wastewater

Thesis submitted to the University of Nottingham for the degree of Doctor of Philosophy

Darren J. D. Dickinson

December 2023

Acknowledgements

Firstly, I would like to thank my supervisor, Dr Jon Hobman, whose guidance and support have been instrumental throughout these past few years. Jon, I appreciate not only your encouragement to pursue my research interests, your faith in my ability, but also your wisdom that, during the many moments of uncertainty, helped to remind me what the point of it all was. Additionally, I extend my thanks to Professor Christine Dodd for her feedback, comments, and valuable suggestions. This thesis has greatly benefited from her contributions and wouldn't be the same without her.

I would also like to thank Dr Phil Hill for his helpful suggestions around plasmid design, as Chapter Five would look very different without him. I'd also like to express my gratitude to Rhidian Ford for her patient and repeated explanations of how Gibson assembly works.

A special mention goes to all the past and present students that have helped me over the years - thank you to Joe, Weijie, Kayley, Reema, and especially to Alex. I appreciate all your help and advice, or just for listening to me vent about things! Many thanks to all the other staff and students in Food Sciences, but especially to Nicos, Stanley, Bailey, Sam, Bader and Josh (sorry everyone else!). My time at Nottingham was better for knowing you all, though our theses might have been finished a lot sooner had we never met.

I am also grateful to the University of Nottingham and the Wellcome Trust for funding this project. Thank you to all those involved in the AAMR DTP at the Universities of Nottingham and Birmingham, especially to my cohort. Your support early on was vital, when none of us had a clue what we were doing.

I would like to thank my mother and sister, Nicola and Sami Dickinson, as well as my mother and father-in-law, Sara and David, who have absolutely no idea what I'm doing but have supported me doing it anyway. Special thanks also to my father, David, without whose support I would never have got this far. Finally, and most importantly, I would like to thank my incredible wife, Rosanna. Thank you for all your love, support and encouragement, especially in the past few months. I really couldn't have done this without you and Luna.

COVID-19 Impact Statement

This project was adversely affected by the COVID-19 pandemic as outlined hereafter. The data presented in Chapters 3 and 4 of this thesis relied on the collection of wastewater samples from treatment plants. In January 2020, a plan was generated to collect samples weekly over an 8-week period. This sampling regimen was planned to be a preliminary one, and the dataset generated by these experiments was to be used as a basis to design further experiments that would require additional sampling. The preliminary sampling protocol started fully in February 2020 but due to the pandemic, only 3-weeks' worth of samples were collected. The WWTP operator did not allow anyone from the University on to their premises to collect samples after that point, due to concern over COVID-19 being detected in sewage, so the full set of samples could never be taken. From the start of this project, the plan was to use a range of culture dependent and independent methods to gain a broader understanding of AMR within wastewater samples, and this preliminary round of sampling was to be used to determine the targets for some culture independent methods. Due to the impact of COVID-19, these methods were never able to be used, and so the analysis in Chapters 3 and 4 of this thesis had to change to only culture dependent methods.

In addition to the sampling issues, access to the laboratory was not allowed after mid-March 2020 until later in the year due to the pandemic. Although the University allowed research to recommence on 10th August, research for this work could not continue until 28th September due to priority access being given to final year PhD students. Additionally, a large proportion of the experiments

in the project required the use of PCR. Due to the high levels of PCR testing used in the UK government's surveillance and diagnosis of SARS-CoV-2 infections, certain consumables required for PCR were in high demand. This necessarily meant that PCR experiments were delayed due to lack of consumables and significant world-wide delays in shipping.

Abstract

Antimicrobial resistance (AMR) is rapidly becoming one of the greatest threats to modern healthcare around the world. The numbers of resistant infections have been rising rapidly over the last few decades, and mobile genetic elements (MGEs) carrying genes that confer resistance to our most valuable antibiotics have played a major role. Antimicrobial resistant bacteria are frequently isolated from wastewater treatment plants, and identification of their associated resistance genes and MGEs can be used to help understand the landscape of AMR in a local environment. The work described here investigated the presence of carbapenemase-producing *Enterobacteriaceae* (CPE) in wastewater from the UK East Midlands. Selective enrichment was used to isolate CPE as well as cephalosporin-resistant bacteria, phenotypic AMR profiles were determined by antimicrobial disc diffusion assay, and detection of beta-lactamase and plasmid genes was carried out using polymerase chain reaction (PCR). Nineteen isolates underwent whole genome sequencing, sixteen of which used Illumina and Oxford Nanopore Technologies sequencing technology to generate hybrid assemblies, which were used to investigate the genetic mechanisms of carbapenem resistance. CPE were identified from both wastewater influent and effluent, and those isolated were identified as *Escherichia coli*, *Citrobacter portucalensis*, *Klebsiella pneumoniae*, and *Klebsiella quasipneumoniae*, while a carbapenemase-producing *Pseudomonas aeruginosa* was also detected. Carbapenemase genes isolated in this work were $bla_{\text{NDM-4}}$, $bla_{\text{NDM-5}}$, $bla_{\text{OXA-181}}$, $bla_{\text{IMP-7}}$ and $bla_{\text{IMP-70}}$, and these were found on IncF, IncX3, IncA/C and IncX3-ColKp3 plasmids. Sharing of highly related

carbapenemase plasmids was seen across multiple sequence types, and in one case, across species, as an IncX3 plasmid was detected in *E. coli* and *K. quasipneumoniae* isolates. Analysis of results showed a greater proportion of NDM-producing *E. coli* were found in this work when compared to previous studies of carbapenemase-producing isolates from clinical and wastewater samples from the UK. Importantly, multidrug resistance regions were commonly associated with IS*26* pseudo compound transposons, and experiments using clustered regularly interspaced short palindromic repeats (CRISPR)/CRISPR-associated protein 9 (Cas9)-based plasmid curing were able to show transposition of the genomic region containing bla_{NDM} and other resistance genes from one plasmid to another. This study highlights the need for more surveillance of the spread of carbapenemase-producing organisms both locally and across the globe.

Table of Contents

Index of Figures

Index of Tables

List of Abbreviations

°C	Degrees Centrigrade
µg	Microgram(s)
µl	Microlitre(s)
µm	Micrometre(s)
A. baumannii	*Acinetobacter baumannii*
A. baylyi	*Acinetobacter baylyi*
aa	Amino Acid(s)
AAC	Aminoglycosde *N*-acetyltransferase
Ae. hydrophila	*Aeromonas hydrophila*
Ae. media	*Aeromonas media*
AIEC	Adherent-Invasive *Eshcerichia coli*
AMC	Amoxicillin-Clavulanic acid
AME	Aminoglycoside Modifying Enzyme
AMP	Ampicillin
Amp^R	Ampicillin resistance
AMR	Antimicrobial Resistance
AMRHAI	Antimicrobial Resistance and Healthcare Associated Infections
ANT	Aminoglycoside *O*-nucleotidyltransferases
APH	Aminoglycoside *O*-phosphotransferases
ARB	Antimicrobial Resistant Bacteria
ARG	Antimicrobial resistance gene
AST	Antibiotic Sensitivity Test
aTc	Anhydrotetracycline
ATCC	American Type Culture Collection
ATM	Aztreonam
Azi^R	Sodium Azide Resistant
AZM	Azithromycin
BLAST	Basic Local Alignment Search Tool
BLDB	Beta-Lactam Database
bp	Base pair(s)
BRIG	BLAST Ring Image Generator
C	Chloramphenicol
C. freundii	*Citrobacter freundii*
C. portucalensis	*Citrobacter portucalensis*
cAMPs	Cationic Antimicrobial Peptides
CARD	The Comprehensive Antibiotic Resistance Database
CDS	Coding Sequence(s)
CFU	Colony Forming Units
CGE	Center for Genomic Epidemiology
cgMLST	Core Genome Multilocus Sequence Type
CIP	Ciprofloxacin
CLSI	Clinical and Laboratory Standards Institute
CPD	Cefpodoxime
CPE	Carbapenemase-Producing *Enterobacteriaceae*
CPO	Carbapenemase-Producing Organism
CRISPR	Clustered Regularly Interspaced Short Palindromic Repeats
CTX	Cefotaxime

DHP-I	Dehydropeptidase-I
DNA	Deoxyribonucleic acid
DPBS	Dulbecco's Phosphate Buffered Saline
DR	Direct Repeat
dsDNA	Double-Stranded Deoxyribonucleic Acid
E. coli	*Escherichia coli*
EARS-Net	The European Antimicrobial Resistance Surveillance Network
ECDC	European Centre for Disease Prevention and Control
EDTA	Ethylenediaminetetraacetic acid
Ent. cloacae	*Enterobacter cloacae*
epicPCR	Emulsion, Paired Isolation and Concatenation PCR
ESBL	Extended-Spectrum Beta-Lactamase
EU	European Union
EUCAST	European Committee on Antimicrobial Susceptibility Testing
ExPEC	Extraintestinal Pathogenic *Escherichia coli*
F	Nitrofurantoin
FDA	Food and Drug Administration
fmol	Femtomole(s)
FOX	Cefoxitin
g	Gram(s)
GLASS	Global Antimicrobial Resistance Surveillance System
GFP	Green Fluorescent Protein
GP	General Practitioner
H_2O	Water
HGT	Horizontal Gene Transfer
Indel	Insertion/Deletion
IR	Inverted Repeat
IS	Insertion Sequence(s)
IS*CR*	Insertion Sequence Common Region
K. pneumoniae	*Klebsiella pneumoniae*
K. quasipneumoniae	*Klebsiella quasipneumoniae,*
Kan^R	Kanamycin Resistant
kbp	Kilobase pairs
Klu. ascorbata	*Kluyvera ascorbata*
Klu. georgiana	*Kluyvera. georgiana*
L	Litre(s)
LB	Lysogeny Broth
LMIC	Low and Middle Income Country
LPS	Lipopolysaccharide
M	Molar
MAC	MacConkey Agar
MAM	Macrolide-Arrest Motif
MBL	Metallo-Beta-Lactamase
Mbp	Megabase pair(s)
MDR	Multidrug Resistant
MEM	Meropenem
MGE	Mobile Genetic Element
MH	Mueller-Hinton
MIC	Minimum Inhibitory Concentration

mL	Millilitre(s)
MLST	Multilocus Sequence Type
mM	Millimolar
MRD	Maximum Recovery Diluent
NA	Nalidixic Acid
NCTC	National Collection of Type Cultures
NEB	New England Biolabs
nm	Nanometres
nM	Nanomolar
OD_{600}	Optical Density at 600 nanometres
OM	Outer Membrane
ONT	Oxford Nanopore Technologies
ORF	Open Reading Frame
OT	Oxytetracycline
P. aeruginosa	*Pseudomonas aeruginosa*
PABA	*p*-aminobenzoic acid
PBP	Penicillin Binding Protein
PBRT	PCR-Based Replicon Typing
PCR	Polymerase Chain Reaction
PCT	Pseudo Compound Transposon
PCU	Population Corrected Unit
PLSDB	Plasmid Database
pMLST	Plasmid Multilocus Sequence Type
pmol	Picomole(s)
PNEC	Predicted No Effect Concentration
psi	Pounds per Square Inch
PSK	Postsegregational Killing
qPCR	Quantitative PCR
R. ornithinolytica	*Raoultella ornithinolytica*
RCR	Rolling Circle Replication
RNA	Ribonucleic Acid
RO	Reverse Osmosis
rpm	Revolutions Per Minute
rRNA	Ribosomal Ribonucleic Acid
S. cattleya	*Streptomyces cattleya*
S. clavuligerus	*Streptomyces clavuligerus*
Sh. oneidensis	*Shewanella oneidensis*
St. aureus	*Staphylococcus aureus*
Sten. maltophilia	*Stenotrophomonas maltophilia*
S10	Streptomycin
SBL	Serine Beta-Lactamase
sgRNA	Single Guide Ribonucleic Acid
SMART	Study for Monitoring Antimicrobial Resistance Trends
SNP	Single Nucleotide Polymorphism
SOC	Super Optimal broth with Catabolite repression
sp.	Species
spp.	Species (plural)
ssDNA	Single-Stranded Deoxyribonucleic Acid
ST	Sequence Type

SXT	Trimethoprim-sulfamethoxazole
TA	Toxin-Antitoxin System
TBX	Tryptone Bile X-glucuronide agar
T4CP	Type IV Coupling Protein
T4SS	Type IV Secretion System
TAE	Tris-Acetate Ethylenediaminetetraacetic acid
TE	Transposable Element
TET	Oxytetracycline
tIS	Transporter Insertion Sequence
Tn	Transposon
Tnp	Transposase
Tris-HCl	Tris(hydroxymethyl)aminomethane hydrochloride
TRPP	Tetracycline Ribosomal Protection Protein
TSB	Tryptone Soya Broth
TU	Translocatable Unit
UDP	Uridine diphosphate
UK	United Kingdom
UKHSA	United Kingdom Health Security Agency
UN	United Nations
UNESCO	United Nations Educational, Scientific and Cultural Organization
USA	United States of America
UV	Ultraviolet
V	Volts
v/v	Concentration Volume per Volume
w/v	Concentration Weight per Volume
WBE	Wastewater-Based Epidemiology
WEF	World Economic Forum
WGS	Whole Genome Sequencing
WHO	World Health Organisation
WWTP	Wastewater Treatment Plant
x *g*	Times Gravity
XDR	Extensively Drug Resistant
zCIM	Zinc-supplemented Carbapenem Inactivation Method

CHAPTER 1: INTRODUCTION

1.1 Antimicrobial discovery

The use of antimicrobials as we know them today began in the early 20th century with Paul Ehrlich and his "magic bullet." From his work using dyes to stain different types of tissue, he aimed to find compounds that could destroy microorganisms at dosage levels that would be safe for use in humans (Winau, Westphal and Winau, 2004; Bosch and Rosich, 2008). He systematically screened various arsenic derivatives based on the toxic drug Atoxyl, used for treatment of infections by trypanosomes at the time (Bosch and Rosich, 2008). In 1909, the compound numbered 606 was found to be effective against syphilis in rabbits, and, following trials in humans, went on to be marketed as the drug Salvarsan (Aminov, 2010). Modifying the chemical structure of Salvarsan led to the production of Neosalvarsan in 1912, a less toxic and more soluble version of the drug (Strebhardt and Ullrich, 2008).

This approach to finding new drugs led to the discovery of sulphonamidochrysoidine, better known as Prontosil, by Gerhard Domagk. Screened using haemolytic *Streptococcus* infected mice, Prontosil was discovered to be an effective antimicrobial in 1932 (Sköld, 2000). Soon after, it was discovered that the drug was metabolised in the body, breaking down into the compound sulphanilamide, which retained all the antimicrobial properties of Prontosil (Sneader, 2001; Gould, 2016). Sulphanilamide was cheap to produce and unpatentable as it had been used for many years in the dye industry, which led to its widespread use as an antimicrobial as the first in the class of sulphonamides (Sneader, 2001; Aminov, 2010).

Meanwhile, penicillin had been discovered by Alexander Fleming in 1928, but he had failed to be able to purify it, and had given up the venture by 1940 (Fleming, 1929; Aminov, 2010). Fortunately, in that same year, a team at Oxford led by Ernest Chain and Howard Florey published a paper on purifying penicillin in quantities high enough for clinical testing (Chain et al., 2005). This breakthrough led to the mass production of penicillin in the 1940s, and eventually to the golden age of antibiotics (Aminov, 2010; Gould, 2016).

1.2 Antimicrobial mechanisms of action

There are a variety of mechanisms of action of different classes of antibiotics, but the most common of these are: inhibition of cell wall synthesis, inhibition of protein biosynthesis, inhibition of DNA replication and inhibition of the folic acid pathway (Kapoor, Saigal and Elongavan, 2017). Another notable mechanism is that of outer membrane (OM) disruption (Mohapatra, Dwibedy and Padhy, 2021).

1.2.1 Inhibition of cell-wall synthesis

Peptidoglycan is an essential component of the bacterial cell wall found outside the cytoplasmic membrane in almost all bacteria (Vollmer, Blanot and De Pedro, 2008). It is formed of alternating polysaccharide chains of *N*-acetylglucosamine and *N*-acetylmuramic acid, with a peptide chain containing 3-5 amino acids attached to the former group. These peptide chains

are typically made up of *L*-Ala-γ-*D*-Glu-*meso*-A_2pm (or *L*-Lys)-*D*-Ala-*D*-Ala. These are cross-linked together to form the lattice-like structure of peptidoglycan, either through direct-linkage of two peptide chains, or through the use of a peptide bridge. These cross-links are typically formed between the peptides at position 4 of one peptide chain to position 3 of the other peptide chain, as shown in **Figure 1.1.** (Vollmer, Blanot and De Pedro, 2008; Liu and Breukink, 2016). A variety of enzymes are involved in peptidoglycan synthesis, the most important of which are the transglycosylases, carboxypeptidases and transpeptidases (Spratt, 1975, 1977; Sauvage et al., 2008). Transglycosylases are responsible for elongating the polysaccharide chains, while carboxypeptidases are responsible for trimming unlinked peptide chains. Transpeptidases catalyse the formation of the cross-linked peptide chains by targeting the *D*-Ala-*D*-Ala dipeptide and cleaving the terminal *D*-Ala from one peptide chain to provide the energy to from the covalent bond with the neighbouring peptide chain (Sauvage et al., 2008; Vollmer, Blanot and De Pedro, 2008; Typas et al., 2012).

As shown in **Figure 1.2**, the beta-lactam antibiotics are structurally similar to the substrate of the transpeptidases, *D*-Ala-*D*-Ala, and so these enzymes are also known as penicillin binding proteins (PBPs). Beta-lactams act as competitive mechanistic inhibitors by binding to these enzymes to form a penicilloyl-enzyme complex, which prevents the PBPs from completing their function of cross-linking the peptidoglycan layers (Bush and Bradford, 2016; Lima et al., 2020). As cell wall synthesis is an ongoing process, parts of the cell wall are being broken down at the same time as new layers of peptidoglycan

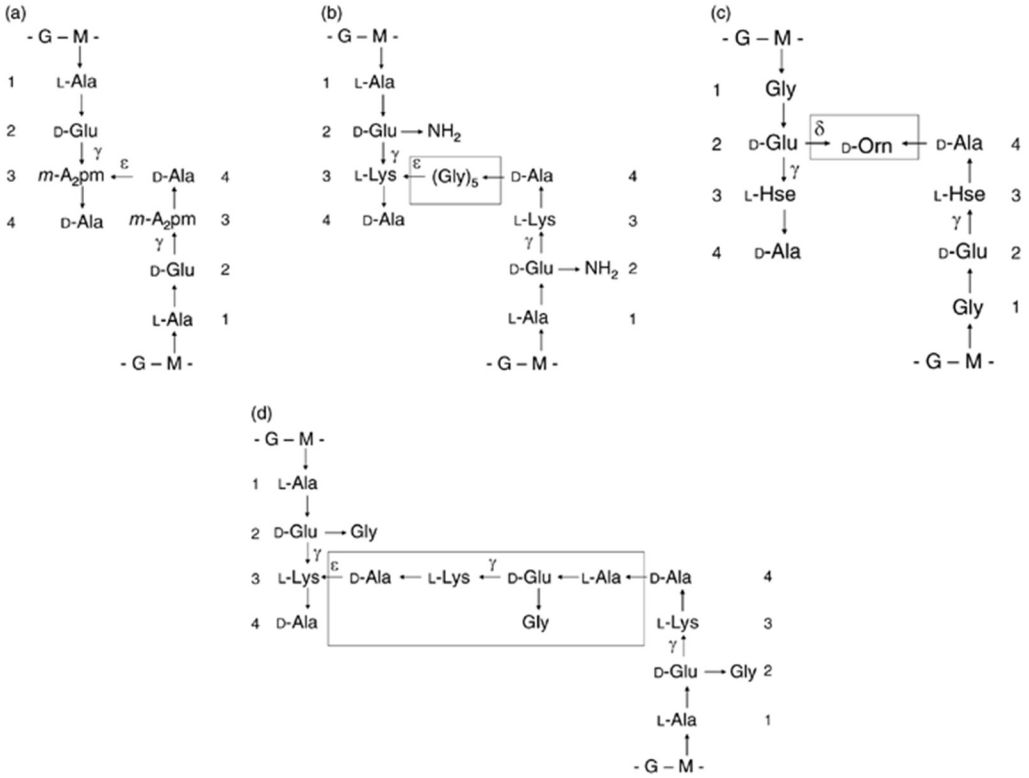

Figure 1.1. Examples of cross-linkage and peptide bridge. (a), *Escherichia coli* (direct cross-link between peptide chains at positions 3 and 4); (b), *Staphylococcus aureus* (cross-link with a pentaglycine bridge between peptide chains at positions 3 and 4); (c), *Corynebacterium pointsettiae* (cross-link with a d-ornithine bridge between peptide chains at positions 2 and 4); (d), *Micrococcus luteus* (cross-link with a bridge consisting of a peptide stem). G, N-acetylglucosamine; M, N-acetylmuramic acid. Republished from Vollmer, Blanot and De Pedro (2008) under Creative Commons CC-BY license.

are being produced. Without new layers being cross-linked due to the action of beta-lactams, the bacterial cell becomes structurally weakened and eventually bursts due to osmotic pressure (Papp-Wallace et al., 2011).

Another example of an antibiotic that inhibits cell wall synthesis is the glycopeptide antibiotic Vancomycin. This binds to the*D*-Ala-*D*-Ala motif of the peptidoglycan precursor, creating a physical barrier that blocks the activity of transglycosylases, and prevents the transpeptidases from cross-linking the peptide chains. Similar to beta-lactam antibiotics, this disruption weakens the bacterial cell wall, ultimately leading to cell death (Mühlberg et al., 2020).

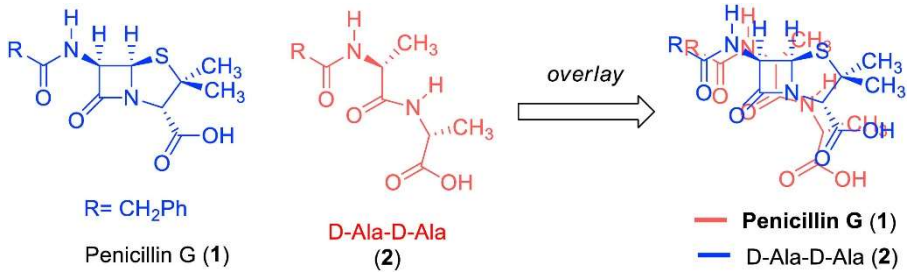

Figure 1.2. The structural similarity of Penicillin G (1, blue), and *D*-Ala-*D*-Ala, a common substrate of Penicillin Binding Proteins (2, red). Republished with permission from Lima et al. (2020). Copyright 2020 Elsevier.

1.2.2 Inhibition of protein synthesis

Aminoglycosides are bactericidal antibiotics that inhibit protein synthesis by binding to the A-site on the 16S ribosomal RNA of the 30S ribosome, altering its conformation (Kotra, Haddad and Mobashery, 2000; Krause et al., 2016). As a result of this, proteins can be mistranslated by induced codon misreading, which leads to incorrect protein structures that can cause damage to the cell. Some aminoglycoside compounds can also block elongation of the polypeptide chain, or prevent initiation entirely, although the specific mechanisms vary by the chemical structure of the various compounds (Wilson, 2014; Krause et al., 2016). Aminoglycosides are unique among the classes of antibiotic that inhibit protein synthesis, as they are bactericidal as opposed to bacteriostatic. This is due to their mechanism of entry into the cell that occurs due to a three-stage process, as shown in **Figure 1.3**. Firstly, as they are polycationic hydrophobic molecules, aminoglycosides bind electrostatically to the negatively charged components of the bacterial cell surface. This results in displacement of divalent cations and increased permeability of aminoglycoside molecules into

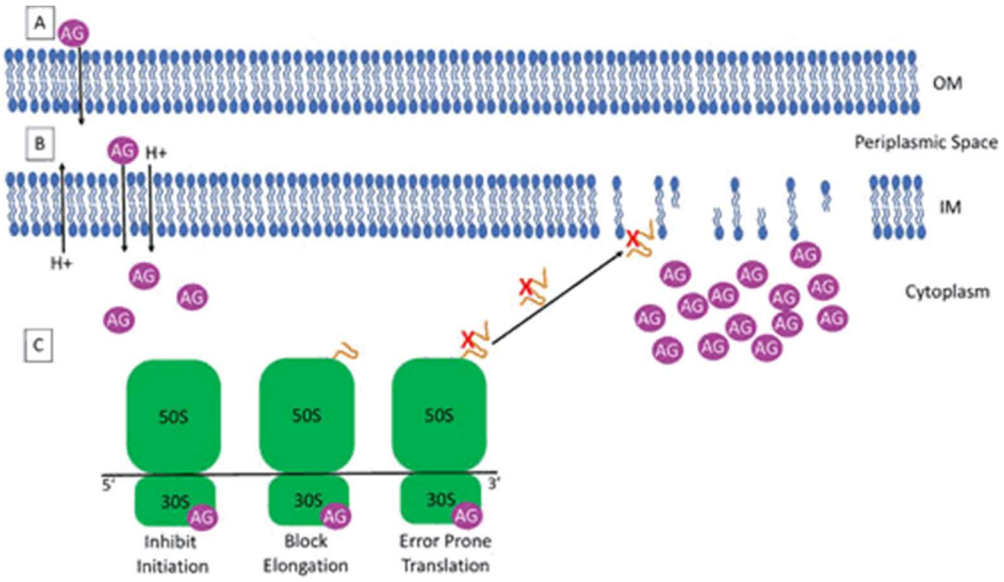

Figure 1.3. The process of aminoglycoside entry into the bacterial cell. A) Positively charged aminoglycoside molecules (AG) enter the cell through electrostatic binding to the negatively charged components of the outer membrane (OM). B) Small numbers of AG cross the inner membrane (IM) using the proton motive force. C) AGs bind to the 30S subunit of rRNA and cause mistranslation, as well as blocking initiation and elongation of translation. Mistranslated proteins are hypothesised to cause damage to the IM, allowing increased amounts of AG to enter the cytoplasm. Republished from Serio et al. (2018) under Creative Commons CC-BY license.

the bacterial cell (Serio et al., 2018). Secondly, small numbers of these molecules cross the cytoplasmic membrane in an energy-dependent manner, known as the energy-dependent phase I (Jana and Deb, 2006; Serio et al., 2018). Once inside the cell, these molecules inhibit protein synthesis as described above and it is hypothesised that mistranslated proteins cause further damage to the cytoplasmic membrane, which increases the concentration of aminoglycosides in the cytoplasm. The final stage is known as the energy-dependent phase II, and this results in the rapid increase of aminoglycoside molecules in the cytoplasm. The combination of damage to the cytoplasmic membrane, mistranslation and inhibition of protein synthesis is what causes their bactericidal activity (Jana and Deb, 2006; Serio et al., 2018).

Tetracyclines act on the same 30S ribosomal subunit to prevent protein synthesis, though are mostly considered bacteriostatic. This is due to the antibiotic physically interfering with the docking of transfer RNA (tRNA) during elongation (Grossman, 2016). This halts protein synthesis without causing translation errors, as seen with aminoglycosides, and typically results in a bacteriostatic effect. Another key difference is their mechanism of entry into the cell: tetracyclines diffuse through porin channels as a metal ion-antibiotic complex, after which the metal ion dissociates, allowing the antibiotic to cross the lipid bilayer as a lipophilic molecule (Chopra and Roberts, 2001).

Macrolide, lincosamide, streptogramin, phenicol and pleuromutilin antibiotics interfere with protein synthesis by binding to the 50S ribosomal subunit (Schwarz et al., 2016; Dinos, 2017). Macrolides are known to target the nascent peptide exit tunnel, through which synthesised protein leaves the ribosome. There, they prevent peptide bond formation between specific sequences known as Macrolide-Arrest Motifs (MAMs) (Vázquez-Laslop and Mankin, 2018). Research into the mechanisms of action of four macrolides (erythromycin, josamycin, spiramycin, and telithromycin), a lincosamide (clindamycin), and a streptogramin (pristinamycin IA) has shown that all these antibiotics promote the dissociation of peptidyl-tRNA from the ribosome (Tenson, Lovmar, and Ehrenberg, 2003). However, their effects vary: josamycin, spiramycin, and clindamycin cause dissociation of peptidyl-tRNAs with 2–4 amino acid residues; erythromycin primarily targets peptidyl-tRNAs with 6–8 residues; pristinamycin IA affects those with 6 residues; and telithromycin induces dissociation of peptidyl-tRNAs containing 9–10 residues.

These findings highlight a shared mode of action among these antibiotics, which is why they are commonly referred to as the MLS antibiotics (macrolide, lincosamide, streptogramin) (Tenson, Lovmar, and Ehrenberg, 2003; Spížek and Řezanka, 2017).

The binding site of chloramphenicol is located in the peptidyl transferase centre of the 50S ribosomal subunit, adjacent to and partially overlapping with the binding site of lincosamide antibiotics. Similarly, pleuromutilins also target the peptidyl transferase centre, although their precise binding position varies depending on the specific drug. These similar binding sites are the reason that these drugs all have the similar bacteriostatic effect of disrupting protein synthesis (Schwarz et al., 2016).

1.2.3 Inhibition of DNA synthesis

During DNA replication, double-stranded DNA (dsDNA) is unwound by the enzyme DNA helicase to provide single-stranded templates for the replication machinery to synthesize new DNA strands. This unwinding generates torsional strain in the DNA molecule, which is relieved by topoisomerase enzymes. These enzymes introduce temporary nicks in the DNA strands, allowing intact sections of dsDNA to pass through before resealing the nicks (Correia et al., 2017).

Quinolone and fluoroquinolone antibiotics disrupt bacterial DNA replication by targeting type-II topoisomerases, specifically DNA gyrase and topoisomerase IV (Pham, Ziora, and Blaskovich, 2019), as shown in **Figure 1.4**. These enzymes

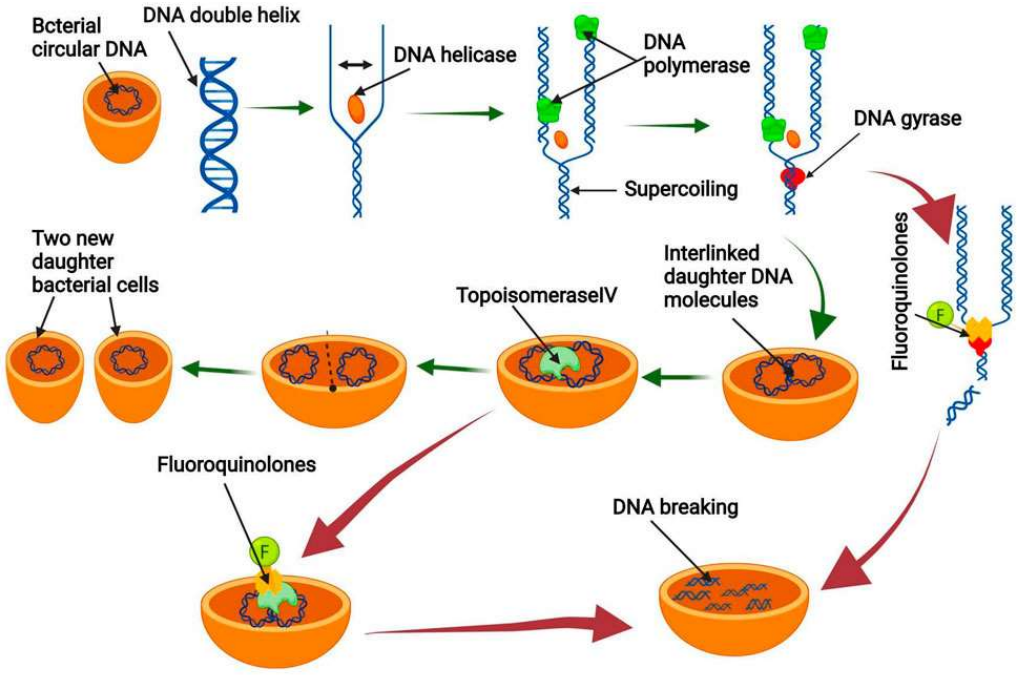

Figure 1.4. Mechanism of DNA replication processes showing the stages at which fluoroquinolones interact with topoisomerase enzymes to inhibit DNA replication. Republished from Halawa et al. (2024) under Creative Commons CC-BY license.

form transient complexes with DNA via covalent bonds between active site tyrosine residues and the 5'-overhangs at DNA breaks, known as cleavage complexes. Quinolones stabilize these cleavage complexes, forming a quinolone-topoisomerase-DNA complex that blocks the progression of the replication machinery at replication forks, thereby inhibiting DNA synthesis (Correia et al., 2017).

Collisions between the replication machinery and these stabilized complexes generate larger, irreversible DNA breaks (Hooper and Jacoby, 2016). This triggers a bacterial stress response that de-represses the SOS repair system, activating DNA repair enzymes. At low quinolone concentrations, this results in bacteriostasis. However, at higher concentrations, the repair mechanisms can

be overwhelmed, leading to incomplete DNA repair, extensive DNA damage, and ultimately bacterial cell death (Correia et al., 2017).

1.2.4 Inhibition of folic acid pathway

Tetrahydrofolic acid, the active form of vitamin B_9, plays a pivotal role in many biochemical reactions including nucleotide synthesis in both eukaryotes and prokaryotes. In bacteria, it is involved in the biosynthesis of methionine, serine and glycine; production of adenine and guanine; production of thymidine monophosphate; and the formation of formyl-methionyl tRNAs (Nixon et al., 2014). Tetrahydrofolic acid is synthesised through a pathway that converts dihydropteroate diphosphate and *p*-aminobenzoic acid (PABA) into dihydropteroic acid. This is then converted to dihydrofolic acid, and finally forms tetrahydrofolic acid by the action of dihydrofolate reductase.

The sulphonamide antibiotics act as competitive antagonists and structural analogues of PABA and are therefore able to disrupt this pathway by replacing PABA in the reaction of the enzyme dihydropteroate synthetase. This inhibits the production of purine bases and amino acids, thereby preventing DNA replication and cell division, which results in a bacteriostatic effect (Ovung and Bhattacharyya, 2021).

Similarly, the diaminopyrimidine antibiotics, such as trimethoprim, act as competitive antagonists for dihydrofolate reductase, another enzyme in the tetrahydrofolic acid pathway, and consequently inhibit DNA replication and cell division in the same manner (Gleckman, Blagg and Joubert, 1981).

1.2.5 Disruption of outer membrane

Structurally, the polymyxin antibiotics a very similar to the cationic antimicrobial peptides (cAMPs) produced by the innate immune system of eukaryotes in response to bacterial infection. These antibiotics consist of a hydrophilic cationic peptide ring and a hydrophobic fatty acid tail structure (Trimble et al., 2016) as can be seen in **Figure 1.5**. The cationic peptide region binds to the lipopolysaccharide (LPS) molecules of the bacterial OM due to electrostatic interactions between the positively charged polymyxin and the negatively charged phosphate groups of the LPS. After binding to the LPS and subsequent displacement of membrane-stabilising cations, the hydrophobicity of the tail structure interacts with the lipid A of the LPS layer on the surface of the OM, which disrupts the membrane structure and leads to increased membrane permeability. These interactions lead to weakening and subsequent disintegration of the membrane followed by cell death due to osmotic pressure. This mechanism has a somewhat similar effect when polymixins interact with the membranes of human cells, which results in the nephrotoxic effect observed in their clinical use. This toxicity is primarily seen in kidney and brain tissue, although recent modifications to dosage and modifications to the formulation have greatly reduced this effect (Mohapatra, Dwibedy and Padhy, 2021).

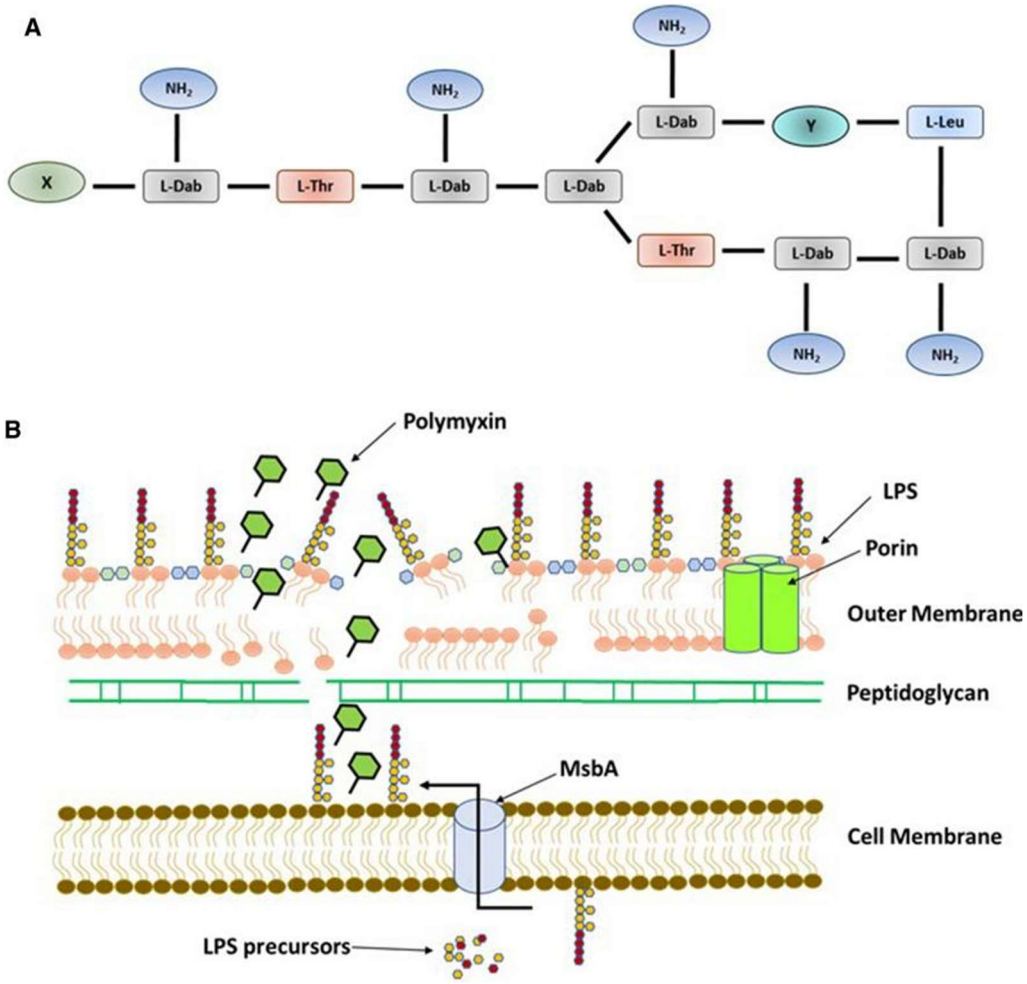

Figure 1.5. Structure of polymyxin antibiotics and their mechanism of action. A) Structure of the polymyxin molecule. Y represents *D*-Phe in the polymyxin B molecule and *D*-Leu in the colistin molecule. X represents the fatty acid chain; Dab- diamino-butyric acid. B) The interaction between the polymyxin molecule and the bacterial outer membrane (OM). Polymyxin molecules interact electrostatically with lipopolysaccharide (LPS) and lead to disruption of, followed by insertion of the polymyxins into, the OM. The antibiotics can also interfere with LPS molecules being transported to the OM. The overall process leads to disintegration of the OM resulting in cell lysis and death. Republished with permission from (Mohapatra, Dwibedy and Padhy, 2021. Copyright Springer Nature 2021.

1.3 Antimicrobial resistance

1.3.1 Origins of antimicrobial resistance

Most of the antimicrobials used today in clinics around the world are derived from natural sources. In fact, over 70% of the antibiotics used now were developed from the secondary metabolites of the actinomycetes (Mak, Xu and Nodwell, 2014; Nothias, Knight and Dorrestein, 2016). Given that antibiotics are produced in natural environments (Clardy, Fischbach and Currie, 2009), it is unsurprising that antimicrobial resistance would also exist in bacteria in those environments, as a defence mechanism against both self-produced antimicrobial molecules as well as those produced by competing organisms. Indeed, studies have shown that antibiotic resistance genes are ancient, with vancomycin, tetracycline and beta-lactam resistance genes having been detected in 30,000 year old Canadian permafrost (D'Costa et al., 2011). Antibiotic resistance has also been detected in the deep subsurface microbiome, as well as an isolated cave microbiome, untouched by anthropogenic sources of antimicrobial use (Brown and Balkwill, 2009; Bhullar et al., 2012). Further evidence from evolutionary analyses shows beta-lactamases are at least two billion years old, while the OXA beta-lactamases specifically were mobilised onto plasmids millions of years ago (Barlow and Hall, 2002; Hall and Barlow, 2004). It seems clear, therefore, that resistance predates the modern development of antimicrobials by humans, and so the "antimicrobial resistance pandemic" as we currently know it is caused by

selection pressure for pre-existing antimicrobial resistance genes (ARGs), or combinations thereof, due to anthropogenic use of antimicrobials.

Sir Alexander Fleming warned of the overuse of antibiotics in 1945, saying that demands for the drug by the public would lead to an era of abuses (Ventola, 2015). This has proven true, as can be seen by the vast amounts of antibiotics prescribed (or simply purchased without prescription) unnecessarily across the globe. As an example of poor antimicrobial stewardship: in the UK in 2011, 51% of patients seen by a GP for a cough or cold-like symptoms were prescribed antibiotics (Hawker et al., 2014), despite this being against medical recommendations. On a larger scale, a study of antibiotic consumption across 76 countries found that antibiotic use per 1,000 population increased 39% between 2000 and 2015 (Klein et al., 2018); while another study estimated global antibiotic consumption to have increased 46% between 2000 and 2018 (Browne et al., 2021). In low- and middle-income countries (LMICs), antibiotics are often available without prescription, either due to lack of regulation, or lack of enforcement of existing regulations (Morgan et al., 2011). In some LMICs, available antimicrobials are often of poor quality, due to inadequate storage, or even outright counterfeit drugs, which do not contain the drug they are marketed as, or not at the concentrations claimed (Ayukekbong, Ntemgwa and Atabe, 2017).

The overuse of antibiotics in agriculture has also contributed to the problem of antimicrobial resistance (AMR), with 70% of all antibiotics defined as medically important in the USA being used in agriculture in 2016 (O'Neill, 2016). The USA Food and Drug Administration (FDA) did eliminate antibiotic use for growth

promotion in 2017, and while this has led to a 32% reduction in agricultural antibiotic use between 2016 and 2020, it is still 86% higher per population corrected unit (PCU) than in the European Union (EU) (Wallinga et al., 2022). Unfortunately, these reductions do not reflect the trends in global consumption of agricultural antibiotics, which is predicted to rise by 8% between 2020 and 2030 (Mulchandani et al., 2023).

The United Nations (UN) has called the AMR crisis a "global health emergency" (UN News, 2018), while the former World Health Organisation (WHO) Director-General, Dr Margaret Chan, has referred to AMR as "a slow-motion tsunami" (WHO, 2016). Globally, it was estimated that six drug-resistant pathogens were responsible for the deaths of at least 700,000 people in 2014 (O'Neill, 2014), and it has been estimated that the total burden of AMR could rise to 10 million by 2050 (O'Neill, 2016), although it is worth noting that this is disputed as too high an estimation (de Kraker, Stewardson and Harbarth, 2016). More recently, it was estimated that 4 of those 6 drug-resistant pathogens were directly responsible for 670,000 deaths in 2019, while the total number of deaths directly caused by drug-resistance that year was 1.27 million (Murray et al., 2022). Undoubtedly, if actions are not taken the AMR crisis will have a dramatic impact on medicine as we know it. Medical treatments such as routine surgery, joint-replacements and caesarean sections all rely on the efficacy of antibiotic therapy. Treatment that requires immunosuppression such as chemotherapy and organ transplantation would be impossible if antibiotics were no longer effective, as indeed is already a problem with the rise of multidrug resistant (MDR) and extensively drug resistant (XDR) bacterial infections (George et al.,

2014). This potential future is what the WHO calls the “post-antibiotic era” (Reardon, 2014), and we must act quickly and effectively to prevent it.

1.3.2 Mechanisms of antimicrobial resistance

Resistance to antimicrobials is produced by four main mechanisms: i) inactivation of the antimicrobial, ii) modification of the target site of the antimicrobial, iii) prevention of the antimicrobial from reaching the target site, and iv) resistance due to global cell adaptive processes (Munita and Arias, 2016). The most common mechanisms are shown in **Figure 1.6**.

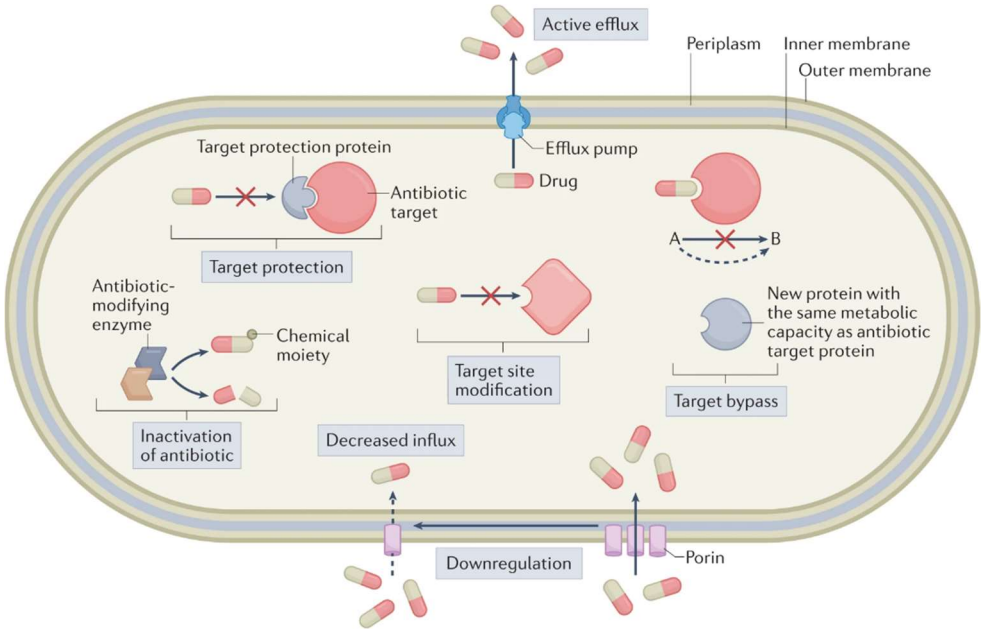

Figure 1.6. Common mechanisms of antimicrobial resistance. Inactivation of antibiotic occurs via enzymatic degradation or modification of the antibiotic. Target protection involves the physical association of a target protection protein that prevents the antibiotic from reaching its target site. Decreased influx involves changes to the membrane structure, often through downregulation or mutations of porins, which reduces the ability of the antibiotic to enter the cell. Target site modification reduces affinity of the antibiotic for the target site, usually through genetic mutation or enzymatic alteration. Active efflux is facilitated by efflux pumps, which export antibiotics and various other compounds out of bacterial cells. Target bypass involves production of another protein for the same function that is not inhibited by the antibiotic. Republished with permission from Darby et al., 2023. Copyright 2023 Springer Nature Limited.

1.3.2.1 Inactivation of the antimicrobial molecule

Antimicrobials can be modified by bacterial mechanisms through both chemical modification and degradation of the molecule itself. Some of the most well described mechanisms of chemical modification are the aminoglycoside modifying enzymes (AMEs) (Garneau-Tsodikova and Labby, 2016; Munita and Arias, 2016). These enzymes are classified based on the form of chemical modification they apply to the aminoglycoside molecule. They consist of the **a**minoglycoside *N*-**ac**etyltransferases (AAC), **a**minoglycoside *O*-**n**ucleotidyl**t**ransferases (ANT), and **a**minoglycoside *O*-**ph**osphotransferases (APH) families of enzymes (Garneau-Tsodikova and Labby, 2016). These enzymes alter the chemical structure of the antibiotics, by modifying the hydroxyl or amino groups, which substantially reduces their affinity for their target (Darby et al., 2023).

Similarly, other antimicrobials that target the 50S ribosomal subunit and inhibit protein biosynthesis are also targets of chemical modification. Lincosamide antibiotics are also modified by bacterial nucleotidyltransferases; macrolide resistance can occur through the production of phosphotransferases and esterases; while streptogramin and phenicol antibiotics are commonly modified by acetyltransferases, such as the chloramphenicol acetyltransferase (CAT) family of enzymes (Darby 2023).

Perhaps the most well-known mechanism of antimicrobial degradation is hydrolysis of beta-lactam antibiotics by the beta-lactamases, which will be discussed in more detail in **§1.5**. Another example of antimicrobial degradation is the tetracycline destructases, such as the Tet(X) family of enzymes, which

catalyse the oxidation of tetracyclines, leading to covalent destruction of the antibiotic scaffold (Markley and Wencewicz, 2018).

1.3.2.2 Modification of the target site of the molecule

Mutations that lead to amino acid substitutions in the target site protein can alter the structure and reduce binding-affinity of the antimicrobial molecule. For example, a common mechanism of fluoroquinolone resistance is due to mutations in the antibiotic target sites of DNA gyrase and/or topoisomerase IV (Redgrave et al., 2014). Although fluoroquinolones are to some extent active against both proteins, they do target a particular protein preferentially, depending on the specific drug and bacterial species. However, they will also bind to the secondary target and exert an antimicrobial effect even if the primary target has been modified (Hooper, 2000). For this reason, alterations of the target site can result in only a small increase in the minimum inhibitory concentration (MIC) of the drug, and high levels of fluoroquinolone resistance are frequently associated with multiple amino acid changes in both DNA gyrase and topoisomerase IV (Hooper, 2000; Munita and Arias, 2016).

Other mechanisms that modify the target site include enzymatic alteration, such as the *erm* family of macrolide resistance genes. These are so named because they are **e**rythromycin **r**ibosomal **m**ethylation genes, that methylate an adenine residue in a conserved region of the 23S ribosomal subunit, causing reduced binding affinity of erythromycin (Leclercq, 2002). The final mechanism in this category is known as target protection. Resistance to tetracycline

antibiotics is caused by a number of different mechanisms, one of which is the production of tetracycline ribosomal protection proteins (TRPPs) such as Tet(M) and Tet(O) (Connell et al., 2003; Wilson et al., 2020). These TRPPs bind to the ribosome in a position that overlaps the tetracycline binding site, which physically displaces the drug. They also produce conformational changes in the tetracycline-binding site of the ribosome that persist after TRPP disassociation, which prevents immediate rebinding of the drug (Wilson et al., 2020).

Another strategy consists of using a different pathway to accomplish a biochemical function to that of the antimicrobial target. Perhaps the most well-known example of this is that of methicillin resistance in *Staphylococcus aureus,* which is due to the acquisition of an exogenous PBP (PBP2a) (Munita and Arias, 2016). PBP2a is homologous to the original target site but has a lower affinity for beta-lactam antibiotics. Even when bound to methicillin, cell wall synthesis is not inhibited as the transpeptidase activity of PBP2a is still maintained (Stapleton and Taylor, 2002; Munita and Arias, 2016; Darby et al., 2023).

Overproduction of the antimicrobial target is another mechanism by which resistance can be conferred. This occurs when the amount of target molecules is increased, effectively overwhelming the ability of the antibiotic to interact with them. Mutations in the promoter regions of the genes encoding dihydropteroate synthase and dihydrofolate reductase can confer resistance to sulphonamide and trimethoprim antibiotics, respectively. These mutations lead to overexpression of the enzymes involved in folate synthesis (as

described in **§1.2.4**), reducing the ability of the antibiotics to inhibit this pathway and allowing bacterial survival (Munita and Arias, 2016).

1.3.2.3 Prevention of the antimicrobial from reaching the target site

The Gram-negative OM is composed of a lipid bilayer that is impermeable to large, charged molecules. To enable the uptake of nutrients and other molecules, the OM also contains water-filled open channels, known as porins, that allow the penetration of hydrophilic molecules across the OM (Pagès, James and Winterhalter, 2008). These channels are the means of entry to the bacterial cell of small hydrophilic antibiotics such as beta-lactams, tetracyclines, phenicols, and fluoroquinolones (Nikaido, 2003). There are three strategies of porin modification used by bacteria that reduce susceptibility to antimicrobials: changes in the type of porin expressed, changes in levels of porin expression, and modifications of the functional properties of the porin channel (Pagès, James and Winterhalter, 2008). The change in expression from the larger porins OmpK35 and OmpK36 for the smaller OmpK37 is responsible for drastic increases in MICs of cephalosporins in *Klebsiella pneumoniae* isolates (Delcour, 2009). The OprD porin of *Pseudomonas aeruginosa* is known to be preferentially used by imipenem to enter the cell, and reduced expression of this protein increases the MIC of the antibiotic (Li et al., 2012). Reduced expression can be conferred through mutational change but can also occur due to regulatory control in response to antimicrobial stress. The regulatory RNA MicC modulates the expression of the porin OmpC in *E. coli*. Expression of *micC*

has been shown to increase in response to the presence of beta-lactams, resulting in downregulation of the porin gene *ompC* as a response (Dam, Pagès and Masi, 2017).

Another major mechanism for preventing antimicrobial access to its target site is through the use of bacterial efflux pumps, which are important for removing many types of harmful compounds from bacterial cells, such as waste cell products, antibiotics, antimicrobial metals, disinfectants and bile salts (Thanassi, Cheng and Nikaido, 1997; Kazama et al., 1998; Hobman and Crossman, 2015; Blanco et al., 2016). Efflux pumps may be substrate specific, such as the Tet(A) and Tet(B), which are the most common method of tetracycline efflux in Gram-negative clinical isolates (Grossman, 2016). Those that have a broader range of substrates are often capable of expelling multiple classes of antibiotic and are known as multidrug efflux pumps. In *P. aeruginosa*, the multidrug efflux pump (Mex) MexAB-OprM is considered the main contributor to antimicrobial resistance, and is capable of removing quinolones, macrolides, tetracycline, chloramphenicol, novobiocin, and most beta-lactams from the cell (Masuda et al., 2000; Lorusso et al., 2022).

The formation of bacterial biofilms also plays a role in preventing antimicrobials from reaching their targets through the production of an extracellular matrix. This biopolymer contains proteins, polysaccharides as well as extracellular DNA, and is able to prevent antimicrobials from reaching bacterial cells (Ciofu et al., 2022; Shree et al., 2023). Another mechanism of resistance mediated by biofilms is that of metabolic heterogeneity, where cells in parts of the biofilm

are metabolically inactive, which prevents antibiotics from acting upon target molecules involved in DNA, protein or cell-wall synthesis (Ciofu et al., 2022).

1.3.2.4 Resistance due to global cell adaptive processes

Bacterial pathogens have evolved sophisticated mechanisms to cope with environmental pressures that allow them to survive in a range of stressful environments, including the human body. Development of resistance to daptomycin and lowered susceptibility to vancomycin by Gram-positive bacteria are clinically relevant examples of resistance phenotypes that are a result of these cellular mechanisms (Munita and Arias, 2016).

Daptomycin is a lipopeptide antibiotic that is structurally and functionally similar to cAMPs produced by the innate immune system (Tran, Munita and Arias, 2015). The antimicrobial activity of daptomycin begins with it forming a complex with calcium ions, giving the molecule a positive charge. This interacts electrostatically with the negatively charged cell membrane, eventually resulting in entry to the cell. Bacteria have evolved systems to protect themselves against cAMPs and possess regulatory mechanisms that are involved in protecting the cell envelope in the presence of cAMPs (Munita and Arias, 2016).

The LiaFSR system of *Enterococcus faecium* and *Enterococcus faecalis* is a stress-response regulatory system that regulates genes for cell wall synthesis, cell division, transmembrane proteins, and cell envelope stress response. Increased activity of LiaFSR in response to daptomycin causes remodelling of

the cell membrane, which is responsible for the resistance phenotype in these bacteria (Tymoszewska, Szylińska and Aleksandrzak-Piekarczyk, 2023). In *St. aureus,* remodelling of the cell membrane results in changes of surface charge which lead to electrostatic repulsion of the positively charged daptomycin-calcium complex away from the cell (Bayer, Schneider and Sahl, 2013; Munita and Arias, 2016).

1.3.3 Natural and acquired resistance

1.3.3.1 Natural antimicrobial resistance

The resistance mechanisms described in the previous section can be further divided into two categories called natural (encompassing both intrinsic and naturally inducible resistance) and acquired resistance. Intrinsic resistance is insusceptibility to an antimicrobial caused by a trait that is: universally shared across a bacterial species, independent of antibiotic selective pressure, and not associated with horizontal gene transfer (HGT) (Cox and Wright, 2013). Perhaps the best-known example of intrinsic resistance is the Gram-negative OM itself, which protects the cell from toxic molecules including antibiotics such as vancomycin, which is unable to penetrate the membrane (Miller, 2016). Another similar example would be Gram-positive bacterial resistance to colistin, as they lack an OM for the antibiotic to act upon. While intrinsic resistance is often caused by these sorts of passive physical properties of cells, it also includes more active mechanisms like antibiotic inactivation, such as the constitutively expressed beta-lactamases of *Acinetobacter baumannii* (Poirel,

Bonnin and Nordmann, 2011b). Other examples of clinically relevant intrinsic resistance mechanisms include bacterial efflux pumps such as the MexAB-OprM as described in **§1.3.2.3**. Naturally inducible resistance mechanisms are those which are found chromosomally, and expressed at basal levels until hyperexpression is triggered by the presence or action of antimicrobials. An example of inducible resistance is the group of enzymes known as AmpC beta-lactamases, which are constitutively expressed in some species, such as *Escherichia coli*, *A. baumannii* and *Shigella* spp.*;* these are plasmid mediated in other members of the *Enterobacteriaceae,* as well as being inducible in other species such as *Enterobacter cloacae*, *Serratia marcescens*, *Citrobacter freundii* and *P. aeruginosa* (Tamma et al., 2019). In the latter group, the regulatory protein AmpR reduces *ampC* expression to very low levels in the absence of beta-lactams (Honoré, Nicolas and Cole, 1986). When cell wall degradation products are produced by the activity of certain beta-lactams, these peptides compete with uridine diphosphate (UDP)–*N*-acetylmuramic acid, the substrate of AmpR. As these cell wall peptides bind to AmpR, it undergoes conformational changes that disable its function, preventing repression and therefore increasing expression of AmpC (Tamma et al., 2019). AmpC is induced by, and capable of hydrolysing, the aminopenicillins, such as ampicillin and amoxicillin, cephamycins such as cefoxitin, and first-generation cephalosporins. Other beta-lactams such as fourth-generation cephalosporins and carbapenems are inducers of AmpC expression but are also able to withstand hydrolysis by the enzyme due to the formation of a stable acyl enzyme complex (Hancock and Bellido, 1996; Sanders et al., 1997).

1.3.3.2 Acquired antimicrobial resistance

Although natural resistance mechanisms pose a problem for the treatment of infections caused by certain bacteria, the current crisis of AMR is primarily caused by the acquisition of resistance mechanisms by previously susceptible bacteria. This development of acquired resistance is caused by two main routes: i) mutational resistance and ii) horizontal gene transfer.

Mutational resistance is caused by single nucleotide polymorphisms (SNPs) and insertions or deletions (indels) in pre-existing genes that result in a resistant phenotype to antimicrobials. These are commonly associated with particular species of bacteria as well as certain antibiotics, dependent on their specific targets. For example, resistance to penicillins in *Streptococcus* is primarily caused by modifications of its PBPs, specifically PBP 2X, PBP 2B, and PBP 1A, which leads to decreased affinity for the antimicrobial molecule and higher MICs (Haenni and Moreillon, 2006). Resistance to fluoroquinolones is commonly caused by mutations in the *gyrA* and *gyrB* or *parC* and *parE* genes encoding for DNA gyrase and DNA topoisomerase IV respectively, as described in **§1.2.3**. In *Mycobacterium tuberculosis*, resistance mechanisms for all of our current therapeutic agents are caused solely by mutations (Dookie et al., 2018). Similarly, the resistance mechanisms of multidrug resistant *Helicobacter pylori* are also caused by mutational changes (Woodford and Ellington, 2007). Mutational changes in natural resistance mechanisms can lead to increased levels of phenotypic resistance, or resistance to new classes of antibiotics, especially when multiple mutational changes have an additive effect on the resistance phenotype. Mutants of the constitutively expressed AmpC beta-

lactamase can result in AmpC overexpression, which has been shown to have increased affinity for third generation cephalosporins such as cefotaxime, as well as carbapenems (Mammeri, Poirel and Nordmann, 2007). Combinations of mutations that cause AmpC and efflux pump overexpression have been shown to cause meropenem resistance in *P. aeruginosa* (Cabot et al., 2011), while AmpC overexpression combined with porin loss can cause carbapenem resistance in *E. coli* (Mammeri et al., 2008).

Horizontal gene transfer is the acquisition of external DNA material and occurs via three mechanisms: i) transformation (incorporation of naked DNA), ii) transduction (bacteriophage-mediated transfer of DNA) and iii) conjugation (transfer of DNA between bacteria via direct contact) (Munita and Arias, 2016), the specifics of which will be covered in more detail in **§1.4**. Briefly, HGT is responsible for the spread of resistance to almost all classes of antibiotics in clinical use (Bennett, 2008), and is capable of transferring a variety of distinct mechanisms. HGT is associated with the common tetracycline resistance gene *tetA*, which encodes an inducible efflux pump (Ball, Shales and Chopra, 1980; Grossman, 2016); plasmid-mediated dihydrofolate reductase, which confers resistance to trimethoprim (Adrian et al., 1998); the majority of aminoglycoside resistance genes (Zhang et al., 2023); the dissemination of sulphonamide resistance genes (Sköld, 2000); and many others. HGT is also primarily responsible for the spread of resistance to our most crucial antibiotics, colistin and the carbapenems, dubbed “last resort” treatments by the WHO (WHO, 2021). The spread of all the most clinically relevant carbapenemases has been brought about by HGT (Halat and Moubareck, 2020), and these will be

addressed in more detail in **§1.5.2**. The mobile colistin resistance gene, *mcr-1,* was first described on a plasmid in 2015, isolated from *E. coli* from food animals (Liu et al., 2016). Phylogenetic analyses have shown that *mcr-1* mobilised into agricultural isolates from an unknown source, and has since then spread into human isolates (Wang et al., 2018), where HGT has played a major role in the global spread of colistin resistance (Castañeda-Barba, Top and Stalder, 2023).

1.4 Mechanisms of horizontal gene transfer

1.4.1 Transformation

Transformation is a process where bacterial cells uptake DNA through the cell wall from their surroundings, followed by stable incorporation into the genome or replication as an independent DNA molecule. Bacteria that can undergo transformation are known as competent, and while many bacteria can be made competent via chemical stress or electroporation, those that can undergo transformation without human intervention are known as naturally competent. Historically, conjugation has often been the main focus in the study of the spread of AMR via HGT, however, recent studies suggest natural transformation may be more important than previously thought (Winter et al., 2021). Naturally competent *A. baumanii* have been shown to incorporate ARGs from extracellular DNA from different species containing multiple ARGs (Traglia et al., 2019). In *A. baylyi,* natural transformation has been shown to result in the uptake of integrons (**§1.4.5**) and a Tn*21*-like transposon (**§1.4.4.3**) from

DNA harvested from many different genera (Domingues et al., 2012). It has also been shown that in *Vibrio cholerae* and *Streptococcus pneumoniae,* the genes that regulate competence are linked to those that regulate neighbour predation (Veening and Blokesch, 2017), which suggests transformation may play a more active role in interspecies gene transfer, and possibly the spread of AMR, than previously thought.

1.4.2 Transduction

Transduction is the process by which a virus transfers genetic material from one bacterium to another. Historically, phage-mediated transfer of host genes was thought to occur by one of two mechanisms: generalised and specialised transduction. Generalised transduction was first discovered in *Salmonella* phage P22 (Zinder and Lederberg, 1952), and is a process by which bacteriophage package any bacterial DNA into phage heads instead of viral DNA due to errors in *pac* site recognition (Chiang, Penadés and Chen, 2019). Specialised transduction, first described in bacteriophage lambda (Morse, Lederberg and Lederberg, 1956), differs from generalised transduction in that bacterial DNA transfer is limited to a specific section on the chromosome. When a lysogenic phage that has integrated into the host chromosome becomes lytic, imprecise excision of phage DNA can lead to adjacent sections of bacterial DNA also being excised and packaged into phage particles by mistake (Chiang, Penadés and Chen, 2019). Recently, the third mechanism of transduction, lateral transduction, was discovered in temperate bacteriophage

of *St. aureus* (Chen et al., 2018). Whereas the previous two mechanisms of transduction are thought to occur due to mistakes in viral replication, bacterial DNA is transferred via lateral transduction as a natural part of the replication of specific bacteriophage. This is because these prophages do not excise from the host chromosome and then begin replication, but replication begins *in situ* within the bacterial genome. The viral capsids are then packaged with DNA until they reach physical capacity, at which point the DNA is cleaved non-specifically. After this, the terminase protein remains attached to the DNA and begins packaging into another capsid, which has been shown to occur up to seven times. This means that large sections of host DNA, up to several hundred kilobases, can be transferred by this mechanism, which has been shown to transfer host DNA at a rate up to one thousand times greater than other forms of transduction (Chen et al., 2018; Davidson, 2018; Chiang, Penadés and Chen, 2019).

Many studies have shown that bacteriophage can transfer ARGs *in vitro*, though a small number have detected ARGs in bacteriophage DNA from environmental samples (Balcazar, 2014). One such study was performed by Colomer-Lluch, Jofre and Muniesa (2011), which found beta-lactamase genes bla_{TEM} and $bla_{\text{CTX-M-9}}$ isolated from bacteriophage DNA in river water and urban wastewater samples from Spain. The same group also found quinolone resistance genes *qnrA* and *qnrS* from urban and farm wastewater (Colomer-Lluch, Jofre and Muniesa, 2014). Another study also found quinolone resistance genes *qnrA, qnrB,* and *qnrS*, as well as beta-lactamase genes $bla_{\text{CTX-M}}$, bla_{SHV} and bla_{TEM} in the phage DNA fraction from environmental wastewater (Marti,

Variatza and Balcazar, 2014). More recent work has also provided genomic evidence that transduction was responsible for the inter-species transfer of ARGs between *Erysipelothrix rhusiopathiae* and *Enterococcus faecalis* as well as *Streptococcus suis* genomes (Gabashvili et al., 2020).

1.4.3 Conjugation

Conjugation was discovered in 1946 by Edward Tatum and Joshua Lederberg, who showed that bacteria could exchange genetic information mediated by a so-called fertility (F) factor (Lederberg and Tatum, 1946; Virolle et al., 2020). It has since been shown that the F factor was a replicative extrachromosomal genetic element, known as a plasmid. Plasmids are DNA molecules capable of replication independent of the bacterial genome, which can be donors or recipients of intracellular exchange. Through conjugation or mobilisation functions they can also be responsible for the intercellular transfer of DNA (Partridge et al., 2018). The process of conjugation begins with cellular interaction during the "mate-seeking" phase, where the conjugative pilus undergoes a dynamic process of extension and retraction. This allows it to locate and pull a potential recipient cell into close proximity with the donor cell. Once a stable mating junction is established, the system seamlessly shifts into the DNA transfer mode, facilitating the exchange of genetic material between the two cells (Hu, Khara and Christie, 2019). Within the donor cell, formation of a complex called the relaxosome assembles at the origin of transfer (*oriT*) of the donor plasmid. Next, the dsDNA is nicked and unwound

to produce single-stranded DNA (ssDNA) which is recruited to the type IV secretion system (T4SS) channel. The ssDNA is then translocated through the T4SS channel, and is then recircularised in the recipient cell, as shown in **Figure 1.7** (Wallden, Rivera-Calzada and Waksman, 2010).

Plasmids were originally classified based on the fact that closely related

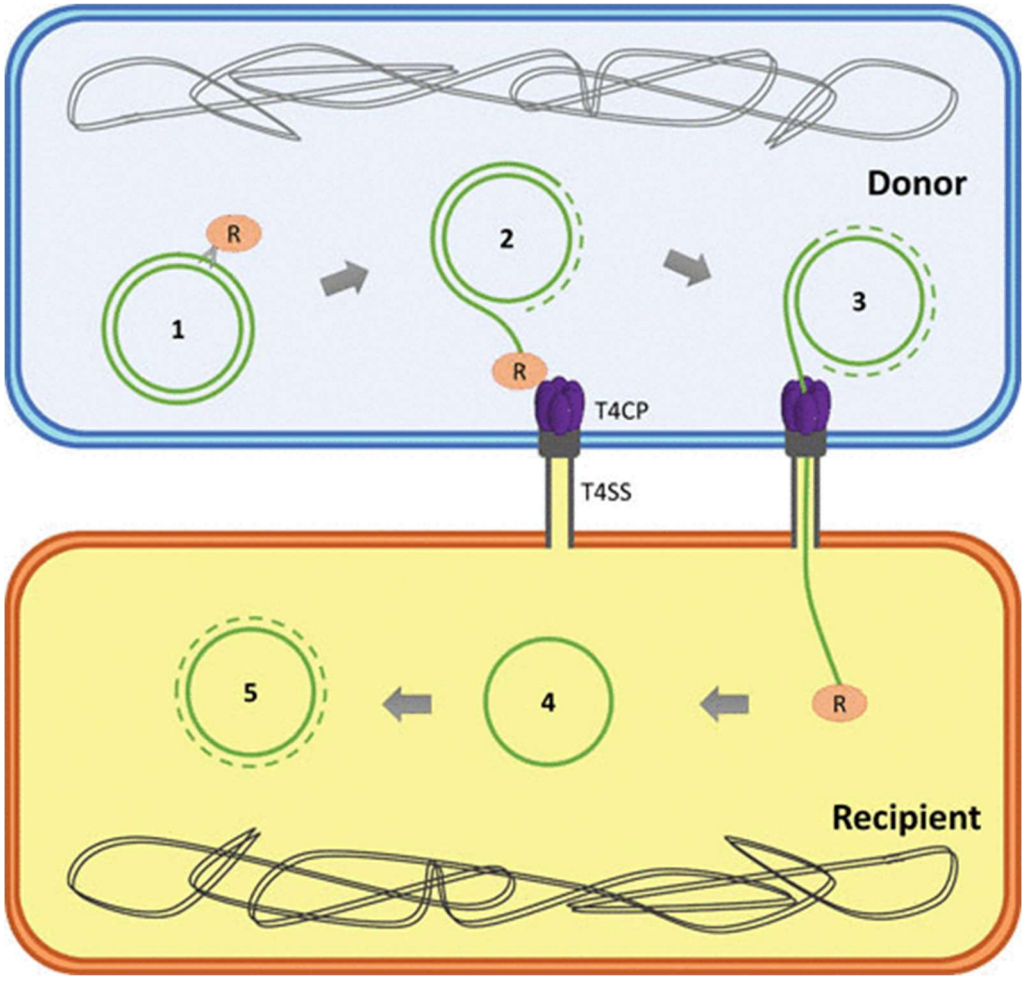

Figure 1.7. Plasmid transfer by conjugation. 1) The relaxase (R) cleaves plasmid DNA and remains covalently bound to the 5' end of the origin of transfer (*oriT*), and DNA relaxation induces the formation of a protein complex called the relaxosome. 2) The Type IV Secretion System (T4SS) protein recruits the relaxosome by interacting with the Type IV Coupling Protein (T4CP), while the plasmid DNA undergoes replication via rolling circle replication (RCR). 3) The leading DNA strand is transferred to the recipient cell through pores formed by the T4SS, facilitated by the T4CP pumping activity. 4) In the recipient cell, the relaxase executes a reverse nicking reaction to recircularise the leading strand. 5) The transferred single-stranded DNA (ssDNA) is then replicated to generate a complete copy of the original plasmid. Republished from Getino and de la Cruz et al. (2018) under Creative Commons CC-BY license.

plasmids cannot stably coexist in the same cell, leading to groupings based on their incompatibility (Inc groups) (Carattoli, 2013). Plasmid incompatibility is defined as the failure of coresident plasmids to be stably inherited in the absence of external selection (Novick, 1987) and occurs when plasmids have the same replication or partitioning system. Most plasmids encode a negative regulation system, such as production of antisense RNAs, which inhibit replication when plasmid copy number is high but allows replication when low. When closely related plasmids in the same cell use similar regulation systems, the same antisense RNAs produced by one plasmid will prevent replication in the other, and vice versa, leading to abnormally low copy number of both plasmids, which leads to plasmid loss over generations. For low copy number plasmids, where random distribution of plasmid copies into daughter cells is not sufficient for guaranteed plasmid inheritance, partition systems are encoded on the plasmids to ensure their retention (Schumacher, 2012). These partition systems rely on plasmid-specific centromere sequences, and when a second plasmid shares an identical centromere, this partitioning process is disrupted, leading to potential plasmid loss over generations (Diaz, Rech and Bouet, 2015).

The IncF, IncI, IncA/C and IncH incompatibility groups are the most common plasmid types found within sequence data from human and animal isolates belonging to the *Enterobacteriaceae* (Rozwandowicz et al., 2018). Although, as Rozwandowicz *et al.* (2018) point out, it is worth noting that large numbers of studies that used whole genome sequencing within the past few years have focused on clinically relevant bacteria, so the plasmid data available to us is

likely biased towards those that encode ARGs. Many plasmids are further classified by plasmid multilocus sequence type schemes (pMLST), such as the IncI1, IncHI2, IncF, IncN and IncA/C groups (Jolley, Bray and Maiden, 2018).

IncF plasmids are low-copy number, conjugative plasmids that range from 45 to 200 kbp. They are considered narrow host range plasmids that are limited to the *Enterobacteriaceae,* and are the most abundant plasmids found in *E. coli* (Rozwandowicz et al., 2018; Pitout and Chen, 2023). Unlike most other plasmid groups, IncF plasmids can contain more than one replicon, and different IncF plasmids can have different functional replicons. This multi-replicon status enables the acquisition of plasmids carrying other IncF replicons that would otherwise be incompatible with each other. The IncF replicons range from FI to FVII, with FI being further subdivided into FIA, FIB and FIC replicons. Additionally, distinct FII replicons exist, each designated by subscripts that denote the genera in which they were initially identified: FII_S (*Salmonella)*, FII_K (*Klebsiella)*, FII_Y (*Yersinia)*, and FII_{Sh} (*Shigella)* (Villa et al., 2010; Partridge et al., 2018). The classic multi-replicon IncF plasmid contains IncFII, IncFIA and IncFIB replicons, and these are the three sequences used for classification in the IncF pMLST scheme (Carattoli et al., 2014; Rozwandowicz et al., 2018).

IncF plasmids are of great importance in the spread of AMR as they have contributed to the spread of MDR *E. coli* clones sequence type (ST) 131 and ST410, which are themselves heavily involved in the global spread of $bla_{CTX\text{-}M\text{-}15}$ and the $bla_{NDM\text{-}5}$ and $bla_{OXA\text{-}181}$ carbapenemases, respectively (Pitout and Chen, 2023). These kind of IncF plasmids have been named “epidemic resistance

plasmids" due to their ability to acquire multiple resistance genes and transfer between strains (Carattoli, 2011; Cantón, González-Alba and Galán, 2012).

1.4.4 Transposable elements

Mobile genetic elements (MGEs) have played a major role in the spread of AMR in Gram-negative bacteria around the globe. MGE is a term used to describe a factor that promotes the intracellular or intercellular exchange of DNA. Intercellular transfer is mostly mediated by plasmids between different bacteria, as described above, while intracellular exchange of DNA commonly occurs between chromosomes and plasmids within cells through the movement of transposable elements (TEs). Insertion sequences (IS) and transposons (Tn) are TEs able to transpose themselves, through the use of a transposase, to other DNA locations somewhat randomly within the cell (Partridge et al., 2018). Insertion sequences are one of the smallest TEs, consisting of a transposase flanked by terminal inverted repeats (IRs) (Chandler and Siguier, 2013). A section of DNA flanked by two copies of the same IS that moves as a discrete unit is often called a compound or composite Tn (Harmer, Pong and Hall, 2020). Insertion sequences such as IS*26* are frequently associated with the formation of multidrug-resistant plasmids (Miriagou et al., 2005).

1.4.4.1 Insertion sequences

The initial definition of an IS was a short, generally phenotypically cryptic, DNA segment encoding only the enzymes essential for transposition, that is capable of insertion into numerous sites within a genome by utilising mechanisms that are independent from DNA homology between the IS and the target site. IS were originally assigned sequential numbers based on the order in which they were discovered, e.g. IS*1*, but now their names also include abbreviations based on the species in which they were discovered, e.g. IS*Kpn26* was discovered in *K. pneumoniae* (Partridge et al., 2018). IS are typically between 0.7-2.5 kbp in length, containing a single open reading frame (ORF) encoding for a transposase (Tnp) and flanked by two inverted repeat (IR) regions (Siguier et al., 2015). These transposase enzymes bind to the IRs and catalyse the mobilisation of the IS to new locations. Insertion sequences are broadly classified into two major types based on the nature of their transposases, those being whether they contain DDE or HUH motifs, which catalyse the cleaving and re-joining of DNA (Siguier et al., 2015).

Insertion sequences with DDE enzymes are the most abundant type found within public databases such as ISFinder (Siguier et al., 2006, 2015). They are so named as the active site of DDE enzymes contains a characteristic motif of three amino acids, two of which are aspartic acids (D), and one which is usually a glutamic acid (E); although sometimes another aspartic acid is found and hence these enzymes are sometimes referred to as DD[E/D] enzymes (Nesmelova and Hackett, 2010). The DDE transposases catalyse cleavage of a single DNA strand, known as the transferred strand, to generate a 3’ OH group

which is then used to attack the phosphodiester bond in the target DNA backbone. However, these enzymes vary in the ways in which the non-transferred strand is processed (Siguier et al., 2015). Some transposases cleave the DNA only at the 3' end, which leads to a branched intermediate with the 3' end bound to the target site and the 5' end attached to the original DNA strand. This intermediate is resolved by DNA replication and results in "copy-in" replicative transposition, where the TE is duplicated, and found at both the donor and target site after transposition. Examples of this type of transposition include Tn*3* and the replicative transposition of the IS*6*-family, and this can be seen in **Figure 1.8A** (Nicolas et al., 2015; Varani et al., 2021). Another major mechanism of DDE transposition is that of the IS*3* family, as shown in **Figure 1.8B**, which has been extensively studied in IS*911* (Hickman and Dyda, 2015). This mechanism involves the 3' OH group attacking the same DNA strand at the other end of the TE, which results in the creation of a ssDNA donor molecule that is replicated to produce a dsDNA TE intermediate, as well as the regeneration of the original DNA strand. As with the previous mechanism, this also results in TE duplication, as one DNA strand is used to create the circular TE intermediate while the other strand is used to regenerate the donor sequence, resulting in two dsDNA IS and known as "copy-out-paste-in" replicative transposition (Siguier et al., 2015).

The other category of DDE transposase mechanisms of action is known as "cut-and-paste" transposition, where the TE is not duplicated, also known as non-replicative transposition. One such mechanism involves the non-transferred strand being cleaved first, several bases within the IS, followed by cleavage of

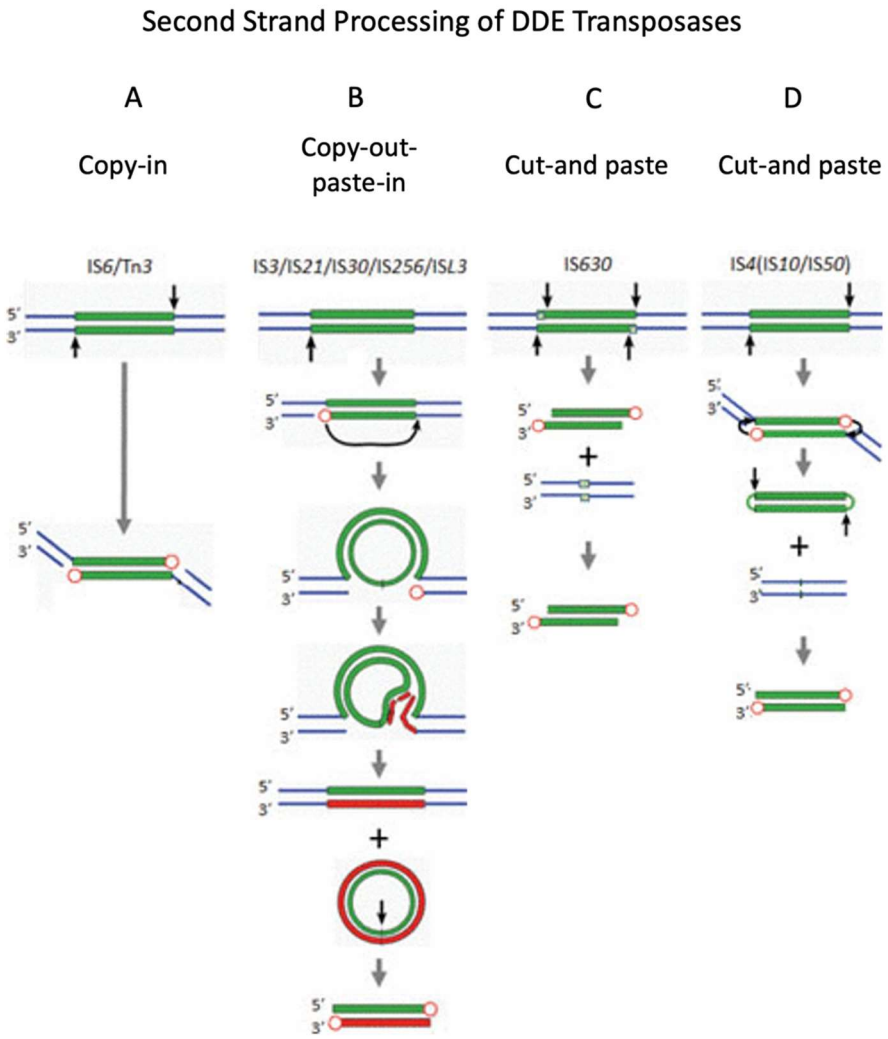

Figure 1.8. DDE transposases of IS families are distinguished by their mechanism of second strand processing. IS are shown as green sections, flanking DNA as blue. Cleavage is shown as bold vertical arrows. 3' OH residues are shown as red circles, replicated DNA is indicated in red. Adapted from Siguier et al. (2015) under Creative Commons CC-BY license.

the transferred strand. This is shown in **Figure 1.8C** and an example of this type of transposition is the action of IS*630* and the prokaryotic Tn Tc1 (Plasterk, 1996; Siguier et al., 2015). Another mechanism involves the 3' OH generated by transferred strand cleavage being used to attack the non-transferred strand to create a hairpin structure which separates the IS from the flanking DNA region, as shown in **Figure 1.8D**. This mechanism is used by the IS*4*-family of IS,

including IS*10* and IS*50*, which mobilise the composite Tns (**§1.4.4.2**) Tn*10* and Tn*5* respectively (Haniford and Ellis, 2015).

In contrast, the HUH enzymes are single-strand nucleases, and include proteins involved in plasmid and bacteriophage rolling-circle replication as well as relaxases involved in plasmid transfer (Chandler et al., 2013). They are named for the two histidine (H) residues separated by a hydrophobic residue at the active site of the enzyme. The IS families that use this kind of transposase include IS*91* and IS*200*/IS*605.* Their mechanism of DNA cleavage uses a tyrosine residue to create a transient 5'- phosphotyrosine intermediate and free 3'-OH at the cleavage site (Chandler et al., 2013; Siguier et al., 2015).

IS are involved in the spread of AMR in a variety of ways. IS transposition can cause truncation/interruption/loss of genes, which can result in resistance to antimicrobials by disruption of repression mechanisms, such as in the case of IS insertion into the repression systems of the Acr family of MDR efflux pumps in *E. coli* and *Salmonella* Typhimurium (Jellen-Ritter and Kern, 2001; Olliver et al., 2005). Experiments have shown that development of cephalosporin and carbapenem resistance can be caused by porin loss due to IS insertion into the *ompK36* gene in *K. pneumoniae* (Hernández-Allés et al., 1999; Lee et al., 2007). Many IS have also been shown to contain -35 and -10 promoter components, and insertion at the correct distance from downstream genes can produce a strong promoter and result in their enhanced expression. IS*Ecp1* has been shown to increase expression of beta-lactamase $bla_{\text{CTX-M}}$ as well as the aminoglycoside resistance gene *rmtC* (Poirel, Decousser and Nordmann, 2003; Wachino et al., 2006).

1.4.4.2 Composite transposons

IS were traditionally defined as TEs that lack phenotypically detectable passenger genes, whereas Tns are TEs that also contain genes that are not responsible for transposition and result in a change in phenotype such as AMR or expression of virulence (Siguier et al., 2015). A distinction is made between unit Tns (**§1.4.4.3**), and composite Tns. The latter are TEs bounded by a pair of the same, or closely related, IS elements that can transpose as a single unit. Either or both of the IS elements can produce the transposase responsible for excision of the composite Tn, while the IR sequences of the IS elements at either flank are used for end recognition (Bennett, 2004). A comparison of IS, composite and unit Tns can be seen in **Figure 1.9**. An example of a composite Tn responsible for the spread of AMR is the aforementioned Tn*5*, which contains a gene conferring resistance to kanamycin between two IS*50* elements that was first discovered in 1974 (Berg et al., 1975). More recently, Tn*125* has been associated with the carbapenemase gene *bla*$_{\text{NDM-1}}$. This Tn contains two copies of IS*Aba125,* and is thought to have been the cause of the mobilisation of *bla*$_{\text{NDM}}$ into the *Enterobacteriaceae* (Bontron, Nordmann and Poirel, 2016).

1.4.4.3 Unit transposons

Unit (also known as complex) Tns are TEs that are not bordered by two IS elements, instead they possess their own transposase gene, as well as a resolvase gene and their own IR sequences for end recognition. Unit Tns that

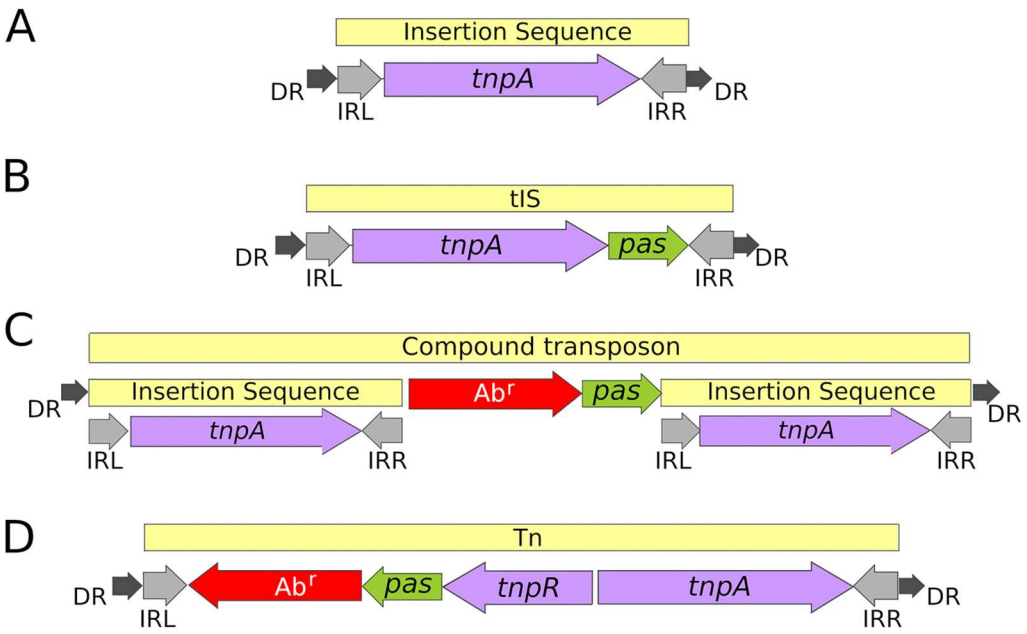

Figure 1.9. Structural arrangement of prokaryotic transposable elements. Genes shown as coloured arrows indicating the direction of expression including transposition genes in purple, antibiotic resistance genes in red and passenger genes in green. The inverted terminal repeats found at the ends of the majority of TEs, IRL and IRR, are shown as grey arrows, and direct target repeats (DR) often produced by insertion are indicated by small black arrows. A) Insertion sequences (IS), composed of a transposase flanked by IRs and generally containing direct repeats of the target site (DR). B) Transporter IS that is similar to IS but also containing passenger gene(s). C) Compound (or composite) transposon formed by two IS genes at either end, which flank passenger genes, often including AMR genes. D) Unit transposons are more heterogeneous structures and include different sets of transposition-related genes that are specific to each transposon family and multiple passenger genes including AMR genes. This specifically is an example of a Tn*3* family transposon. Republished from Ross et al. (2021) under Creative Commons CC-BY license.

are often associated with antimicrobial resistance include Tn*3*, which has been heavily associated with the dissemination of the *bla*$_{TEM}$ beta-lactamases (Partridge and Hall, 2005). Various derivatives of this transposon family are responsible for the spread of other AMR genes including those that confer resistance to macrolides, lincosamides and, streptogramins, as well as aminoglycosides, tetracyclines and vancomycin (Nicolas et al., 2015). The Tn*3*-derivative Tn*21* contains a mercury resistance operon as well as a class 1 integron (**§1.4.5**), that commonly confers resistance to sulphonamides and aminoglycosides (Liebert, Hall and Summers, 1999).

1.4.4.4 Transporter IS

Over the past few years, new TEs have been described that blur the lines between Tns and IS. The transporter insertion sequences, known as tIS, are IS that carry additional open reading frames, such as transcription regulators, methyltransferases and ARGs, and an example is shown in **Figure 1.9** (Siguier, Gagnevin and Chandler, 2009; Siguier et al., 2015). IS*1595* contains a transposase as well as a chloramphenicol resistance gene, which would traditionally define it as a transposon, but it has been classified as a tIS based on sequence similarity to other IS families (Siguier, Gagnevin and Chandler, 2009).

1.4.4.5 Pseudo compound transposons

Pseudo Compound Transposons (PCTs) are TEs that are bounded by directly oriented IS*26*-family elements. They were originally thought to be standard composite Tns, until it was discovered that these structures do not move together as a single unit (Harmer, Pong and Hall, 2020). Instead, "transposition" of these structures occurs via a two-step process, which will be detailed in **§1.4.4.6**.

1.4.4.6 IS*26*

IS*26* is a member of an IS family that was originally named after IS*6,* which was first described in 1975 as the composite transposon Tn*6*. IS*26* was discovered

in 1982, found within the composite transposon Tn*2680* and in 1985, Tn*2680* was shown to be homologous to Tn*6* by restriction digest analysis (Iida et al., 1982; Mollet et al., 1985; Harmer and Hall, 2019). As IS*6* has never been sequenced, while IS*26* has been extensively characterised and is the IS most commonly associated with ARGs in Gram-negative bacteria, it has been suggested that this family be referred to as the IS*6*/IS*26* family (Harmer and Hall, 2019), whilst the description 'IS*26* family' has been used more recently (Harmer, Pong and Hall, 2020). However, a recent review by another research group has continued to use IS*6* family (Varani et al., 2021), which is how the family is still described in the ISFinder database, and the correct nomenclature is still in dispute (Hall, 2022; Varani et al., 2022).

IS*26* is 820 bp in length, while its DDE transposase, Tnp26, is 234 aa in length and encoded by the 705 bp *tnp26* gene. The IS is bounded by 14-bp terminal IRs, and generates 8 bp target site duplications (TSDs) when it mobilises via replicative transposition (Mollet, Iida and Arber, 1985; Pong et al., 2021). The structure of IS*26* can be seen in **Figure 1.10**.

IS*26* is also known to form arrays of multiresistant loci containing numerous IS*26* genes within multidrug resistance plasmids, as shown in **Figure 1.11** (Miriagou et al., 2005; Harmer, Moran and Hall, 2014; Harmer and Hall, 2019; Varani et al., 2021). These arrays, or sections of them, were previously referred to as composite Tns (Harmer, Pong and Hall, 2020), as it was assumed that they mobilised with two IS*26* elements together at either end bracketing a central DNA segment, similar to Tn*5* (Haniford and Ellis, 2015; Harmer, Pong and Hall, 2020).

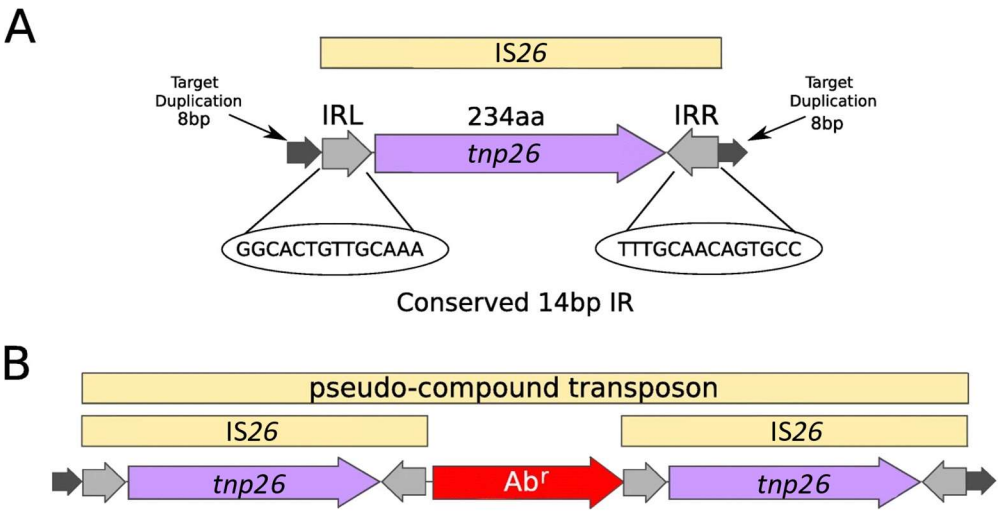

Figure 1.10. The structure of IS*26*. Genes shown as coloured arrows indicating the direction of expression including the transposase gene *tnp26* in purple, and antibiotic resistance gene in red. The inverted terminal repeats, IRL and IRR, are shown as grey arrows, and target duplication produced during replicative transposition shown as dark grey arrows. A) The structure of a single IS*26* element. B) The structure of IS*26* pseudo compound transposons. Adapted from Varani et al. (2021) under Creative Commons CC-BY license.

Mobilisation of IS*26* was first studied in the 1980s, and the IS was shown to form cointegrates between two DNA molecules: a donor containing an IS*26* gene, and a second target molecule (Iida et al., 1984; Harmer and Hall, 2020). This method is replicative, as the IS*26* element is duplicated along with the 8-bp target site, and can be seen in **Figure 1.12A**. Resolution of the cointegrate occurs via RecA-dependent homologous recombination, and the donor and target DNA molecules are separated, while the IS*26* gene appears to have "transposed" to the target molecule (Harmer and Hall, 2020).

It is now known that IS*26* has a second method of mobilisation that is responsible for these arrays of resistance regions. Experiments have shown that when two DNA molecules both contain an IS*26* gene, cointegrate formation can occur between them in a targeted mechanism, where the transposase of one IS*26* targets the other IS*26* element to form the cointegrate.

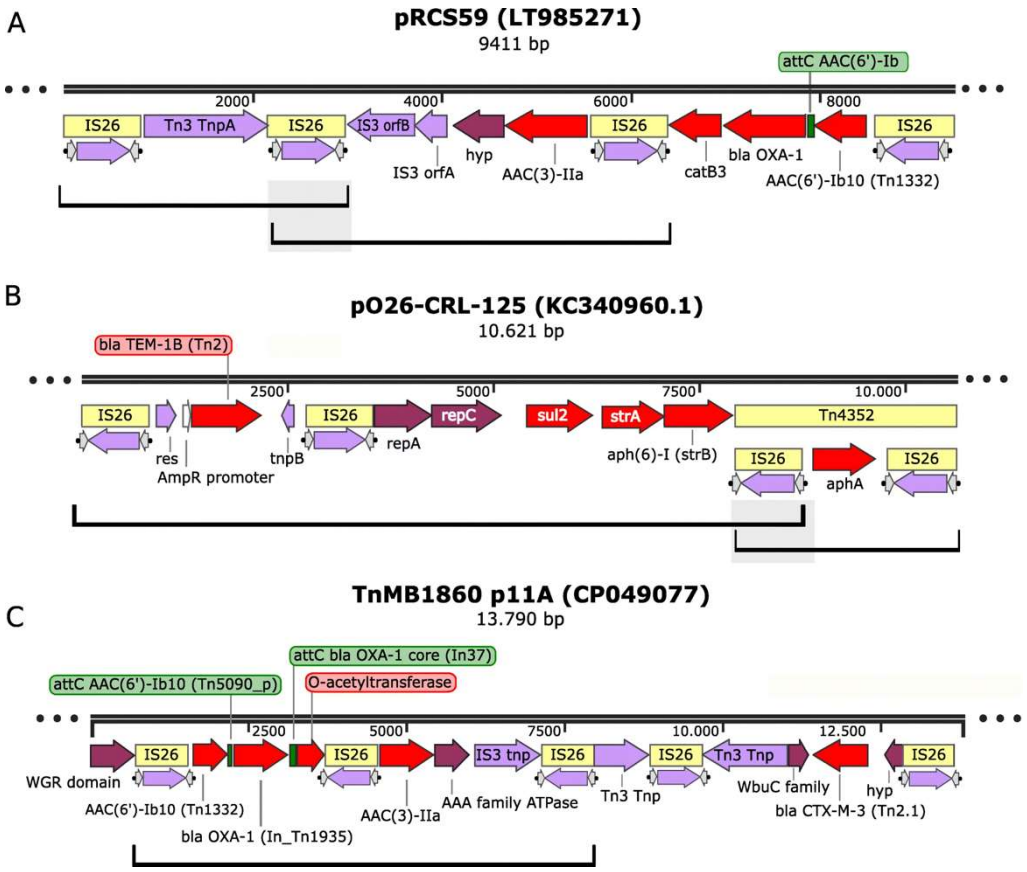

Figure 1.11. Arrays of IS*26* elements in multidrug resistance regions. Genes shown as coloured arrows indicating the direction of expression including transposition genes in purple, antibiotic resistance gene in red, and other genes in maroon. The inverted terminal repeats, IRL and IRR, are shown as grey arrows adjacent to IS*26* elements, and target duplication produced during replicative transposition shown as black circles. Grey boxes show overlapping IS*26* elements between pseudo-compound transposons (PCT). A) Array of IS*26* genes in plasmid pRCS59, horizontal bracket shows region forming two potential overlapping PCTs. B) Array of IS*26* genes in plasmid pO26-CRL-125, horizontal bracket shows region forming two potential overlapping PCTs. C) Array of IS*26* genes in MDR chromosomal region of Sequence Type (ST) 131 isolate that was transferred to plasmid p11A; horizontal bracket showing two inversely oriented IS*26* elements that will not form a PCT. Republished from Varani et al. (2021) under Creative Commons CC-BY license.

Additionally, cointegrate formation is conservative (non-replicative), as shown in **Figure 1.12B**, and occurs at a rate of over 50 times greater than the replicative mechanism, making it the preferred method of movement if an IS*26* gene is present on the target molecule (Harmer, Moran and Hall, 2014; Harmer and Hall, 2016). The arrays of IS*26*-ARG-IS*26* regions seen above are a result of cointegrate formation of different IS*26* containing molecules. Furthermore,

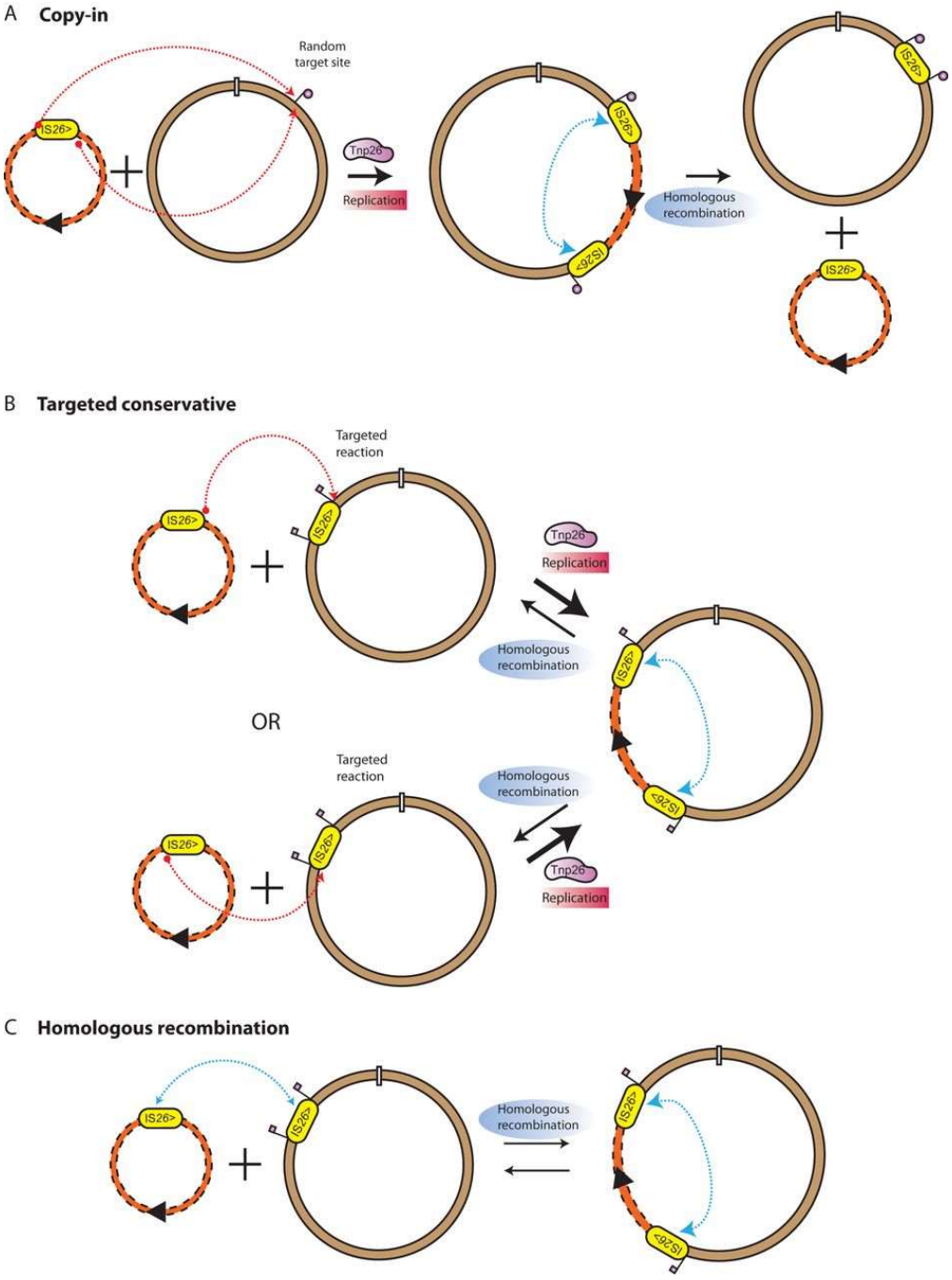

Figure 1.12. The three mechanisms of cointegrate formation of IS*26*. A) Copy-in method. B) Targeted conservative method. C) Homologous recombination. IS*26* elements are shown in yellow ovals with orientation indicated by ">". Target site and subsequent duplications are shown by flags. Relative frequencies of the different reactions are shown by the thickness of the arrows. Republished from Harmer and Hall (2020) under Creative Commons CC-BY license.

sections of these arrays found between two directly oriented IS*26* genes can excise, via homologous recombination, to form a DNA molecule containing a single IS*26* and the central DNA segment found between two adjacent IS*26* genes, and this circular molecule is known as a Translocatable Unit (TU) (Harmer, Moran and Hall, 2014; Harmer and Hall, 2016). As TUs contain an IS*26,* they will preferentially insert adjacent to other IS*26* genes, which leads to the formation of these arrays of IS*26*-flanked sequences, and means that once a DNA molecule contains IS*26,* it is predisposed to acquire further IS*26* TUs adjacent to this region (Harmer, Moran and Hall, 2014; Harmer, Pong and Hall, 2020). As these TUs are formed by an IS*26*-flanked region, but only a single IS*26* mobilises with the excised DNA, they are referred to as Pseudo Compound Transposons (PCT) (Harmer, Pong and Hall, 2020).

The mechanism of IS*26* mobility has been shown to form cointegrates between large plasmids, creating new fusion plasmids such as the MDR IncHI2 with the IncF virulence plasmid in *Salmonella* Enteritidis (Wong, Chan and Chen, 2017); formation of the carbapenemase-producing, fosfomycin and aminoglycoside resistance plasmid PT18 in *Proteus mirabilis* (Hua et al., 2020); and a virulence plasmid and carbapenemase-producing plasmid in *K. pneumoniae* (Tian et al., 2023). IS*26* is also responsible for inversions of large DNA segments in MDR plasmids, due to replicative transposition and cointegrate formation within the same DNA molecule. Resolution of cointegrates that are formed by inversely oriented IS*26* genes results in inversion of the bracketed DNA segment (He et al., 2015; Harmer, Pong and Hall, 2020; Li et al., 2023). Direct evidence of PCT transfer between a bacterial chromosome and conjugative plasmid has been

shown by Oliva et al*.,* (2018), where the 8.7 kbp and 14.5 kbp PCTs found on a *Salmonella* chromosome were detected on the IncFII plasmid of a transconjugant, formed via the targeted conservative mechanism of IS*26.*

1.4.5 Integrons

Integrons are genetic elements that contain a site-specific recombination system able to integrate, express and exchange specific DNA elements, called gene cassettes. Integrons consist of three elements: a tyrosine recombinase gene known as an integrase, encoded by *intI,* which is responsible for recombination within the integron; the recombination site *attI*, recognised by the integrase; and a promoter, located upstream of the integration site, necessary for expression of the gene cassettes (Domingues, da Silva and Nielsen, 2012). Integrons were originally discovered in the late 1980s, and were thought to be MGEs themselves, but their supposed mobility was due to the fact that the first integrons to be characterised were discovered within transposons (Mazel, 2006). Integrons are classified into 5 groups, based on the relatedness of their integrase genes, of which classes 1-3 have been most extensively studied due to their association with MDR bacteria (Mazel, 2006; Domingues, da Silva and Nielsen, 2012). Of these, the class one integrons are the most abundant amongst clinical isolates, due to their association with a wide variety of MGEs (Deng et al., 2015). Usually, class one integrons have three distinct genetic regions, two of which are highly conserved and flank the third central variable region where cassettes are located. The 5'-conserved

region includes the integrase gene *intI1*, the recombination site *attI1*, and the promoter P_c. The 3'-conserved region contains the *qacE*Δ1 gene, which encodes an incomplete version of a protein responsible for resistance to disinfectants such as quaternary ammonium compounds (QACs); the *sul1* gene, which encodes for sulphonamide resistance; and *orf5,* an open reading frame of unknown function (Domingues, da Silva and Nielsen, 2012). A wide variety of other gene cassettes have been discovered on integrons, including those that confer resistance to beta-lactams, aminoglycosides, lincosamides, phenicols and fluoroquinolones (Partridge et al., 2009, Partridge et al. 2018). An increasing number of class 1 integrons are associated with Insertion Sequences with a Common Region (IS*CR*), and known as IS*CR*-linked or "complex" class 1 integrons (Toleman, Bennett and Walsh, 2006a; Domingues, da Silva and Nielsen, 2012). IS*CR* elements resemble the unusual insertion sequence IS*91,* in that they lack IRs, and are thought to transpose using rolling-circle replication (termed rolling-circle transposition), and are sometimes referred to as IS*91*-like elements (Toleman, Bennett and Walsh, 2006b).

1.4.6 Co-selection

Co-occurrence is the phenomenon in which bacteria carry genes conferring resistance to different antimicrobials within the same bacterial isolate or population. Co-occurrence may refer to the presence of multiple genes that confer resistance to the same or different type of antimicrobial, such as antibiotics, antimicrobial metals or biocides. Co-selection is a term used when

selection for one type of resistance will lead to preservation of these other co-occurring resistances alongside the mechanism under selection. This can be due to cross-resistance, which is caused by selection for a single resistance mechanism that confers resistance to multiple antimicrobials, or co-resistance, where genes conferring resistance to different antimicrobials are located together on MGEs such as a plasmid, transposon or integron (Chapman, 2003; Hobman, 2017). Examples of cross-resistance include the AcrAB-TolC MDR efflux pump of the *Enterobacteriaceae*, which can confer resistance to a broad range of molecules that are toxic to the cell such as macrolides, beta-lactams, aminocoumarins, rifamycins, quinolones, oxazolidones, and tetracyclines (Kobylka et al., 2020). Another example is the *aac(6')-Ib-cr* variant of the AAC family, which is capable of acetylating both aminoglycosides and fluoroquinolones (Vetting et al., 2008). Co-resistance is frequently linked with integrons because of their diverse gene cassettes that provide resistance to multiple antibiotic classes. Moreover, these integrons are commonly situated on the same MGEs as genes conferring resistance not only to other antibiotics but also to antimicrobial metals (Gillings et al., 2015). The transposon Tn*21* contains ARGs on an integron alongside a mercury resistance operon, and so selection for these antimicrobials can lead to co-selection of mercury resistance, and vice versa (Liebert, Hall and Summers, 1999; Pal et al., 2017). The ability of MGEs to confer resistance to multiple antibiotic classes, as well as biocides and antimicrobial metals, is a major factor in the rising levels of multidrug resistant bacteria (MDR) seen all over the world. This is of major importance, not only because MDR infections are associated with higher levels

of morbidity and mortality, but treatment options become severely limited (Schultsz and Geerlings, 2012).

1.5 History of beta-lactams and beta-lactamases

Of all the antibiotic classes used from the beginning of the 'antibiotic era' to the modern day, by far the most widely used in the treatment of bacterial infections are the beta-lactams (Bush and Bradford, 2016). Famously discovered by Alexander Fleming in 1928, it wasn't until the 1940s that penicillin could be produced in large enough quantities to be reliably used as an antibiotic (Gaynes, 2017). Within a year, 4 strains of *Staphylococcus* were found in hospitalised patients that were resistant to penicillin (Rammelkamp and Maxon, 1942; Lobanovska and Pilla, 2017) and by the end of the 1960s, resistance to penicillin was found in over 80% of staphylococcal isolates from both community-acquired and hospital-acquired infections (Lowy, 2003). This prompted the search for new antibiotics in order to treat these resistant infections, leading to a cycle of antibiotic discovery and ever-increasing levels of AMR.

In the decades that followed the production of penicillin, synthesised modifications to the side chain of the beta-lactam ring were used to develop various semi-synthetic penicillin derivatives in order to generate a wider spectrum of activity (Kong, Schneper and Mathee, 2010). Alongside this, widespread screening of environmental organisms led to the discovery of entirely new classes of antibiotics, as well as many novel beta-lactams. The

discovery of penicillinase-resistant cephalosporin C, from the fungus *Cephalosporium acremonium* (Abraham and Newton, 1961), led to the development of hundreds of new cephalosporin antibiotics to treat bacterial infections (Bush and Bradford, 2016). The fact that cephalosporins were resistant to common penicillinases made them ideal for treatment of the most clinically relevant penicillinase-producing bacteria of the time, *St. aureus.* They were also found to be effective against streptococcal infections as well as non-beta-lactamase-producing Gram-negative bacteria (Bush and Bradford, 2016).

The first penicillinase was described over 80 years ago, found in *Escherichia* (then *Bacillus) coli* by Abraham and Chain (Abraham and Chain, 1940). However, it was not thought to be clinically relevant at the time since penicillin was used to treat Gram-positive infections (Drawz and Bonomo, 2010). The first plasmid-mediated beta-lactamase in Gram-negative bacteria was discovered in the 1960s, isolated from an *E. coli* bloodstream infection in a patient named Temoniera, leading to the designation TEM (Bradford, 2001). As this enzyme began to appear in other bacterial species, especially *Haemophilus influenzae* and *Neisseria gonorrhoeae*, this led to increased efforts in research to find compounds that could either inhibit, or were resistant to, degradation by beta-lactamases (Bush and Bradford, 2016; Bush, 2018). This led to the development of second and third-generation cephalosporins, that were stable against this enzyme, and with greater activity against the Gram-negative bacteria likely to carry it (Bush and Bradford, 2016), as shown in **Figure 1.13**.

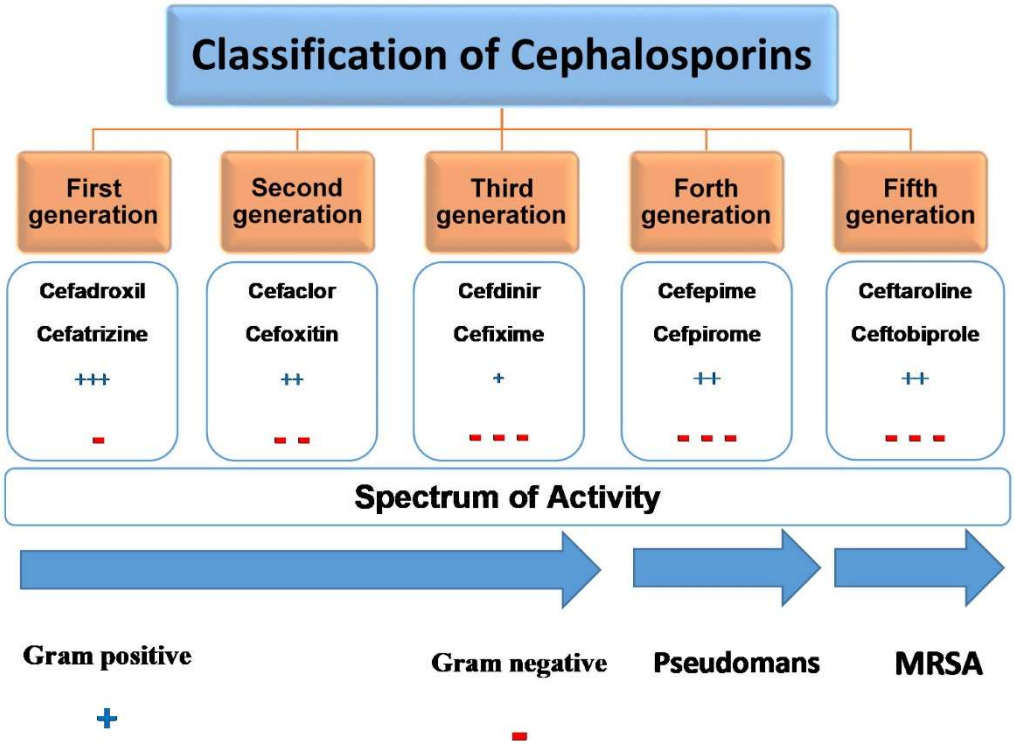

Figure 1.13. Classification of different generations of cephalosporins. First-generation cephalosporins are active mostly against Gram-positive bacteria. Second/third-generation are more active against Gram-negative bacteria. Fourth-generation drugs have increased activity against *Pseudomonas* infections, while fifth-generation cephalosporins have increased activity against methicillin-resistant *Staphylococcus aureus* (MRSA). Republished from Zaid Alkilani et al., (2024) under Creative Commons CC-BY license.

Unfortunately, with as little as 3 amino acid substitutions, the TEM-1 penicillinase is capable of hydrolysing these broad spectrum cephalosporins (Sougakoff, Goussard and Courvalin, 1988). This new enzyme was named TEM-3, and was the first extended-spectrum beta-lactamase (ESBL) to be discovered (Bradford, 2001). These enzymes are usually found on MGEs and are characterised by their ability to hydrolyse the oxyimino-cephalosporins (third and fourth-generation cephalosporins) as well as monobactams (Cantón, González-Alba and Galán, 2012).

As the number of clinically relevant beta-lactamases increased during the 1960s and 70s, the need for a way to combat these enzymes became ever more important (Drawz and Bonomo, 2010; Papp-Wallace et al., 2011). Since the actinomycetes were (and still are) the largest known producer of natural antimicrobial compounds, vast amounts of these bacteria were grown in fermentation broths and screened for the production of useful compounds (Watve et al., 2001). In 1976, the compounds olivanic acid and clavulanic acid were isolated from *Streptomyces olivaceus* and *S. clavuligerus* respectively; these were the first beta-lactamase inhibitors (Brown et al., 1976). Around the same time, the first of the carbapenems, a compound named thienamycin, was isolated from *S. cattleya* during soil-screening for antibiotics that inhibit the synthesis of the bacterial cell wall. This was found to have a broad spectrum of antibiotic activity and was not inhibited by the presence of many beta-lactamases that usually conferred resistance to earlier penicillins and cephalosporins (Kahan et al., 1979).

Thienamycin was found to be very chemically unstable in solution, and so could not be used in concentrations necessary to have an antimicrobial effect *in vivo* (Kahan et al., 1983; Papp-Wallace et al., 2011). This led to the development of synthetic derivatives of thienamycin, firstly the *N*-formimidoyl derivative imipenem. Imipenem was shown to be chemically stable, however it was inactivated by the enzyme dehydropeptidase-I (DHP-I) found in the human renal brush border (Kropp et al., 1982). For imipenem to be clinically useful it was found it must be administered with the DHP-I inhibitor cilastatin (Norrby et al., 1983). The development of later carbapenems led to the addition of a

methyl group that confers resistance to DHP-I, which removes the need for co-administration with cilastatin (Zhanel et al., 1998). Further changes to the chemical side chain have resulted in the later clinically available carbapenems such as meropenem and ertapenem. These changes in the side chain of meropenem are also shown to increase its activity against Gram-negative bacteria (Zhanel et al., 2007). The structure of the carbapenems can be seen in **Figure 1.14**.

As rising resistance to penicillins led to a wider use of cephalosporins, so increased levels of cephalosporin resistance led to wider use of carbapenems (McLaughlin et al., 2013). As ever, the increase in clinical use has been swiftly followed by an increase in resistance (Papp-Wallace et al., 2011).

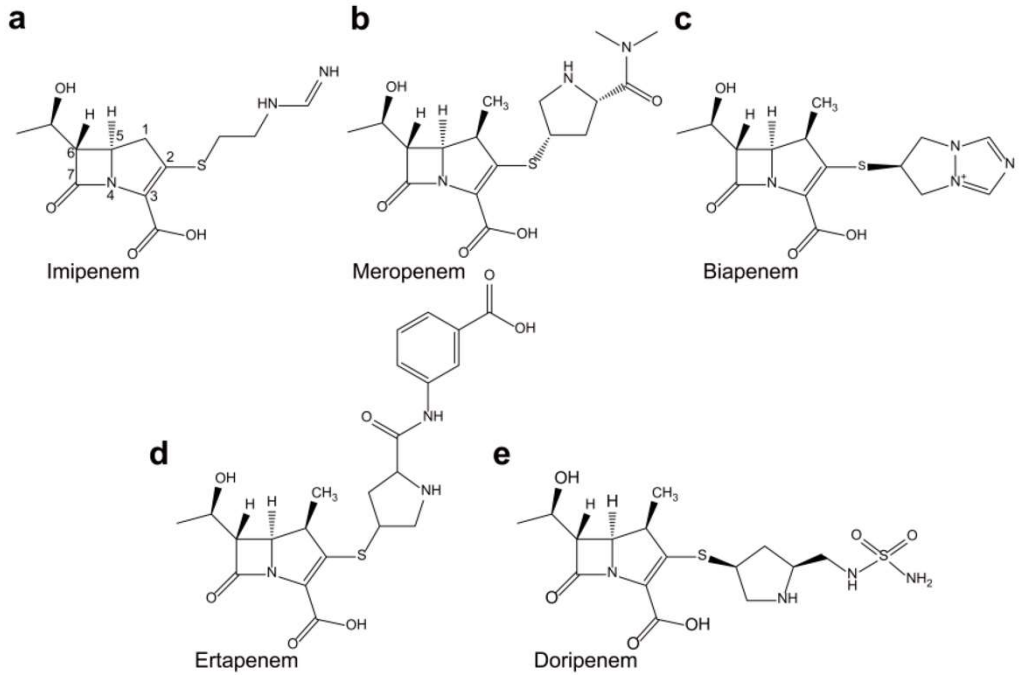

Figure 1.14. Chemical structures of (a) imipenem; (b) meropenem; (c) biapenem; (d) ertapenem; and (e) doripenem. The beta-lactam nucleus is numbered. The addition of the methyl group at position 1 prevents the inactivation of later carbapenems by **d**e**h**ydro**p**eptidase-I (DHP-I). Republished from Jeon et al. (2015) under Creative Commons CC-BY license.

The first identified transferrable carbapenemase was IMP-1 (named for Imipenem-resistant *Pseudomonas*), found in Japan in 1988, followed by VIM in Italy in 1996 (Verona Integron-encoded Metallo-beta-lactamase) (Meletis, 2016). Also in 1996, *Klebsiella pneumoniae* carbapenemase (KPC) was detected in the USA (Yigit et al., 2001), and in 2008, the New Delhi Metallo-beta-lactamase (NDM) enzyme was discovered in a patient in Sweden (Yong et al., 2009).

1.5.1 Extended spectrum beta-lactamases

Surveillance studies in the 1970s found that an average of 63% of all ampicillin-resistant bacteria contained one of either the TEM-1 or TEM-2 penicillinases (Bush, 2018). Throughout the 1980s and 1990s, after the introduction of the oxyimino-cephalosporins, the most common ESBLs were enzymes descended from these TEM penicillinases, as well as the SHV enzymes (Bradford, 2001; Bush, 2018). Like the TEM enzymes, the SHV ESBLs (named for **S**ulf**h**ydryl reagent **V**ariable) are derivatives of the penicillinase SHV-1, with the ESBL SHV-2 differing by only a single aa (Liakopoulos, Mevius and Ceccarelli, 2016; Castanheira, Simner and Bradford, 2021). Another class of beta-lactamases, the OXA enzymes, were named for their greater levels of activity against Oxacillin. In 1991, the first example of an ESBL of the OXA class, OXA-11, was discovered in a *P. aeruginosa* isolate. It was found to be transferable, and differed from OXA-10 by only 2 aa (Evans and Amyes, 2014).

However, the landscape of ESBLs changed dramatically in the 1990s with the rise of the CTX-M enzymes. Initially found in *E. coli* in Munich in 1989, CTX-M-1 was named for its preferential hydrolytic activity against cefotaxime (CTX, and M for Munich) (Cantón, González-Alba and Galán, 2012). Almost at the same time, this enzyme was isolated in France under the name MEN-1, and a related beta-lactamase, named CTX-M-2, was isolated from *Salmonella* Typhimurium in Argentina (Bauernfeind et al., 1996).

During the late 1990s, new CTX-M enzymes were detected spreading quickly throughout the globe. In 1996, CTX-M-3 was detected in Poland, followed by France in 1998 and Taiwan in 1999 (Cantón, González-Alba and Galán, 2012). Another example of this rapid dissemination is CTX-M-9, initially found in Spain and Brazil in 1996, it was then identified in China the following year. Evidence from these countries showed that CTX-M enzymes soon became prevalent in areas previously dominated by TEM and SHV ESBLs (Cantón, González-Alba and Galán, 2012). This was especially true of the CTX-M-15 enzyme, which has become dominant in most regions of the world (Cantón, González-Alba and Galán, 2012; Bevan, Jones and Hawkey, 2017), and by 2004 was found in approximately 90% of ESBL-producing bacteria referred to the UK Antibiotic Resistance Monitoring and Reference Laboratory (Livermore, 2012). Exceptions include China, South-East Asia and Spain, where CTX-M-14 is often dominant; and South America, where CTX-M-2 is prevalent. However, data appear to show that although the displacement of other CTX-M enzymes by CTX-M-15 is slower compared to displacement of TEM and SHV ESBLs, levels of

CTX-M-15 are increasing in both Spain and South America (Cantón, González-Alba and Galán, 2012).

It has now been demonstrated that these enzymes are highly related to chromosomal ESBLs found in various *Kluyvera* spp. (Bevan, Jones and Hawkey, 2017). CTX-M-2 is identical to the ESBL found in *Klu. ascorbata* (Di Conza et al., 2002), while CTX-M-14 is identical to an enzyme found in *Klu. georgiana* isolated in Guyana (Olson et al., 2005). It is highly likely that insertion sequences, such as the IS*Ecp*1 element frequently found upstream of CTX-M-14 and CTX-M-15, played a major role in their spread from chromosomal to plasmid-mediated enzymes (Bevan, Jones and Hawkey, 2017).

1.5.2 Carbapenemases

Carbapenemases are the current pinnacle of beta-lactamase evolution, as the spectrum of activity of these enzymes includes nearly all hydrolysable beta-lactams (Queenan and Bush, 2007). They belong to two major families that differ by the hydrolytic mechanism at their active site. The first carbapenemase to be discovered was produced by a *Bacillus cereus* mutant 569/H/9, whose ancestral strain was first isolated in the 1950s, decades before the discovery of thienamycin (Kuwabara, 1970; Davies, Abraham and Melling, 1974; Davies, 1975). This, and other enzymes also isolated from *Bacillus* spp. in the early 1980s, differed from previously known beta-lactamases at the time as they were found to be inhibited by ethylenediaminetetraacetic acid (EDTA), which established them as metallo-beta-lactamases (MBL) (Carfi et al., 1995; Halat

and Moubareck, 2020). Many carbapenemases studied around the same time were also chromosomally-encoded MBLs found in opportunistic pathogens such as *Aeromonas hydrophila* and *Stenotrophomonas maltophilia* (Saino et al., 1982; Iaconis and Sanders, 1990). These enzymes require at least one zinc ion at the active site that facilitates hydrolysis of the beta-lactam ring (Palzkill, 2013). They are contrasted with the more common serine beta-lactamases, which contain a serine residue at the active site, as shown in **Figure 1.15**, and are inhibited by beta-lactamase inhibitors such as clavulanic acid and tazobactam (Queenan and Bush, 2007). In the early 1980s, the serine-carbapenemase *Serratia marcescens* enzyme (SME) was discovered in a *Serratia marcescens* strain first isolated in 1982 (Yang, Wu and Livermore, 1990). Shortly afterwards, the imipenem-hydrolysing-beta-lactamase (IMI) was

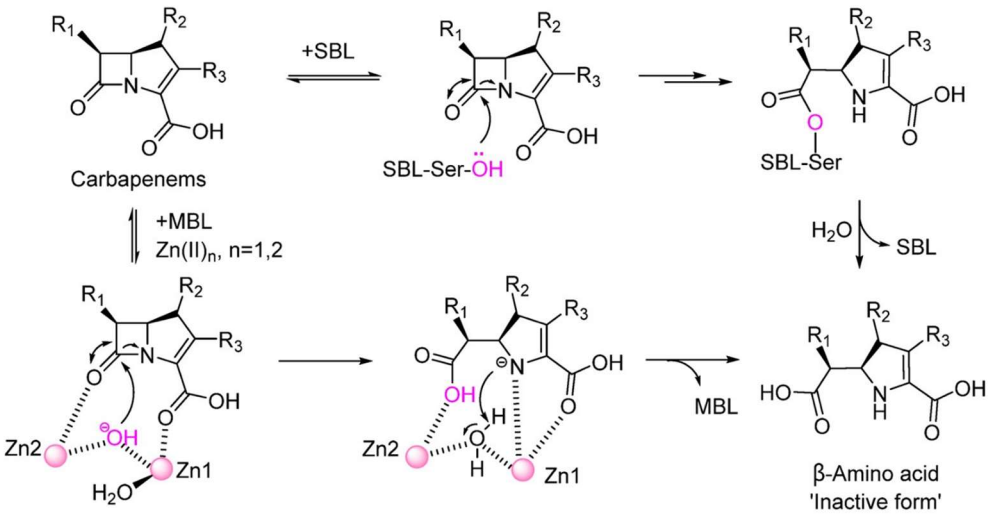

Figure 1.15. Mechanisms for Metallo-Beta-Lactamases (MBL) and Serine-Beta-Lactamases (SBL) catalysed hydrolysis of carbapenems. The top-right shows the serine residue covalently bonded to the broken beta-lactam ring, whereas MBLs bind through electrostatic interactions, shown bottom left by dashed lines. Republished with permission from Wang et al. (2019). Copyright 2019 American Chemical Society.

found in *Ent. cloacae* in 1984 (Rasmussen et al., 1996). Notably, all these carbapenemases were isolated before the clinical introduction of imipenem in 1985. At this time, the spread of carbapenem resistance was limited to clonal expansion, as all the previously described enzymes were chromosomally encoded (Queenan and Bush, 2007). This would change with the discovery and dissemination of the so-called "big five" carbapenemases: IMP, VIM, KPC, NDM and OXA-48-like (Hopkins et al., 2022).

1.5.2.1 The first transferrable imipenemase

In 1988 the first transferable carbapenemase was discovered in Japan. Known as imipenemase (IMP), this was identified as an MBL harboured on a conjugative plasmid in a *P. aeruginosa* isolate (Watanabe et al., 1991). Shortly afterwards, this enzyme spread into the *Enterobacteriaceae* in Japan and was first isolated in Europe from an *A. baumannii* strain in Italy in 1997 (Senda et al., 1996; Cornaglia et al., 1999). Around the same time, the Verona integron-encoded MBL (VIM) enzyme was spreading amongst *P. aeruginosa* isolates in Europe, and was subsequently detected in *Enterobacteriaceae* isolates in the early 2000s (Queenan and Bush, 2007). Although these MBLs were distributed across the world in the mid 2000s, reports of outbreaks tended to be small, restricted in duration and geographic location (Queenan and Bush, 2007; Halat and Moubareck, 2020).

1.5.2.2 Klebsiella pneumoniae carbapenemase

The first *Klebsiella pneumoniae* carbapenemase (KPC) enzyme was isolated in the US in 1996 (Yigit et al., 2001). A serine carbapenemase, KPC is capable of hydrolysing all beta-lactams and is often carried on MGEs such as Tn*4401* and a variety of plasmids (Hansen, 2021). Similarities to the spread of the CTX-M enzymes can be seen in the dissemination of the KPC beta-lactamases. They are strongly associated with a particular sequence type of *K. pneumoniae*, ST258, an MDR isolate which was previously responsible for over three-quarters of all outbreaks of KPC-producing *K. pneumoniae* in the US (Kitchel et al., 2009; Chen et al., 2014). Since their discovery there, KPC producers have spread globally and are now endemic in parts of South America and China, as well as Greece, Italy, and Poland (Baraniak et al., 2011; Nordmann, Naas and Poirel, 2011; Munoz-Price et al., 2013). From there, KPC enzymes have been detected nearly everywhere in Europe (Munoz-Price et al., 2013).

1.5.2.3 New Delhi Metallo-beta-lactamase

In contrast to the mostly clonal dissemination of KPC, the New Delhi Metallo-beta-lactamase (NDM) carbapenemase has been associated with many different sequence types in both *E. coli* and *K. pneumoniae*, none of which appear as predominantly as ST131 or ST258 (Wu et al., 2019). In 2008 the first case of *K. pneumoniae* with NDM-1 was found in a Swedish patient who had recently returned from India (Yong et al., 2009). This was of particular concern because the plasmid on which this gene was transmitted also conferred

resistance to aminoglycosides, macrolides, rifampicin, sulfamethoxazole and aztreonam (a monobactam not usually hydrolysed by NDM) (Walsh, 2010). Unlike the previously described carbapenemases, the dissemination of NDM after its initial detection was dramatic in its rapidity. By 2011, just 3 years after its discovery, NDM had been isolated from patients with direct links to the Indian subcontinent in Australia, Austria, Belgium, Canada, Finland, France, Germany, Ireland, Italy, Hong Kong, Japan, Kuwait, the Netherlands, New Zealand, Norway, Oman, Singapore, Spain, Switzerland, Taiwan, the UK and the USA (Johnson and Woodford, 2013). Also of note, within that time, NDM had spread to *C. freundii, Ent. cloacae, E. coli, Morganella morganii, Proteus mirabilis, Providencia rettgeri* and *Salmonella* spp. A retrospective investigation into Carbapenemase-Producing *Enterobacteriaceae* (CPE) isolated from Indian hospitals in 2006-2007 found *Ent. cloacae, E. coli* and *K. pneumoniae* isolates that harboured NDM in New Delhi, predating the original finding in Sweden (Castanheira et al., 2011). A contributing factor to this rapid global dissemination may have been the community spread of NDM within India, which, alongside global travel, facilitated the distribution of NDM. A 2010 analysis of environmental water samples detected $bla_{\text{NDM-1}}$ by polymerase chain reaction (PCR) in 51/171 samples in New Delhi, while NDM-producing bacteria were cultured from 2 drinking-water samples in the same study (Walsh et al., 2011). This clearly showed that the problem of NDM was not confined to nosocomial outbreaks, as had been the case for previous carbapenemases (Johnson and Woodford, 2013).

1.5.2.3.1 NDM variants

As of 2017, 17 variants of NDM had been isolated (Khan, Maryam and Zarrilli, 2017); the Beta-Lactam Database (BLDB) shows that number is now up to 61 (Naas et al., 2017), and the spread of these genes can be seen all across the globe (Walsh, 2010). The NDM enzyme is a 270 aa protein that contains 2 zinc ions at its active site which is responsible for hydrolysis of beta-lactams. NDM variants commonly contain between 1 and 5 aa substitutions compared to NDM-1 (Wu et al., 2019). The most common aa substitution is M154L, which is found in the single mutant NDM-4, as well in double mutants such as NDM-5. This mutation has been shown to increase affinity for zinc ions, which leads to enhanced carbapenemase activity under conditions of zinc-deprivation, such as might occur during infection (Bahr et al., 2017). It has also been reported that variants containing the V88L substitution, such as NDM-5, exhibit enhanced carbapenemase activity through an unknown mechanism (Hornsey, Phee and Wareham, 2011; Wu et al., 2019).

1.5.2.3.2 Genetic context of *bla*$_{NDM}$

The genetic contexts of all known *bla*$_{NDM}$ sequences share two common features. An intact or truncated insertion sequence, IS*Aba125,* is almost always found upstream, and this provides the -35 region of a promoter for *bla*$_{NDM}$; while a bleomycin resistance gene, *ble*$_{MBL}$, is always found downstream (Poirel, Bonnin and Nordmann, 2011a; Partridge and Iredell, 2012; Wu et al., 2019). Further downstream of *ble*$_{MBL}$, there is often a complete or remnant set of genes, including *trpF*, *dsbD* (also referred to as *dsbC* or *tat*), *cutA1* and *groES*-

groEL (Wu et al., 2019). Previous examination of the *bla*$_{NDM}$ gene revealed the first 19 bp sequence is identical to that of the aminoglycoside resistance gene *aphA6.* This showed *bla*$_{NDM}$ is actually a chimeric gene, formed by the fusion of an unknown metallo-beta-lactamase and *aphA6* (Toleman et al., 2012). It is thought that this unknown MBL was mobilised along with the *ble*$_{MBL}$ to the *groES-groEL* region of the chromosome by a downstream IS*CR*27 in *Acinetobacter* (Toleman et al., 2012; Wu et al., 2019). This likely inserted downstream of IS*Aba125* and *aphA6*, which then fused with the MBL to create *bla*$_{NDM}$ and this whole genetic region (Poirel et al., 2012; Toleman et al., 2012). At some point, this sequence transposed upstream of another IS*Aba125* element, which then formed the composite transposon Tn*125* (Partridge and Iredell, 2012; Poirel et al., 2012). This composite transposon is the source of the mobilisation of *bla*$_{NDM}$ into the *Enterobacteriaceae* and can be seen in **Figure 1.16**. From there, this element has been interrupted or truncated by a variety of mobile elements, leading to a variety of complex genetic contexts surrounding *bla*$_{NDM}$ (Wu et al., 2019). In an analysis of over 2000 genomes, Acman et al. found that the more ancestral sequence containing a complete Tn*125* is now almost exclusively found in *Acinetobacter* and *Klebsiella* (Acman et al., 2022).

1.5.2.4 OXA-48-like carbapenemases

The enzyme OXA-48 was first discovered in a *K. pneumoniae* isolate from Turkey in 2001. Although other members of the OXA family are capable of low

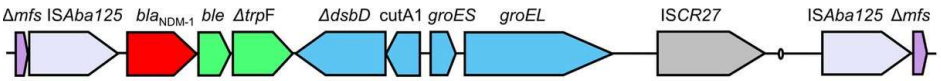

Figure 1.16. Structure of Tn*125.* This composite transposon is formed by two directly oriented IS*Aba125* elements and is believed to be responsible for the mobilisation of *bla*$_{NDM}$ into the *Enterobacteriaceae*. Republished with permission from Jones et al. (2014). Copyright 2014, American Society for Microbiology.

levels of carbapenem hydrolysis, the OXA-48 enzyme was capable of hydrolysing carbapenems at higher rates. However, carriage of OXA-48 alone results in only modest increases in MIC to carbapenems, though when combined with other resistance mechanisms such as porin-loss it can lead to significant levels of carbapenem resistance (Halat and Moubareck, 2020). Sequence analysis showed that OXA-48 shared only 46% aa identity with the ESBL OXA-10, and only 36% aa identity with the weak-carbapenemase OXA-23 (Poirel et al., 2004). Later studies showed that *Shewanella oneidensis*, a waterborne environmental bacterium, harboured the OXA-48 enzyme, while OXA-48-like derivatives OXA-181 and OXA-204 have also been found in the same genus (Mairi et al., 2018). This shows the OXA-48-like enzymes have a distinct origin from other OXA beta-lactamases, such as the OXA-23 enzyme first discovered in *Acinetobacter* (Mugnier et al., 2010). Since their discovery, the OXA-48-like enzymes have disseminated globally due to the spread of a broad host-range plasmid harbouring the OXA-48 gene within a composite transposon Tn*1999.* The most common derivative of OXA-48, OXA-181, was found to be mobilised from the *Sh. oneidensis* chromosome by IS*Ecp1,* followed by incorporation into Tn*2013* and the subsequent transmission into ColE2, IncX3, IncN1, and IncT plasmids (Potron, Poirel and Nordmann, 2011). Since

their discovery in Turkey, OXA-48-like-producing organisms have been found as the source of nosocomial and community outbreaks in many parts of the world and are now considered endemic in large parts of the Mediterranean and Middle East. On top of this, hospital outbreaks have been reported in Australia, China, Mexico, South Africa, as well as many European countries, while there are case reports of OXA-48 producing organisms in North and South America as well as many other countries (Mairi et al., 2018; Pitout et al., 2019).

1.5.3 Classification of beta-lactamases

There are two major classification systems for beta-lactamase enzymes. Firstly, the Ambler system is based on primary structure that originally classified beta-lactamases into 2 molecular classes, A and B (Ambler, 1980). These were distinguished by their use of either serine or zinc ions for beta-lactam hydrolysis, with serine-based beta-lactamases forming class A and the MBLs in class B. This system was further expanded when groups of serine-based beta-lactamases were discovered that appeared distinct from the class A enzymes. Thus, class C consisted of the AmpC beta-lactamases while class D contains the OXA family of enzymes (Hall and Barlow, 2005). In this system, the enzymes TEM, SHV, CTX-M and KPC are all group A beta-lactamases, while group B contains the NDM, VIM and IMP enzymes.

The other classification system was proposed by Bush in 1989, further refined in 1995 by Bush, Jacoby and Medeiros, and once again in 2010 (Bush and Jacoby, 2010). This system is based on functional classification of the enzymes

and their abilities to hydrolyse particular classes of antibiotics as well as their resistance to inhibitors. Group 1 consists of the molecular class C cephalosporinases that are chromosomally encoded, such as the AmpC enzymes. Group 2 consists of the molecular groups A and D serine-beta-lactamases. Subgroups include the ESBLs, such as the TEM, CTX-M and OXA enzymes, as well as the serine-based carbapenemases such as KPC. Group 3 contains the molecular class B metallo-beta-lactamases such as NDM, VIM and IMP (Bush and Jacoby, 2010). A diagram of both functional and structural classifications can be seen in **Figure 1.17**.

In 2010, around 850 beta-lactamases had been identified (Drawz and Bonomo, 2010), and by 2018 that number was up to 2770 (Bush, 2018). Today, the BLDB shows that number is up to 8154 (Naas et al., 2017). This is likely due in large part to the increasing availability of whole-genome sequencing allowing

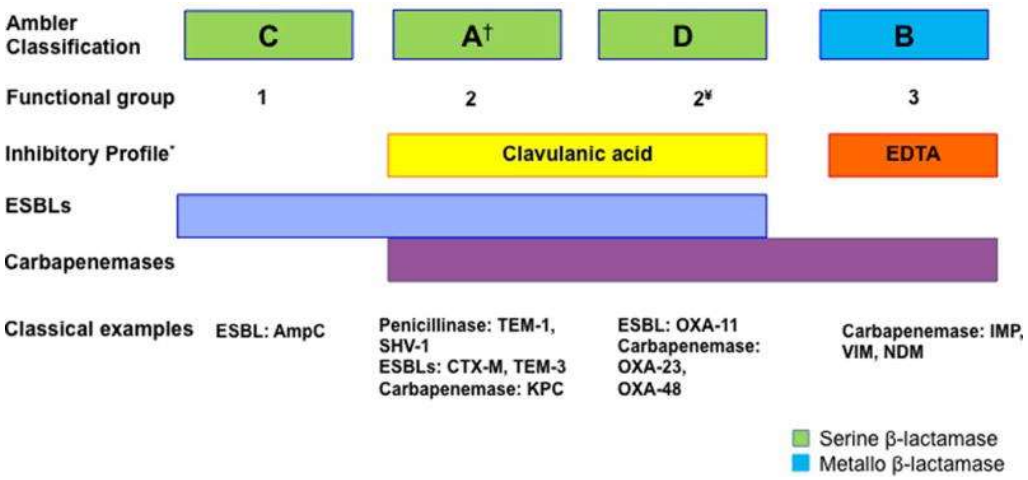

Figure 1.17. Classification schemes of beta-lactamases. The molecular classification of beta-lactamases follows the Ambler classification. The main functional groups of the Bush-Jacoby-Medeiros scheme are also shown. † Class A enzymes are the most diverse and include penicillinases, ESBLs and carbapenemases. ¥ Ambler class D enzymes belong to the functional group/subgroup 2d. * Class A enzymes belonging to the subgroup 2br are resistant to clavulanic acid inhibition. Republished from Munita and Arias (2016) under Creative Commons CC-BY license.

greater detection of beta-lactamase variants, as well as the continual rise of new AMR genes due to selection pressure of antibiotics.

1.6 AMR detection in wastewater

For decades, the importance of local and national surveillance of AMR to guide treatment guidelines and intervention strategies has been acknowledged. The first international AMR surveillance program was The European Antimicrobial Resistance Surveillance Network (EARS-Net), with its precursor, EARS, initiated in 1998. EARS-Net relies on routine clinical antimicrobial susceptibility data from clinical laboratories, reported to the European Centre for Disease Prevention and Control (ECDC) (ECDC, 2023a). The data include only invasive isolates (blood and cerebrospinal fluid) and encompass eight bacterial pathogens: *E. coli*, *K. pneumoniae*, *P. aeruginosa*, *Acinetobacter spp*., *Streptococcus pneumoniae*, *St. aureus*, *Enterococcus faecalis* and *Enterococcus faecium*. On a more global scale, the Global Antimicrobial Resistance Surveillance System (GLASS) was introduced in October 2015 by the World Health Organization (WHO) to support its overarching global action plan on AMR (WHO, 2023), while the industry-sponsored Study for Monitoring Antimicrobial Resistance Trends (SMART) recently completed its 20th year (Aarestrup and Woolhouse, 2020; Cantón et al., 2023).

Wastewater-based epidemiology (WBE) utilises the analysis of wastewater as an epidemiological approach to gather information about human populations

on a community scale via sampling undertaken at wastewater treatment plants (WWTPs) (Choi et al., 2018; Chau et al., 2022). This approach has been used successfully to monitor illicit drug use, as well as pathogen surveillance, including SARS-CoV-2 (Chau et al., 2022). The use of WBE for the surveillance of AMR has been reviewed multiple times (Fahrenfeld and J. Bisceglia, 2016; Aarestrup and Woolhouse, 2020; Chau et al., 2022), and it has been suggested that the implementation of a global sewage-based AMR surveillance system would complement and augment current AMR surveillance efforts, so contributing to meeting the key objectives of AMR surveillance at a global scale (Aarestrup and Woolhouse, 2020).

A variety of methods have been used to detect AMR in wastewater (Karkman et al., 2018; Pazda et al., 2019). These can be grouped into two broad categories of culture-dependent and culture-independent methods. Culture-dependent methods may have a variety of downstream processes, but they rely on the ability to isolate and grow specific bacteria in the laboratory. After isolation, methods include phenotypic characterisation such as: disc diffusion assays, MIC measurement, as well as immunochromatographic detection of AMR proteins, such as beta-lactamases. Molecular approaches are also used that include PCR detection of AMR genes, and increasingly whole genome sequencing is being used to determine the entire genetic environment of ARGs and their host organisms. Of course, the usual limitations of culture based approaches apply, in that only a fraction of environmental bacteria can be grown in the laboratory, and the use of specific selection methods will strongly

bias the types of bacteria isolated (Walsh and Duffy, 2013; Karkman et al., 2018).

Culture-independent methods can be used to overcome these limitations. Metagenomic approaches, where the DNA of the entire microbial community is sequenced, are used to detect the full range of ARGs in a particular environment (Bengtsson-Palme et al., 2019; Hendriksen et al., 2019; Kneis, Berendonk and Heß, 2019). Issues with this approach are that the number of ARGs in a particular environment may be low, and so a number of ARGs may be below the limit of detection (Fitzpatrick and Walsh, 2016). A possible way to overcome these issues is the use of quasi-metagenomics, recently used in the detection of enteric pathogens in food safety (Hyeon, Li, et al., 2018; Hyeon, Mann, et al., 2018; Forghani et al., 2020). Quasi-metagenomics refers to the sequencing of a modified microbiome of concentrated DNA, using selective enrichment for target organisms. This method, also described as culture-enriched metagenomics in the literature, has been used to profile the cystic fibrosis lung microbiota, as well as the beta-lactam resistome of a WWTP (Whelan et al., 2020; Zhang, Zhang and Ju, 2022).

Quantitative PCR (qPCR) is often used to determine the level of a number of resistance genes in a particular sample, and this is especially useful for comparing across multiple WWTPs, or between the influent and effluent of a WWTP (Karkman et al., 2016; McConnell et al., 2018; Cacace et al., 2019). A disadvantage of standard metagenomic and qPCR approaches is that, since the bacterial cells are lysed to allow DNA isolation, any extrachromosomal DNA is sequenced separately from that of the host organism (Karkman et al., 2018).

This makes it impossible to determine the host of particular plasmids, which limits the use of these techniques. Possible methods to overcome this include inverse PCR, which, combined with long-read sequencing has also been used to investigate the genetic environment of specific ARGs (Pärnänen et al., 2016). This is where DNA with suspected ARGs is digested and circularised. Then, PCR amplification of the target gene using only a single primer will amplify the entire circularised section. These sections of DNA can then be sequenced, and the resulting reads will contain not only the ARG of interest, but those upstream and downstream as well.

Another method that is able to link ARGs and their host organisms is the use of proximity ligation with shotgun sequencing to create chimeric reads of DNA that contain sections of chromosome and plasmids from the same cell (Stalder et al., 2019). This technique uses chromosome conformation capture (3C), a method first used to understand the higher order structure of eukaryotic DNA within the nucleus (Barutcu et al., 2016), to bind DNA sections that are close together in 3D space. DNA is then digested, circularised and sequenced, and this has been used to link ARGs from plasmids to their host organisms from a wastewater sample in the USA (Stalder et al., 2019). Other methods include Emulsion, Paired Isolation and Concatenation PCR (epicPCR), which is able to link the 16S rRNA gene from a single bacterial cell with another gene of interest and amplify this product via PCR (Spencer et al., 2016). This has recently been used to detect the host range of specific ARGs in WWTPs in Finland (Hultman et al., 2018). High-throughput single-cell genomic sequencing has also been

used to analyse the distribution of ARGs in an environmental sample (Lan et al., 2017), and could be an important method in the future.

1.7 Aims and objectives

It is known that AMR diversity and abundance varies geographically, and the analysis of wastewater has been proposed as an economically and ethically feasible way of surveillance of AMR (Hendriksen et al., 2019). Research suggests that surveillance of bacterial populations in WWTPs can serve as a proxy for surveillance of clinically relevant bacteria carried within the human population (Newton et al., 2015). This information could be used to recognise current and future trends in the spread of AMR, potentially leading to better control and prevention of antimicrobial infections.

This introduction has highlighted the threat of the rapid dissemination of ARGs of serious concern and underscored the importance of MGEs in the spread of AMR. The aim of this study was to investigate the presence of antimicrobial resistant enterobacteria in the raw sewage of WWTPs and receiving water in the East Midlands, as a proxy for the surveillance of AMR in the human population of that area. The Urban Waste Water Treatment Directive of the European Commission also suggests sampling of treated effluent to determine the transmission risk of environmental AMR, therefore the presence of these bacteria in the effluent of WWTPs was also investigated (European Commission, 2022; Larsson, Flach and Laxminarayan, 2023). The goal of this was to identify the genetic mechanisms by which bacteria in this area are

resistant to our most useful antibiotics, the beta-lactams, with a specific focus on the beta-lactams of "last resort", the carbapenems. Additionally, the mobility of the resistance mechanisms was given special attention. To meet these aims, a range of phenotypic and molecular-based approaches were used that not only enabled the identification of which AMR genes are present and in which species, but helped understand the wider genetic environments that enable these MDR bacteria to emerge and disseminate in the human population.

The main objectives included:

i. Isolation and phenotypic characterisation of cephalosporin and carbapenem resistant enterobacteria from raw and treated sewage and receiving waters via disc diffusion assay.

ii. Genotypic characterisation of relevant AMR genes through PCR and whole genome sequencing.

iii. Characterisation of the MGEs of carbapenem resistant isolates, including conjugation assays to determine mobility of MGEs and associated ARGs.

iv. Investigation of genetic relatedness of isolates across a range of time points, are similarities in phenotypic and PCR results due to clonality or the spread of related MGEs?

v. Determination of sequence similarity of MGEs from collected wastewater isolates with other published MGE sequences from the UK.

vi. Investigation into the intracellular mobility of MGEs containing carbapenemase genes.

CHAPTER 2: MATERIALS AND METHODS

2.1 Growth and maintenance

2.1.1 Bacterial Strains

The strains used in this study can be found in **Table 2.1**. Strains listed as controls were used as positive and negative controls for the antibiotic susceptibility testing disc diffusion assay (**§2.3.1**), while ATCC 25922 and NCTC 13476 were also used as controls for the zinc-supplemented carbapenem inactivation method (**§2.3.2**).

Table 2.1. Strains used in this study.

Strain name	Description	Use	Reference
ATCC 25922	*E. coli* FDA strain Seattle 1946 [DSM 1103, NCIB 12210]	Negative control	American Type Culture Collection (ATCC)
NCTC 13476	*E. coli* containing bla_{IMP}	Positive control	National Collection of Type Cultures (NCTC)
NCTC 13353	*E. coli* strain EO 487 encoding $bla_{CTX\text{-}M\text{-}15}$	Positive control	NCTC
CV601 kan^R rif^R gfp^+	*E. coli* K-12 derivative resistant to kanamycin and rifampicin that includes green fluorescent protein (*gfp*)	Conjugation recipient	(Smalla et al., 2000)
J53 Azi^R	*E. coli* K-12 derivative resistant to sodium azide	Conjugation recipient	(Yi et al., 2012)
NEB® 5-alpha Competent *E. coli*	Chemically competent derivative of DH5α	Transformation recipient	C2987H, New England Biolabs (NEB), Hitchin, UK.

2.1.2 Media

All media were prepared using reverse osmosis (RO) water and sterilised by autoclaving at 121°C for 15 minutes at 15 psi, unless specified otherwise. Where appropriate, supplements were added to the media once it had cooled to 50°C. All growth media were obtained from Sigma-Aldrich, Gillingham, UK, unless specified otherwise.

2.1.2.1 Lysogeny broth (Lennox) and Lysogeny broth (Lennox) with agar

Lysogeny broth (LB) was prepared to a final concentration of 10 g L^{-1} tryptone, 5 g L^{-1} sodium chloride and 5 g L^{-1} yeast extract. LB with agar used the same concentrations with the addition of 15 g L^{-1} agar.

2.1.2.2 Mueller-Hinton broth and agar

Mueller-Hinton (MH) broth was prepared to a final concentration of 2 g L^{-1} beef infusion solids, 17.5 g L^{-1} casein hydrolysate and 1.5 g L^{-1} starch. MH agar used the same concentrations with the addition of 17 g L^{-1} agar.

2.1.2.3 Tryptone Soya Broth (Thermo Fisher Scientific)

Tryptone Soya Broth (TSB) was prepared to a final concentration of 17 g L^{-1} pancreatic digest of casein, 3 g L^{-1} enzymatic digest of soya bean, 5 g L^{-1} sodium chloride, 2.5 g L^{-1} dipotassium hydrogen phosphate and 2.5 g L^{-1} glucose.

2.1.2.4 MacConkey agar

MacConkey agar (MAC) was prepared to a final concentration of 17 g L^{-1} peptone, 3 g L^{-1} proteose peptone, 10 g L^{-1} lactose, 1.5 g L^{-1} bile salts no. 3, 5 g L^{-1} sodium chloride, 13.5 g L^{-1} agar, 0.03 g L^{-1} neutral red and 0.001 g L^{-1} crystal violet.

2.1.2.5 Tryptone Bile X-glucuronide agar

Tryptone Bile X-glucuronide agar (TBX) was prepared to a final concentration 15 g L^{-1} agar, 1.5 g L^{-1} bile salts, 0.075 g L^{-1} X-β-*D*-glucuronide and 20 g L^{-1} peptone.

2.1.2.6 *Brilliance* CRE agar (Thermo Fisher Scientific)

Brilliance CRE agar containing 15 g L^{-1} peptones, 2 g L^{-1} carbohydrates, 5.1 g L^{-1} titanium oxide, 1 g L^{-1} chromogenic mix, 19 mL L^{-1} antibiotic mix (*sic*) and 15 g L^{-1} agar was purchased as prepared medium.

2.1.2.7 CHROMagar mSuperCARBA agar

CHROMagar™ mSuperCARBA™ agar (CHROMagar, Paris, France) was prepared to a final concentration 15 g L^{-1} agar, 20 g L^{-1} peptones, 5 g L^{-1} sodium chloride, 0.8 g L^{-1} chromogenic and selective mix, 1.7 g L^{-1} growth factors and 2 mL L^{-1} growth factors mix supplement. RO water was used to make the desired volume before bringing to the boil on a hotplate. This was followed by the addition of 0.25 g L^{-1} 'selective mix supplement' once the agar had cooled to 50°C.

2.1.2.8 Super Optimal broth with catabolite repression (SOC) medium (Thermo Fisher Scientific)

Super Optimal broth with catabolite repression (SOC) medium containing 2% tryptone, 0.5% yeast extract, 10 mM sodium chloride, 2.5 mM potassium chloride, 10 mM magnesium chloride, 10 mM magnesium sulphate, and 20 mM glucose was purchased as prepared medium (Thermo Fisher Scientific, Loughborough, UK).

2.1.2.9 SOC Outgrowth Medium (New England Biolabs)

SOC Outgrowth Medium containing 2% vegetable peptone, 0.5% yeast extract, 10 mM sodium chloride, 2.5 mM potassium chloride, 10 mM magnesium chloride, 10 mM magnesium sulphate and 20 mM glucose was purchased as prepared medium (New England Biolabs (NEB), Hitchin, UK).

2.1.3 Antimicrobial stock solutions

All antibiotic powders used in selective liquid or plate culture were obtained from Sigma-Aldrich, prepared at 500X working concentration using Milli-Q purified water (Millipore), filter sterilised using a 0.22 µm filter (Sartorius, Epsom) and stored in aliquots at -20°C, unless specified otherwise.

2.1.3.1 Ampicillin

100 mg mL^{-1} of ampicillin sodium salt was dissolved in water and used at a working concentration of 100 µg mL^{-1}.

2.1.3.2 Cefotaxime

1 mg mL^{-1} of cefotaxime sodium salt was dissolved in sterile water and used at a working concentration of 2 µg mL^{-1}.

2.1.3.3 Kanamycin

25 mg mL^{-1} of kanamycin sulphate was dissolved in sterile water and used at a working concentration of 50 µg mL^{-1}.

2.1.3.4 Rifampicin

10 mg mL^{-1} of rifampicin (Thermo Fisher Scientific) was dissolved in 95% (v/v) ethanol and used at a working concentration of 50 µg mL^{-1}.

2.1.3.5 Meropenem

For meropenem selection, 1 mg mL^{-1} of meropenem trihydrate (APExBIO, Texas, USA) was dissolved in sterile water and used at a working concentration of 2 µg mL^{-1}. For minimum inhibitory confirmation, 10 mg mL^{-1} of meropenem trihydrate was dissolved in sterile water, filter sterilised using a 0.22 µm filter (Sartorius, Epsom, UK), and used on the same day at the required concentrations.

2.1.3.6 Sodium azide

100 mg mL^{-1} of sodium azide was dissolved in sterile water and used at a working concentration of 100 µg mL^{-1}.

2.1.3.7 Anhydrotetracycline

220 µg mL^{-1} of anhydrotetracycline hydrochloride (APExBIO) was dissolved in 50% (v/v) ethanol, stored in an opaque container at -20°C and used at a working concentration of 200 ng mL^{-1}.

2.1.4 Buffers and Solutions

All chemicals were supplied by Thermo Fisher Scientific unless specified otherwise. RO water was used to bring solutions to required volumes.

2.1.4.1 Maximum Recovery Diluent

Maximum Recovery Diluent (MRD) was prepared to a final concentration 8.5 g L^{-1} sodium chloride and 1 g L^{-1} peptone and sterilised by autoclaving.

2.1.4.2 Dulbecco's Phosphate Buffered Saline

Dulbecco's Phosphate Buffered Saline (DPBS) was prepared to a final concentration of 8.5 g L^{-1} sodium chloride, 2.16 g L^{-1} sodium phosphate dibasic, 0.2 g L^{-1} potassium chloride and 0.2 g L^{-1} potassium phosphate monobasic and sterilised by autoclaving.

2.1.4.3 Ethylenediaminetetraacetic acid

Ethylenediaminetetraacetic acid (EDTA) was prepared as a 0.5 M solution by dissolving 186.1 g of EDTA in 800 mL of RO water, adjusted to pH 8.0 with 1 M sodium hydroxide and sterilised by autoclaving.

2.1.4.4 Tris(hydroxymethyl)aminomethane hydrochloride

Tris(hydroxymethyl)aminomethane hydrochloride (Tris-HCl) was prepared as a 1 M solution by dissolving 121.1 g of Tris base in 800 mL of RO water, adjusted to either pH 8.0 or pH 7.5 with 1 M hydrochloric acid, brought to a final volume of 500 mL with RO water and sterilised by autoclaving.

2.1.4.5 Tris-EDTA buffer

Tris-EDTA buffer was prepared to a final concentration of 10 mM Tris-HCl (pH 7.5) and 1 mM EDTA and sterilised by autoclaving.

2.1.4.6 Tris-acetate-EDTA buffer

Tris-acetate-EDTA (TAE) buffer was prepared to a final concentration of 40 mM Tris-HCl, 1 mM EDTA and 20 mM glacial acetic acid, adjusted to pH 8.0 with either 1 M hydrochloric acid or 1 M sodium hydroxide.

2.1.4.7 Glycerol

Glycerol solution was prepared to a final concentration of 50% or 10% (v/v) as required and sterilised by autoclaving.

2.1.4.8 Ethanol

Ethanol solution was mixed with sterile RO water to a final concentration of 80% or 95% (v/v) as required.

2.1.4.9 4% Rhamnose

4% (w/v) of L-Rhamnose monohydrate (Sigma-Aldrich) was dissolved in sterile Milli-Q purified water and filter sterilised using a 0.22 µm filter (Sartorius).

2.1.4.10 Zinc sulfate

240 mM Zinc sulfate was dissolved in sterile Milli-Q purified water and filter sterilised using a 0.22 µm filter (Sartorius).

2.1.5 Growth conditions

Bacterial liquid cultures were routinely grown in LB broth for 18 hours at 37°C with shaking at 200 rpm (Medline Scientific™ ISF-7100 Floor Standing Incubator Shaker). Bacterial cultures were routinely grown on LB agar plates for 18 hours at 37°C. Where appropriate, antimicrobial stock solutions (Section 2.1.3) were added to the media so that the final concentrations were as follows: 2 µg mL^{-1} meropenem, 2 µg mL^{-1} cefotaxime, 50 µg mL^{-1} kanamycin, 50 µg mL^{-1} rifampicin and 100 µg mL^{-1} sodium azide.

2.1.6 Long term storage of bacterial strains

A single bacterial colony was inoculated into 3 mL LB broth and incubated at 37°C for 18 hours with shaking at 200 rpm. 500 µl of this overnight culture was mixed with 500 µl of sterile 50% glycerol in a 2 mL cryogenic storage tube and stored at -80°C.

2.2 Environmental sampling

2.2.1 Wastewater and river sampling

2.2.1.1 Wastewater collection

Samples were taken from two separate wastewater treatment plants in the East Midlands between October 2019 and July 2022. The first, WWTP A, serves a local village and university campus; while the second, WWTP B, serves a local city that has a major hospital. Before the COVID-19 pandemic, a total of five samples were collected. First, from WWTP A in October 2019, then WWTP B in January 2020, and both A & B in February 2020 and on two occasions in March 2020. After the COVID-19 lockdown in March 2020, it was not possible to collect wastewater influent, and so effluent samples were collected from WWTP B on two occasions in May and July 2022.

Influent and effluent samples were collected in 200 mL volumes in sterile containers from their respective inlet or outlet pipes and transferred to the laboratory at ambient temperature. Samples from WWTP A were transported to the laboratory within 20 minutes, and samples from WWTP B within an hour. Samples taken in May and July 2022 were collected in 4 x 1 L volumes and transported on ice instead.

2.2.1.2 River water collection

At the same time as collecting wastewater in May and July 2022, samples were also taken from the river which wastewater treatment plant B discharges into. Sample points were 1) 100 m upstream of the effluent discharge point, 2)

100 m downstream of the effluent discharge point and 3) 200 m downstream of the effluent discharge point. Samples were collected in 4 x 1 L volumes in sterile containers and transported to the laboratory on ice within 1 hour.

2.2.2 Bacterial isolation

Wastewater and river water samples were diluted ten-fold in sterile MRD in triplicate and 100 µl of each dilution was spread onto an individual series of agar plates that were incubated at 37°C for 18 hours. The agar plates used in 2019 and 2020 were: LB, *Brilliance* CRE, MAC, TBX, and MAC/TBX supplemented with 2 µg mL^{-1} meropenem. The agar plates used in 2022 were LB, mSuperCARBA, MAC, TBX and MAC/TBX supplemented with 2 µg mL^{-1} meropenem or 2 µg mL^{-1} cefotaxime.

Colonies matching the morphology of *E. coli* on CRE and mSuperCARBA agar plates (red/pink colonies) and TBX agar plates (blue/green colonies) were streaked for single colonies on TBX agar and incubated for 37°C for 18 hours. Colonies matching the morphology of other *Enterobacteriaceae* on CRE and mSuperCARBA agar plates (blue colonies) or MAC plates (pink colonies) were streaked for single colonies on MAC agar and incubated at 37°C for 18 hours. Once pure cultures were obtained, these were then inoculated onto LB agar and incubated at 37°C for 18 hours and then put into long term storage (**§2.1.6**).

2.2.3 Water filtration

50 mL of water from river water or wastewater samples from WWTP B was vacuum filtered through sterile 0.22 µm Durapore PVDF Membrane Filters (MilliporeSigma, Feltham, UK) in a sterile magnetic filter funnel (Cytiva, Marlborough, MA, USA). The filters were transferred to the surface of individual LB, CRE or mSuperCARBA and TBX/MAC agar plates supplemented with 2 µg mL^{-1} meropenem, 2 µg mL^{-1} cefotaxime or 100 µg mL^{-1} ampicillin (as above) and incubated at 37°C for 18 hours. Pure cultures of isolates were then obtained as in **§2.2.2**.

2.2.4 Enriched isolation

Due to the low numbers of carbapenem-resistant isolates expected to be found in wastewater effluent and river water, bacteria from these samples were enriched by overnight growth in broth supplemented with meropenem. Triplicate samples of 50 mL of water were vacuum filtered through 0.22 µm Durapore PVDF Membrane Filters (MilliporeSigma) and these were transferred to 50 mL of TSB supplemented with 2 µg mL^{-1} meropenem and incubated at 37°C for 18 hours with shaking at 200 rpm. Ten-fold serial dilutions of these overnight cultures were performed and 100 µl of each dilution was spread onto agar plates listed in **§2.2.3**. Pure cultures of isolates were then obtained as in **§2.2.2** and stored as in **§2.1.6**.

2.2.5 Indole Testing

Each isolate was screened for the production of indole using the RapID Spot Indole Reagent (Remel, Thermo Fisher, Dartford UK). The *p*-dimethylaminocinnamaldehyde within the reagent reacts with indole to produce a blue-green colour. A single colony was inoculated into a drop of reagent in a sterile petri dish and mixed using a sterile loop. An isolate was considered positive for indole production if a blue-green colour change was observed within three minutes, and negative if no colour change was observed in that time.

2.2.6 Oxidase Testing

Oxidase test strips (MilliporeSigma) were used to touch a single colony, and an isolate was considered positive for oxidase production if a colour change was observed within one minute, and negative if no colour change was observed in that time.

2.3 Antimicrobial susceptibility testing

2.3.1 Disc diffusion assay

All isolates were screened for antimicrobial susceptibility using a modified Kirby-Bauer disc diffusion method as recommended by the Clinical and Laboratory Standards Institute (CLSI) (CLSI, 2012). Isolates were inoculated onto LB agar plates and incubated at 37°C for 18 hours before colonies from

these plates were suspended in Mueller-Hinton broth, adjusted to a turbidity of around a 0.5 McFarland standard. Mueller-Hinton agar plates were inoculated from this suspension using a sterile swab by swabbing in three directions across the surface of the plate. Antibiotic discs were added to the surface of the agar plate using a 16-disc antibiotic disc dispenser (i2a diagnostics, Montpellier, France) within 15 minutes of inoculation. The following antibiotics were used: Ampicillin 10 µg (AMP), Amoxicillin-clavulanic acid 20 µg and 10 µg (AMC), Cefoxitin 30 µg (FOX), Cefotaxime 30 µg (CTX), Cefpodoxime 10 µg (CPD), Aztreonam 30 µg (ATM), Meropenem 10 µg (MEM), Streptomycin 10 µg (S10), Oxytetracycline 30 µg (OT), Ciprofloxacin 5 µg (CIP), Nalidixic Acid 30 µg (NA), Trimethoprim-sulfamethoxazole 1.25 µg and 23.75 µg (SXT), Chloramphenicol 30 µg (C), Nitrofurantoin 300 µg (F) and Azithromycin 15 µg (AZM). All antibiotics were procured from i2a diagnostics. The breakpoints used for determination of susceptible, increased susceptibility or resistant results were taken from the CLSI M100 and M45 documents, or where not available, breakpoints determined by the European Committee on Antimicrobial Susceptibility Testing (EUCAST) were used instead (CLSI, 2016, 2019; EUCAST, 2019).

2.3.2 Zinc-supplemented carbapenem inactivation method (zCIM)

Each isolate was screened for carbapenemase production using the zinc-supplemented carbapenem inactivation method (Lucena Baeza et al., 2019). A full 10 µl inoculation loop of bacteria was suspended in 400 µl TSB

supplemented with zinc sulphate (0.3 mM final concentration) in a sterile microcentrifuge tube. A single 10 µg meropenem disc was added to the tube and the mixture was incubated at 37°C for 2 hours. After incubation, the disc was removed from the tube and placed on a Mueller-Hinton agar plate previously inoculated with a lawn of meropenem-susceptible *E. coli* ATCC 25922 as in **§2.3.1**. A fresh 10 µg meropenem disc was then placed on each plate as a control. After 18-hour incubation at 37°C, the zones of inhibition around the discs were measured, and isolates with zone diameters of ≤20 mm were recorded as positive for carbapenemase production. The zCIM was also performed on strains NCTC 13476 and ATCC 25922 as positive and negative controls respectively.

2.3.3 Minimum inhibitory concentration

The minimum inhibitory concentration (MIC) of meropenem on carbapenemase-producing isolates was measured by the agar dilution method (Wiegand, Hilpert and Hancock, 2008). Pure cultures of bacterial isolates were grown on LB agar at 37°C for 18 hours. A single colony of each isolate was inoculated into 4 mL LB broth and incubated at 37°C for 18 hours with shaking at 200 rpm. Each culture was diluted ten-fold and an optical density reading was taken using a Jenway 7205 spectrophotometer at 600 nm with a 1cm path length (Cole-Palmer Instrument Company Ltd, St. Neots, UK). A dilution series from 10^{0}-10^{-7} was performed and 100 µl of the 10^{-6} and 10^{-7} dilutions were spread onto LB agar in triplicate and incubated at 37°C for 18 hours. Colonies

were counted and the corresponding colony forming units (CFU) mL^{-1} calculated.

Table 2.2. Concentration of meropenem used in Mueller-Hinton agar plates.

Concentration (µg mL^{-1})	**0**	**0.5**	**1**	**2**	**4**	**8**	**16**	**32**	**64**	**128**	**256**
Volume of 10 mg mL^{-1} solution (µl)							40	80	160	320	640
Volume of 1 mg mL^{-1} solution (µl)				50	100	200					
Volume of 1 mg mL^{-1} solution (µl)		125	250								
Volume of H_2O (µl)	1000	875	750	950	900	800	960	920	840	680	360

Agar plates were prepared by adding 1 mL of various concentrations of meropenem solution to 24 mL of Mueller-Hinton agar cooled to 50°C. The concentrations used can be seen in **Table 2.2**.

A single colony of each isolate was again inoculated into 4 mL LB broth and incubated at 37°C for 18 hours with shaking at 200 rpm. Each culture was diluted ten-fold and an optical density reading was taken at 600 nm. This reading was compared to the previous one and its corresponding CFU mL^{-1} to calculate the current CFU mL^{-1}. An amount of culture was mixed with sterile MRD in the wells of a 96-well plate such that each well contained 100 µl of each culture at 1 x 10^8 CFU mL^{-1}. A 48-pin stainless steel replicator (Sigma-Aldrich) was used to transfer the inocula to triplicate Mueller-Hinton agar plates supplemented with meropenem. The replicator was sterilised by soaking in ethanol and passing through a Bunsen burner flame in between inoculating each set of triplicate plates. The plates were left to dry and then incubated at 37°C for 18 hours.

To confirm that the size of the bacterial inoculum was appropriate, 10 µl of the contents of each well was diluted in 990 µl sterile MRD (10^{-2} dilution), followed by a serial dilution to 10^{-5}, at which point 100 µl of the 10^{-4} and 10^{-5} dilutions were spread onto LB agar and incubated at 37°C for 18 hours. After incubation, colonies were counted and the MIC result considered valid if there were 50-200 colonies on the 10^{-5} plate, i.e., the bacterial suspension contained 0.5-2.0 x 10^{8} CFU mL^{-1}.

Valid MICs were recorded as the lowest concentration of meropenem that inhibited all growth of that isolate on all three agar plates inoculated; single colonies were discounted for this purpose.

2.4 DNA preparation

2.4.1 Crude DNA extraction

Pure cultures of bacterial isolates were grown on LB agar at 37°C for 18 hours. A single colony was suspended in 100 µl sterile Milli-Q purified water in a sterile microcentrifuge tube and placed in a heating block set to 100°C for 30 minutes. After centrifugation at 16,000 x *g* for 5 minutes (Eppendorf, 5417c, Eppendorf, Hamburg, Germany), the supernatant was transferred to a fresh sterile microcentrifuge tube.

2.4.2 Genomic DNA extraction for sequencing

The Monarch® HMW DNA Extraction Kit for Tissue (NEB) was used to extract DNA for whole genome sequencing, following the manufacturer's protocol for Gram-negative bacteria. Briefly, 1.5 mL of overnight culture was centrifuged, and the pellet was resuspended in cold DPBS (**§2.1.4.2**). Lysozyme and HMW gDNA Tissue Lysis Buffer were added, followed by incubation in an Eppendorf ThermoMixer® Comfort thermal mixer (Eppendorf) at 37°C for 10 minutes at 1400 rpm. Proteinase K was added and then homogenisation was carried out by incubating in a thermal mixer at 56°C for 30 minutes at 1400 rpm, followed by incubation with RNase A. The DNA was separated from protein by the addition of Protein Separation Solution and centrifugation for 10 minutes at 16,000 x *g*. DNA was transferred to a fresh tube using a wide-bore 1000 µl pipette, followed by the addition of DNA capture beads and isopropanol. The tubes were mixed on a Grant-bio, PTR-60 vertical rotating mixer (Grant Instruments, Royston, UK) to attach DNA to the beads, which were then washed twice with gDNA Wash Buffer, followed by incubation with elution buffer at 56°C for 5 minutes at 300 rpm. The eluate was then centrifuged for 30 seconds at 16,000 x *g* through a bead retainer to remove the beads, and then stored at ambient temperature overnight to encourage the DNA to dissolve into solution, before use in downstream applications.

2.4.3 DNA quality control

2.4.3.1 Quantification of DNA Concentration using a Nanodrop 1000 Spectrophotometer

The amount and purity of DNA was quantified using a Nanodrop 1000 (Thermo Fisher Scientific) by measuring the absorbance of UV light of a 1 µl volume of DNA. Purity was assessed by calculating the absorbance value ratios at 260/280 nm and 260/230 nm. A ratio of ~1.8 for 260/280 nm and ~2.0-2.2 for 260/230 nm is considered pure for DNA.

2.4.3.2 Quantification of DNA Concentration using a Qubit 3 Fluorometer

The amount of DNA was quantified using the Qubit 3 fluorometer and Qubit dsDNA HS Assay kit (Thermo Fisher Scientific). Briefly, the fluorometer was calibrated using the standards included in the assay kit, and then 1-10 µl of sample was mixed with 190-199 µl of Qubit dsDNA reagent and buffer solution in a thin walled 0.5 mL PCR tube. The samples were then quantified by the fluorometer measuring the fluorescent signals emitted by the dyes used in the reagent when bound to the sample DNA and excited by visible light at 502 nm.

2.4.3.3 DNA size determination using an Agilent 2200 TapeStation

The size of DNA fragments was determined by electrophoresis using the Agilent 2200 TapeStation with the Genomic DNA ScreenTape system (Agilent

Technologies, Wokingham, UK). Samples and a DNA ladder were prepared by mixing 10 µl Genomic DNA Sample Buffer with 1 µl genomic/ladder DNA in a 0.2 mL PCR tube. Tubes were centrifuged briefly (Mini Fuge PLUS, STARLAB, Milton Keynes, UK), followed by vortexing at 2000 rpm for 1 minute in a Thermo Fisher Scientific, IKA MS 3 mixer (Thermo Fisher Scientific), and then a final brief centrifugation. Tubes were then loaded into an Agilent 2200 TapeStation device and size was determined using a gel matrix to resolve nucleic acid samples according to molecular weight by electrophoresis. This process uses micro-channels filled with a sieving polymer and fluorescent dye that separates DNA molecules according to size.

2.4.4 Plasmid Purification

Plasmids were purified from isolates using the Monarch® Plasmid Miniprep Kit (NEB). All centrifugation steps were carried out at 16,000 x *g*. A single colony was inoculated into 20 mL LB broth and incubated at 37°C for 18 hours with shaking at 200 rpm. 1.5 mL of this overnight culture was centrifuged for 30 seconds and resuspended in 200 µl Plasmid Resuspension Buffer. The cell walls were broken down and the DNA denatured by alkaline lysis, by the addition of 200 µl Plasmid Lysis Buffer. This alkaline solution was then neutralised by the addition of 400 µl of Plasmid Neutralization Buffer. The plasmid DNA dissolved in solution while the larger genomic DNA fragments formed a precipitate with other cell debris, and these were separated by centrifugation for 5 minutes. The supernatant containing plasmid DNA was transferred to a spin column and

the DNA bound to the silica membrane by centrifugation for 1 minute. 200 µl of Plasmid Wash Buffer 1 was added and the column centrifuged for 1 minute to remove cellular components. This was followed by the addition of 400 µl of Plasmid Wash Buffer 2 and a 1-minute centrifugation to remove trace buffer components. Finally, DNA was eluted in 30 µl nuclease-free water by centrifuging for 1 minute.

2.5 Polymerase chain reaction (PCR)

A Bio-Rad C1000 thermal cycler (Bio-Rad, Watford, UK) was used for all PCR reactions. Unless specified otherwise, the reaction mixture contained 10 µl DreamTaq Green PCR Master Mix (2X) (Thermo Fisher Scientific), 1 µl forward primer, 1 µl reverse primer, x µl template DNA (1-2 ng plasmid DNA, or 5-50 ng gDNA), and the final volume was made up to 20 µl with the addition of nuclease-free water in a 0.2 mL PCR tube.

2.5.1 Primers

All primers were synthesised by Sigma-Aldrich, using desalt purification to a concentration of 100 µM in nuclease-free water. Working stocks were prepared at 10 µM by dilution in nuclease-free water and stored at -20°C.

Table 2.3. List of primers used in ESBL detection.

Primer name	Sequence	Product Size (bp)	Reference
CTX-M Fw	CGCTTTGCGATGTGCAG	550	(Poirel et al., 2001)
CTX-M Rv	ACCGCGATATCGTTGGT		
TEM Fw	GAGTATTCAACATTTCCGTGTC	861	(Zaniani et al., 2012)
TEM Rv	TAATCAGTGAGGCACCTATCTC		
SHV Fw	TTATCTCCCTGTTAGCCACC	795	(Weill et al., 2004)
SHV Rv	GATTTGCTGATTTCGCTCGG		
OXA-1 Fw	ATGAAAAACACAATACATATCAACTTCGC	820	(Hasman et al., 2005)
OXA-1 Rv	GTGTGTTTAGAATGGTGATCGCATT		
OXA-2 Fw	ACGATAGTTGTGGCAGACGAAC	602	(Hasman et al., 2005)
OXA-2 Rv	ATYCTGTTTGGCGTATCRATATTC		

Table 2.4. List of primers used in acquired carbapenemase detection.

Primer name	Sequence	Product Size	Reference
NDM Fw	GGTTTGGCGATCTGGTTTTC	621	(Poirel et al., 2011)
NDM Rv	CGGAATGGCTCATCACGATC		
KPC Fw	CGTCTAGTTCTGCTGTCTTG	798	
KPC Rv	CTTGTCATCCTTGTTAGGCG		
OXA-48 Fw	GCGTGGTTAAGGATGAACAC	438	
OXA-48 Rv	CATCAAGTTCAACCCAACCG		
BIC Fw	TATGCAGCTCCTTTAAGGGC	537	
BIC Rv	TCATTGGCGGTGCCGTACAC		
AIM Fw	CTGAAGGTGTACGGAAACAC	322	
AIM Rv	GTTCGGCCACCTCGAATTG		
DIM Fw	GCTTGTCTTCGCTTGCTAACG	699	
DIM Rv	CGTTCGGCTGGATTGATTTG		
GIM Fw	TCGACACACCTTGGTCTGAA	477	
GIM Rv	AACTTCCAACTTTGCCATGC		
SIM Fw	TACAAGGGATTCGGCATCG	570	
SIM Rv	TAATGGCCTGTTCCCATGTG		
IMP Fw	GGAATAGAGTGGCTTAAYTCTC	232	
IMP Rv	GGTTTAAYAAAACAACCACC		
VIM Fw	GATGGTGTTTGGTCGCATA	390	
VIM Rv	CGAATGCGCAGCACCAG		
SPM Fw	AAAATCTGGGTACGCAAACG	271	

SPM Rv	ACATTATCCGCTGGAACAGG		

Table 2.5. List of primers used in PCR-based replicon typing.

Primer name	Sequence	Product Size	Reference
HI1 Fw	GGAGCGATGGATTACTTCAGTAC	471	(Carattoli et al., 2005)
HI1 Rv	TGCCGTTTCACCTCGTGAGTA		
HI2 Fw	TTTCTCCTGAGTCACCTGTTAACAC	644	
HI2 Rv	GGCTCACTACCGTTGTCATCCT		
I1-Iγ Fw	CGAAAGCCGGACGGCAGAA	139	
I1-Iγ Rv	TCGTCGTTCCGCCAAGTTCGT		
X Fw	AACCTTAGAGGCTATTTAAGTTGCTGAT	376	
X Rv	TGAGAGTCAATTTTTATCTCATGTTTTAGC		
L/M Fw	GGATGAAAACTATCAGCATCTGAAG	785	
L/M Rv	CTGCAGGGGCGATTCTTTAGG		
N Fw	GTCTAACGAGCTTACCGAAG	559	
N Rv	GTTTCAACTCTGCCAAGTTC		
FIA Fw	CCATGCTGGTTCTAGAGAAGGTG	462	
FIA Rv	GTATATCCTTACTGGCTTCCGCAG		
FIB Fw	TCTGTTTATTCTTTTACTGTCCAC	683	(Villa et al., 2010)
FIB Rv	CTCCCGTCGCTTCAGGGCATT		(Carattoli et al., 2005)
W Fw	CCTAAGAACAACAAAGCCCCCG	242	

W Rv	GGTGCGCGGCATAGAACCGT		
Y Fw	AATTCAAACAACACTGTGCAGCCTG	765	
Y Rv	GCGAGAATGGACGATTACAAAACTTT		
P Fw	CTATGGCCCTGCAAACGCGCCAGAAA	534	
P Rv	TCACGCGCCAGGGCGCAGCC		
FIC Fw	GTGAACTGGCAGATGAGGAAGG	262	
FIC Rv	TTCTCCTCGTCGCCAAACTAGAT		
A/C Fw	GAGAACCAAAGACAAAGACCTGGA	465	
A/C Rv	ACGACAAACCTGAATTGCCTCCTT		
T Fw	TTGGCCTGTTTGTGCCTAAACCAT	750	
T Rv	CGTTGATTACACTTAGCTTTGGAC		
FIIS Fw	CTGTCGTAAGCTGATGGC	270	
FIIS Rv	CTCTGCCACAAACTTCAGC		
FII Fw	CTGATCGTTTAAGGAATTTT	258-262	(Villa et al., 2010)
FII Rv	CACACCATCCTGCACTTA		
K/B/O Fw	GCGGTCCGGAAAGCCAGAAAAC	160	(Carattoli et al., 2005)
K Rv	TCTTTCACGAGCCCGCCAAA		
B/O Rv	TCTGCGTTCCGCCAAGTTCGA	159	
X3 Fw	GTTTTCTCCACGCCCTTGTTCA	351	(Johnson et al., 2012)
X3 Rv	CTTTGTGCTTGGCTATCATAA		

Table 2.6. List of other primers used in this study.

Primer name	Sequence	Product Size	Reference
GFP Fw	ATATAGCATGCGTAAAGGAGAAGAACTTTTCA	714	(Andersen et al., 1998)
GFP Rv	CTCTCAAGCTTATTTGTATAGTTCATCCATGC		
16S rRNA 8 Fw	AGAGTTTGATCCTGGCTCAG	1503	(Weisburg et al., 1991)
16S rRNA 1492 Rv	GGTTACCTTGTTACGACTT		(Eden et al., 1991)
IncP *oriT* Fw	CAGCCTCGCAGAGCAGGAT	110	(Götz et al., 1996)
IncP *oriT* Rv	CAGCCGGGCAGGATAGGTGAAGT		
***colA* Fw**	ACGAACATCACGAAATCTGAC	143	This study
***colA* Rv**	AAAGCCTCCACCACAACAC		

Table 2.7. List of primers used to generate fragments for Gibson assembly, and to check correct assembly of plasmid.

Primer name	Sequence	Product Size	Reference
CasTet Fw	TTATAAGGTACCCTCTGGGCCTCATGGGCCGGTTATAATCCCTATCAGTGATAGAGATTG	5180	This study
CasTet Rv	CCAGTATTACGCGTTCAGGGCAGGGTCGTTAAATAG		
***ccdA* Fw**	CCCTGCCCTGAACGCGTAATACTGGTGTATAC	326	
***ccdA* Rv**	CGCACAATGTTTATAGGTGTAAACCTTAAACTG		
***pemI* Fw**	GGTTTACACCTATAAACATTGTGCGTTAAAGCC	392	
***pemI* Rv**	GACTACCTGCTGAGCGAGACAAGCCAGATTTC		
IS*26* Fw	GGCTTGTCTCGCTCAGCAGGTAGTCGTCGAAG	938	
IS*26* Rv	GTCGTCAGCTTGTACAAGCAGGCATCACGAAG		
KanRep Fw	ATGCCTGCTTGTACAAGCTGACGACCGGGTC	2174	
KanRep Rv	GTTGAGCTCGTTGATGCGGCCTTGACGGCCACTGACAGGAAAATGGGCCATTG		
IS*26* no ATs Fw	CCCTGCCCTGAACCAGCAGGTAGTCGTCGAAG	938	
CasTet no ATs Rv	GACTACCTGCTGGTTCAGGGCAGGGTCGTTAAATAG	5180	
Var Fw	GTGCAGAGCCAGCCTTCTTA	1947	
Var Rv	CCATCCTATGGAACTGCCTC		

2.5.2 Extended spectrum beta-lactamase (ESBL) PCR

All isolates were screened for five beta-lactamase genes: *bla*$_{\text{CTX-M}}$, *bla*$_{\text{TEM}}$, *bla*$_{\text{SHV}}$, *bla*$_{\text{OXA-1}}$ and *bla*$_{\text{OXA-2}}$. PCR cycling conditions for *bla*$_{\text{CTX-M}}$, *bla*$_{\text{TEM}}$, *bla*$_{\text{SHV}}$ and *bla*$_{\text{OXA-2}}$ primers (**Table 2.3**) were as follows: an initial denaturation at 95°C for 5 minutes, followed by 35 cycles of 95°C for 30 seconds, 55°C for 1 minute and 72°C for 1 minute with a final extension at 72°C for 5 minutes. For *bla*$_{\text{OXA-1}}$, conditions were as follows: an initial denaturation at 95°C for 5 minutes, followed by 35 cycles of 95°C for 1 minute, 51°C for 1 minute and 72°C for 1 minute with a final extension at 72°C for 5 minutes.

2.5.3 Multiplex PCR for acquired carbapenemase genes

Isolates exhibiting carbapenemase production in the zCIM assay were screened for acquired carbapenemase genes in three multiplex PCR reactions (Poirel et al., 2011). These multiplex reactions contained primers for 1: *bla*$_{\text{NDM}}$, *bla*$_{\text{KPC}}$, *bla*$_{\text{OXA-48}}$ and *bla*$_{\text{BIC}}$; 2: *bla*$_{\text{AIM}}$, *bla*$_{\text{DIM}}$, *bla*$_{\text{GIM}}$ and *bla*$_{\text{SIM}}$; 3: *bla*$_{\text{IMP}}$, *bla*$_{\text{VIM}}$, and *bla*$_{\text{SPM}}$ (**Table 2.4**). The reaction mixture for multiplexes 1 and 2 contained 12.5 µl Qiagen Master Mix (2X) (Qiagen, Manchester, UK), 0.25 µl of each forward primer, 0.25 µl of each reverse primer, x µl template DNA (5-50 ng gDNA) and were made up to a final volume of 25 µl using nuclease-free water. Multiplex reaction 3 contained 12.5 µl Qiagen Master Mix (2X) (Qiagen), 0.5 µl of each forward primer, 0.5 µl of each reverse primer, x µl template DNA (5-50 ng gDNA) and were made up to a final volume of 25 µl using nuclease-free

water. The PCR cycling conditions used were as follows: an initial denaturation at 94°C for 10 minutes, followed by 35 cycles of 94°C for 30 seconds, 52°C for 40 seconds and 72°C for 50 seconds with a final extension at 72°C for 5 minutes.

2.5.4 *bla*$_{NDM}$ PCR

For confirmation of *bla*$_{NDM}$ transfer, a simplex PCR using the *bla*$_{NDM}$ primers (**Table 2.4**) and cycling conditions in **§2.5.3** were used.

2.5.5 PCR-Based Replicon Typing

All isolates were screened for the presence of plasmids using PCR-based replicon typing (PBRT), using the primers described in Caratolli et al. (2005), with the updated FIB forward primer described in Villa et al. (2010). This involved 5 multiplex reactions containing primer sets for the following plasmid replicons: 1 – HI1, HI2, I1-Iγ; 2 – X, L/M, N; 3 – FIA, FIB, W; 4 – Y, P, FIC; 5 – A/C, T, FII$_S$. Additionally, there were 2 simplex reactions for replicons K and B/O. The F$_{repB}$ replicon PCR from Carattoli *et al*. (2005) was replaced with the FII replicon PCR as described in Villa *et al*. (2010). Finally, a simplex PCR for the X3 plasmid replicon was also used (Johnson et al., 2012), and all of these can be found in **Table 2.5**. The reaction mixture for the multiplex PCRs contained 10 µl DreamTaq Green PCR Master Mix (2X) (Thermo Fisher Scientific), 0.5 µl of each forward primer, 0.5 µl of each reverse primer, x µl template DNA (5-50 ng

gDNA), and the final volume was made up to 20 µl with the addition of nuclease-free water in a 0.2 mL PCR tube. Simplex PCR reaction mixtures were as described in **§2.5**. Cycling conditions for the multiplex PCRs were as follows: an initial denaturation at 94°C for 5 minutes, followed by 35 cycles of 94°C for 1 minute, 60°C for 30 seconds and 72°C for 1 minute with a final extension at 72°C for 5 minutes. Conditions for the K, B/O and X3 replicons were identical except for use of an annealing temperature of 52°C; and the FII replicon PCR was identical except for use of an annealing temperature of 54°C.

2.5.6 Green fluorescent protein (GFP) PCR

Transconjugants were confirmed by screening for the presence of the GFP gene present in the genome of the *E. coli* recipient strain CV601. Primer sequences are detailed in **Table 2.6**. The reaction conditions were as follows: an initial denaturation at 95 °C for 5 minutes followed by 35 cycles of 94°C for 1 minute, 54°C for 2 minutes, 72°C for 1 minute with a final extension of 72°C for 10 minutes.

2.5.7 16S rRNA PCR

All isolates had their 16S rRNA gene amplified by PCR for species/genus identification purposes. Primer sequences are detailed in **Table 2.6**. Cycling conditions were as follows: an initial denaturation at 95°C for 5 minutes,

followed by 35 cycles of 95°C for 30 seconds, 55°C for 1 minute and 72°C for 1 minute with a final extension at 72°C for 5 minutes.

2.5.8 IncP *oriT* PCR

To confirm transformation of plasmid pCURE2 into recipient cells, PCR detection of the *oriT* gene found on that plasmid was performed. Primer sequences are detailed in **Table 2.6**. PCR cycling conditions were as follows: an initial denaturation at 94°C for 5 minutes, followed by 35 cycles of 94°C for 1 minute, 59°C for 30 seconds and 72°C for 30 seconds with a final extension at 72°C for 5 minutes.

2.5.9 *colA* PCR

To check for the transformation of plasmid pFREE/pFREE_IncF into recipient cells, PCR detection of the *colA* replicon found on that plasmid was performed. Primer sequences are detailed in **Table 2.6**. PCR cycling conditions were as follows: an initial denaturation at 94°C for 5 minutes, followed by 35 cycles of 94°C for 1 minute, 52°C for 30 seconds and 72°C for 1 minute with a final extension at 72°C for 5 minutes.

2.5.10 Amplification of fragments for Gibson assembly

All PCR reaction mixtures contained 25 µl Q5® Hot Start High-Fidelity 2X Master Mix (NEB), 2.5 µl forward primer, 2.5 µl reverse primer, x µl template DNA (5-50 ng plasmid DNA), and the final volume was made up to 50 µl with the addition of nuclease-free water in a 0.2 mL PCR tube. The following fragments were amplified with primers listed in **Table 2.7** and used the following cycling conditions: **CasTet** – an initial denaturation at 98°C for 30 seconds, followed by 35 cycles of 98°C for 10 seconds, 70°C for 20 seconds and 72°C for 3 minutes, with a final extension of 72°C for 5 minutes; ***ccdA*** and ***pemI*** – an initial denaturation at 98°C for 30 seconds, followed by 35 cycles of 98°C for 10 seconds, 69°C for 20 seconds and 72°C for 20 seconds, with a final extension of 72°C for 2 minutes; **IS*26*** – an initial denaturation at 98°C for 30 seconds, followed by 35 cycles of 98°C for 10 seconds and a combined annealing and extension at 72°C for 40 seconds, with a final extension of 72°C for 2 minutes; and **KanRep** – an initial denaturation at 98°C for 30 seconds, followed by 35 cycles of 98°C for 10 seconds and a combined annealing and extension at 72°C for 1 minute, with a final extension of 72°C for 2 minutes. After using these primers unsuccessfully, the fragment ***ccdA_pemI*_IS*26*** was amplified using *ccdA* Fw and IS*26* Rv primers (**Table 2.7**), using an initial denaturation at 98°C for 30 seconds, followed by 35 cycles of 98°C for 10 seconds and a combined annealing and extension at 72°C for 60 seconds, with a final extension of 72°C for 2 minutes.

2.5.10.1 PCR to confirm plasmid assembly

PCR primers were designed to amplify products that would span the insertion sites and show that the plasmid had assembled properly. There were known as "sgRNA" and "Var"; and used the following reaction mixtures: 10 µl Q5® Hot Start High-Fidelity 2X Master Mix (NEB), 1 µl forward primer, 1 µl reverse primer, x µl template DNA (5-50 ng plasmid DNA), and the final volume was made up to 20 µl with the addition of nuclease-free water in a 0.2 mL PCR tube. PCR cycling conditions were as follows: an initial denaturation at 98°C for 30 seconds, followed by 35 cycles of 98°C for 10 seconds, 67°C for 20 seconds and 72°C for 40 seconds, with a final extension of 72°C for 2 minutes. A PCR to amplify across both insertion sites in one reaction was also used and contained the Var Fw and sgRNA Rv primers using an extension time of 2 minutes instead of 40 seconds.

2.5.11 Agarose gel electrophoresis

Unless specified otherwise, a 1% (w/v) gel was prepared by adding 0.5-2 g of agarose (Sigma-Aldrich) to 50-200 mL 1X TAE buffer. The agarose was dissolved by microwave heating. The agarose was cooled to around 50°C and ethidium bromide added to a final concentration of 0.5 µg mL^{-1} before being poured into a casting tray containing a well comb and allowed to cool to enable the gel to set. The set gel was transferred to a gel tank containing 1X TAE buffer and 5 µl of PCR product, or 50 µl for fragments used in Gibson assembly, was loaded into each well, with 5 µl of either 100 bp or 1 kb Quick-Load® DNA ladder (NEB)

added as a reference. PCR products generated using Q5® Hot Start High-Fidelity 2X Master Mix (**§2.5.10**) were mixed with Gel Loading Dye, Purple (NEB) in a 1:5 ratio of dye: product before loading. The agarose gel was electrophoresed at 100 V for 30 minutes, unless specified otherwise.

2.5.12 Gel visualisation

DNA was visualised and imaged using a UV trans illuminator (Gel Doc XR+, Bio-Rad).

2.5.13 Purification of PCR products

2.5.13.1 Purification by DNA purification kit

PCR products prepared for Sanger sequencing were purified using the Monarch® PCR & DNA Cleanup Kit (NEB). Briefly, the PCR product was diluted using Monarch® DNA Cleanup Binding Buffer and centrifuged at 16,000 x *g* for 1 minute through a spin column to bind the amplified DNA to the silica membrane. PCR reaction components were then removed by the addition of Monarch® DNA Wash Buffer, and DNA was eluted by centrifugation at 16,000 x *g* for 1 minute in 16 µl of nuclease-free water.

2.5.13.2 Purification by gel extraction

PCR products used for Gibson assembly were purified using the QIAquick® Gel Extraction Kit (Qiagen). Briefly, the PCR products were visualised using a UV

transilluminator (UPV TM-20, now Analytik Jena, Jena, Germany) following gel electrophoresis. DNA fragments were then excised from the agarose gel using a sterile scalpel and placed in a sterile 1.5 mL microcentrifuge tube. The weight of the gel fragment was determined and then a 3:1 volume of Buffer QG: agarose slice was added to the tube, followed by incubation at 50°C for 10 minutes to dissolve the agarose. Isopropanol was added to the solution and then DNA was bound to the silica membrane in a spin column by centrifugation. Buffer PE was used to wash through the spin column and DNA was then eluted in 30 µl nuclease-free water by centrifugation.

2.5.14 Sanger sequencing of purified PCR products

Purified PCR products were quantified using a Nanodrop 100 spectrophotometer (**§2.4.3.1**) and were sent to Eurofins Genomics for Sanger sequencing using the respective forward and reverse primer sequences in **§2.5.1**. Sequences were analysed using SnapGene (www.snapgene.com) and the Basic Local Alignment Search Tool (BLAST) (Altschul et al., 1990).

2.6 Conjugation of plasmids encoding carbapenem-resistance.

Isolates that harboured acquired carbapenemase genes and plasmid replicons were subject to a conjugation assay, in order to determine whether the identified plasmids were transmissible.

2.6.1 Recipient strains

Descriptions of the *E. coli* K-12 CV601 and J53 strains used in conjugation experiments can be found in **Table 2.1**.

2.6.2 Conjugation into *E. coli* CV601

A single colony of each isolate was inoculated into 20 mL LB broth supplemented with 2 µg mL^{-1} meropenem and incubated statically at 37°C for 18 hours. At the same time, a single colony of CV601 was inoculated into 20 mL LB broth and incubated at 37°C for 18 hours with shaking at 200 rpm. After incubation, triplicate cultures of the recipient were refreshed by inoculating 0.5 mL of overnight culture into 4.5 mL fresh LB broth and incubated at 37°C for 2.5 hours with shaking at 200 rpm. Triplicate 5 mL donor and refreshed recipient cultures were then centrifuged for 10 minutes at 1,487 x *g* (Hettich EBA 12R) and the resulting pellets were each resuspended in 5 mL DPBS. Centrifugation was performed once again, after which the pellets were resuspended in 500 µl of DPBS. This suspension was serially diluted ten-fold to 10^{-8}, and 100 µl of the 10^{-6}-10^{-8} dilutions were spread onto LB agar and incubated at 37°C for 18 hours to determine the number of donors and recipients per 100 µl of culture. One hundred microlitres of donor suspension was then mixed with an equal volume of recipient and gently mixed in a sterile microcentrifuge tube. Once mixed, 200 µl of the donor and recipient mixture was inoculated onto an LB agar plate as a single spot, followed by incubation

for 18 hours at 37°C. The following day, 1.5 mL PBS was added to the agar plates and the spot was retrieved by using a sterile spreader to mix the entire bacterial culture with PBS, which was then transferred to a 1.5 mL microcentrifuge tube. This suspension was serially diluted ten-fold to 10^{-4} and 100 µl of each dilution was spread onto LB agar supplemented with 50 µg mL^{-1} kanamycin, 50 µg mL^{-1} rifampicin and 2 µg mL^{-1} meropenem and incubated at 37°C for 18 hours. Ten colonies from each replicate plate (30 colonies in total from 3 replicates), were patch plated onto separate LB agar plates containing 1) rifampicin and kanamycin and 2) meropenem, and these plates were incubated at 37°C for 18 hours. Replicate colonies that were capable of growth on both antimicrobial-supplemented agars were presumed to be transconjugants. To confirm this, DNA extractions were performed (**§2.4.1**), and these were used in PCR reactions to detect the presence of the genes bla_{NDM} and GFP (**§2.5**). Confirmed transconjugants were subjected to antibiotic sensitivity testing as detailed in **§2.3.1**, to determine the resistances to antibiotics conferred by the conjugated plasmid.

2.6.3 Conjugation into *E. coli* J53 Azi^R

For IS*26* mobilisation, the plasmid pDD128_IncF was conjugated into *E. coli* K-12 J53 Azi^R, as both the original isolate and CV601 are resistant to kanamycin, which was the desired selection mechanism for further transformation experiments. These experiments used a modified method from that detailed in

§2.6.2; in these the selective agar plates used contained 100 µg mL^{-1} sodium azide in place of the kanamycin and rifampicin antibiotics.

2.6.4 Determination of efficiency of conjugation

Efficiency of conjugation was determined using the following formula:

$$Efficiency\ of\ conjugation = \frac{CFU\ ml^{-1}\ of\ transconjugants}{CFU\ ml^{-1}\ of\ donors}$$

2.7 IS*26* mobilisation

2.7.1 Preparation of electrocompetent *E. coli* cells

An overnight culture of recipient *E. coli* CV601 or J53 Azi^R cells was freshly grown by transferring 100 µl of overnight culture into an 9.9 mL of sterile LB broth and incubating for ~2.5 hours at 37°C with shaking at 200 rpm, until the culture reached an optical density of 0.4 at 600 nm. 1 mL of this culture was transferred to a 1.5 mL microcentrifuge tube and centrifuged at 20,000 x *g* for 30 seconds at 4°C (1-16k, Sigma Laboratory Centrifuges, Osterode, Germany). The bacterial pellet was resuspended in 1 mL of sterile ice-cold 10% glycerol and centrifuged again. This step was repeated once more. Finally, the washed bacterial cell pellet was resuspended in 40 µl ice-cold 10% glycerol and either placed on ice to be used immediately or stored at -80°C for future use.

2.7.2 Transformation of plasmid DNA into electrocompetent cells

50 ng of plasmid DNA was added to a 40 µl aliquot of electrocompetent *E. coli* cells and transferred to a pre-chilled 2 mm electrode gap electroporation cuvette (FBR-202, Flowgen Bioscience, Hessle, UK). This transformation mixture was electroporated at 2,500 V with a time constant of 4 ms (Eppendorf Electroporator 2510, Eppendorf). 960 µl of SOC medium (**§2.1.2.8**) pre-warmed to 37°C was immediately added and the electroporated cell culture was incubated at 37°C for 1 hour. One hundred microlitre dilutions of this electroporated culture were spread onto LB agar supplemented with the relevant antibiotic and incubated at 37°C for 18 hours.

2.7.3 Plasmid curing using pCURE2

Attempts were made to cure IncF plasmids from transconjugant DD128J53 using the plasmid pCURE2 (Hale et al., 2010). The plasmid was purified via MiniPrep (**§2.4.4**), and transformed into electrocompetent DD128J53 cells (**§2.7.1** and **§2.7.2**). PCR detection of the IncP *oriT* gene (**§2.5.8**) was used to confirm transformation of pCURE2 into recipient cells, while PCR detection of IncF replicons was used to detect plasmid curing (**§2.5.5**).

2.7.4 Patch plating of transconjugants.

A patch plating method was used to confirm that transformants contained pCURE2. Putative transconjugant colonies were streaked onto numbered sections of multiple agar plates, containing meropenem, kanamycin and 5% sucrose separately. Colonies were counted as transformants if they were able to grow on agar containing kanamycin and not able to grow on agar containing sucrose.

2.7.5 Design of pFREE_IncF plasmids

The plasmid pFREE (**Figure 2.1**) (Lauritsen et al., 2017) was used as a template to create pFREE_IncF (**Figure 2.2**), which was made up of six DNA fragments: the CasTet region containing the clustered regularly interspaced short palindromic repeats (CRISPR)-Cas9 gene from *Streptococcus pyogenes* and TetR repressor amplified from pFREE; the KanRep region containing the kanamycin resistance gene and ColA replicon also amplified from pFREE; *pemI* containing the *pemI* antitoxin gene found on environmental plasmid pDD128_IncF (**§4.2.4**); the *ccdA* region containing the *ccdA* antitoxin gene found on pDD128_IncF; the IS*26* region containing the IS*26* gene found on pDD128_IncF; and single guide RNA (sgRNA) region containing the sgRNA array from pFREE, with the spacers replaced with ones to target IncF replicons. Two further plasmids were also designed: pFREE_IncF_No_Ats that did not contain the *pemI* and *ccdA* regions to test whether the antitoxin genes were necessary

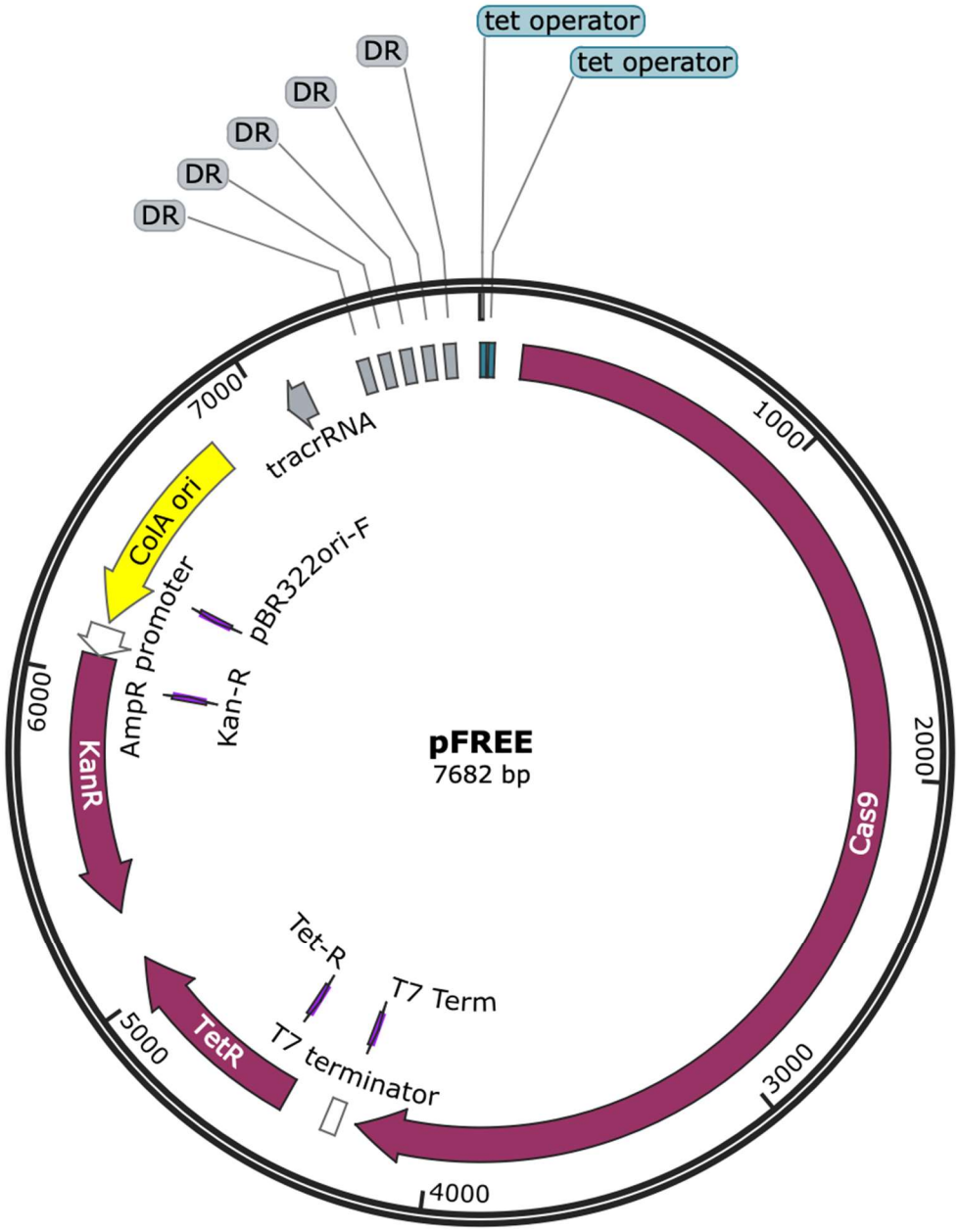

Figure 2.1. Plasmid map of unmodified pFREE (Lauritsen et al., 2017). CRISPR-Cas9 guide RNAs are located between direct repeats labelled "DR". The plasmid contains the TetR repressor for inducible Cas9 expression, as well as kanamycin resistance gene *aph(3')-I* as a selectable marker.

for the cells to survive curing of the IncF plasmid; and pFREE_IncF_No_IS*26* that did not contain the IS*26* region to show that rates of IS*26* mobilisation were lower when the recipient plasmid did not contain an IS*26* gene. The plasmids

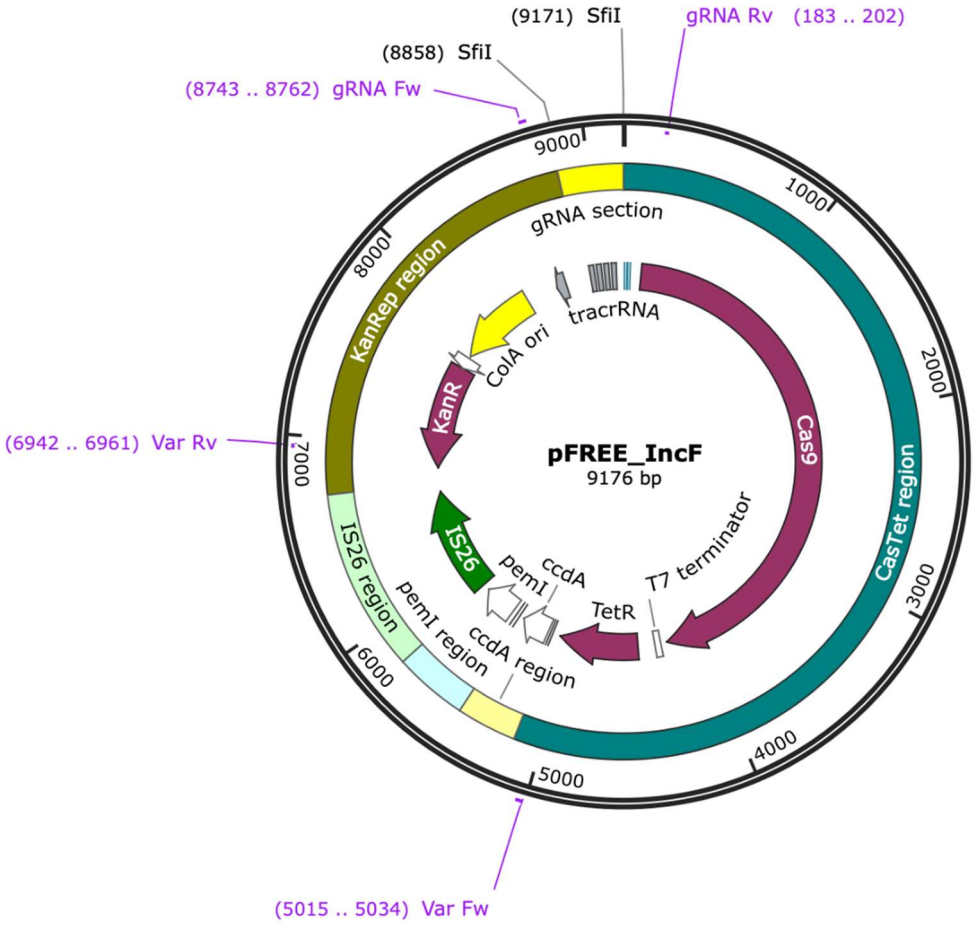

Figure 2.2. Plasmid map of modified plasmid pFREE_IncF, derived from pFREE. KanRep and CasTet regions were amplified by PCR using pFREE as template, *ccdA*, *pemI* and IS*26* regions were amplified by PCR using environmental plasmid pDD128_IncF as template, and sgRNA section was synthesised by Thermo Fisher Scientific and digested using SfiI. Final plasmid was assembled using Gibson assembly. Primers for sgRNA and Var sections were used to check the inserts were assembled properly. Primers Var Fw-sgRNA Rv were used to check complete assembly.

were designed to be assembled using Gibson assembly (Gibson et al., 2009), which uses DNA fragments with overlapping regions of homology at their ends. The reaction mixture contains a DNA exonuclease, DNA polymerase and DNA ligase. The exonuclease creates overhangs at the 5' end of each fragment that allows the created single stranded ends to anneal; the polymerase fills the gaps

produced by this process, and the ligase seals the DNA strands resulting in an unbroken molecule of DNA comprised of the various designed fragments.

2.7.5.1 Design of CRISPR-Cas9 guide RNA

Available sequences of the IncFII (FII_1-114), IncFIA (FIA_1-25) and IncFIB (FIB_1-78) replicons were downloaded from PubMLST.org (Jolley, Bray and Maiden, 2018) and aligned using MUSCLE in SnapGene with default settings (Edgar, 2004). The FII, FIA and FIB consensus (with ambiguous bases input as in FII_2, FIA_4 and FIB_32 respectively) sequences were used as inputs in the Custom Alt-R™ CRISPR-Cas9 guide RNA design tool to generate potential sgRNA target sequences (Integrated DNA Technologies). The 5 potential sgRNA sequences with the highest on-target score were compared to the replicon alignments to select the sequence with 100% identity to the highest number of replicons. All generated sequences were screened against bacterial chromosomal assemblies to check for potential off-target matches with ≥90% sequence identity. The final sgRNA array was synthesised by Thermo Fisher Scientific and incorporated into a plasmid that can be seen in **Figure 2.3**.

2.7.5.2 Promoter prediction for antitoxin genes

The online tool BPROM was used to predict promoter sequences upstream of the *ccdA* and *pemI* ORFs, so that these could be incorporated into the amplified sequences (Solovyev and Salamov, 2011).

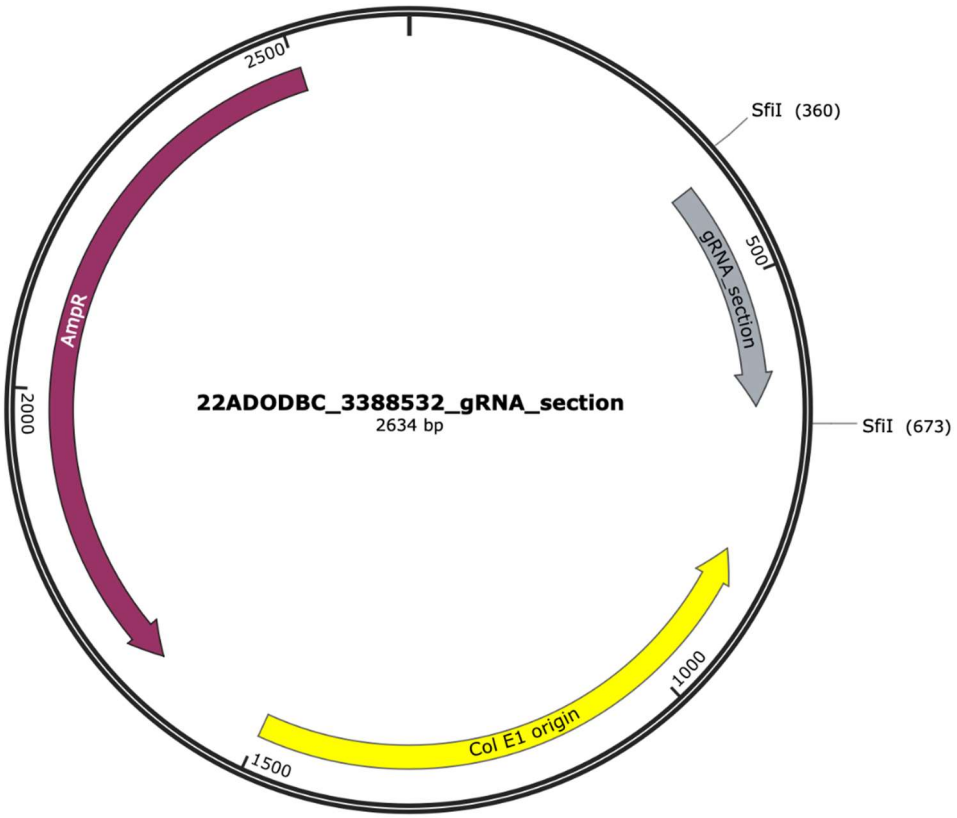

Figure 2.3. Plasmid map of synthesised sgRNA array contained within a pMA-RQ (AmpR) plasmid vector. This sgRNA section is flanked by SfiI restriction sites which were used to digest the plasmid and purify the sgRNA section.

2.7.5.3 Primer design for Gibson assembly

Primers were designed using the NEBuilder® Assembly Tool (v. 2.7.0) (https://nebuilder.neb.com/) using a minimum overlap of 25 nucleotides and a minimum primer length of 18 nucleotides. The sgRNA section was originally planned to be amplified by PCR, but upon synthesis of the fragment this was changed to be by plasmid extraction and restriction digest by SfiI. The primers for the fragments either side were modified to reintroduce the SfiI target sites, so that the sgRNA array could be easily replaced in any future modifications of the plasmid. The final fragment sizes can be found in **Table 2.8**.

Table 2.8. Fragments used in Gibson assembly of pFREE_IncF

Fragment	Size (bp)
CasTet region	5138
ccdA region	300
pemI region	368
IS*26* region	912
KanRep region	2132
sgRNA region	326
ccdA – IS*26* region	1606

2.7.6 Digestion of sgRNA section using SfiI

Plasmid DNA was extracted via Miniprep (**§2.4.4**) and quantified using a Nanodrop 1000 spectrophotometer (**§2.4.3.1**) before SfiI digestion (NEB). The restriction enzyme mixture contained 1 µl SfiI (20,000 units mL^{-1}), 5 µl NEB rCutSmart™ Buffer, 1 µg plasmid DNA, and was made up to a final volume of 50 µl using nuclease-free water in a 0.2 µl tube. This mixture was incubated in a water bath at 50°C for 15 minutes, followed by gel electrophoresis and DNA purification of the correct band size via gel extraction (**§2.5.13.2**). The resulting purified DNA was quantified using a Nanodrop spectrophotometer and stored at 2-8°C.

2.7.7 Gibson assembly of pFREE_IncF

DNA fragments generated in **§2.5.10** were combined with the digested DNA fragment from **§2.7.6** to create pFREE_IncF using the NEBuilder® HiFi DNA Assembly Cloning Kit (NEB). The assembly mixture contained varying amounts of each DNA fragment (**§5.2.5**), 10 µl NEBuilder® HiFi DNA Assembly Master

Mix (2X) and was made up to a final volume of 20 µl using nuclease-free water in a 0.2 mL tube. The assembly mixture was incubated in a thermal cycler (Bio-Rad, C1000) at 50°C for 1 hour and then placed on ice.

2.7.8 Transformation of HiFi Assembly mixture into chemically competent cells

DNA from the assembly mixture (**§2.7.7**) was transformed into chemically competent *E. coli* K-12 DH5α cells supplied with the NEBuilder® HiFi DNA Assembly Cloning Kit (**Table 2.1**). Two microlitres of the assembly mixture was added to 50 µl of chemically competent DH5α cells that had been thawed on ice. After 30 minutes incubation on ice, the cells were subjected to heat shock by immersion in a water bath for 30 seconds at 42°C, and then placed back on ice for 2 minutes. 950 µl of ambient temperature SOC Outgrowth Medium (**§2.1.2.9**) was added to the cells, followed by incubation at 37°C for 1 hour with shaking at 300 rpm. Dilutions were then spread onto pre-warmed LB agar plates supplemented with 50 µg mL^{-1} kanamycin and incubated at 37°C for 18 hours.

2.7.9 Extraction of pFREE-IncF from DH5α

Single colonies from **§2.7.8** were streaked onto LB agar plates supplemented with 50 µg mL^{-1} kanamycin and incubated at 37°C for 18 hours. Plasmids were extracted from these cultures via Miniprep (**§2.4.4**), quantified by NanoDrop

1000 spectrophotometer (**§2.4.3.1**) and checked for correct assembly via PCR (**§2.5.10.1**) as shown by the primer sites in **Figure 2.2**.

2.7.10 Sequencing of constructed plasmids

Plasmid extractions were quantified using a Qubit 3 Fluorometer (**§2.4.3.2**) and analysed using long-read sequencing conducted by Plasmidsaurus (https://www.plasmidsaurus.com/).

2.7.11 Transformation of pFREE-IncF into DD128J53

Plasmids were then transformed into an electrocompetent transconjugant (**§2.6.3** and **§2.7.1**) as in **§2.7.2**, with the use of LB agar supplemented with 50 µg mL^{-1} kanamycin to select for transformants in place of ampicillin. Single colonies from these plates were streaked onto LB agar plates supplemented with 50 µg mL^{-1} kanamycin, followed by DNA extraction (**§2.4.1**) and PCR detection of both IncFII and *colA* plasmid replicons (**§2.5.5** and **§2.5.9**).

2.7.12 Induction of the CRISPR-Cas9 system in pFREE-IncF

To determine that the CRISPR-Cas9 system was able to target and cleave the intended plasmid DNA, a single colony of transconjugant transformant was suspended in 100 µl MRD, and 10 µl of this suspension was used to inoculate sterile LB broth supplemented with various combinations of antibiotics and

inducers. These were as follows: 50 µg mL^{-1} kanamycin, both 50 µg mL^{-1} kanamycin and 2 µg mL^{-1} meropenem, and LB broth without supplement, all additionally containing 0.2% rhamnose and 200 ng mL^{-1} anhydrotetracycline (aTc); while the same supplements without rhamnose and aTc were used as controls. These broths were incubated at 37°C for 18 hours with shaking at 200 rpm. Each culture was diluted ten-fold and 100 µl of each dilution was spread onto LB agar containing the following supplements: 50 µg mL^{-1} kanamycin, 2 µg mL^{-1} meropenem, both 50 µg mL^{-1} kanamycin and 2 µg mL^{-1} meropenem, and LB broth without supplement. These plates were incubated at 37°C for 18 hours and colonies were counted the next day. A select number of single colonies were subcultured onto LB agar and incubated at 37°C for 18 hours, followed by DNA extraction (**§2.4.1**) and detection of FII, FIA, *colA* and bla_{NDM} genes by PCR (**§2.5**). Isolates where *colA* and bla_{NDM} were detected but no IncF replicons were present were suspected positive for IS*26* mobilisation.

2.8 Whole Genome Sequencing

2.8.1 External supplier sequencing

Genome sequencing was conducted by MicrobesNG (http://www.microbesng.com). Isolates to be sent for short-read sequencing were first grown on LB agar incubated overnight at 37°C. One colony from each plate was inoculated into 100 µl DPBS and a 10 µl loop was used to streak onto

LB agar. This was done in such a way that around one third of the plate would be covered by a lawn of bacteria, while the rest was used to streak for single colonies. This was used both as a purity check and to grow enough bacteria to be harvested for sequencing. After overnight incubation at 37°C, a loop was used to transfer all the bacterial culture from the plate to barcoded Microbank™ tubes provided by MicrobesNG, which were then sent at ambient temperature to arrive at MicrobesNG within two days.

Isolates sent for combined long and short-read sequencing were grown as above until the inoculation into 100 µl DPBS step. A loop was then used to streak for single colonies onto LB agar, and the remaining liquid was inoculated into flasks containing 20 mL LB broth supplemented with 2 µg mL^{-1} meropenem. These were then incubated overnight at 37°C at 200 rpm. The LB plates were used to determine that the cultures were pure, and the optical density of the broth was measured at 600 nm. These readings were used to determine the amount of culture to be harvested, such that the total amount of bacteria would equate to at least 5 x 10^9 cells, or OD_{600} of 10.0. Cells were then centrifuged at 1,487 x *g* for 5 minutes (Hettich EBA 12R), washed in 1 mL PBS, centrifuged again, and resuspended in 0.5 mL 1 x DNA/RNA Shield (Zymo Research, Irvine, CA, USA) in 1.5 mL microcentrifuge tubes. These were packaged and sent to MicrobesNG as above.

A copy of the MicrobesNG sequencing and bioinformatics methods can be found here (MicrobesNG, 2021). Briefly, cells were lysed, and genomic DNA was purified using SPRI beads, followed by quantification using a Quant-iT dsDNA HS kit (Thermo Fisher Scientific). Genomic DNA libraries were prepared

using the Nextera XT Library Prep Kit (Illumina, Cambridge, UK) and quantified by the Kapa Biosystems Library Quantification Kit (Sigma-Aldrich). Sequencing was performed on Illumina sequencers (HiSeq/NovaSeq) with a 250 bp paired end protocol. Reads underwent adapter trimming using Trimmomatic followed by *de novo* assembly via SPAdes and annotation using Prokka (Bankevich et al., 2012; Bolger, Lohse and Usadel, 2014; Seemann, 2014).

For the enhanced genome service, in addition to the methods described above, long-read genomic libraries were prepared with the SQK-LSK109 kit (Oxford Nanopore Technologies (ONT), Oxford, UK) using 400-500 ng of high molecular-weight DNA. Barcoded samples were pooled together into a single sequencing library and loaded onto a flow cell in a GridION sequencer (ONT). Reads were trimmed using Trimmomatic; enhanced assembly was performed using Unicycler, and this was also annotated using Prokka (Bolger, Lohse and Usadel, 2014; Seemann, 2014; Wick et al., 2017b).

2.8.2 In-house sequencing

Ten presumptive IS*26* mobilised isolates were selected for long-read sequencing to confirm that mobilisation had occurred, alongside the original pFREE_IncF transformed transconjugant as a control. Since MicrobesNG did not perform sequencing on genetically modified organisms, this was performed within the laboratory using the ONT MinION sequencer on a R10.4.1 flow cell. Additionally, since data encompassing more than eleven bacterial genomes can reliably be generated using a multiplex barcoding kit, all

transconjugants were also selected for sequencing. Finally, two isolates that had only undergone short-read sequencing by MicrobesNG were selected so that better plasmid assemblies could be generated using long-read data. All reagents in this section were supplied by ONT unless specified otherwise.

2.8.2.1 DNA repair and end-prep

For each isolate to be sequenced, DNA extractions from **§2.4.2** were quantified using a Qubit 3 fluorometer (**§2.4.3.2**), and 400 ng gDNA was prepared in a total volume of 11 µl. This DNA sample was combined with 1 µl Diluted DNA Control Sample, 0.875 µl NEBNext® FFPE DNA Repair Buffer, 0.875 µl Ultra II End-prep Reaction Buffer, 0.75 µl Ultra II End-prep Enzyme Mix and 0.5 µl NEBNext® FFPE DNA Repair Mix (NEB) in a 0.2 mL PCR tube. The reagents were mixed by flicking the tube, and it was briefly centrifuged (Mini Fuge PLUS, STARLAB) then incubated in a thermal cycler at 20°C for 5 minutes followed by 65°C for 5 minutes. 15 µl of resuspended AMPure XP Beads was added to each tube and mixed by flicking gently, followed by incubation on a rotator mixer (PTR-60, Grant Instruments) at ambient temperature for 5 minutes. The samples were briefly centrifuged and placed on a NEBNext® Magnetic Separation Rack (NEB) until a pellet formed. The supernatant was removed and 200 µl of freshly prepared 80% (v/v) ethanol was used to wash the beads whilst they remained in the 0.2 mL PCR tube on the magnetic rack and then removed. This wash step was repeated once more, then the 0.2 mL tubes were briefly centrifuged and placed back on the magnetic rack and the pellets allowed to dry for 30 seconds. The tubes were removed from the magnetic rack and the

pellets were resuspended in 10 µl nuclease-free water, centrifuged briefly and incubated at ambient temperature for 2 minutes. Finally, the tubes were placed back on the magnetic rack until the eluate was clear and colourless. The suspended samples were then aspirated and transferred to a clean 1.5 mL DNA LoBind tube (Eppendorf).

2.8.2.2 Native barcode ligation

End-prepped DNA was quantified using a Qubit 3 fluorometer (**§2.4.3.2**), and an equal concentration of each sample was used for barcode ligation using the Native Barcoding Kit 24 V14 (SQK-NBD114.24). Each sample was assigned a unique barcode and 7.5 µl end-prepped DNA was added to 2.5 µl native barcode and 10 µl Blunt/TA Ligase Master Mix (NEB) in a 0.2 mL PCR tube. The reagents were mixed by gently flicking the tubes, briefly centrifuged and incubated at ambient temperature for 20 minutes. 2 µl of EDTA was then added to each tube and mixed by flicking to stop the ligation reaction. The barcoded samples were pooled together in a clean 1.5 mL DNA LoBind tube and mixed with 0.4X AMPure XP Beads. This tube was mixed by flicking and incubated on a rotator mixer (PTR-60, Grant Instruments) at ambient temperature for 10 minutes. After a brief centrifugation, the tube was placed on a MagneSphere® Technology Magnetic Separation Stand (Promega, Southampton, UK) for 5 minutes, until a pellet formed. The supernatant was removed and 700 µl of freshly prepared 80% (v/v) ethanol was used to wash the beads whilst they remained on the magnetic rack. While still on the rack, the supernatant was again removed and this wash and supernatant removal

step was repeated once more, then the tube was briefly centrifuged and placed back on the magnetic rack and the pellet allowed to dry for 30 seconds. The tube was removed from the magnetic rack and the pellet resuspended in 35 µl nuclease-free water by gentle flicking. The tube was incubated at 37°C for 10 minutes, with gentle flicking for 10 seconds every 2 minutes to encourage DNA elution. Finally, the tube was placed back on the magnetic rack until the eluate was clear and colourless, when it was extracted and transferred to a clean 1.5 mL DNA LoBind tube.

2.8.2.3 Adapter ligation and clean-up

30 µl of pooled barcode sample was mixed with 5 µl Native Adapter, 10 µl NEBNext® Quick Ligation Reaction Buffer (5X) and 5 µl Quick T4 DNA Ligase (NEB) in a clean 1.5 mL DNA LoBind tube and incubated at ambient temperature for 20 minutes. 20 µl of resuspended AMPure XP Beads were added to the tube and mixed by flicking, followed by incubation on a rotator mixer (PTR-60, Grant Instruments) at ambient temperature for 10 minutes. The tube was briefly centrifuged and placed on the magnetic rack until a pellet formed. The supernatant was removed, and the pellet was washed by resuspending it in 125 µl of Long Fragment Buffer by gentle flicking, then returned to the magnetic rack until a pellet formed. This wash step was repeated once more, then the tube was briefly centrifuged and placed back on the magnetic rack and the pellet allowed to dry for 30 seconds. The tube was removed from the magnetic rack and the pellet resuspended in 15 µl Elution Buffer by gentle flicking. The tube was incubated at 37°C for 10 minutes, with

gentle flicking for 10 seconds every 2 minutes to encourage DNA elution. Finally, the tube was placed back on the magnetic rack until the eluate was clear and colourless, when it was then extracted and transferred to a clean 1.5 mL DNA LoBind tube.

2.8.2.4 Library quantification and size determination

The amount of DNA was determined by quantification using a Qubit 3 fluorometer (**§2.4.3.2**), and average fragment size was determined using an Agilent 2200 TapeStation system (**§2.4.3.3**). These values were used to determine the molar amount of DNA using the following formula, where Q is the quantity of DNA and N is the average size:

$$Q\ \mu g \times \frac{pmol}{660\ pg} \times \frac{10^6}{1\ \mu g} \times \frac{1}{N} = x\ pmol$$

The library was adjusted to 10-20 fmol in 12 µl by the addition of Elution Buffer and stored on ice until ready to load onto the flow cell.

2.8.2.5 Priming and loading the MinION flow cell

Flow cell priming mix was prepared by adding 5 µl of 50 mg mL^{-1} Bovine Serum Albumin (Thermo Fisher Scientific) and 30 µl Flow Cell Tether to 1170 µl Flow Cell Flush, and the solution was mixed by pipette. After removing any bubbles from the priming port, 800 µl of the priming mix was loaded onto the flow cell via the priming port and then incubated at ambient temperature for 5 minutes. During this time, 12 µl of DNA library was mixed with 25.5 µl resuspended Library Beads and 37.5 µl Sequencing Buffer to prepare the library for loading.

After the incubation time, the SpotON sample port cover was opened and a further 200 µl priming mix loaded into the priming port. Immediately after this step, the library was mixed by gently pipetting up and down and loaded onto the flow cell via the SpotON sample port in a dropwise fashion. The sequencing experiment was started using the MinKNOW software from ONT (v. 22.12.7) until the required coverage was achieved, assuming an average genome size of 5 Mb.

2.8.2.6 Flow cell wash

Between sequencing experiments, the flow cell underwent a wash procedure to eliminate DNA from previous samples. A flow cell wash mix was prepared by combining 2 µl of Wash Mix with 398 µl of Wash Diluent and mixed by pipette before being placed on ice. Subsequently, all liquid was removed from the flow cell waste port and then the wash mix was loaded onto the flow cell via the priming port. After 1 hour, all liquid was again removed from the flow cell waste port and then 500 µl of Storage Buffer was loaded onto the flow cell via the priming port. Finally, all liquid was once more removed from the flow cell waste port, and the flow cell was stored at 4°C until the next sequencing experiment.

2.9 Bioinformatics tools

2.9.1 Assembly and annotation of whole genome sequences

All sequencing runs were operated through MinKNOW. Basecalling was also performed through MinKNOW using the FLO-MIN114 DNA Kit (400 bps) - Fast settings. Reads were de-multiplexed using the native barcode sequences and assigned as passed or failed reads based on their quality score by MinKNOW. Passed read files were concatenated and the adapter sequences removed using PoreChop (Wick et al., 2017a). Read files were quality checked using FastQC (v. 0.12.0) (Andrews, 2010) and long-read only assemblies were generated using Flye (v. 2.9.2) (Kolmogorov et al., 2019). Assemblies were polished using medaka (v. 1.0.3) (Oxford Nanopore Technologies), analysed using Quast (v. 5.0.2) (Gurevich et al., 2013), and then annotated using Prokka (v. 1.14.6) (Seemann, 2014). Where previous short-read sequences existed for the same isolate, hybrid assemblies were instead generated using Unicycler (v. 0.4.8) (Wick et al., 2017b), followed by polishing and annotation via medaka and Prokka respectively.

2.9.2 Post-assembly processing of whole genome sequences

2.9.2.1 ResFinder and PointFinder

Assemblies of sequenced isolates were screened for acquired genes and point mutations that confer antimicrobial resistance using ResFinder and PointFinder

(v. 4.1) with default settings (Camacho et al., 2009; Zankari et al., 2017; Bortolaia et al., 2020).

2.9.2.2 Multi Locus Sequence Typing (MLST)

Predicted sequence types of sequenced isolates were determined by inputting the assemblies into MLST (v. 2.0.9) (Wirth et al., 2006; Jaureguy et al., 2008; Camacho et al., 2009; Larsen et al., 2012).

2.9.2.3 Core Genome Multi Locus Sequence Typing

Core Genome Multi Locus Sequence Type (cgMLST) was determined using cgMLSTFinder 1.2 (v. 1.0.1) using the Enterobase database (Clausen, Aarestrup and Lund, 2018; Zhou et al., 2020).

2.9.2.4 PlasmidFinder

Plasmid replicons were detected in assemblies using PlasmidFinder 2.1 (v. 2.0.1) using the Enterobacterales database with default settings (Camacho et al., 2009; Carattoli et al., 2014).

2.9.2.5 Plasmid MultiLocus Sequence Typing

Plasmid multilocus sequence typing (pMLST) analysis of the assembled genomes was performed using pMLST 2.0 (v. 0.1.0) (Carattoli et al., 2014).

2.9.2.6 The Comprehensive Antibiotic Resistance Database Resistance Gene Identifier

Antimicrobial resistance genes of genome assemblies were also predicted using the Resistance Gene Identifier web portal from the Comprehensive Antibiotic Resistance Database (CARD) (Alcock et al., 2020). The criteria used was set to Perfect, Strict and Loose hits including ≥95% identity Loose hits to be deemed as Strict.

2.9.2.7 Genome comparisons

Similarity of plasmids with any previously described plasmid was determined by performing a Mash (v. 2.3) distance search against the Plasmid Database (PLSDB) with the PLSDB webserver (v. 2021_06_23_v2) (Ondov et al., 2016; Galata et al., 2019; Schmartz et al., 2022) and BLAST (Altschul et al., 1990). Core genome alignments were performed using Roary (v3.13.0) (Page et al., 2015), and a phylogenetic tree was made using Mashtree (v0.37) (Katz et al., 2019). Sequence comparison images were created with BLAST Ring Image Generator (BRIG) (Alikhan et al., 2011), Easyfig (Sullivan, Petty and Beatson, 2011), and SnapGene (www.snapgene.com). Comparisons of SNPs between isolates were performed using snippy (Seemann, 2015) through the Galaxy platform (The Galaxy Community, 2024).

CHAPTER 3: PHENOTYPIC AND GENOTYPIC IDENTIFICATION OF CEPHALOSPORIN AND CARBAPENEM-RESISTANT BACTERIA IN WASTEWATER

3.1 Introduction

One of the key recommendations of the Review on Antimicrobial Resistance chaired by Jim O'Neill was for increased surveillance of AMR (O'Neill, 2016). One way to achieve this is the analysis of the influent of wastewater treatment plants (WWTPs), a concept first proposed in the 1970s (Grabow and Prozesky, 1973; Linton et al., 1974). Now known as wastewater-based epidemiology, a number of studies in recent years have used this method to monitor the levels of SARS-CoV-2 in local human populations (Barcellos et al., 2023).

It has been shown that the increasing levels of AMR in the human population is mirrored by increasing levels of resistance found in local WWTPs (Reinthaler et al., 2013; Kwak et al., 2015), and recent studies have found that WWTPs contain high levels of ESBL producing *E. coli,* predominantly of the CTX-M type (Korzeniewska and Harnisz, 2013; Bréchet et al., 2014). Furthermore, as acquired carbapenem resistance spreads around the globe, mobile carbapenemase genes have been detected in WWTPs in many different countries, including China, India, Japan, Saudi Arabia, South Africa, the United States, the United Kingdom and multiple sites across Europe (Mantilla-Calderon et al., 2016; Yang et al., 2016; Codjoe and Donkor, 2017; Ludden et al., 2017; Subirats et al., 2017; Zurfluh et al., 2017; Lamba et al., 2018; Proia et al., 2018; Cahill et al., 2019; Hoelle et al., 2019; Sekizuka et al., 2019; Alexander, Hembach and Schwartz, 2020; Ebomah and Okoh, 2020; Makowska et al., 2020; Flach et al., 2021).

Recent focus on the One Health approach to AMR has also highlighted the importance of WWTPs, as release of both treated and untreated sewage into receiving waters may be one of the main sources of AMR dissemination into the environment via the spread of Antimicrobial Resistant Bacteria (ARB) as well as antimicrobials themselves (Bouki, Venieri and Diamadopoulos, 2013; Rizzo et al., 2013). The concentration below which an antimicrobial is predicted to have no effect on selection for resistance is known as the Predicted No Effect Concentration (PNEC) (Bengtsson-Palme and Larsson, 2016), and studies have shown that concentrations of antimicrobials above the PNEC but well below the MIC for a particular organism still drive the selection of antimicrobial resistance genes (ARGs) (Sandegren, 2014; Jutkina et al., 2016, 2018). During water treatment within WWTPs, although total numbers of bacteria are shown to be lower in the effluent than the influent, in some cases the relative abundance of specific ARGs is found to be higher (Alexander et al., 2015; Amador et al., 2015; Hiller et al., 2019). A recent investigation into the impact of wastewater treatment in the UK suggests that this may be dependent on the specific WWTPs and ARGs. It was found that macrolide and tetracycline genes were less prevalent in effluent when compared to influent, while the relative abundance of *qacEΔ1* genes increased. The relative abundance of other genes such as *sul1*, *qnrS* and *intI1* differed depending on the particular WWTP site (UKWIR, 2022).

Diversity and abundance of AMR genes varies geographically, and the analysis of wastewater has been proposed as an economically and ethically feasible way to survey the local prevalence of AMR (Hendriksen et al., 2019). All CPE isolated

from municipal wastewater in the UK to date have been collected from treatment plants downstream of hospitals. Two studies have isolated CPE from UK municipal wastewater directly (Ludden et al., 2017; Gibbon et al., 2021). Another study sampled hospital wastewater effluent and detected multiple CPE strains (White et al., 2016); while carbapenemase genes have also been detected in metagenomes from UK municipal wastewater samples (Chau et al., 2023). Of the previous studies on municipal wastewater, Ludden et al. (2017) sampled multiple WWTPs across East Anglia on a single occasion, Gibbon et al. (2021) sampled hospital and municipal wastewater over the course of a week, while Chau et al. (2023) took samples for metagenomic sequencing over the course of three days. The present study aimed to expand on this existing knowledge by sampling in a geographical area not yet studied for the presence of CPE using a longer timeframe to better understand the prevalence of CPE in UK wastewater.

3.1.1 Aims and objectives

The aim of this study was to investigate the presence of ESBL and carbapenemase-producing *Enterobacteriaceae* (CPE) in the raw and treated sewage of two WWTPs in the East Midlands, one of which is downstream of a major hospital. Samples were also taken from the receiving waters into which the WWTPs discharge, to determine whether any resistant bacteria found in the effluent could also be detected further downstream. The main objective was to determine if carbapenemase-producing bacteria and cephalosporin-

resistant *Enterobacteriaceae* could be isolated from any of the samples taken, and to determine and compare the AMR profiles of any such bacteria.

3.2 Results

3.2.1 Isolation of cephalosporin-resistant bacteria

Samples were collected from: i) a small WWTP, referred to as WWTP A, that serves a university campus as well as a village with a population of circa 2000 people; and ii) a large WWTP B downstream of a major hospital that serves a population of circa 620,000 people. Samples were collected on five occasions between October 2019 and March 2020, and two further occasions between May and July 2022.

A total of 158 colonies were subcultured from multiple samples that were divided into: 61 isolates from agars selective for cephalosporin resistance, and 97 isolates from agars selective for carbapenem resistance. Colonies were chosen from selective chromogenic plates that matched the diagnostic characteristics of *Enterobacteriaceae*: purple colonies on MacConkey, blue (*Klebsiella*) or pale pink (*E. coli*) from Brilliance™ CRE agar and mSuperCARBA, and blue colonies from TBX agar (**§2.2.2**). The isolates were subject to analysis as shown in **Table 3.1**.

The cephalosporin resistant isolates were collected from the influent of WWTP A (n=33), the effluent of WWTP B (n=16), and the river into which WWTP B discharges (n=12). 30 isolates were presumptively identified as *E. coli* based on

Table 3.1. Breakdown of the analysis performed on different groups of isolates.

Antibiotic selection	Family	No. of isolates	Analysis
Cephalosporin	*Enterobacteriaceae*	40	AST, PCR
	Non-replicate	38	χ^2
	Non-*Enterobacteriaceae*	21	AST, PCR
Carbapenem	*Enterobacteriaceae*	59	AST, PCR
	Non-replicate	34	χ^2
	CPE	20	MIC
	Unique CPE	18	Conjugation assays, **WGS**
	Non-*Enterobacteriaceae*	38	AST, PCR
	Carbapenem-hydrolytic	8	MIC
	Carbapenemase-producing	1	**WGS**

Indented values indicate a subset of the isolates. All isolates underwent antimicrobial susceptibility testing (AST) and PCR detection of plasmid replicon and antimicrobial resistance genes. Data from non-replicate isolates was used in a Chi-squared test of association (χ^2). All carbapenem-hydrolytic isolates were used in minimum inhibitory concentration (MIC) assays. Unique carbapenemase-producing isolates were subjected to whole genome sequencing (WGS) (**Chapter 4**). Carbapenemase-producing *Enterobacteriaceae* (CPE) refers to *Enterobacteriaceae* isolates that have been confirmed to hydrolyse carbapenems and contain a carbapenemase gene. Unique CPE refers to those that have unique plasmid replicon and antimicrobial resistance gene PCR results from others isolates from the same sample.

positive indole and negative oxidase results (**§2.2.5** and **§2.2.6**). 16S rRNA sequencing (**§2.5.7**) was carried out to determine the species/genus of the isolates so that the correct antimicrobial breakpoints could be used to interpret the disc diffusion assays, and the results can be seen in **Table 3.2**. Thirty-two of 63 isolates were identified to species level, while the remaining 31 were only identified to the level of genus. Forty isolates belonged to the *Enterobacteriaceae* family; while 12 were identified as *Pseudomonas* sp., 8 as *Aeromonas* sp. and the remaining isolate as *Sten. maltophilia*.

Figure 3.1 shows the percentage of all *Enterobacteriaceae* isolates with sensitive, increased susceptibility, and resistant results to each antibiotic determined by the disc diffusion assay (**§2.3.1**). All isolates were resistant to ampicillin (AMP), cefpodoxime (CPD), and cefotaxime (CTX). Most isolates were

Table 3.2. Results of 16S rRNA sequencing of cultures isolated from cephalosporin-selective agars.

Genus	Species	Number of isolates
Aeromonas		8
	Ae. media	3
	Ae. hydrophila	1
Enterobacter		1
Escherichia		31
	E. coli	20
Klebsiella		8
	K. pneumoniae	8
Pseudomonas		12
Stenotrophomonas		1
	Sten. maltophilia	1

Species was determined by percentage identity of BLAST hits >98.65% with only a single species with the highest percentage identity. Where multiple species shared the same percentage identity as the target sequence, the isolate was considered identified to the genus level instead.

resistant to aztreonam (ATM) (29/40, 72.5%), amoxicillin/clavulanic acid (AMC) (23/40, 57.5%), ciprofloxacin (CIP) (21/40, 52.5%) and azithromycin (AZM) (33/40, 67.5%). Just under half of the isolates were resistant to trimethoprim-sulphamethoxazole (SXT), streptomycin (S10), nalidixic acid (NA), and tetracycline (TET) (all 19/40, 47.5%). Only a small proportion of isolates were resistant to cefoxitin (FOX) (9/40, 22.5%), chloramphenicol (C) (8/40, 20%)

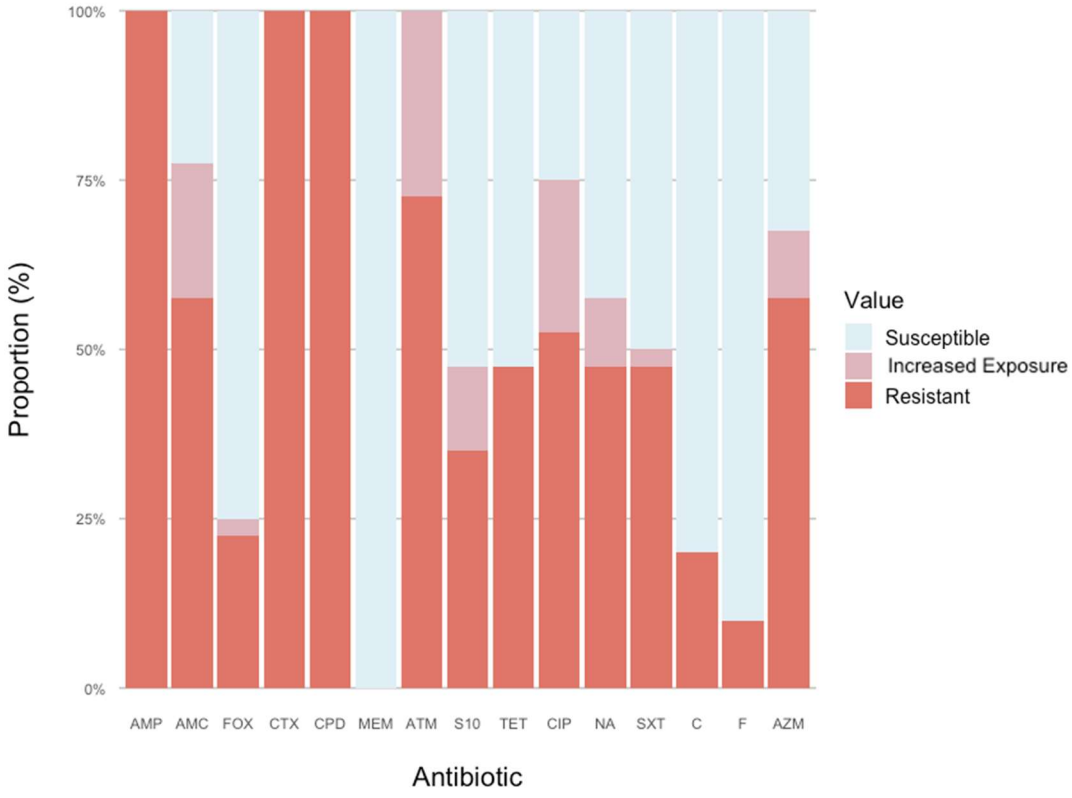

Figure 3.1. Stacked bar graph showing the proportion of *Enterobacteriaceae* isolated from cephalosporin-selective agar that had phenotypically susceptible, increased suceptibility, and resistant results to 15 antibiotics. Antibiotic abbreviations: Ampicillin (AMP), Amoxicillin-clavulanic acid (AMC), Cefoxitin (FOX), Cefotaxime (CTX), Cefpodoxime (CPD), Aztreonam (ATM), Meropenem (MEM), Streptomycin (S10), Oxytetracycline (TET), Ciprofloxacin (CIP), Nalidixic Acid (NA), Trimethoprim-sulfamethoxazole (SXT), Chloramphenicol (C), Nitrofurantoin (F) and Azithromycin (AZM).

and nitrofurantoin (F) (4/40, 10%); and all isolates were susceptible to meropenem (MEM). All but one (39/40, 97.5%) isolate were resistant to three or more classes of antibiotics and so would be considered multidrug resistant. PCR results showed that 95% (38/40) of cephalosporin resistant isolates contained at least one of either $bla_{\text{CTX-M}}$, bla_{TEM} or bla_{SHV}, while there were no positive results for $bla_{\text{OXA-1}}$, $bla_{\text{OXA-2}}$, or any of the acquired carbapenemase genes (**§2.5.2** and **§2.5.3**). Of the 16 isolates containing a single beta lactamase resistance gene, 7 isolates harboured $bla_{\text{CTX-M}}$, 7 contained bla_{TEM} and 2

contained *bla*$_{SHV}$. Of the 19 isolates harbouring 2 beta-lactamase genes, 11 contained both *bla*$_{CTX-M}$ and *bla*$_{SHV}$, while the remaining 8 contained both *bla*$_{CTX-M}$ and *bla*$_{TEM}$. A further three isolates contained all three genes, while two did not contain any of the selected genes.

The PCR-based replicon typing (PBRT) (**§2.5.5**) results showed that 62.5% (25/40) of isolates contained IncFII plasmid replicons, 40% (16/40) contained IncFIA replicons, 25% (10/40) contained IncFIB replicons, and 17.5% (7/40) contained IncI replicons, while none of the other plasmid replicons were detected in these isolates.

These results were combined with those of the antibiotic sensitivity test (AST) disc diffusion assays to create a map that can be seen in **Figure 3.2**. The figure shows that the isolates cluster broadly by sample point/time, presumably since the influent samples were taken only on one occasion, while the other sample dates included multiple sample points. Effluent samples appear mostly to cluster together with other river isolates, with three also interspersed with *E. coli* isolated from the influent. In terms of species clustering, the *K. pneumoniae* isolates form a subcluster with one other *E. coli*, mainly due to them not containing any of the plasmid replicons found in the PBRT scheme. The map shows there are three isolates, DD77, DD83 and DD87 that form a subcluster that has identical results for the AST disc diffusion assay, beta-lactamase detection and PBRT. Given that these were isolated from the same sample point on the same date and are all *Escherichia*, it is likely these isolates are replicates of the same organism.

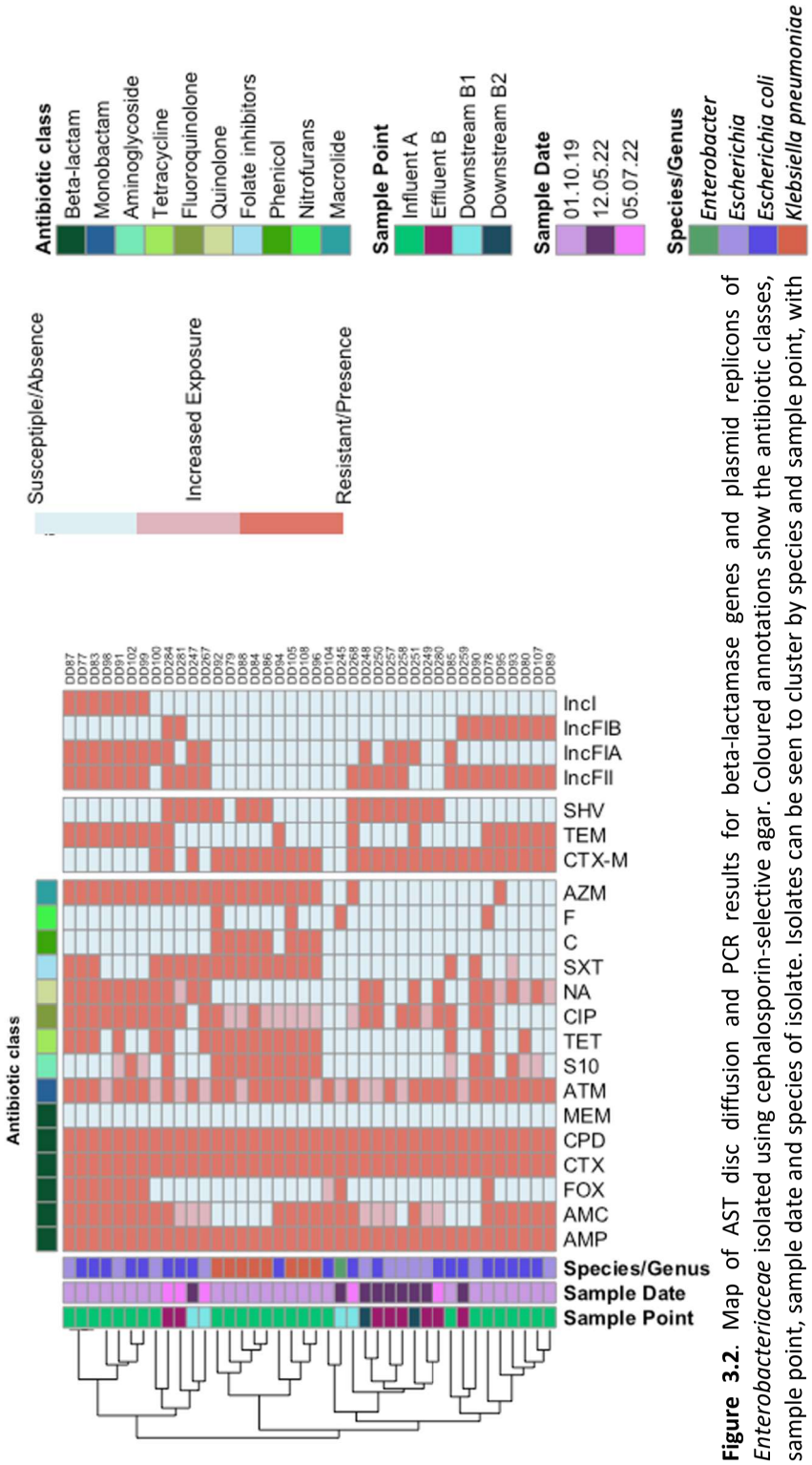

Figure 3.2. Map of AST disc diffusion and PCR results for beta-lactamase genes and plasmid replicons of *Enterobacteriaceae* isolated using cephalosporin-selective agar. Coloured annotations show the antibiotic classes, sample point, sample date and species of isolate. Isolates can be seen to cluster by species and sample point, with *K. pneumoniae* forming a subcluster in the middle of the map, and effluent and river water isolates of *Escherichia* forming a subcluster below. Antibiotic abbreviations: Ampicillin (AMP), Amoxicillin-clavulanic acid (AMC), Cefoxitin (FOX), Cefotaxime (CTX), Cefpodoxime (CPD), Aztreonam (ATM), Meropenem (MEM), Streptomycin (S10), Oxytetracycline (TET), Ciprofloxacin (CIP), Nalidixic Acid (NA), Trimethoprim-sulfamethoxazole (SXT), Chloramphenicol (C), Nitrofurantoin (F) and Azithromycin (AZM).

3.2.1.1 Cephalosporin-resistant non-*Enterobacteriaceae*

The results of the disc diffusion assay for *Aeromonas* isolates can be seen in **Figure 3.3.** Only eight of the antibiotics tested are recommended by the CLSI for the treatment of *Aeromonas* sp. infections, so only these results are shown. All of the isolates were resistant to cefotaxime, while 87.5% (7/8) were resistant to cefoxitin. All were susceptible to meropenem, aztreonam, tetracycline and chloramphenicol. 87.5% (7/8) were susceptible to trimethoprim-sulfamethoxazole while only 37.5% (3/8) were susceptible to ciprofloxacin. Only one isolate contained any of the tested beta-lactamase genes; DD270 harboured both bla_{TEM} and bla_{OXA-1}. DD244 was positive for an IncP replicon, while the other isolates contained no other plasmids from the PBRT scheme.

For *Pseudomonas* isolates other than *P. aeruginosa*, the CLSI (CLSI, 2019) does not recommend the use of the AST disc diffusion assay, therefore no breakpoints are available. The only breakpoints available for *P. aeruginosa* for the antibiotics tested are for meropenem, aztreonam and ciprofloxacin. Of these, 50% of the *Pseudomonas* isolates (6/12) were resistant to aztreonam, 8.3% were resistant to ciprofloxacin (1/12), and none were resistant to meropenem.

The only antibiotic recommended by the CLSI for the treatment of *Stenotrophomonas* is trimethoprim-sulfamethoxazole, to which the single *Sten. maltophilia* isolate was susceptible.

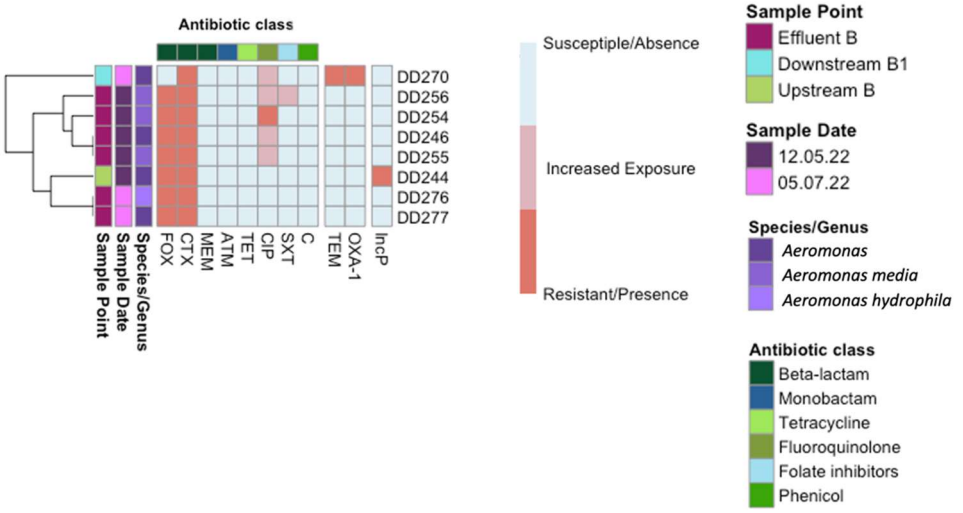

Figure 3.3. Map of disc diffusion and PCR results of *Aeromonas* isolated from cephalosporin-selective agar. Coloured annotations show the antibiotic classes, sample point, sample date and species of isolate. Antibiotic abbreviations: Cefoxitin (FOX), Cefotaxime (CTX), Meropenem (MEM), Aztreonam (ATM), Oxytetracycline (TET), Ciprofloxacin (CIP), Trimethoprim-sulfamethoxazole (SXT), Chloramphenicol (C).

3.2.2 Selection for carbapenemase-producing *Enterobacteriaceae*

The carbapenem-resistant isolates were mostly isolated from the influent of WWTP B (n=73), with the remainder from the effluent of the same WWTP (n=21) and 100 m downstream of the effluent point (n=3) the river into which it discharges. Forty-four isolates were presumptively identified as *E. coli* based on indole and oxidase results. 16S rRNA sequencing was carried out as previously described and the results are shown in **Table 3.3**. Thirty-nine out of 97 isolates were identified to species level, with the remaining 58 could only be identified to genus level. Compared to the indole/oxidase results, only 40 isolates were identified as either *Escherichia* or *E. coli*, with the remaining 4

Table 3.3. Results of 16S rRNA sequencing of cultures isolated from carbapenem-selective agar.

Genus	Species	Number of isolates
Aeromonas		28
	Ae. media	9
Citrobacter		6
	C. freundii	2
Enterobacter		2
Enterococcus		3
Escherichia		40
	E. coli	25
Pseudomonas		7
Klebsiella		2
Klebsiella/Raoultella		1
Klebsiella/Enterobacter		5
Raoultella		3
	R. ornithinolytica	2

Species was determined by percentage identity of BLAST hits >98.65% with only a single species with the highest percentage identity. Where multiple species shared the same percentage identity as the target sequence, the isolate was considered identified to the genus level instead. Right-justified numbers indicate isolates identified to genus level, while left-justified numbers indicated isolates identified to species level.

identified as *Raoultella* or *Klebsiella*/*Raoultella*. Other *Enterobacteriaceae* identified were six *Citrobacter*, two *Enterobacter*, and two *Klebsiella*. Of the 38 non-*Enterobacteriaceae* isolated, 28 were identified as *Aeromonas*, 7 as *Pseudomonas* and 3 as *Enterococcus*.

Figure 3.4 shows the proportion of *Enterobacteriaceae* isolates that had sensitive, increased susceptibility, or resistant results to the antibiotics tested

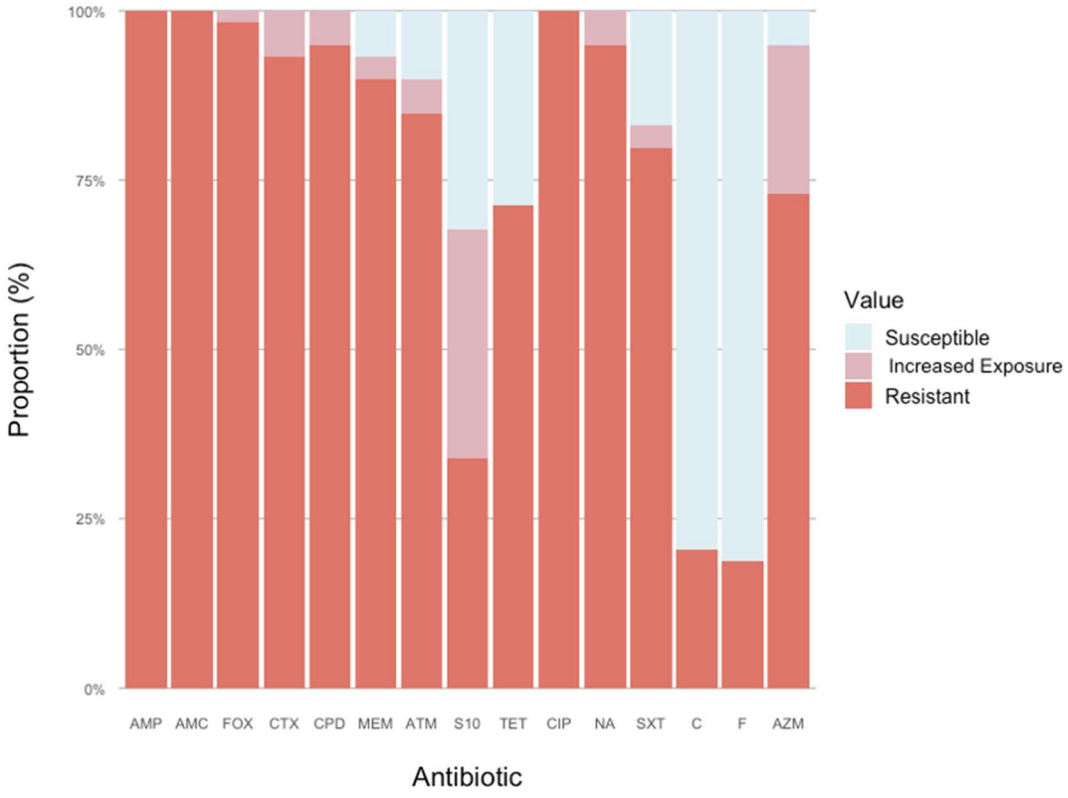

Figure 3.4. Stacked bar graph showing the proportion of Enterobacteriaceae isolated from carbapenem-selective agar that had susceptible, increased susceptibility and resistant results to the following 15 antibiotics: Ampicillin (AMP), Amoxicillin-clavulanic acid (AMC), Cefoxitin (FOX), Cefotaxime (CTX), Cefpodoxime (CPD), Aztreonam (ATM), Meropenem (MEM), Streptomycin (S10), Oxytetracycline (TET), Ciprofloxacin (CIP), Nalidixic Acid (NA), Trimethoprim-sulfamethoxazole (SXT), Chloramphenicol (C), Nitrofurantoin (F) and Azithromycin (AZM).

according to CLSI standard AST disc diffusion assay (**§2.3.1**). All isolates were resistant to ampicillin (AMP), amoxicillin-clavulanic acid (AMC), and ciprofloxacin (CIP)). Large numbers of isolates were resistant to cefoxitin (FOX) (58/59, 98%), cefotaxime (CTX) (55/59, 93%), cefpodoxime (CPD) (56/59, 95%), meropenem (MEM) (53/59, 90%), aztreonam (ATM) (50/59, 85%), nalidixic acid (NA) (56/59 95%), and sulfamethoxazole (SXT) (47/59, 80%. Seventy-one percent (42/59) were resistant to tetracycline (TET), while 66% (39/59) were resistant to azithromycin (AZM).

As with isolates from selective agar supplemented with cephalosporins, the majority of isolates were susceptible to chloramphenicol (C) and nitrofurantoin (F). Only 20% (12/59) and 19% (11/59) were resistant to chloramphenicol and nitrofurantoin respectively, while only 34% (20/59) were resistant to streptomycin (S10). All isolates were resistant to three or more classes of antibiotic, with one that was resistant to all antibiotics tested. This was DD140, identified as *Enterobacter.*

Isolates from cephalosporin-selective agar were phenotypically resistant to between 3 and 11 antibiotics, while those from carbapenem-selective agar were resistant to between 6 and 15, and the percentage of isolates with each resistance profile can be seen in **Figure 3.5.** Overall, the median number of phenotypic resistances was 11 for isolates from carbapenem-selective agar compared to 7.5 for isolates from cephalosporin-selective agar. As carbapenem-resistant isolates would be expected to be resistant to a greater number of beta-lactam antibiotics when compared to cephalosporin-resistant isolates, the median number of phenotypic resistances to non-beta-lactam antibiotics was also compared. Isolates from carbapenem-selective agar had a median of 5 phenotypic resistances results compared to 3 for cephalosporin-selective isolates, and a Mann-Whitney/Wilcoxon rank-sum test confirmed that these distributions were significantly different ($p = 0.0008165$). This shows that isolates from carbapenem-selective agar were more likely to be phenotypically resistant to non-beta-lactam antibiotics, suggesting co-occurrence of resistance mechanisms.

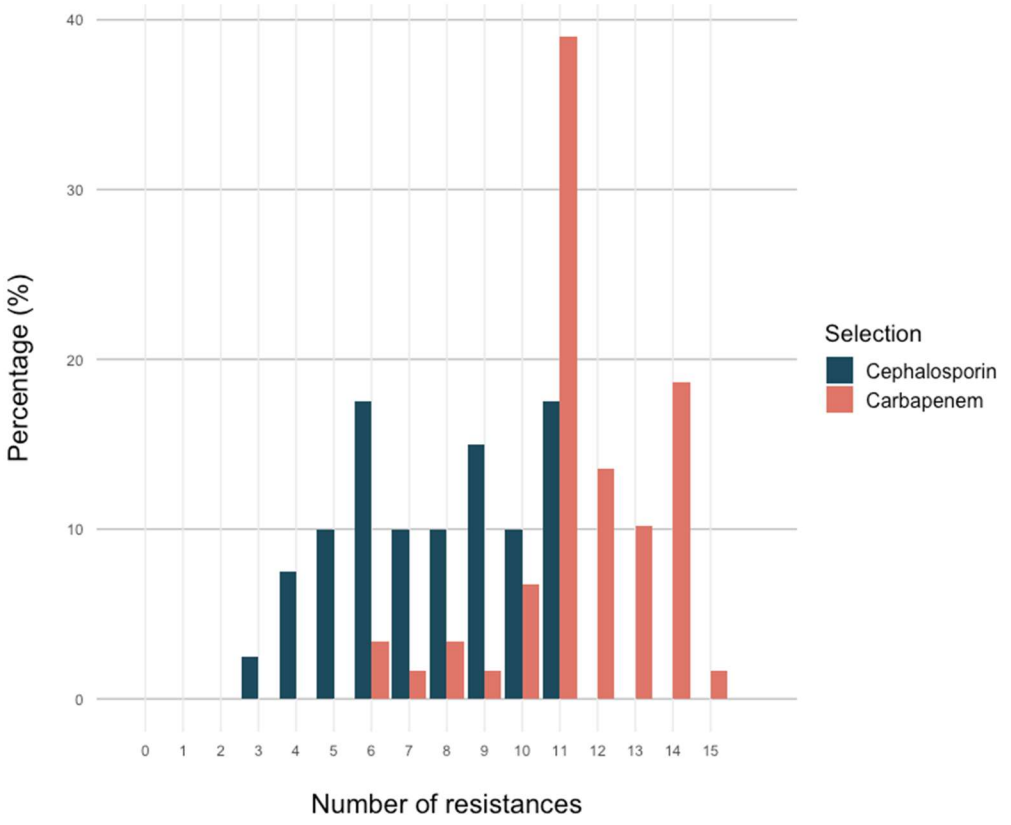

Figure 3.5. Comparison of the range of phenotypic results to antibiotics of isolates from cephalosporin and carbapenem-selective agar. Isolates from cephalosporin-selective agar were resistant to between 3 and 11 antibiotics (median 7.5); from carbapenem-selective agar it was between 6 and 15 antibiotics (median 11).

Forty-two out of 59 isolates had a positive result to the zCIM test (**§2.3.2**), identifying them as carbapenemase-producers. PCR detection of common carbapenemase genes showed that 39 of these were positive for *bla*$_{NDM}$, while the remaining 3 strains contained *bla*$_{IMP}$. Additionally, five of the *bla*$_{NDM}$-containing isolates also were positive for carriage of OXA-48-like carbapenemase genes. Thirty-eight of thirty-nine isolates containing *bla*$_{NDM}$ belonged to the *Escherichia* genus, with the remaining isolate identified as *Klebsiella* spp. Two of the isolates producing *bla*$_{IMP}$ were identified as *Citrobacter* and the other as *Klebsiella.* Eight of the carbapenemase producers

were isolated from the effluent of WWTP B, while the majority were isolated from the influent of the same WWTP.

These data were combined with PCR results from the PBRT and other beta-lactamase detection tests as well as the AST disc diffusion assay results to generate a map as seen in **Figure 3.6**. The map shows that these results cluster by genera, as *Escherichia* forms the entirety of the bottom subcluster, with the remaining *Enterobacteriaceae* and three *Escherichia* making up the top subcluster. However, there are several points on the map where multiple isolates have identical AST and PCR results. **Figure 3.6D** shows a selection of 10 isolates with identical results, though 5 are split between sample dates and 2 were collected from the effluent rather than the influent. For this reason, a second map was produced, where isolates with identical results were removed, unless they differed solely by sample date/sample point, which resulted in the removal of 23 *Escherichia* isolates.

Of the resulting 36 non-replicated isolates, 3 contained 4 of the tested beta-lactamase genes, 10 contained 3 beta-lactamase genes, 13 contained 2 separate genes, and 4 isolates only had 1 beta-lactamase gene, while 6 isolates were negative for all tested beta-lactamase genes (**§2.5.2** and **§2.5.3**). The gene detected most often was still bla_{NDM}, at 19/36 isolates, with bla_{CTX-M} found in 18/36 isolates. Unlike the cephalosporin-selective agar isolates, a high proportion of these contained bla_{OXA-1} at 15/36. Of the other beta-lactamases, 11/36 contained bla_{TEM}, 4/36 contained bla_{SHV}, 3 contained bla_{IMP} and 2 contained bla_{OXA-48}.

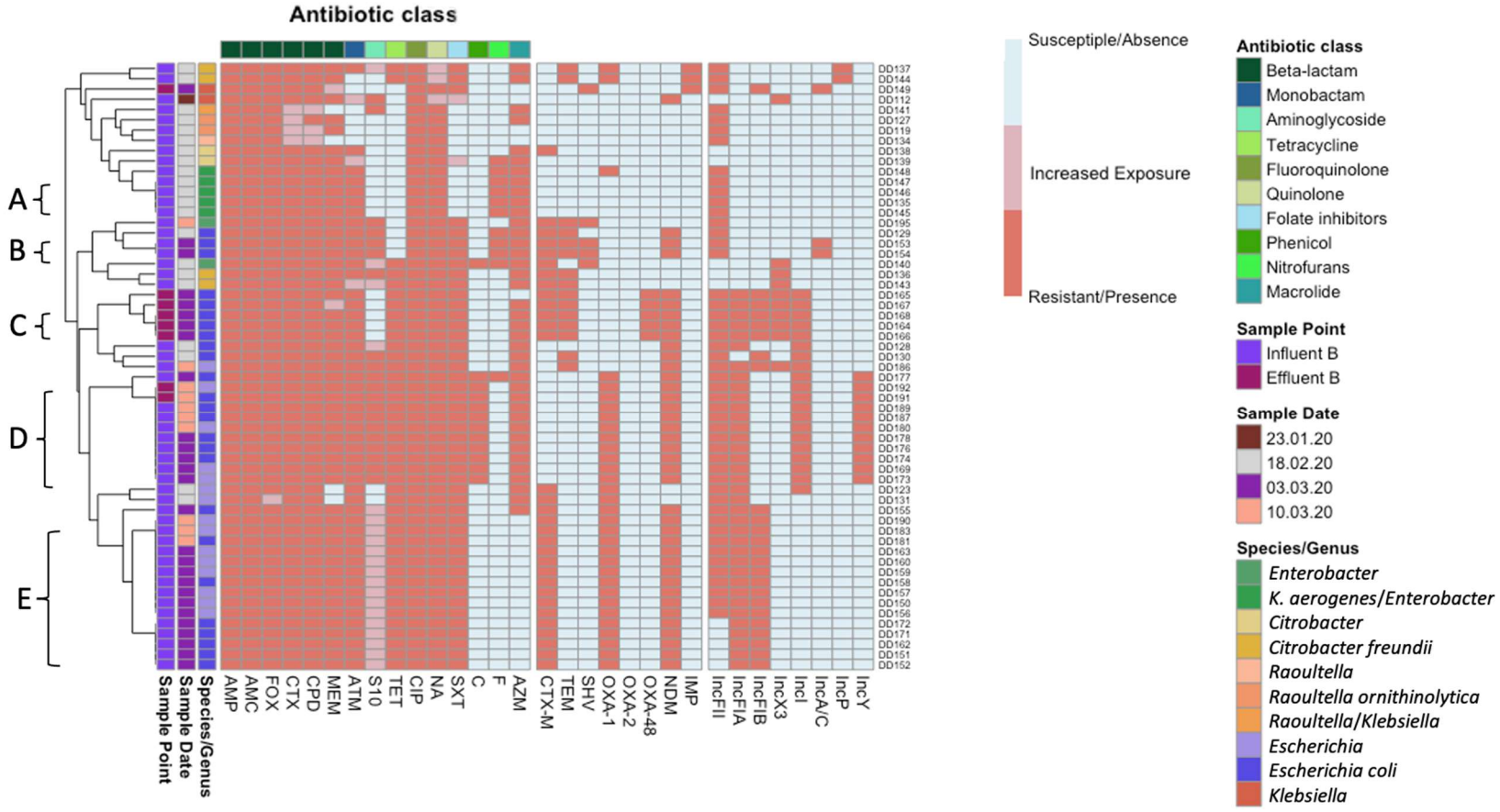

Figure 3.6. Map of AST disc diffusion assays and PCR results of *Enterobacteriaceae* isolated from carbapenem-selective agar. Coloured annotations show the antibiotic classes, sample point, sample date and species of isolates. Isolates can be seen to cluster by species and sample date, with non-*Escherichia* forming a subcluster at the top of the map. A-E highlight isolates with identical disc diffusion and PCR results. Antibiotic abbreviations: Ampicillin (AMP), Amoxicillin-clavulanic acid (AMC), Cefoxitin (FOX), Cefotaxime (CTX), Cefpodoxime (CPD), Aztreonam (ATM), Meropenem (MEM), Streptomycin (S10), Oxytetracycline (TET), Ciprofloxacin (CIP), Nalidixic Acid (NA), Trimethoprim-sulfamethoxazole (SXT), Chloramphenicol (C), Nitrofurantoin (F) and Azithromycin (AZM).

The plasmid replicon detected most often was IncFII, contained in 28/36 isolates (**§2.5.5**). The IncFIA and IncFIB replicons were found in 17 and 12 isolates respectively. Of the other incompatibility groups, 10 isolates contained IncI plasmids, and 7 IncX3 replicons were also detected. There were also 4 IncY replicons found, as well as 2 IncP and 2 IncA/C replicons. The AST and PCR patterns in **Figure 3.7** form two main subclusters, seemingly based on their plasmid replicon PCR results. The lower subcluster, comprised mainly of non-*Escherichia Enterobacteriaceae*, contained 21 plasmid replicons, while the top subcluster that was comprised solely of *Escherichia* contained 61 replicons.

3.2.2.1 Carbapenem-resistant non-*Enterobacteriaceae*

A map was generated for the *Aeromonas* isolates as done previously (**§3.2.1.1**), and this again showed a subcluster of replicate isolates, which were removed before a new map was generated, which can be seen in **Figure 3.8**. Much higher levels of antimicrobial resistance were found in these *Aeromonas* isolates than those recovered from cephalosporin-selective agars. Similarly, 88% (21/24) of isolates were resistant to cefoxitin, while 71% (17/24) were resistant to cefotaxime. However, 42% (10/24) were resistant to meropenem, and 50% (12/24) were resistant to tetracycline, which compared with 0% from the cephalosporin-selective isolates. Seventy-five percent (18/24) were resistant to ciprofloxacin, 25% (6/24) to trimethoprim-sulfamethoxazole, while 4% were resistant to aztreonam and chloramphenicol (1/24). Of the *Aeromonas* isolates

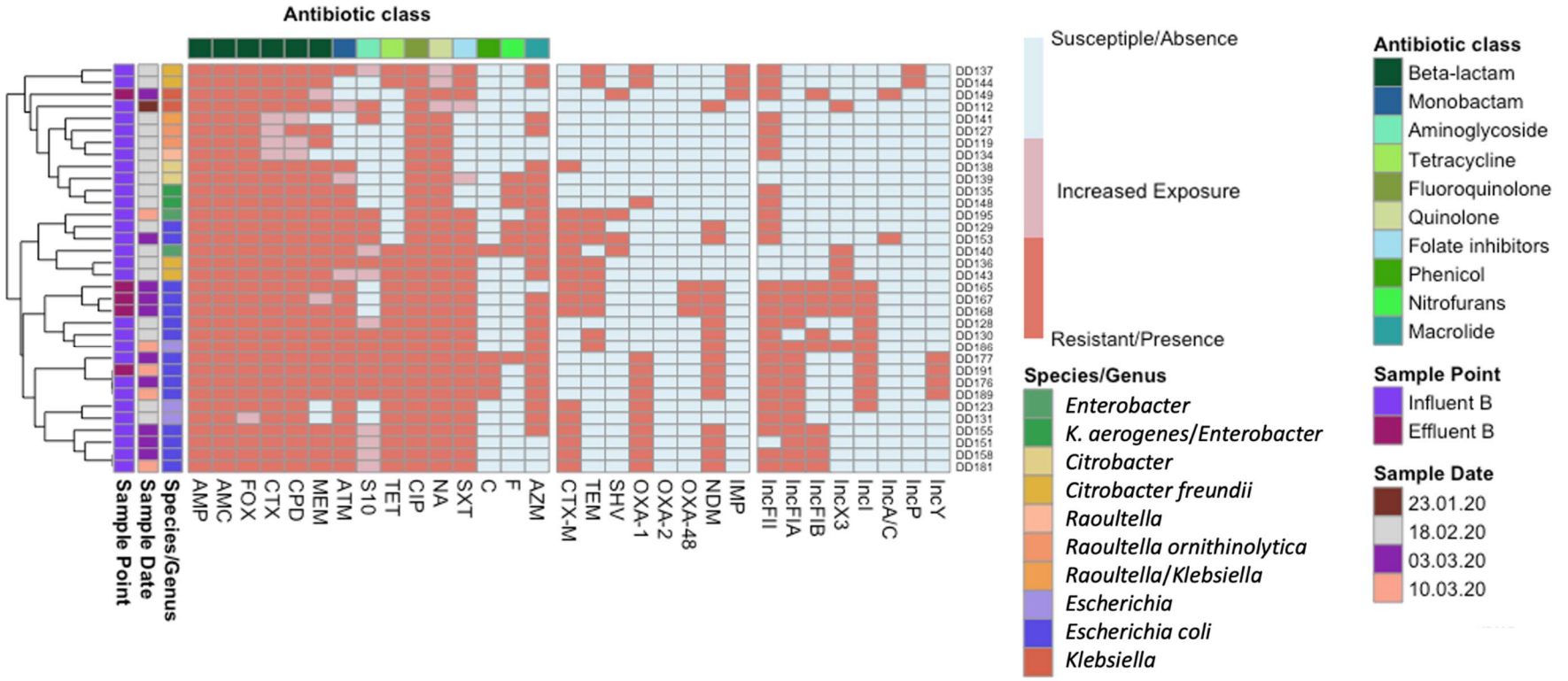

Figure 3.7. Map of AST disc diffusion and PCR results of *Enterobacteriaceae* isolated from carbapenem-selective agar. Coloured annotations show the antibiotic classes, sample point, sample date and species of isolate. Replicated isolates shown in **Figure 3.6** have been removed. Antibiotic abbreviations: Ampicillin (AMP), Amoxicillin-clavulanic acid (AMC), Cefoxitin (FOX), Cefotaxime (CTX), Cefpodoxime (CPD), Aztreonam (ATM), Meropenem (MEM), Streptomycin (S10), Oxytetracycline (TET), Ciprofloxacin (CIP), Nalidixic Acid (NA), Trimethoprim-sulfamethoxazole (SXT), Chloramphenicol (C), Nitrofurantoin (F) and Azithromycin (AZM).

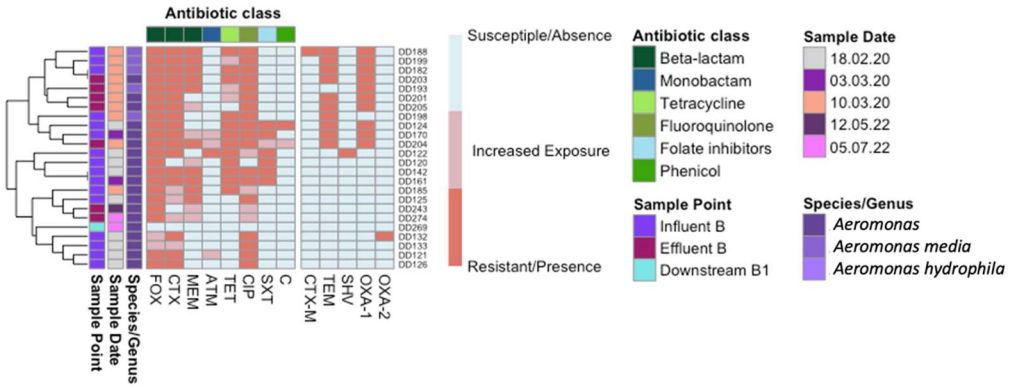

Figure 3.8. Map of disc diffusion and PCR results of *Aeromonas* isolated from carbapenem-selective agar. Coloured annotations show the antibiotic classes, sample point, sample date and species of isolate. Antibiotic abbreviations: Cefoxitin (FOX), Cefotaxime (CTX), Meropenem (MEM), Aztreonam (ATM), Oxytetracycline (TET), Ciprofloxacin (CIP), Trimethoprim-sulfamethoxazole (SXT), Chloramphenicol (C).

subcultured from cephalosporin-selective agar, only 12.5% (1/8) were phenotypically resistant to any of the 4 non-beta-lactam antibiotics tested, while the remainder were susceptible. Those isolated from carbapenem-selective agar had larger numbers of phenotypic resistances, as only 12.5% (3/24) of the non-replicated isolates were susceptible to all antibiotics tested. Four percent (1/24) were resistant to all non-beta-lactam antibiotics, 12.5% (3/24) were resistant to 3, 29.2% (7/24) were resistant to 2 and 41.7% (10/24) resistant to only 1. The difference between these distributions was shown to be statistically significant via the MWW test ($p = 0.0004712$).

Another difference was the numbers of beta-lactamase genes detected in these isolates. From cephalosporin-selective agar, only a single *Aeromonas* isolate contained a beta-lactamase gene, compared to 13 of 24 isolates from carbapenem-selective agar. Nine of these contained both bla_{TEM} and bla_{SHV}, with one containing $bla_{CTX\text{-}M}$ as well. A single isolate was positive for $bla_{OXA\text{-}2}$,

which was the only *bla*$_{OXA-2}$ detected in this study and so was confirmed using Sanger sequencing. Seven *Aeromonas* isolates were positive for carbapenemase production using the zCIM test but no carbapenemase genes were detected by PCR.

Of the seven *Pseudomonas* isolates, three were resistant to aztreonam, while one was resistant to both meropenem and ciprofloxacin. The latter isolate was identified as *P. aeruginosa* which was also positive for carbapenemase production using the zCIM test. PCR detection confirmed this, with the detection of *bla*$_{IMP}$ from isolate DD202. No other beta-lactamase genes were detected via PCR.

Of the three *Enterococcus* isolates, only two distinct disc diffusion assay patterns were seen for the five antibiotics recommended for use by the CLSI (CLSI, 2019). One pattern was resistance to ampicillin, ciprofloxacin and nitrofurantoin, increased suceptibility to tetracycline and susceptible to chloramphenicol. The difference in the other AST pattern was susceptibility to nitrofurantoin. None of the isolates were positive for plasmid replicons or beta-lactamase genes.

3.2.2.2 Comparison of genera isolated by agar

The genus identified most often across all samples was *Escherichia* and it was also the most common genus of isolates that were positive for carbapenemase production. As TBX agar was used to isolate bacteria in this study, and this agar is used specifically to isolate *E. coli*, analysis was performed to try and

determine whether the large numbers of *Escherichia* isolated was due to selection bias from the use of TBX agar. **Figure 3.9** shows the proportion of genera isolated on different agars. Overall, there were 38 strains isolated on CRE agar, 76 strains isolated on MacConkey agar, 35 on TBX agar and 9 on mSuperCARBA. The large number of isolates on MacConkey agar was due to the first sample of 33 isolates from WWTP A, which was meant as a preliminary sample and used only MacConkey agar for isolation. The number of isolates identified as *Enterobacteriaceae* from each agar type was 55% (21/38) of isolates from CRE agar, 66% (50/76) from MacConkey agar, 80% (28/35) from TBX agar and 0% from mSuperCARBA.

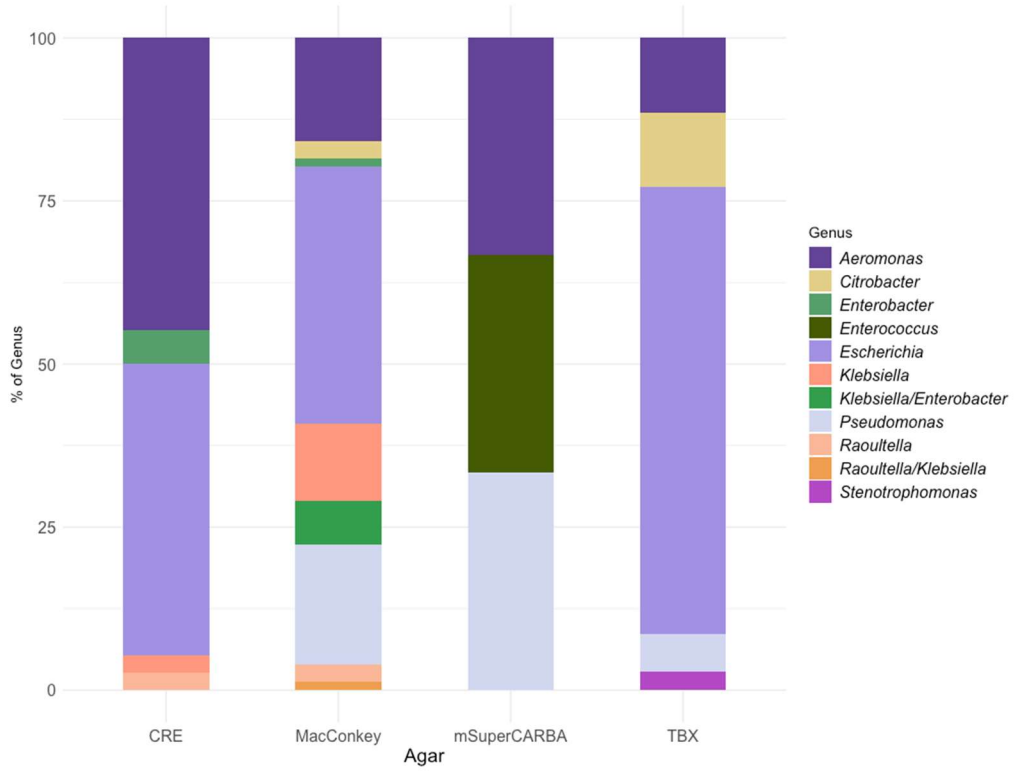

Figure 3.9. Percentage of isolates identified as a particular species by type of isolation agar. The highest proportions of *Enterobacteriaceae* were isolated from MacConkey and TBX agars.

Escherichia made up 45% (17/38) of those strains isolated from CRE agar, 39% (30/76) from MacConkey and 68% (24/35) from TBX agar. A Chi-Squared test of association was performed to test the association between the identification of *Escherichia* and the use of TBX agar, and no significant association was found (p=0.082).

3.2.3 Phenotypic-Genotypic Association using Chi-Squared test

Chi-Squared tests of association were performed between AST disc diffusion assay and PCR results of non-replicate isolates for those combinations with acceptable expected values, and these can be seen **Figure 3.10**. There were multiple significant associations between various beta-lactamase genes and resistance to beta-lactams, while plasmid genes were associated with a small number of resistances. Carriage of bla_{NDM} was associated more phenotypic resistances than any other beta-lactamase or plasmid gene. It was associated with resistance to meropenem, ampicillin, cefoxitin and trimethoprim-sulfamethoxazole. Association with beta-lactam resistance is unsurprising but trimethoprim-sulfamethoxazole resistance may suggest co-occurrence of different resistance genes among isolates harbouring bla_{NDM}.

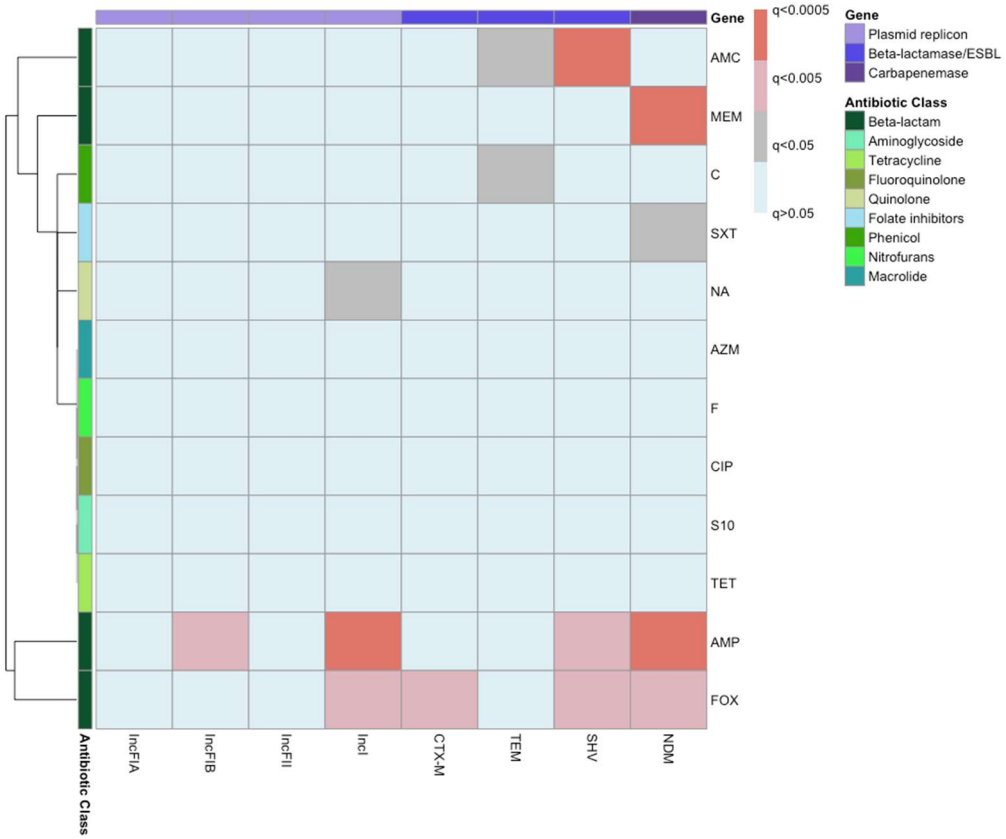

Figure 3.10. Heatmap showing the associations between resistance genes and resistant phenotypes as identified by chi-squared tests with false discovery rate corrections. Associations with lower adjusted p values (q) are shown as coloured squares. Associations with adjusted p value (q) > 0.05 were considered non-significant. Tests of association were only performed when expected values were all >3 or all >2 and 50% >5. Carriage of *bla*$_{NDM}$ was associated with resistance to ampicillin, cefoxitin, meropenem, and trimethoprim-sulfamethoxazole, which was the most associations of all beta-lactam and plasmid genes.

3.2.4 Minimum inhibitory concentration of meropenem on carbapenem-hydrolytic isolates

Minimum inhibitory concentrations (MICs) of meropenem were determined using the agar dilution method for all 50 carbapenem-hydrolytic isolates (**§2.3.3**). The CLSI breakpoint for meropenem resistance determined by MIC is >4 µg mL^{-1} for *Enterobacteriaceae* and *Aeromonas* sp., and >8 µg mL^{-1} for

P. aeruginosa (CLSI, 2016, 2019). MICs ranged from 16 μg mL^{-1} to greater than 128 μg mL^{-1}, and both MIC50 and MIC90s were 128 μg mL^{-1}, with the full results shown in **Table 3.4**. Of the 39 *Escherichia* isolates containing bla_{NDM}, 32 had an MIC of 128 μg mL^{-1}, 5 had an MIC of 64 μg mL^{-1} and the remaining 2 had MICs of >128 μg mL^{-1}. The *Klebsiella* isolate that also encoded bla_{NDM} had an MIC of 64 μg mL^{-1}. The isolates positive for bla_{IMP} had MICs of 16 μg mL^{-1} for the *Klebsiella* isolate, 64 and 128 μg mL^{-1} for the two *Citrobacter* isolates and 128 μg mL^{-1} for the *Pseudomonas* isolate. NCTC 13476, which also contains bla_{IMP}, was used as a control and had an MIC of 64 μg mL^{-1}. Three of the *Aeromonas* isolates with unidentified carbapenemases had MICs of 16 μg mL^{-1}, two had results of 32 μg mL^{-1}, and the remaining isolate had an MIC of 128 μg mL^{-1}.

3.2.5 Conjugation experiments

PCR results from **§3.2.2** showed that all isolated CPE also contained plasmid replicons. Experiments were performed to determine whether the carbapenemase genes could be transferred to a recipient *E. coli* by conjugation (**§2.6.2**), to see if these genes were found on conjugable plasmids. The recipient strain used for these experiments was the K12 derivative *E. coli* CV601 kan^R rif^R gfp^+, which was resistant to the antibiotics kanamycin and rifampicin, and also expressed the GFP protein (**§2.1.1**). This was chosen as a number of CPE did not show phenotypic resistance to streptomycin, and it was thought that the

Table 3.4. Results of MICs of meropenem for all carbapenem-hydrolytic isolates.

Isolate	Genus/Species	Carbapenemase	MIC (μg mL^{-1})
DD112	*Klebsiella*	*bla*$_{NDM}$	64
DD120	*Aeromonas*	Unknown	32
DD125	*Aeromonas*	Unknown	16
DD128	*Escherichia coli*	*bla*$_{NDM}$	128
DD129	*Escherichia coli*	*bla*$_{NDM}$	128
DD130	*Escherichia coli*	*bla*$_{NDM}$	64
DD137	*Citrobacter freundii*	*bla*$_{IMP}$	64
DD144	*Citrobacter freundii*	*bla*$_{IMP}$	128
DD149	*Klebsiella*	*bla*$_{IMP}$	16
DD150	*Escherichia*	*bla*$_{NDM}$	64
DD151	*Escherichia coli*	*bla*$_{NDM}$	128
DD152	*Escherichia coli*	*bla*$_{NDM}$	128
DD153	*Escherichia coli*	*bla*$_{NDM}$	128
DD154	*Escherichia coli*	*bla*$_{NDM}$	128
DD155	*Escherichia coli*	*bla*$_{NDM}$	64
DD156	*Escherichia*	*bla*$_{NDM}$	128
DD157	*Escherichia*	*bla*$_{NDM}$	128
DD158	*Escherichia coli*	*bla*$_{NDM}$	128
DD159	*Escherichia*	*bla*$_{NDM}$	128
DD160	*Escherichia*	*bla*$_{NDM}$	64
DD161	*Aeromonas*	Unknown	128
DD162	*Escherichia coli*	*bla*$_{NDM}$	128
DD163	*Escherichia*	*bla*$_{NDM}$	64
DD164	*Escherichia coli*	*bla*$_{NDM}$/*bla*$_{OXA-48}$	128
DD165	*Escherichia coli*	*bla*$_{NDM}$/*bla*$_{OXA-48}$	128
DD166	*Escherichia coli*	*bla*$_{NDM}$/*bla*$_{OXA-48}$	128
DD167	*Escherichia coli*	*bla*$_{NDM}$/*bla*$_{OXA-48}$	128
DD168	*Escherichia coli*	*bla*$_{NDM}$/*bla*$_{OXA-48}$	128
DD169	*Escherichia*	*bla*$_{NDM}$	>128
DD171	*Escherichia coli*	*bla*$_{NDM}$	128
DD172	*Escherichia coli*	*bla*$_{NDM}$	128
DD173	*Escherichia*	*bla*$_{NDM}$	>128
DD174	*Escherichia coli*	*bla*$_{NDM}$	128
DD176	*Escherichia coli*	*bla*$_{NDM}$	128
DD177	*Escherichia coli*	*bla*$_{NDM}$	128
DD178	*Escherichia coli*	*bla*$_{NDM}$	128
DD180	*Escherichia*	*bla*$_{NDM}$	128
DD181	*Escherichia coli*	*bla*$_{NDM}$	128
DD183	*Escherichia*	*bla*$_{NDM}$	128
DD185	*Escherichia*	*bla*$_{NDM}$	128
DD186	*Escherichia*	*bla*$_{NDM}$	128

DD187	*Escherichia coli*	*bla*$_{NDM}$	128
DD189	*Escherichia coli*	*bla*$_{NDM}$	128
DD190	*Escherichia*	*bla*$_{NDM}$	128
DD191	*Escherichia coli*	*bla*$_{NDM}$	128
DD192	*Escherichia coli*	*bla*$_{NDM}$	128
DD202	*Pseudomonas aeruginosa*	*bla*$_{IMP}$	128
DD243	*Aeromonas*	Unknown	16
DD269	*Aeromonas*	Unknown	16
DD270	*Aeromonas*	Unknown	32
ATCC25922	*Escherichia coli*	*bla*$_{IMP}$	0.25
NCTC13476	*Escherichia coli*	None	64

ability to use double antibiotic selection would prevent the growth of the MDR donors. Additionally, GFP expression was chosen so that transconjugants could be identified on conjugation assay plates directly using UV light.

The AST and PCR results of the CPE isolates are shown in **Figure 3.11**. There were two nodes where isolates had identical AST and PCR patterns, however these were collected from different samples, either by date or sample type and so were not replicates of the same organism. However, DD144 and DD167 were excluded from further experiments, as although their AST patterns were slightly different, the fact that they were isolated from the same samples as other isolates with identical PCR results (DD137 and DD168 respectively) implied they may have been clonal isolates of the same organisms. The remaining 18 CPE were considered unique CPE and used in conjugation assays, the results of which can be seen in **Table 3.5**. The highest efficiency of conjugation was 1.36×10^{-5} from DD176, while the lowest was 9.30×10^{-8} from DD137, the *C. freundii* isolate. No transconjugants were recovered from experiments using DD128, DD129 and DD130 as donors. The AST disc diffusion

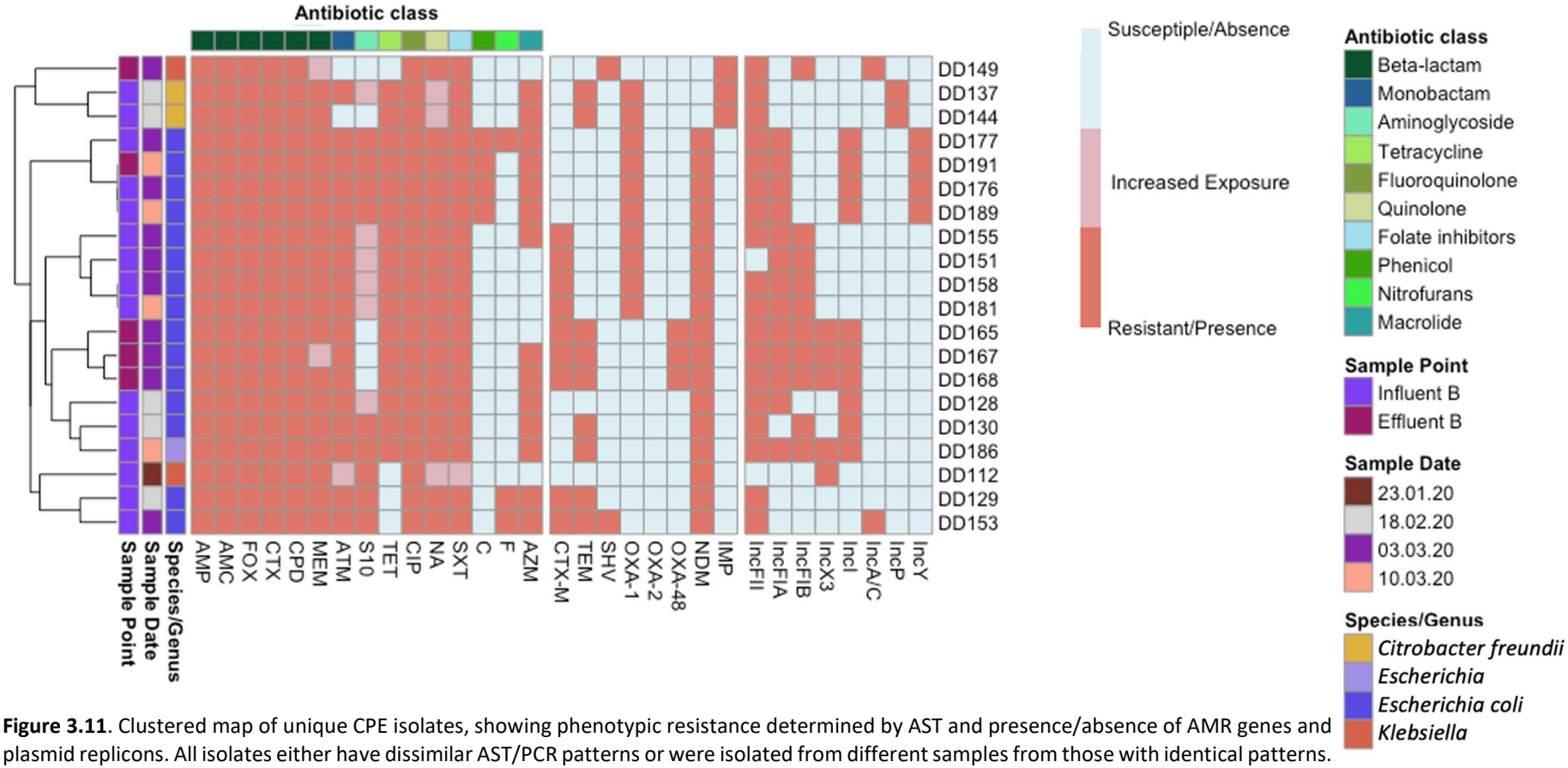

Figure 3.11. Clustered map of unique CPE isolates, showing phenotypic resistance determined by AST and presence/absence of AMR genes and plasmid replicons. All isolates either have dissimilar AST/PCR patterns or were isolated from different samples from those with identical patterns. Antibiotic abbreviations: Ampicillin (AMP), Amoxicillin-clavulanic acid (AMC), Cefoxitin (FOX), Cefotaxime (CTX), Cefpodoxime (CPD), Aztreonam (ATM), Meropenem (MEM), Streptomycin (S10), Oxytetracycline (TET), Ciprofloxacin (CIP), Nalidixic Acid (NA), Trimethoprim-sulfamethoxazole (SXT), Chloramphenicol (C), Nitrofurantoin (F) and Azithromycin (AZM).

assay showed a number of transconjugants had lost resistance to certain antibiotics when compared to the results of their respective donors. The most phenotypic resistance losses were seen in DD186, in which the transconjugant was no longer resistant to aztreonam, streptomycin, tetracycline, ciprofloxacin, nalidixic acid and azithromycin. All transconjugants were resistant to all penicillins, cephalosporins and meropenem, which was expected, while aztreonam, which is not hydrolysed by MBLs, was the most common resistance loss. DD191/DD176/DD189 and DD151/DD158/DD181 shared patterns of phenotypic resistance gain and loss suggesting their donor strains have the same resistance genes encoded on their plasmid containing the carbapenemase gene. Many transconjugants only lost one or two phenotypic resistances when compared to their donors, suggesting that the majority of resistance genes are found on the carbapenemase plasmid.

Table 3.5. Results of conjugation assays and sequencing of transconjugants.

Isolate	Species	Efficiency of Conjugation	Phenotypic Resistance Change
DD149	*K. pneumoniae*	3.78×10^{-6}	*ATM⁻ CIP⁻* **AMP⁺ AMC⁺ FOX⁺ CTX⁺ CPD⁺ MEM⁺ SXT⁺**
DD137	*C. freundii*	9.30×10^{-8}	*CIP⁻* **AMP⁺ AMC⁺ FOX⁺ CTX⁺ CPD⁺ MEM⁺ SXT⁺ AZM⁺**
DD177	*E. coli*	3.20×10^{-5}	*ATM⁻ S10⁻ CIP⁻ NA⁻ C⁻ F⁻* **AMP⁺ AMC⁺ FOX⁺ CTX⁺ CPD⁺ MEM⁺ TET⁺ SXT⁺ AZM⁺**
DD191	*E. coli*	4.61×10^{-6}	*ATM⁻ S10⁻ CIP⁻ NA⁻ C⁻* **AMP⁺ AMC⁺ FOX⁺ CTX⁺ CPD⁺ MEM⁺ TET⁺ SXT⁺ AZM⁺**
DD176	*E. coli*	1.36×10^{-5}	*ATM⁻ S10⁻ CIP⁻ NA⁻ C⁻* **AMP⁺ AMC⁺ FOX⁺ CTX⁺ CPD⁺ MEM⁺ TET⁺ SXT⁺ AZM⁺**
DD189	*E. coli*	2.56×10^{-5}	*ATM⁻ S10⁻ CIP⁻ NA⁻ C⁻* **AMP⁺ AMC⁺ FOX⁺ CTX⁺ CPD⁺ MEM⁺ TET⁺ SXT⁺ AZM⁺**
DD155	*E. coli*	8.90×10^{-8}	*CIP⁻ NA⁻* **AMP⁺ AMC⁺ FOX⁺ CTX⁺ CPD⁺ ATM⁺ MEM⁺ TET⁺ SXT⁺ AZM⁺**
DD151	*E. coli*	2.56×10^{-7}	*CIP⁻ NA⁻* **AMP⁺ AMC⁺ FOX⁺ CTX⁺ CPD⁺ ATM⁺ MEM⁺ TET⁺ SXT⁺**
DD158	*E. coli*	7.66×10^{-8}	*CIP⁻ NA⁻* **AMP⁺ AMC⁺ FOX⁺ CTX⁺ CPD⁺ ATM⁺ MEM⁺ TET⁺ SXT⁺**
DD181	*E. coli*	3.36×10^{-7}	*CIP⁻ NA⁻* **AMP⁺ AMC⁺ FOX⁺ CTX⁺ CPD⁺ ATM⁺ MEM⁺ TET⁺ SXT⁺**
DD165	*E. coli*	9.41×10^{-7}	*ATM⁻ TET⁻ SXT⁻ AZM⁻* **AMP⁺ AMC⁺ FOX⁺ CTX⁺ CPD⁺ MEM⁺ CIP⁺**
DD168	*E. coli*	5.86×10^{-7}	*ATM⁻ NA⁻* **AMP⁺ AMC⁺ FOX⁺ CTX⁺ CPD⁺ MEM⁺ TET⁺ CIP⁺ AZM⁺**
DD128	*E. coli*	1.57×10^{-5}	*ATM⁻ CIP⁻ NA⁻* **AMP⁺ AMC⁺ FOX⁺ CTX⁺ CPD⁺ MEM⁺ TET⁺ SXT⁺ AZM⁺**
DD186	*E. coli*	9.58×10^{-6}	*ATM⁻ S10⁻ TET⁻ CIP⁻ NA⁻ AZM⁻* **AMP⁺ AMC⁺ FOX⁺ CTX⁺ CPD⁺ MEM⁺ SXT⁺**
DD112	*K. quasipneumoniae*	4.03×10^{-5}	*ATM⁻ CIP⁻* **AMP⁺ AMC⁺ FOX⁺ CTX⁺ CPD⁺ MEM⁺**

Efficiency of conjugation measured per donor CFU. Phenotypic resistance change refers to the loss of phenotypic resistance of transconjugants compared to donors (shown in red) as well as the gain of phenotypic resistance compared to original recipient strain (shown in bold); both measured by disc diffusion test. No transconjugants were recovered for DD129, DD153 and DD130. Identical resistance changes in DD191, DD176 and DD189; DD151, DD158 and DD181 may suggest the donor strains are related. Antibiotic abbreviations: Ampicillin (AMP), Amoxicillin-clavulanic acid (AMC), Cefoxitin (FOX), Cefotaxime (CTX), Cefpodoxime (CPD), Aztreonam (ATM), Meropenem (MEM), Streptomycin (S10), Oxytetracycline (TET), Ciprofloxacin (CIP), Nalidixic Acid (NA), Trimethoprim-sulfamethoxazole (SXT), Chloramphenicol (C), Nitrofurantoin (F) and Azithromycin (AZM).

3.3 Discussion

A total of 158 cephalosporin or carbapenem resistant bacterial isolates were collected from wastewater and river water and characterised to determine their AMR profiles. The primary aim of this chapter was to determine whether CPE could be isolated from wastewater in the East Midlands, and a total of 36 unique CPE were isolated, both from the influent (n=32) and effluent (n=4) of a WWTP that serves a major city and hospital. In addition, eight carbapenem-hydrolytic non-*Enterobacteriaceae* were isolated, with seven identified as belonging to the *Aeromonas* genus and one *P. aeruginosa.*

3.3.1 Multidrug resistance in *Enterobacteriaceae*

MDR bacteria were isolated from both cephalosporin and carbapenem selective agars. All but one of the *Enterobacteriaceae* isolated from agars supplemented with cephalosporins were resistant to three or more classes of antibiotic, and were therefore classed as MDR according to the definition used by Magiorakos et al. (2012)(. All *Enterobacteriaceae* isolated on agar supplemented with carbapenems were classed as MDR and were more likely to be resistant to a greater number of non-beta-lactam antibiotics. Furthermore, there was a significant association with harbouring bla_{NDM} and being resistant to multiple other classes of antibiotic, more so than for any other beta-lactam or plasmid replicon. All isolates but one containing bla_{NDM} were classified as *Escherichia*, and all of those also contained IncF plasmid

replicons. Additionally, IncF plasmids were also found in 26/29 non-replicate *Escherichia* isolated from cephalosporin selective agar. These data are consistent with previous studies showing that IncF plasmids are most associated with *E. coli* and often contain ESBL and carbapenemase genes (Rozwandowicz et al., 2018). The majority of CPE contained plasmids that were able to be transferred to a recipient strain through conjugation. These included two *Klebsiella* and one *Citrobacter* isolate, the plasmids of which were transferred into *E. coli.* Many transconjugants had identical patterns of phenotypic resistance gain and loss compared to their donor strains, and this suggests these are closely related. Of the assays that were not successful, those donors had previously been found to contain plasmid replicons, so this suggests either the carbapenemase genes are chromosomally encoded, or their plasmids are not conjugable. This will be investigated further in **Chapter 4**.

3.3.2 Comparison of CPE with UK epidemiology data

Overall, 20 non-duplicate CPE were identified in this study. These included 16 *Escherichia* and a single *Klebsiella* isolate containing bla_{NDM}. Two of the *Escherichia* isolates were also positive for bla_{OXA-48}, showing they contained two distinct carbapenemase genes. The remaining CPE were identified as two *C. freundii* and one *Klebsiella* sp. harbouring bla_{IMP}.

Early data on national NDM-producing isolates collected from the UK Health Security Agency (UKHSA; formerly Public Health England) Antimicrobial

Resistance and Healthcare Associated Infections (AMRHAI) between 2008 to 2013 found that *E. coli* only made up 26% of isolates, while *Klebsiella* spp. made up the majority at 59% (Jain et al., 2014). Data from AMRHAI collected from clinical isolates in East Anglia between 2006 and 2015 showed 43% of CPE produced NDM and only 41% of CPE were identified as *E. coli* (Ludden et al., 2017). In the West Midlands between 2007 and 2014, NDM was found in the majority of CPE at 58%, however only 22% of those were *E. coli* (Findlay et al., 2017).

In October 2020, UKHSA published the Framework of Actions to contain CPE (UKHSA, 2020), which requires diagnostic laboratories to notify UKHSA upon detection of CPE and their resistance mechanism. Analysis of this surveillance data from October 2020 to March 2023 showed similar results to the previous studies, that *K. pneumoniae* is most frequently found in the UK (32.9% of isolates), while *E. coli* makes up 31.0% of the species detected (UKHSA, 2023). The data on specific carbapenemases showed that OXA-48-like genes were most abundant (36.7%), with NDM (28.5%) and KPC (26.1%) the next most common. Of the *Escherichia* strains, OXA-48-like made up the highest proportion of carbapenemase genes at 40.9% of detected isolates, with NDM at 36.1% and KPC 20.2%. Among *Klebsiella* species, once again OXA-48-like carbapenemases are most abundant at 39.2%, with KPC the next most common at 31.7% and NDM at 24.7%, while IMP makes up only 2.8%. In *Citrobacter* isolates, IMP is relatively rare at 5.4%, behind OXA-48-like (42.8%), KPC (25.1%), and NDM (22.2%). These data differed geographically, and in the East Midlands, OXA-48-like carbapenemases make up an even higher proportion at

65.3%. NDM was found in 24.9% of carbapenemase producers, with KPC and IMP much lower than at the national level at 5.9% and 2.7% respectively.

Considering the data on CPE specifically in UK wastewater, Ludden et al. (2017) found only 22% of those detected in East Anglia contained an NDM carbapenemase, while the majority contained OXA-48. Of the detected CPE, only 11% were identified as *E. coli*. A study by Gibbon et al. (2021), which selected for *Klebsiella* in Southwest England hospital effluent and local wastewater influent, found only the OXA-48 carbapenemase. These data seem to suggest that although the prevalence of specific carbapenemases and bacterial species varies between studies and geographic locations, *E. coli* and NDM appear to be generally less abundant than other species and genotypes in the UK. These results are in contrast with this study, where the majority of carbapenemases detected were NDM, and *E. coli* the predominant carrier, with all *E. coli* CPE isolates producing this carbapenemase. Although OXA-48-like carbapenemases were detected, they were found in only 10% of non-duplicate CPE, much lower than the 40.9% found in *Escherichia* by UKHSA.

3.3.3 Carbapenem-hydrolytic non-*Enterobacteriaceae*

Seven *Aeromonas* and one *P. aeruginosa* isolate were positive for carbapenem hydrolysis, with the latter identified as containing the carbapenemase gene bla_{IMP}. The *Aeromonas* isolates were not positive for any of the carbapenemase genes tested. However, although acquired carbapenemase genes have been found in *Aeromonas* species, carbapenem resistance is more often caused by

the production of chromosomal carbapenemases intrinsic to certain *Aeromonas* species (Janda and Abbott, 2010). Whereas carbapenem-resistant *P.* aeruginosa have been designated one of the three critical priority pathogens by the World Health Organisation (WHO, 2017). Nationally, IMP carbapenemases make up 21.0% of those found in *P. aeruginosa* isolates, which makes it less common than VIM (33.6%) and NDM (27.3%) (UKHSA, 2023). This *P*. *aeruginosa* containing bla_{IMP} was the only *Pseudomonas* isolate to be resistant or have increased susceptibility to all three antibiotics that are recommended for use by the CLSI used in this study.

3.3.4 Comparison of influent and effluent isolates

Overall, only eight non-duplicate *Enterobacteriaceae* isolated on cephalosporin-selective agar were found from the effluent of WWTP B. Five of these clustered with other *Escherichia* that were isolated from river water samples. The others clustered with influent samples, but none shared the same AST and PCR profiles as those within their clusters. This is unsurprising as the three samples that used cephalosporin-selective agar were collected across a much longer timeframe than those using carbapenem selective-agars, with effluent samples being collected years later than influent samples.

On carbapenem-selective agar, there were only four non-duplicate isolates found in the effluent samples. These were identified as one bla_{IMP}-containing *Klebsiella* sp. and three bla_{NDM}-containing *E. coli.* The *Klebsiella* isolate clustered with other non-*Escherichia* isolates, while two of the *E. coli* formed a

small subcluster by themselves. However, the remaining *E. coli* isolate formed an identical cluster with two other *E. coli* samples isolated from the influent of the same WWTP, both from separate sample time points. This effluent sample was collected only one week after a previous influent sample, so it was possible that these organisms could be genetically related, and this is investigated in more detail in **Chapter 4**.

CPE were detected in the effluent of WWTP B in March 2020 from two separate samples, but neither sample taken in 2022 detected any CPE. Since the number of CPE isolated from influent samples also varied across time points, it is entirely possible that this is just seasonal variation. Previous studies have found seasonal variation in the bacterial communities of WWTPs (Zhang et al., 2018). However, seasonal patterns seem to vary by location; a study in China found a higher abundance of ARGs in winter (Su et al., 2017), whereas a comparison in the USA found ARG abundance was highest in Spring (Joseph et al., 2019). Another possibility is that recent upgrades to the WWTP in 2021 have improved the treatment process such that the abundance of CPE is much lower than was the case using the old treatment processes.

3.3.5 Conclusion

The aim of this chapter was to determine whether *Enterobacteriaceae* with acquired carbapenem resistance could be detected from local UK WWTPs that have previously not been sampled for these types of ARB. Results showed this was indeed possible and multiple isolates sharing the same AST and PCR

patterns were isolated from both treated and untreated wastewater sampled a week apart. Compared to *Enterobacteriaceae* isolates from cephalosporin-selective agars, those with carbapenem resistance had higher levels of resistance to non-beta-lactam antibiotics, while harbouring bla_{NDM} was associated with more phenotypic resistances than any other ARG or plasmid replicon. Similarly, even *Aeromonas* isolates from carbapenem-selective agar had higher levels of resistance to non-beta-lactams when compared to those from cephalosporin-selective agar, and the only carbapenemase-producing *Pseudomonas* had the most resistant results of all *Pseudomonas* isolates to the antibiotics tested. It has been shown that efflux pumps contribute to increased levels of MDR, as they can be responsible for the efflux of multiple different classes of antibiotic (Meletis, 2016); however, this work shows that higher levels of MDR are also associated with carbapenemase production. This has serious implications for our treatment of bacterial infections, as there become fewer antimicrobial therapies available for the treatment of these critical priority pathogens.

3.3.6 Future work

This chapter describes preliminary work to assess the feasibility of isolating CPE from wastewater and environmental samples, using the methods described. At the time of sampling there was only one published paper describing CPE from municipal wastewater samples taken in the UK. The selection for CPE was used to determine whether any could be detected, and then longer-term

experiments were planned to gather more data than is present here. However, the COVID-19 pandemic meant that sampling had to be stopped in March 2020 and it has not been possible to take any further influent samples. The effluent and river sampling of 2022 was designed to determine whether CPE could still be detected in the WWTP effluent, as they were in 2020.

Future work would include negotiating to be able to take influent samples once again, in order to be able to monitor the presence of CPE over a longer period. Recent work has shown that composite samples, that are a combination of multiple samples over the course of a day, are preferable to the short-term grab samples taken in this study (Chau et al., 2022), given the transient nature of ARB in wastewater. With this in mind, future samples would use composite sampling.

Carbapenemase-producing bacteria identified in this chapter will be further investigated in **Chapter 4**, especially focusing on the relatedness of CPE strains that cluster together on the map in **Figure 3.11** with specific focus on the plasmids harboured by these MDR stains. Future work would include a wider combination of phenotypic and genotypic analyses, such as qPCR for the determination of ARG relative abundance between sample points, as well as metagenomic approaches. Furthermore, there are several experiments that could be performed on the existing isolates, such as identification of the carbapenemases produced by the *Aeromonas* isolates, and PCR detection of mobile genetic elements such as *intI*, IS*26* and *ISEcp*1 in the *Enterobacteriaceae.* Lastly, the antimicrobials used to determine sensitivity in this study were chosen to represent a wide range of antimicrobial classes,

where resistance may be found in isolates of environmental as well as human and veterinary origin. With the knowledge that many of these isolates contain ARGs of concern such as *bla*$_{NDM}$ and *bla*$_{OXA-48}$, which are commonly detected in human-derived isolates, the use of antibiotics for use specifically to treat CPE such as fosfomycin or beta-lactamase inhibitor combinations for sensitivity testing could be performed.

CHAPTER 4: GENOMIC ANALYSIS OF CARBAPENEMASE-PRODUCING ISOLATES

4.1 Introduction

Whole genome sequencing has been used for a wide variety of applications, such as identification of rare human diseases, genome-wide association studies, mapping genomes of novel organisms, finishing genomes of known organisms, comparative genomics between samples, as well as many others (Krier, Kalia and Green, 2016; Illumina, 2023). The use of whole genome sequencing enables detection of clonal isolates responsible for the dissemination of AMR. Perhaps the most well-known examples of these are the clonal spread of the bla_{KPC}-producing *K. pneumoniae* clone ST258 (Bowers et al., 2015), and that of $bla_{CTX\text{-}M\text{-}15}$ through *E. coli* ST131 (Stoesser et al., 2016). Previous work on UK wastewater has shown that CPE strains of clonal origin can be found in hospital wastewater at different time points (White et al., 2016). Increasingly, long-read whole genome sequencing (WGS) data are being used to characterise MDR plasmids that have spread between strains, which helps us to understand non-clonal dissemination of AMR genes. Plasmids are notoriously difficult to assemble using short-read data alone, due to repetitive regions of DNA, especially those containing multiple MGEs which can often also be found on the host chromosome, even more so when there are multiple plasmids within the same cell (Arredondo-Alonso et al., 2017). Therefore, the use of Oxford Nanopore Technologies sequencers is ideal for the resolution of plasmid sequences, due to longer read lengths that can overcome these repetitive regions, in many cases generating the full plasmid sequence in a single read. This use of long-read sequencing has previously enabled

identification of identical carbapenem-resistance plasmids discovered in different bacterial species from municipal wastewater in East Anglia (Ludden et al., 2017). Additionally, a study comparing 3,697 plasmid sequences of bloodstream infections and wastewater isolates in Oxfordshire found that 19% of these were formed of 225 groups of identical plasmids, many of which were shared across species (Matlock et al., 2023). These studies highlight why long-read WGS is vital to our understanding of the spread of AMR.

Chapter 3 showed that MDR isolates from wastewater contained carbapenemase genes *bla*$_{NDM}$, *bla*$_{OXA-48}$-like and *bla*$_{IMP}$. These genes are commonly associated with MGEs in the *Enterobacteriaceae* (Mathers, 2016; Pitout et al., 2019), and all those isolates belonging to this family in **Chapter 3** also contained plasmid replicons that are strongly associated with AMR (Rozwandowicz et al., 2018). This chapter seeks to investigate this further, by generating and analysing WGS data to understand the genetic context of these MDR isolates.

4.1.1 Aims and objectives

The previous chapter showed that carbapenemase-producing bacteria with identical phenotypic antimicrobial resistance patterns, as well as genotypic patterns of ARGs and plasmid replicons, were isolated from different samples from the same WWTP at different time points or locations. The aims of this chapter were to determine whether these identical patterns were caused by the isolates themselves being clonal, or the spread of identical plasmids

between isolates; and to identify the genetic context of the carbapenemase genes harboured by these bacteria.

4.2 Results

All of the unique CPE isolated in **Chapter 3**, as described in **§3.2.5**, were subject to WGS performed externally. In addition, the *P. aeruginosa* isolate DD202 was also included for WGS. Although other carbapenem resistant non-*Enterobacteriaceae* were isolated in **Chapter 3**, DD202 was the only one to contain evidence of acquired carbapenem-resistance, as none of the *Aeromonas* isolates were positive for any of the carbapenemase genes tested by PCR (**§3.2.2.1**). This resulted in a total of 19 organisms sent for WGS, comprised of 15 *E. coli* isolates, the *Klebsiella* isolates DD112 and DD149, the *C. freundii* isolate DD137, and the *P. aeruginosa* isolate DD202. Originally, 12 isolates underwent both long-read and short-read sequencing, with a further 7 for short-read sequencing only (**§2.8.1**). Two isolates, DD153 and DD155 were later sequenced in-house using long-read sequencing (**§2.8.2**) and these data combined with short-read data to produce a combined assembly.

4.2.1 Genome assembly

Table 4.1 shows the assembly statistics for the sequenced isolates. All of those assembled using both long-read and short-read sequencing data were

Table 4.1. Assembly statistics for the sequenced isolates.

Isolate	No. of contigs	Largest contig (bp)	Total length (bp)	N50 (bp)	Illumina or Combined
DD153	68	355,394	4,947,432	183,592	Illumina
DD155	66	786,960	5,309,479	145,641	Illumina
DD177	61	593,877	5,119,229	192,949	Illumina
DD181	82	738,883	5,403,526	240,212	Illumina
DD189	53	593,877	5,120,620	200,008	Illumina
DD112	27	4,872,239	5,595,098	4,872,239	Combined
DD128	4	5,212,517	5,494,739	5,212,517	Combined
DD129	3	4,869,615	4,921,671	4,869,615	Combined
DD130	8	4,863,231	5,098,155	4,863,231	Combined
DD137	17	4,667,704	5,587,169	4,667,704	Combined
DD149	45	5,208,047	6,134,145	5,208,047	Combined
DD151	28	5,164,288	5,638,736	5,164,288	Combined
DD153	6	4,861,820	5,020,120	4,861,820	Combined*
DD155	2	5,119,709	5,283,181	5,119,709	Combined*
DD158	7	5,115,716	5,486,835	5,115,716	Combined
DD165	7	4,754,964	5,021,818	4,754,964	Combined
DD168	7	4,755,030	5,026,952	4,755,030	Combined
DD176	4	4,906,150	5,165,591	4,906,150	Combined
DD186	16	4,838,282	5,131,797	4,838,282	Combined
DD191	4	4,909,719	5,185,139	4,909,719	Combined
DD202	1	6,953,711	6,953,711	6,953,711	Combined

** Assemblies were generated from Illumina short-read sequencing performed by MicrobesNG combined with Oxford Nanopore sequencing performed internally. All other assemblies were performed by MicrobesNG.*

resolved into a smaller number of contigs (2-45 contigs) when compared to those assembled using short-read sequencing alone (49-82 contigs). The longest contig was 6,953,711 bp long and comprised the entire *P. aeruginosa* assembly of DD202. The isolates DD153 and DD155 were originally sequenced

via the Illumina platform alone and this resulted in assemblies containing 68 and 66 contigs respectively, with N50s of 183,592 and 145,641 bp. These were later also sequenced on the Oxford Nanopore MinION platform and these reads were used to create combined assemblies that reduced the number of contigs to 6 and 2 respectively and increased the N50 to 4,861,820 and 5,119,709 bp respectively.

4.2.2 Taxonomic distributions

The results of the Kraken analysis (**§2.8.1**) of the taxonomic distribution of sequencing reads can be seen in **Table 4.2**. The NDM-producing *Klebsiella* was identified as *K. quasipneumoniae,* while all the other NDM-producers were identified as *E. coli*. The other two *Enterobacteriaceae* containing bla_{IMP} were identified as *K. pneumoniae* and *C. portucalensis* (previously identified as *C. freundii* by 16S*),* and the taxonomic distribution of DD202 matched the 16S identification of *P. aeruginosa.* 80.38% of the DD202 reads matched that species identification, whereas for the *Enterobacteriaceae* isolates, those figures ranged from 23.70% to 75.01%.

4.2.3 Multi-Locus Sequence Typing and core genome Multi Locus Sequence Typing

E. coli isolate whole genome sequences were inputted into the Centre for Genetic Epidemiology (CGE) MLST and cgMLSTFinder tools (**§2.9.2.2**, **§2.9.2.3**)

Table 4.2. Taxonomic distribution of sequencing reads, as identified by Kraken software.

Isolate	Most frequent genus	Most frequent genus (%)	Most frequent species	Most frequent species (%)
DD112	*Klebsiella*	69.61	*K. quasipneumoniae*	23.70
DD128	*Escherichia*	77.57	*E. coli*	75.01
DD129	*Escherichia*	52.52	*E. coli*	50.35
DD130	*Escherichia*	50.22	*E. coli*	47.42
DD137	*Citrobacter*	83.76	*C. portucalensis*	57.22
DD149	*Klebsiella*	63.93	*K. pneumoniae*	32.21
DD151	*Escherichia*	77.36	*E. coli*	74.66
DD153	*Escherichia*	52.83	*E. coli*	51.06
DD155	*Escherichia*	77.11	*E. coli*	74.40
DD158	*Escherichia*	73.92	*E. coli*	70.89
DD165	*Escherichia*	47.08	*E. coli*	45.49
DD168	*Escherichia*	47.01	*E. coli*	45.26
DD176	*Escherichia*	36.69	*E. coli*	33.95
DD177	*Escherichia*	34.01	*E. coli*	34.01
DD181	*Escherichia*	70.04	*E. coli*	67.62
DD186	*Escherichia*	54.56	*E. coli*	52.80
DD189	*Escherichia*	36.48	*E. coli*	34.07
DD191	*Escherichia*	35.89	*E. coli*	33.42
DD202	*Pseudomonas*	94.30	*P. aeruginosa*	80.38

to identify the relatedness of the isolates, and the results can be seen in **Table 4.3**. Overall, there were six different sequence types detected amongst the *E. coli* isolates: ST101, ST205, ST361, ST405, ST940 and ST2851. Of these, multiple isolates were identified that belong to ST101, ST361, ST405 and ST2851, while the ST205 and ST940 groups contained only a single isolate. The ST101 isolates DD129 and DD153 that were isolated from WWTP influent samples and

Table 4.3. Results of CGE MLST and cgMLSTFinder tools to identify the sequence types of *E. coli* isolates.

Isolate	Sample point	Sample date	MLST	cgMLST
DD129	Influent	18.02.20	101	**104245**
DD153	Influent	03.03.20	101	**104245**
DD130	Influent	18.02.20	205	141815
DD176	Influent	03.03.20	361	**115891**
DD177	Influent	03.03.20	361	**115891**
DD189	Influent	10.03.20	361	**115891**
DD191	Effluent	10.03.20	361	**115891**
DD128	Influent	18.02.20	405	141146
DD151	Influent	03.03.20	405	106034
DD155	Influent	03.03.20	405	110910
DD158	Influent	03.03.20	405	**129352**
DD181	Influent	10.03.20	405	**129352**
DD186	Influent	10.03.20	940	110891
DD165	Effluent	03.03.20	2851	129451
DD168	Effluent	03.03.20	2851	129451

Core genome MLST results that were detected in multiple samples collected on different weeks or from a different sample point are shown in bold.

collected on 18.02.20 and 03.03.20 respectively, were found to have identical core genome MLST (cgMLST) results. The ST361 isolates, DD176, DD177, DD189 and DD191, were also found to have identical cgMLST results. DD176 and DD177 were collected from the influent on 03.03.20; DD189 was collected from the influent on 10.03.20; and DD191 was collected from the effluent on 10.03.20. DD177 was found to have the same cgMLST result as the other three, despite having a different AST result. The five ST405 isolates, DD128, DD151, DD155, DD158 and DD181, were found to be made up of four separate cgMLSTs, with DD158 and DD181, which were isolated from influent samples collected on 03.03.20 and 10.03.20, having identical cgMLST results. The same was true of ST2851 isolates DD165 and DD168, which were identified as the same core genome sequence type. Overall, there were six different sequence

types using the MLST scheme and nine using the cgMLST scheme, and the discrepancy between the two was found in the ST405 isolates.

4.2.4 Plasmid Replicon Detection and Sequence Typing

All assemblies were inputted into the CGE PlasmidFinder and pMLST tools (**§2.9.2.4**, **§2.9.2.5**), to detect plasmid replicons and their corresponding sequence type and the results can be seen in **Table 4.4.** PCR results from **§3.2.2** showed that all *Enterobacteriaceae* isolates contained IncF plasmids, while the *P. aeruginosa* isolate DD202 did not contain any of the plasmid replicons in the PBRT scheme. Analysis of the sequence data confirmed this, as there were no plasmids detected in DD202, while all other sequenced isolates contained IncF plasmids of various sequence types. A number of isolates were found to have identical pMLST results, including those isolated from different samples and belonging to different *E. coli* sequence types.

4.2.5 Resistance Gene Detection

The assemblies were inputted into the CGE ResFinder tool (**§2.9.2.1**), CARD Resistance Gene Identifier tool (**§2.9.2.6**), and CGE PointFinder tool (**§2.9.2.1**), in order to detect the presence and subtype of ARGs in the assembled sequences, and the results can be seen in **Table 4.5**. The carbapenemase genes detected in **Chapter 3** were identified as *bla*$_{\text{NDM-4}}$,

Table 4.4. Plasmid replicons detected in genome assemblies of isolates.

Isolate	Species	Sequence Type	Plasmid replicon	Plasmid size (bp)	pMLST
DD129	*E. coli*	ST101	IncFII	49,758	**F2:A-:B-**
DD153	*E. coli*	ST101	IncC IncFII	101,123 49,758	**F2:A-:B-**
DD130	*E. coli*	ST205	IncFIB (H89) IncFII IncFIB IncIγ Col156	113,585 90,309 16,139 5,091	*F66:A-:B32*
DD176	*E. coli*	ST361	IncFII IncFIA IncY IncIγ	122,175 89,634 47,632	F2:A4:B-
DD177	*E. coli*	ST361	IncFII IncFIA IncY IncIγ	- - -	F2:A4:B-
DD189	*E. coli*	ST361	IncFII IncFIA IncY IncIγ	- - -	F2:A4:B-
DD191	*E. coli*	ST361	IncFII IncFIA IncY IncIγ	123,996 89,634 61,790	F2:A4:B-
DD128	*E. coli*	ST405	IncFII IncFIA p0111 IncIγ	120,294 97,552 64,376	F2:A4:B-
DD151	*E. coli*	ST405	p0111 IncFII IncFIA IncFIB IncB/O/K/Z	99,371 97,185 85,738	F1:A1:B49
DD155	*E. coli*	ST405	IncFII IncFIA IncFIB	163,463	F1:A2:B33
DD158	*E. coli*	ST405	IncFII IncFIA IncFIB p0111 IncFII	149,168 95,656 72,721	***F31/36:A4:B1*** ***F35:A-:B-***
DD181	*E. coli*	ST405	IncFII IncFIA IncFIB p0111 IncFII	- - -	***F31/36:A4:B1*** ***F35:A-:B-***

DD186	*E. coli*	ST940	IncFII IncFIA IncFIB IncX3 IncIγ	142,480 46,161 71,037	F36:A1:B33
DD165	*E. coli*	ST2851	IncFII IncFIB IncX3 ColKP3 IncIγ	90,423 51,479 26,272	*F66:A-:B32*
DD168	*E. coli*	ST2851	IncFII IncFIB IncX3 ColKP3 IncIγ	95,416 51,479 26,272	*F66:A-:B32*
DD112	*K. quas.*	N/A	$IncFII_K$ $IncFIB_K$ IncFIA(HI1) repB IncX3	142,577 48,790 46,161	K1:A13:B-
DD137	*C. port.*	N/A	IncHI1A IncHI1B $IncFII_{Yp}$ IncC IncFII(SARC14)	299,854 170,608 140,924 120,997	Y3:A-:B-
DD149	*K. pneu.*	N/A	$IncFII_K$ $IncFIB_K$ IncC $IncFII_K$ repB	378,559 169,477 130,171	K5:A-:B- K7:A-:B-
DD202	*P. aeru.*	N/A	-	-	-

DD177, D181 and DD189 were assembled from short-read data, and so plasmid size could not be determined. DD202 did not contain any plasmid replicons. Matching pMLST results across isolates are highlighted using formatting, i.e. bold, italics, underlined, bold and italic. K. quas. – Klebsiella quasipneumoniae; C. port. – Citrobacter portaculensis; K. pneu. – Klebsiella pneumoniae; P. aeru. – Pseudomonas aeruginosa.

carried chromosomally; bla_{NDM-5}, carried chromosomally, on IncF, and IncX plasmids; $bla_{OXA-181}$, carried on IncX3-ColKp3 fusion plasmids; bla_{IMP-70} in the *C. portucalensis* isolate DD137 and *K. pneumoniae* isolate DD149; carried on IncC plasmids, and bla_{IMP-7} in the *P. aeruginosa* isolate DD202, carried chromosonally. All isolates contained *sul1*, except DD186 which

Table 4.5. Resistance genes detected in each isolate using ResFinder, PointFinder and CARD.

DD129 ST101						
Chromosome					**IncFII**	
***bla*$_{NDM-4}$**	*aac(3)-Iia*	*mdtG*	*parC*			
bla$_{CTX-M-15}$	*aadA2*	*msbA*	*emrK*	*H-NS*		
bla$_{TEM-1A}$	*baeSR*	*pmrF*	*emrY*	*marAR*		
qacEΔ1 x2	*cpxA*	*bacA*	*acrABR*	*mdtEF*	*bla*$_{TEM-1B}$	
mdf(A)	*kdpE*	*eptA*	*acrDE*	*mdtMN*	*mph(A)*	
sul1 x 2	*ampC*	*yojI*	*acrF*	*mdtO*	*rmtB*	
dfrA12	*ampC1*	*emrABR*	*acrS*	*mdtP*	*mrx*	
ble$_{MBL}$	*ampH*	*gyrA*	*CRP*	*soxRS*		
aph(3'')-Ib	*EF-Tu*	*gyrR*	*evgAS*	*tolC*		
aph(6)-Id	*glpT*	*mdtH*	*gadX*			
DD153 ST101						
Chromosome					**IncFII**	**IncC**
***bla*$_{NDM-5}$**	*aac(3)-Iia*	*mdtG*	*parC*			
bla$_{CTX-M-15}$	*aadA2*	*msbA*	*emrK*	*H-NS*		
bla$_{TEM-1A}$	*baeSR*	*pmrF*	*emrY*	*marAR*		
qacEΔ1	*cpxA*	*bacA*	*acrABR*	*mdtEF*	*bla*$_{TEM-1B}$	*bla*$_{SHV-12}$
mdf(A)	*kdpE*	*eptA*	*acrDE*	*mdtMN*	*mph(A)*	*qacEΔ1*
sul1	*ampC*	*yojI*	*acrF*	*mdtO*	*rmtB*	*aac(3)-IId*
dfrA12	*ampC1*	*emrABR*	*acrS*	*mdtP*	*mrx*	*aac(6')-Ib3*
ble$_{MBL}$	*ampH*	*gyrA*	*CRP*	*soxRS*		
aph(3'')-Ib	*EF-Tu*	*gyrR*	*evgAS*	*tolC*		
aph(6)-Id	*glpT*	*mdtH*	*gadX*			
DD130 ST205						
Chromosome					**IncFII:B**	
dfrA1	*vanG*	*emrABR*	*acrF*			
aadA1	*mrx*	*gyrA*	*acrS*	*mdtEF*		
baeSR	*msbA*	*mdtH*	*CRP*	*mdtMN*	***bla*$_{NDM-5}$**	*dfrA12*
cpxA	*pmrF*	*parC*	*evgAS*	*mdtO*	*bla*$_{TEM-1B}$	*ble*$_{MBL}$
kdpE	*sat2*	*emrK*	*gadX*	*mdtP*	*qacEΔ1*	*mph(A)*
leuO	*arnT*	*emrY*	*H-NS*	*rsmA*	*tetB*	*aadA2*
EF-Tu	*bacA*	*tetR*	*kpnE*	*soxRS*	*sul1*	*qepA4*
glpT	*eptA*	*acrABR*	*kpnF*	*tolC*		
mdtG	*yojI*	*acrDE*	*marAR*			
DD176 DD177 DD189 DD191 ST361						
Chromosome					**IncFII:A**	**IncIγ**
bla$_{OXA-1}$	*ampC1*	*bacA*	*emrY*	*marAR*	***bla*$_{NDM-5}$**	
mdf(A)	*ampH*	*eptA*	*acrABR*	*mdtEF*	*qacEΔ1*	
aadA1	*sitABCD*	*yojI*	*acrDE*	*mdtMN*	*tetA*	
qepA1	*EF-Tu*	*emrABR*	*acrF*	*mdtO*	*mph(A)*	*bla*$_{CMY-145}$
catA1	*glpT*	*gyrA*	*acrS*	*mdtP*	*sul1*	
baeSR	*mdtG*	*gyrR*	*CRP*	*soxRS*	*dfrA12*	
cpxA	*emrE*	*mdtH*	*evgAS*	*tolC*		

kdpE *ampC*	*msbA* *pmrF*	*parC* *emrK*	*gadX* *H-NS*		ble_{MBL} *aadA2* *mrx*	
DD128 ST405						
Chromosome					**IncFII:A**	**IncIγ**
baeSR *cpxA* *kdpE* *ampC* *ampC1* *ampH* *sitABCD* *EF-Tu*	*cyaA* *glpT* *mdtG* *emrE* *msbA* *pmrF* *bacA* *eptA*	*ugd* *yojI* *emrABR* *gyrA* *gyrR* *mdtH* *parC* *emrK*	*emrY* *acrABR* *acrDE* *acrF* *acrS* *CRP* *evgAS* *gadWX*	*H-NS* *marAR* *mdtEF* *mdtN* *mdtO* *mdtP* *soxRS* *tolC*	bla_{NDM-5} *qacEΔ1* *tetA* *mph(A)* *sul1* *dfrA12* ble_{MBL} *aadA2*	$bla_{CMY-145}$
DD151 ST405						
Chromosome					**IncFII:A:B**	
baeSR *cpxA* *kdpE* *leuO* *sitABCD* *EF-Tu* *cyaA* *glpT* *mdtG*	*vanG* *emrE* *msbA* *pmrF* *arnT* *bacA* *eptA* *ugd* *yojI*	*emrABR* *gyrA* *mdtH* *parC* *emrK* *emrY* *tetR* *acrABR* *acrDE*	*acrF* *acrS* *CRP* *evgAS* *gadWX* *H-NS* *kpnE* *kpnF* *marAR*	*mdtEF* *mdtN* *mdtO* *mdtP* *rsmA* *soxRS* *tolC*	bla_{NDM-5} $bla_{CTX-M-15}$ bla_{OXA-1} *qacEΔ1*x2 *tetB* *sul1* x2 *dfrA12* *dfrA17*	ble_{MBL} *aac(6')-Ib-cr* *aac(3)-IId* *aadA2* *aadA5* *catB3Δ* *tmrB*
DD155 ST405						
Chromosome					**IncFII:A:B**	
mdf(A) *baeSR* *cpxA* *kdpE* *ampC* *ampC1* *ampH* *EF-Tu*	*cyaA* *glpT* *mdtG* *emrE* *msbA* *pmrF* *bacA* *eptA*	*ugd* *yojI* *emrABR* *gyrA* *gyrR* *mdtH* *parC* *emrK*	*emrY* *acrABR* *acrDE* *acrF* *acrS* *CRP* *evgAS* *gadWX*	*H-NS* *marAR* *mdtEF* *mdtN* *mdtO* *mdtP* *soxRS* *tolC*	bla_{NDM-5} $bla_{CTX-M-15}$ bla_{OXA-1} *qacEΔ1* *tetA* *mph(A)* *sul1*	*dfrA12* ble_{MBL} *aac(6')-Ib-cr* *aadA2* *catB3Δ* *mrx*
DD158 DD181 ST405						
Chromosome					**IncFII:A:B**	
mdf(A) *baeSR* *cpxA* *kdpE* *ampC* *ampC1* *ampH* *sitABCD*	*cyaA* *glpT* *mdtG* *emrE* *msbA* *pmrF* *bacA* *eptA*	*yojI* *emrABR* *gyrA* *gyrR* *mdtH* *parC* *emrK* *emrY*	*acrABR* *acrDE* *acrF* *acrS* *CRP* *evgAS* *gadWX* *H-NS*	*mdtEF* *mdtN* *mdtO* *mdtP* *soxRS* *tolC*	bla_{NDM-5} $bla_{CTX-M-15}$ bla_{OXA-1} *qacEΔ1 x2* *tetA* *sul1 x2* *dfrA12*	*dfrA17* ble_{MBL} *aac(6')-Ib-cr* *aadA2* *aadA5* *catB3Δ*

EF-Tu	*ugd*	*tetR*	*marAR*			

DD186 ST940						
Chromosome			**IncFII:A:B**	**IncX3**	**IncIγ**	**Unknown**
tetB *dfrA1* *aadA1* *baeSR* *cpxA* *kdpE* *leuO* *EF-Tu* *glpT* *mdtG* *vanG* *mrx* *msbA* *pmrF* *sat2*	*arnT* *bacA* *eptA* *yojI* *emrABR* *gyrA* *mdtH* *parC* *emrK* *emrY* *tetR* *acrABR* *acrDE* *acrF* *acrS*	*CRP* *evgAS* *gadX* *H-NS* *kpnE* *kpnF* *marAR* *mdtEF* *mdtMN* *mdtO* *mdtP* *rsmA* *soxRS* *tolC*	*mph(A)* *ermB*	***bla*$_{NDM-5}$** *ble*$_{MBL}$	*bla*$_{CMY-42}$	*sul2* *bla*$_{TEM-1B}$ *aph(6)-Id* *aph(3'')-Ib*

DD165 DD168 ST2851						
Chromosome				**IncFII:B**	**IncX3 ColKP3**	**IncIγ**
bla$_{CTX-M-15}$ *mdf(A)* *baeSR* *cpxA* *kdpE* *ampC* *ampC1* *ampH* *EF-Tu* *glpT*	*mdtG* *msbA* *pmrF* *bacA* *eptA* *yojI* *emrABR* *gyrA* *gyrR* *mdtH*	*parC* *emrK* *emrY* *tetR* *acrABR* *acrDE* *acrF* *acrS* *CRP* *evgAS*	*gadX* *H-NS* *marAR* *mdtEF* *mdtMN* *mdtO* *mdtP* *soxRS* *tolC*	***bla*$_{NDM-5}$** *bla*$_{TEM-1B}$ *qacEΔ1* *tetA* *mph(A)* *sul1* *dfrA12* *ble*$_{MBL}$ *aadA2* *qepA4 x2* *mrx*	***bla*$_{OXA-181}$** *qnrS1*	*bla*$_{CMY-42}$

DD112 *K. quasipneumoniae*						
Chromosome					**IncFIA (HI1)**	**IncX3**
bla$_{OKP-B-2}$ *bla*$_{OKP-B-15}$ *fosA* *baeR* *leuO*	*EF-Tu* *uhpT* *vanG* *msbA* *arnT*	*lptD* *marAR* *eptB* *emrR* *acrR*	*adeF* *CRP* *H-NS* *kpnE* *kpnF*	*kpnG* *kpnH* *oqxA* *oqxB* *rsmA*	*bla*$_{DHA-1}$ *qacEΔ1* *sul1* *aph(3'')-Ib* *aph(6)-Id* *qnrB4*	***bla*$_{NDM-5}$** *ble*$_{MBL}$

DD137 *C. portaculensis*						
Chromosome			**IncFII$_{YP}$**	**IncFII (SARC14)**	**IncC**	**Unknown**

bla$_{CMY-49}$ *qnrB1* *baeR* *cpxA* *kdpE* *leuO* *EF-Tu* *glpT* *mdtG*	*uhpT* *vanG* *mrx* *msbA* *pmrF* *sat2* *arnT* *emrBR* *acrA*	*CRP* *H-NS* *kpnE* *kpnF* *marAR* *rsmA* *soxS*	*bla*$_{TEM-1B}$ *qacEΔ1* *sul1* *dfrA12* *mph(A)* *aac(3)-IId* *aadA2* *tmrB* *merACPRT*	*bla*$_{OXA-1}$ *tetA* *aac(6')-Ib-cr* *catB3Δ* *pcoABCD* *ERS* *arsABCD* *silABCEFP* *RS*	***bla*$_{IMP-70}$** *qacEΔ1* *sul1* *dfrA1* *aac(6')-Ib3* *sat2* *merACPRT*	*bla*$_{OXA-35}$ *qacEΔ1* *sul1* *aac(3)-Ib* *aadA10*
DD149 *K. pneumoniae*						
Chromosome					**IncC**	**Unknown**
bla$_{SHV-42}$ *fosA* *baeR* *leuO* *EF-Tu*	*uhpT* *vanG* *msbA* *arnT* *emrR*	*emrY* *acrA* *adeF* *CRP* *H-NS*	*kpnE* *kpnF* *kpnG* *kpnH* *lptD*	*marAR* *oqxA* *oqxB* *ramR* *rsmA*	***bla*$_{IMP-70}$** *qacEΔ1* *sul1* *dfrA1* *ere(A)* *aac(6')-Ib3* *aph(3')-Ia* *sat2* *merACPRT*	*qacEΔ1* *sul1* *qnrA1*
DD202 *P. aeruginosa*						
Chromosome						
***bla*$_{IMP-70}$** *bla*$_{OXA-488}$ *bla*$_{PAO}$ *qacEΔ1* *sul1* *aph(3')-IIb* *aac(3)-Ic* *aac(6')-Ib3* *aac(6')-Ib-cr*	*aadA2b* *aadA6* *catB7* *fosA* *arnA-arnT* *basRS* *mexAB-oprM* *mexCD-oprJ* *mexEF-oprN*	*mexGHI-opmD* *muxABC-opmB* *triA-opmH* *bcr-1* *cprR* *cprS* *cpxR* *emrE* *gyrA*	*mexJK* *mexL* *mexM* *mexN* *mexP* *mexQ* *mexR* *mexS* *mexT*	*mexV* *mexW* *mexY* *mexZ* *nalC* *nalD* *nfxB* *opmE* *parR*	*parS* *pdc-35* *pmpM* *rsmA* *soxR* *vanW* *yajC*	

Carbapenemase genes are highlighted in red. Unknown refers to genes detected on circular contigs with no known plasmid replicons. E. coli isolates are identified by their respective sequence types, while other isolates are identified by their respective species.

contained *sul2*. All those containing *bla*$_{NDM}$ also harboured *ble*$_{MBL}$, a bleomycin resistance gene, while all *E. coli* isolates except DD186 also contained *dfrA12*, *aadA2* and *qacEΔ1*. Notably, all isolates that contained the chloramphenicol

resistance gene *catB3Δ* were determined to be phenotypically susceptible to this antibiotic via AST in **§3.2.2.**

4.2.6 Sequence similarity of isolates

The software snippy was used to determine the number of SNPs between isolates to identify whether those within sequence types were of clonal origin, and the results can be seen in **Table 4.6**. Isolates were considered to be from the same source if they contained 20 or fewer SNPs (Pightling et al., 2018).

The ST101 isolates DD129 and DD153 were identified as clonal with only 2 SNPs detected between them. These were isolated from WWTP influent two weeks apart, and the plasmid replicon and ARG results above show that in this time, DD153 had gained an additional IncC plasmid when compared to DD129. Additionally, the carbapenemase gene detected in DD153 was $bla_{\text{NDM-5}}$, while the gene identified in DD129 was $bla_{\text{NDM-4}}$.

The ST405 isolates DD158 and DD181 were isolated from samples collected a week apart and these were also identified as clonal with only three SNPs detected between them.

Of the ST361 isolates, DD176 and DD177 were isolated from WWTP influent on 03.03.20, DD189 was isolated from WWTP influent on 10.03.20, while DD191 was isolated from WWTP effluent on 10.03.20. DD176 and DD177 were thought to be non-clonal due to their differing AST results (**§3.2.2)**, but with 0 SNPs between their chromosomes and only 1 SNP difference in their Inclγ

Table 4.6. Sequence similarity of suspected clonal isolates.

Isolate ID 1	Isolate ID 2	Sample Date 1	Sample Date 2	ST	SNP Distance
DD129	DD153	18.02.20	03.03.20	ST101	2
DD158	DD181	03.03.20	10.03.20	ST405	3
DD176	DD177	03.03.20	03.03.20	ST361	1 (IncIγ)
DD176	DD189	03.03.20	10.03.20	ST361	1 (IncIγ)
DD176	DD191	03.03.20	10.03.20*	ST361	1
DD168	DD165	03.03.20*	03.03.20*	ST2851	1

**These samples were collected from the effluent of the wastewater treatment plant, while all others in this table were collected from the influent.*

plasmid sequences this analysis showed that they were clonal isolates. DD189 had the same result as DD177, with only a single SNP between the IncIγ plasmids, while DD191 had a single chromosomal SNP when compared to DD176. This shows that isolates from a clonal origin were detected in three separate samples: influent on 03.03.20, influent on 10.03.20 and effluent on 10.03.20.

The isolates DD168 and DD165 were also thought to be non-clonal due to differing AST results (**§3.2.2)**, but this analysis showed they had a single SNP between them. However, their IncF plasmids differed by around 5 kbp in size, which analysis showed was due to a duplication of the sequence containing an IS*91* transposase, *groL*, *qepA4* and *ynaI*. The read files of DD165 however showed that this is an error in assembly, as multiple read files contained the repeated section, including one that was 94,593 bp in length.

Additionally, the plasmids from DD128 and the ST361 isolates that had identical pMLST results in **Table 4.4** were found to be very similar. The IncF plasmid of DD128 had 4 SNPs, a 6 bp deletion, a 47 bp deletion, two 1.8 kbp IS*Ec37* insertions and a 15 kbp region between two IS*26* sequences that is inverted when compared to the plasmid of DD191, as shown in **Figure 4.1A**.

Similarly, the plasmids of DD130 and DD168 were shown to be almost identical, with only 2 SNPs as well as the duplication of a region containing an IS*91* transposase, *groL*, *qepA4* and *ynaI* in pDD168_IncF, as well as the insertion of a hypothetical protein upstream of an IS*1A* element. The region on DD168 that is located between IS*26* elements was found to be inversely oriented in DD130 and was missing one of the IS*26* genes as shown in **Figure 4.1B**. This implies that the IncF plasmid of DD130 is an ancestor of that found in DD168, and that IS*26* replicated via a copy-in mechanism and caused the intervening DNA sequence to change orientation. Analysis of the direct repeats shows this to be the case, as the 8 bp target site where IS*26* does not exist in DD130 is duplicated in DD168.

Finally, the IncX3 plasmids contained in DD112 and DD186 that were both 46,181 bp in length were found to be almost identical, with only 1 SNP between them. As DD112 was isolated on 23.01.20 while DD186 was isolated on 10.03.20, this represents the longest period between isolation of related plasmids. This is also the only occasion in this work where the same plasmid was detected in differing species, as DD112 was identified as *K. quasipneumoniae,* and DD186 as *E. coli*.

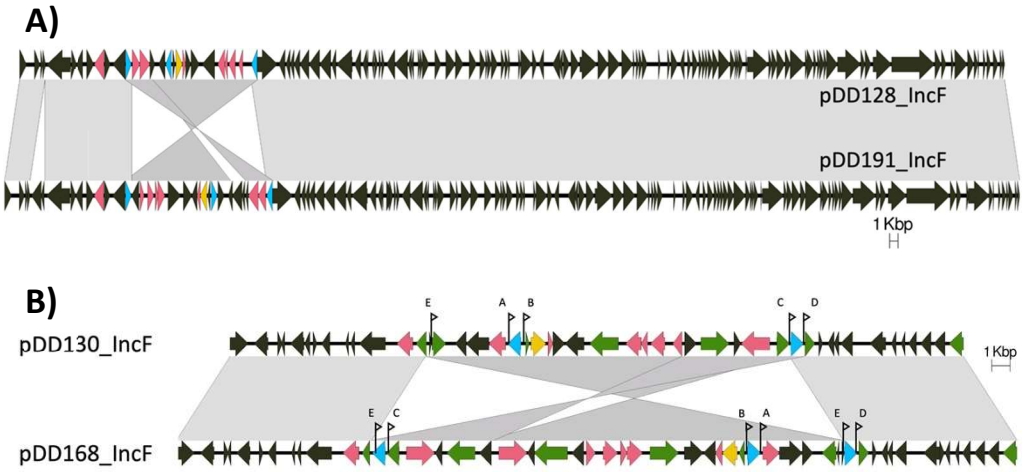

Figure 4.1. A) Alignment of the IncF plasmids of DD128 and DD191. The region containing all-but-one of the ARGs on both plasmids is inverted and found between two inversely oriented copies of IS*26.* B) Alignment of regions surrounding *bla*$_{NDM}$ on the IncF plasmids of DD130 and DD168. Antimicrobial resistance genes are represented by red arrows, mobile genetic elements by green arrows, IS*26* genes by blue arrows, while remaining coding sequences (CDS) are represented by black arrows. The locations of IS*26* direct repeats and target site on pDD130_IncF are represented by flags, with letters showing homologous repeats. The copy-in mechanism of IS*26* has resulted in an extra IS*26* element on pDD168_IncF and inversion of the intervening region.

4.2.7 Genetic context of *bla*$_{NDM}$

As all but one *bla*$_{NDM}$ isolate in this study contained *bla*$_{NDM-5}$, a BLAST search was conducted to find other isolates containing *bla*$_{NDM-5}$. As NDM genotypes can differ by a single base pair, a BLAST search for 100% identity to *bla*$_{NDM-5}$ was conducted in September 2021, and this resulted in 331 hits. The same search in September 2023 resulted in 641 hits, and the breakdown of the country metadata of these sequences can be seen in **Table 4.7**, grouped by global region. The vast majority of *bla*$_{NDM-5}$ sequences recovered originate from Asia, with only 16.6% in 2021 and 17.4% in 2023 being from outside the continent.

Table 4.7. Global distribution of *bla*$_{NDM-5}$ sequences found in Genbank in 2021 and 2023.

Region	2021	2023
East Asia	51.7%	49.1%
South Asia	27.2%	23.2%
Southeast Asia	4.5%	10.3%
Europe	8.8%	6.9%
North America	4.8%	6.9%
Other	3.0%	3.6%

In 2021, a BLAST search of *bla*$_{NDM-5}$ found 4 sequences isolated from the UK, whereas in 2023 there were 9, and these were all downloaded to produce a comparison of the regions surrounding the *bla*$_{NDM-5}$ gene. These sequences included a *K. pneumoniae* from a blood sample in London (Turton et al., 2019); 7 *E. coli* strains isolated from other UK hospitals (Turton et al., 2022), (unpublished, CP133853); and an *E. coli* isolated from the wound of a Springer spaniel in Liverpool (Reynolds et al., 2019, accession number: CP031653.1). Additionally, another sequence not found in Genbank was also used, the *E. coli* isolate VRES0316 found in wastewater described by Ludden et al. in 2017. **Figure 4.2** shows an alignment using BLAST of all these UK strains alongside the assembled plasmids from this study, except for DD130 and DD165 which were not used due to their similarity to DD168. The region surrounding *bla*$_{NDM-5}$ on the DD112 IncX3 plasmid only shares the beta-lactamase itself, the bleomycin

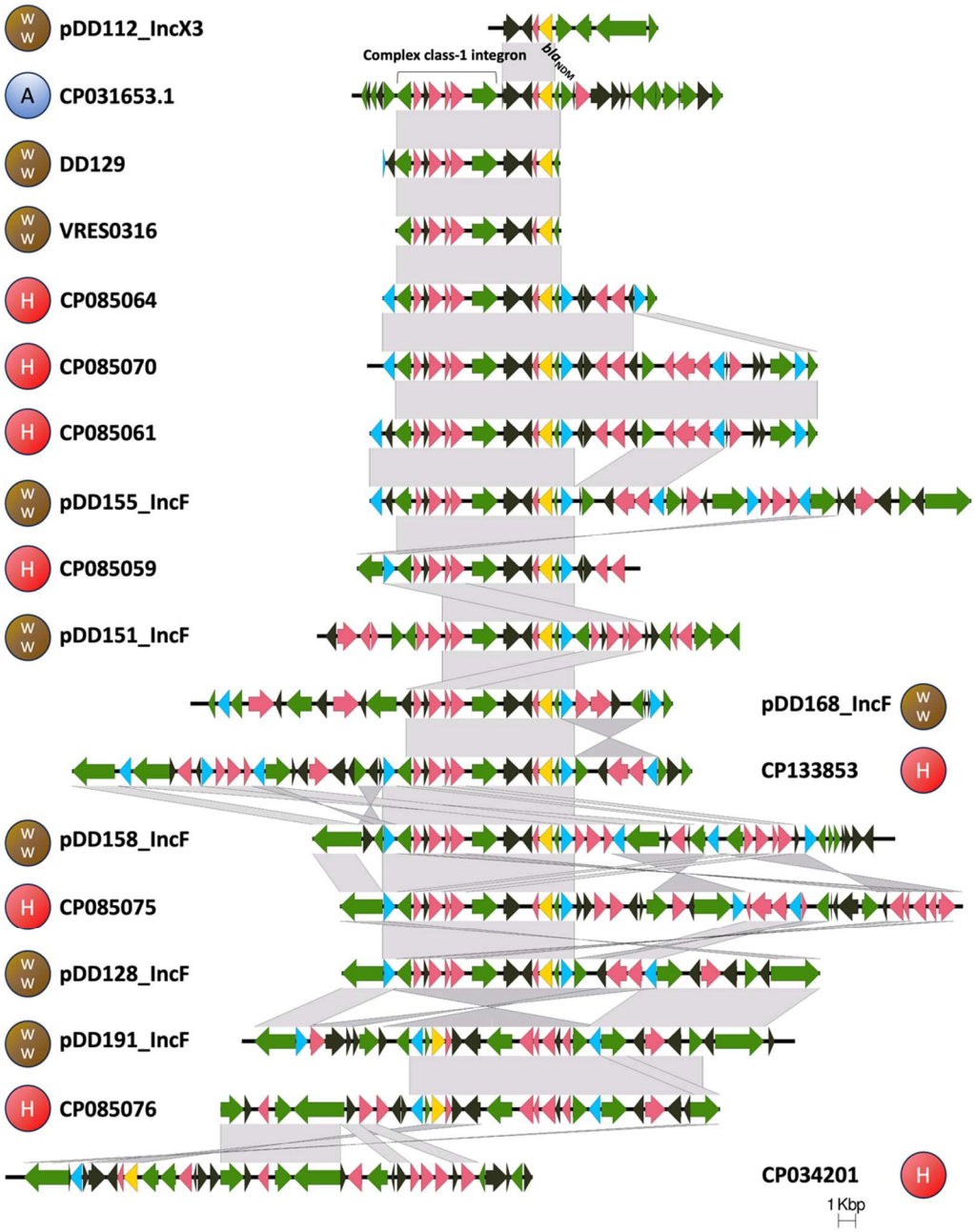

Figure 4.2. Alignment of the *bla*$_{NDM}$ regions of isolates in this study compared to others from the UK. Antimicrobial resistance genes are represented by red arrows, *bla*$_{NDM}$ by yellow arrows, mobile genetic elements by green arrows, IS*26* genes by blue arrows, while remaining coding sequences (CDS) are represented by black arrows. Sequences are annotated by bacterial isolation source: WW – isolated from wastewater, A – isolated from an animal source, H – hospital isolate. The genomic region surrounding *bla*$_{NDM}$ is conserved across the majority of the sequences. Only the *Klebsiella* isolates CP034201 and pDD112_IncX3 shared less than 10 kbp homology with other sequences.

resistance gene, and genes *trpF* and *dsbD* with the other sequences. Both DD129 and CP031653.1 contained their *bla*$_{NDM}$ genes on the chromosome; while the VRES0316 sequence was generated using short-read data so it is unknown whether the NDM is chromosomal or plasmid-based. All the remaining sequences contained at least 1 IS*26* gene within 3 kbp of their *bla*$_{NDM}$ gene, with up to 5 being detected in DD158 and CP133853. The majority of these conserved sequences also included the complex class 1 integron containing IS*CR1, sul1, qacEΔ1, aadA2, dfrA12* and the integrase *intI1.*

4.2.8 Genetic context of *bla*$_{IMP}$

The carbapenemase gene of *P. aeruginosa* isolate DD202, *bla*$_{IMP-7}$, was located within a class 1 integron, also containing *sul1*, *aadA2b*, and *aac(6')-Ib3*, as shown in **Figure 4.3**. This integron was found between two other insertion sequences, IS*6100* and an IS*1182*-family transposase.

The *bla*$_{IMP-70}$ gene of *C. portaculensis* isolate DD137 was found on its IncC plasmid, contained within a class 1 integron, alongside *aac(6')-Ib3, sul1* and *qacEΔ1*. In the *K. pneumoniae* isolate DD149, *bla*$_{IMP-70}$ was once again found within an integron on an IncC plasmid. In this isolate, an *ereA* gene had inserted into the integron, which was otherwise identical to that found in DD137*,* as can be seen in **Figure 4.3B**. Both sequences contained significant regions of homology, including another integron upstream of *bla*$_{IMP-70}$, as well as a

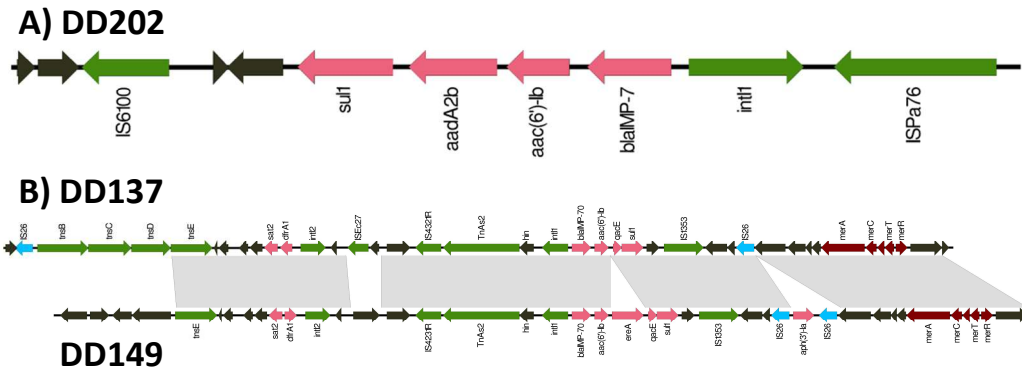

Figure 4.3. A) The genetic region around *bla*$_{IMP-7}$ on the chromosome of *P. aeruginosa* isolate DD202. B) Alignment of the regions surrounding *bla*$_{IMP-70}$ on the IncC plasmids of *C. portaculensis* isolate DD137 and *K. pneumoniae* isolate DD149. Antimicrobial resistance genes are represented by red arrows, mobile genetic elements by green arrows, IS*26* genes by blue arrows, mercury resistance genes by maroon arrows, while remaining coding sequences (CDS) are represented by black arrows.

mercury resistance operon downstream. In DD149, an IS*26* PCT had formed containing the aminoglycoside phosphotransferase gene *aph(3')-1a*.

4.2.9 Transconjugant sequencing and analysis

The transconjugants produced in **Chapter 3** were subject to in-house sequencing using the ONT MinION platform (**§2.8.2**). The assemblies were inputted into PlasmidFinder (**§2.9.2.4**) to determine the plasmid replicons that were mobilised from donor to recipient in the conjugation assays, the results of which can be seen in **Table 4.8**. Plasmid analysis explained why no transconjugants were recovered for DD129 or DD153 in conjugation assays in the previous chapter. This was due to their IncF plasmids missing genes from the *tra* operon which is responsible for conjugation (See **Appendix Figure 8.1**). Similarly, no results were found for DD130 which also lacks *tra* genes, although

Table 4.8. Results of conjugation assays and sequencing of transconjugants

Isolate	Plasmid replicons detected in donor	Plasmid replicons detected in transconjugant
DD112	IncFII(K), IncFIB(K), IncFIA(HI1), repB, **IncX3**	IncX3
DD128	**IncFII**, **IncFIA**, Inclγ, p0111	IncFII, IncFIA
DD129	IncFII	-
DD130	Col156, IncFII, IncFIB, IncFIB(H89), Inclγ	-
DD137	**IncC**, IncFII(SARC14), IncFII(Yp), IncHI1A, IncHI1B,	IncC, IncFII(Yp)
DD149	**IncC**, IncFII(K), IncFIB(K), repB	IncC
DD151	IncB/O/K/Z, **IncFII**, **IncFIA**, **IncFIB**, p0111	IncFIA, IncFIB
DD153	IncC, IncFII	-
DD155	**IncFII**, **IncFIA**, **IncFIB**	IncFII, IncFIA, IncFIB
DD158	Col(BS512), **IncFII**, **IncFIA**, **IncFIB**, p0111	IncFIA, IncFIB
DD165	**IncFII**, **IncFIB**, Inclγ, *IncX3-ColKP3*	IncX3-ColKP3
DD168	**IncFII**, **IncFIB**, Inclγ, *IncX3-ColKP3*	IncFII, IncFIB, Inclγ, IncX3-ColKP3
DD176	**IncFII**, **IncFIA**, IncY Inclγ	IncFII, IncFIA
DD186	IncFII, IncFIA, IncFIB, Inclγ, **IncX3**	IncX3
DD191	**IncFII**, **IncFIA**, IncY Inclγ	IncFII, IncFIA

Plasmid replicons detected via ResFinder in donor and transconjugant assemblies. Donor plasmids containing carbapenemase genes are shown in bold (bla$_{NDM}$) and italics (bla$_{OXA-181}$).

transconjugants had been recovered from assays involving DD165 and DD168 which had very similar plasmids. However, DD165 and DD168 also contained an IncX3-ColKP3 fusion plasmid containing *bla*$_{IMP}$, which in the case of DD165 has conjugated alone, and in DD168 has transferred to CV601 alongside the IncF plasmid containing *bla*$_{NDM.}$ There were 2 transconjugants, CV601:DD151 and and CV601:DD158, where a plasmid replicon was missing from the expected assembly. In both cases, the IncFIA and IncFIB replicons were detected, but the IncFII genes were missing. The lowest efficiency of conjugation from **Chapter 3** was from DD137, and bioinformatic analysis showed its IncC plasmid again does not contain *tra* genes, and this is explained

by the transconjugant also harbouring the IncFII(Yp) plasmid from DD137, which does. The next lowest efficiency was found from DD155, which may be explained by the fact that pDD155_IncF was the largest carbapenem-resistance IncF plasmid found in this study at 163 kbp. Overall, the results show that the plasmids of DD130, DD165, DD168 and DD137 are mobilisable, while the carbapenemase plasmids from all other conjugation assays are conjugable.

4.2.9.1 Donor YRIN/YRIK insertion and aztreonam resistance

As described in **§3.2.5**, the most common phenotypic loss of resistance in the conjugation assays was to aztreonam, which suggested that aztreonam resistance of the donors was not carried on their carbapenemase plasmids. Sadek et al. (2020) showed that aztreonam-avibactam resistance in CPE was caused by the isolates in that study having a combination of *bla*$_{CMY}$ genes alongside insertions of four amino acids, either YRIN or YRIK, in their PBP3 genes. An investigation into the loss of aztreonam resistance in transconjugants from **Chapter 3** showed that all *E. coli* donor sequences contained an insertion of these amino acids in their PBP3 gene that confers resistance to aztreonam (Sadek et al., 2020). Isolates DD128, DD155, DD158 and DD181 have the YRIK insertion and DD129, DD130, DD151, DD153, DD165, DD168, DD176, DD177, DD186, DD189 and DD191 have YRIN at 1000-1011 of their gene encoding PBP3. Additionally, 8 out of 15 *E. coli* donors harboured *bla*$_{CMY}$ enzymes, found entirely on IncIγ plasmids.

4.3 Discussion

In this chapter, the use of WGS showed that *E. coli* strains isolated from wastewater samples taken multiple weeks apart were clonal. Three separate isolates were detected on multiple occasions, determined by the use of WGS and cgMLST, including one found within multiple influent samples and an effluent sample a week later. This is the first time the same CPE has been detected in both the influent and effluent of a UK WWTP. Similar to previous studies, these CPE were detected in municipal UK wastewater sampled from the influent and effluent of WWTPs downstream of hospitals (Ludden et al., 2017; Gibbon et al., 2021). In another previous study, the same carbapenemase-producing strain was recovered in hospital wastewater at multiple time points over a two-month period (White et al., 2016), so the continual release of the same CPE from UK hospitals may explain why the same CPE strains were found at multiple time points.

Using resistance gene databases, a wide array of ARGs were detected, conferring resistance to almost all classes of antibiotics. All *E. coli* isolates contained the YRIN(K) insertion in their PBP3 protein recently shown to reduce susceptibility to Aztreonam (Alm, Johnstone and Lahiri, 2015). This is the only clinically used beta-lactam not degraded by MBLs, while avibactam inhibits serine-beta-lactamases, so Aztreonam-Avibactam combination therapy has been proposed for treatment of infections caused by CPE, and is currently under commercial development (Sadek et al., 2020). However, production of CMY enzymes, particularly CMY-42, as well as an insertion of four amino acids

(YRIN or YRIK) in the PBP3 gene is associated with increased MICs to this combination (Sadek et al., 2020). Four of the ST405 strains all contained the YRIK insertion while all others contain YRIN; while over 50% of sequenced *E. coli* isolates also produced CMY enzymes.

All sequenced isolates contained MDR plasmids with a high level of relatedness to those isolated from clinical samples around the world and belonged to sequence types previously associated with clinical infections (**§4.3.1**), suggesting these bacteria have the ability to cause severe and difficult to treat infections. 15 out of 19 isolates were confirmed to be *E. coli,* while the remaining strains were identified by Kraken analysis as *K. pneumoniae*, *K. quasipneumoniae*, *C. portucalensis*, and *P. aeruginosa*. The majority of the carbapenemase genes detected were *bla*$_{NDM}$, which were almost exclusively carried on IncFII plasmids, aside from two isolates which harboured their *bla*$_{NDM}$ genes on IncX3 plasmids. Of the sixteen sequenced *E. coli* isolates, only one contained *bla*$_{NDM-4}$ while the remainder harboured *bla*$_{NDM-5}$. Another isolate with identical cgMLST result and IncF plasmid compared to the *bla*$_{NDM-4}$-producing strain was found two weeks later and discovered to then contain *bla*$_{NDM-5}$, which is caused by a single aa substitution, potentially showing the evolution of *bla*$_{NDM}$ over time. Additionally, multiple unique isolates contained the same *bla*$_{NDM-5}$-producing plasmids, including *E.* coli strains DD130 and DD165; DD128 and DD191; as well as the *K. quasipneumoniae* isolate DD112 and *E. coli* DD186 sharing an IncX3 plasmid. Ludden et al. (2017) postulated that plasmids shared between species detected in UK wastewater were shared within the wastewater treatment plant itself, based on 0 SNP differences and

the base mutation rate of 14 SNPs per genome per year. The results in this chapter, that of an IncX3 plasmid found in two separate species 47 days apart with only 1 SNP difference, both from influent samples, suggest that although this is possible, there is certainly recent interspecies plasmid transfer going on prior to the wastewater treatment process.

4.3.1 Sequence types of *E. coli* isolates

Of the 15 sequenced *E. coli* isolates, the sequence types detected in this study were ST405 (5/15), ST361 (4/15), ST101 (2/15), ST2851 (2/15), ST205 (1/15) and ST940 (1/15). As well as being associated with NDM (Dadashi et al., 2019), ST405 is also an epidemic clone causing extraintestinal infections that is partly responsible for the global distribution of CTX-M-15 (Coque et al., 2008). ST101 is an MDR clone associated with nosocomial outbreaks caused by MBL-producing strains as well as non-outbreak related extraintestinal infections across Europe and Asia (Santos et al., 2020). Although reports of ST361 are relatively rare, it has been found producing NDM in clinical samples and hospital screening in South Korea, China, Nepal and Bangladesh (Shrestha et al., 2017; Hossain et al., 2020; Park et al., 2020). It has also been detected in Europe harbouring an OXA-48-like carbapenemase (Hammerum et al., 2020; Chudejova et al., 2021), as well as in ESBL-producing veterinary isolates (Freitag et al., 2017; Zogg et al., 2018; Shnaiderman-Torban et al., 2020). ST2851 is even less common, though it has once been found harbouring $bla_{\text{NDM-5}}$ in a surveillance network of clinical samples across Switzerland and Germany

(Chakraborty et al., 2021), as well as in wastewater from a German hospital, though its resistance genes are not described (Muller et al., 2018). An ST2851 isolate has also been found in a urine sample of a German patient that is almost identical to those found in this study (100% ID over 99% query cover) (Nordmann et al., 2021). Reports of ST940 and ST205 are also rare, but an ST940 isolate has previously been found harbouring *bla*$_{\text{NDM-5}}$ on an IncF plasmid in a clinical sample from the United States (Flerlage et al., 2020); while an ST205 has been described containing a *bla*$_{\text{OXA-181}}$ carbapenemase (Peirano et al., 2022). A review of NDM-producing bacteria in clinical settings around the world found that out of 212 *E. coli* isolates, ST101, ST167, ST131 and ST405 were the most common sequence types (Dadashi et al., 2019). However, another review in the same year found that. of 305 NDM-containing *E. coli* sequences deposited in GenBank, ST167, ST410 and ST617 were most prevalent (Wu et al., 2019). A more recent analysis of UK CPE found the sequence types ST405, ST648, ST167 and ST1702 were the most common carriers of *bla*$_{\text{NDM-5}}$ (Turton et al., 2022). The most commonly detected sequence type in this study was ST405, which aligns with Turton et al. (2022) and Dadashi et al. (2019), while two ST101 isolates were also detected. The ST2851 isolate was found recently in Germany so it is possible that this is due to recent importation of this strain to the UK. It is likely that the data from this study represents a brief snapshot of the CPE in this particular area, and more samples would be needed to generate a more robust picture of the ST of CPE in this region.

Considering the plasmids containing *bla*$_{NDM}$, Wu et al. (2019) found in the UK that *bla*$_{NDM}$ were most commonly associated with the IncC, IncL/M and IncX plasmid groups. Worldwide, *bla*$_{NDM-5}$ is often associated with IncFII plasmids, though IncX3 plasmids have been found to be more common (Wu et al., 2019). Of those that are carried on IncFII plasmids, the FY4:A-:B36 and F2:A-:B- allele types have been found to be most abundant (Wu et al., 2019). Similarly, of the 525 plasmid contigs containing *bla*$_{NDM}$ analysed by Acman et al. (2022), 48% contained IncX3 replicons, with IncFII as the next most common replicon type. However, when looking at Europe, the IncFII plasmids were found to be most common, with IncN also highly detected (Acman et al., 2022). This study found that *bla*$_{NDM}$ was found mostly on IncFII plasmids (12/16 isolates), with others on IncX3 (2/16) or chromosomally inserted in isolates with IncFII plasmids (2/16). The F2:A4:B- plasmid was detected in multiple sequence types, while F2:A-:B- was also detected, and the latter of which aligns with Wu et al. (2019). Overall, the incompatibility groups in this study seem to align with Acman et al. (2022), in that IncF replicons were most common in this part of the world, and the discrepancy with the previous investigation by Wu et al. (2019) may be due to the geographic distribution of sequence data in current databases.

It is important to point out that the vast majority of the data in other studies is generated in Asia. Of the 597 GenBank sequences containing *bla*$_{NDM}$ with location data available in Wu et al., 61.2% were from East Asia, South East Asia or the Indian subcontinent (Wu et al., 2019). Of the 269 *E. coli* sequences with known locations, the percentage was 88.2%, while only 1.1% were from the UK. Of the 212 *E. coli* sequences with known locations reviewed by Dadashi et

al. (2019), the prevalence of Asian isolates was similarly high, at 68.4%; while UK isolates made up only 5.2%. No specific percentages were available for Acman et al., though the study mentions that East and South East Asian countries make up the majority of collection sites, with China representing 31.8% of all isolates (Acman et al., 2022). For *bla*$_{\text{NDM-5}}$ specifically, this number is even higher, as shown by BLAST analysis in this work, where 82.6% of *bla*$_{\text{NDM-5}}$ sequences identified through BLAST analysis were found to be from Asia.

4.3.2 Genetic context of *bla*$_{\text{NDM}}$

It has been estimated that the UK is the second largest reservoir of *bla*$_{\text{NDM-1}}$ producers, behind the Indian subcontinent (Khan, Maryam and Zarrilli, 2017). In the West Midlands in 2017, 87% of *bla*$_{\text{NDM}}$ producers harboured *bla*$_{\text{NDM-1}}$, while *bla*$_{\text{NDM-5}}$ made up 9% (6/69) and *bla*$_{\text{NDM-4}}$ only 1% (1/69) (Findlay et al., 2017). Data from a recent review shows Europe is similar, with *bla*$_{\text{NDM-1}}$ being the most dominant genotype found in clinical isolates at 83% (65/78), with *bla*$_{\text{NDM-5}}$ making up 8% (6/78) and *bla*$_{\text{NDM-4}}$ (2/78) being only 3% (Dadashi et al., 2019). However, a more recent study on UK CPE involved the analysis of 1010 *E. coli* isolates submitted to UKHSA, found that 89 of the 105 *bla*$_{\text{NDM}}$ isolates contained *bla*$_{\text{NDM-5}}$ (Turton et al., 2022). While the *bla*$_{\text{NDM}}$ genotypes identified in this study are a small sample size so far, it is noteworthy that no *bla*$_{\text{NDM-1}}$ has been found considering the sequence types are clinically associated.

All the *bla*$_{\text{NDM}}$ sequences found in this study contained the common features of *ble*$_{\text{MBL}}$, *trpF* and *dsbD* immediately downstream, which were previously

shown to be found on the Tn*125* transposon that mobilised *bla*$_{NDM}$ and these associated genes into the *Enterobacteriaceae* (Bontron, Nordmann and Poirel, 2016). The strains with the *bla*$_{NDM}$ gene harboured on IncF plasmids contained truncated IS*Aba125* genes immediately upstream, while those found on IncX3 plasmids contained an intact IS*Aba125* gene, with an IS*5* inserted between, showing these are distinct lineages. Downstream sequences in which IS*CR1* has inserted adjacent to *dsbD* and is followed by *sul1*, as is the case for the majority of isolates in this study, are found almost exclusively on IncF plasmids in *Klebsiella* and *E. coli* (Acman et al., 2022). As IS*CR1* replicates via rolling-circle replication, the orientation of the transposase in most cases prevents it from mobilising *bla*$_{NDM}$ (Ilyina, 2012; Acman et al., 2022). However, Acman et al. (2022) found other IS elements that are heavily associated with *bla*$_{NDM}$, including IS*5*, predominantly found upstream on IncX3 plasmids from East Asia; IS*3000*, forming the composite transposon Tn*3000* in predominantly *Klebsiella* isolates; as well as IS*26.* The section containing IS*CR1* is followed by *intI1* in all but the ST2851 isolates, which have a further insertion between *dfrA12* and *intI1*. However, the upstream regions are more variable, as they contain a variety of different resistance genes contained within IS*26* arrays. These arrays can be seen in **Figure 4.2**, where the majority of isolates contain at least three IS*26* elements in the region around their *bla*$_{NDM}$ gene. In DD155, this region contains five copies of IS*26*, in both orientations, and the sequences between these elements contained every resistance gene found on that IncF plasmid.

4.3.3 Genetic context of other carbapenemase genes

The *bla*$_{OXA-181}$ gene was found on an IncX3-ColKP3 fusion plasmid, contained within an IS*26* PCT. This matches the results found by an investigation into the plasmids carrying *bla*$_{OXA-181}$ found in GenBank, which determined that 64/81 contained both IncX3 and ColKP3 replicons (Yu et al., 2022). These isolates also contained *bla*$_{NDM}$, which has previously been described in both *K. pneumoniae* and *E. coli* in Korea, Nepal and China (Ahn et al., 2019; Sherchan et al., 2020; Tao, Tan and Chen, 2023).

The *bla*$_{IMP}$ genes detected in this study were *bla*$_{IMP-7}$ and *bla*$_{IMP-70}$, both found within integrons, on IncC plasmids as well as on a *P. aeruginosa* chromosome. The *bla*$_{IMP}$ gene has been detected within integrons since 1995 (Arakawa et al., 1995), and a review in 2005 showed that most *bla*$_{IMP}$ genes are in fact found on class 1 integrons, though some have been detected within class-3 integrons as well (Walsh et al., 2005). A *P. aeruginosa* isolate in Malaysia was found to contain *bla*$_{IMP-7}$ in 2002, just as in DD202 (Ho et al., 2002), and has since been discovered in Eastern Europe, Canada and Australia (Cornaglia, Giamarellou and Rossolini, 2011; McCarthy et al., 2017).

The only published reports of *bla*$_{IMP-70}$ come from *Providencia* isolates from urine samples in Japan, where the gene was found on IncA/C plasmids (Iwata et al., 2020; Watanabe et al., 2022). In this study it was found on an IncC plasmid in both *K. pneumoniae* and *C. portucalensis.* This new species of *Citrobacter* was first described in 2017, found in a water sample in Portugal (Ribeiro et al., 2017), and has since been characterised harbouring *bla*$_{NDM}$ and

bla$_{KPC}$ in China (Cao et al., 2021; X. Luo et al., 2022) It was previously identified as *C. freundii* through 16S sequencing in **Chapter 3**, but Kraken analysis of the entire genome showed that 57.22% of reads were identified as *C. portucalensis* instead. This appears to be the first report of this species in the UK, though it is worth noting that previous studies which solely used 16S identification would have labelled this as *C. freundii.*

4.3.4 Co-occurrence and co-selection of AMR

All the isolates sequenced in this chapter contained multiple AMR genes conferring phenotypic resistance to a variety of antibiotic classes, as shown in **Chapter 3**. Many of these genes co-occur in the same cell, as many isolates contained multiple plasmids that harboured different ARGs, as well as containing further ARGs or disinfectant resistance genes on the host chromosome. However, many of these resistance genes were found on genomic regions that are highly conserved across multiple different plasmids. Previous *in silico* analysis has shown that carbapenemase genes spread through the human microbiome via clonal spread of bacterial strains, plasmid transfer, and transfer between plasmids via smaller MGEs such as transposons (Sheppard et al., 2016). The fact that the *bla*$_{NDM}$ gene found on IncF plasmids in this study was often surrounded by other ARGs all contained within an IS*26* PCT shows that selection for any of these resistance genes has the potential to select for all of the resistance genes contained within that PCT, if not all the ARGs in the entire plasmid. Indeed, in the case of DD155, all the ARGs on the

IncF plasmid were contained within an IS*26* PCT, so this cluster of ARGs has the potential to spread via the methods above as a single unit of selection.

The *C. portucalensis* strain DD137 contained genes that confer resistance to mercury, arsenic, silver and copper, all found on plasmids that contained ARGs. A large-scale study of bacterial sequences containing ARGs and antimicrobial metal resistance genes found that, although mercury resistance is commonly found near ARGs on MGEs, other metal resistance genes rarely co-occur with AMR genes on plasmids (Pal et al., 2015). Previous works have described how antimicrobial metal resistance may be playing a role in the maintenance of AMR in certain bacterial populations, and vice versa (Hobman and Crossman, 2015; Hobman, 2017; Pal et al., 2017). In wastewater specifically, although a previous study found no association between the presence of antimicrobial metals and ARGs in a Swedish WWTP (Bengtsson-Palme et al., 2016), a recent investigation into AMR in 10 UK WWTPs found that the presence of copper was significantly correlated with prevalence of ARGs (UKWIR, 2022). That the *C. portucalensis* isolated in this study contains multiple antimicrobial metal resistance gene operons on plasmids, either close to or within IS*26* PCTs in the same cell as $bla_{\text{IMP-70}}$ contained within an IS*26* PCT, implies that there is the potential for co-selection of metal and antibiotic resistance genes in this isolate. Overall, the amount of ARGs, combined with the fact that nearly every isolate in this study contained a conserved class 1 integron as well as the antimicrobial metal resistance genes described here shows there is potential for co-selection of a large variety of mechanisms alongside carbapenem resistance in these isolates.

4.3.5 ARG presence and phenotypic susceptibility

A number of isolates exhibiting susceptibility to chloramphenicol (§3.2.2) were found to carry the *catB3Δ* gene, encoding part of a chloramphenicol acetyltransferase (**Table 4.5**). Initially, these genes were annotated as *catB3* using ResFinder. However, further investigation into the genotype-phenotype discordance revealed that these genes were a truncated and non-functional variant of *catB3,* usually referred to as *catB4*, as described by Graf et al. (2024). Graf et al. proposed renaming this variant as *catB3Δ* to reflect its truncated nature. They identified that the truncation occurred due to the insertion of an IS*26* element, and in this study, *catB3Δ* was consistently detected immediately upstream of an IS*26* element in all relevant isolates. This highlights, once again, the significant role of IS*26* in shaping antimicrobial resistance (AMR) mechanisms, as well as the issues with inferring phenotypic resistance from WGS data alone.

4.3.6 Conclusion

The prevalence of various genotypic factors of CPE such as species, plasmid content, carbapenemase gene and specific genotype clearly vary by geographical region (Acman et al., 2022); and the data we have on the spread of bla_{NDM} is dominated by sequences from elsewhere in the world. This chapter adds to the data on UK CPE and shows that bla_{NDM} is being spread by IncFII and

IncX3 plasmids amongst enterobacteria in this area. These plasmids often contain multiple other ARGs so selection for various classes of antimicrobial has the potential to select for carbapenem resistance in these isolates. For global surveillance of the spread of AMR to be effective, more research is needed on the spread of CPE within Europe and the UK. This chapter is part of that necessary research and adds to our knowledge of the MGEs responsible for the spread of carbapenemases in the UK.

4.3.7 Future work

A recent review on the surveillance of AMR in wastewater argued that composite samples of wastewater, where multiple samples are taken over a time period and then mixed together, enable a more representative collection of the bacterial species at that time point compared to a single grab sample (Chau et al., 2022). However, another study by Chau et al. found that *bla*$_{NDM}$ was detected in metagenomic data from a grab sample but not the corresponding composite sample for that day (Chau et al., 2023). Any future work collecting wastewater would ideally take this into account and collect both grab and composite samples. The original goal of this study was to use a combination of culture-dependent and culture-independent approaches to determine the prevalence of AMR in wastewater. While unfortunately this had to change due to the COVID-19 pandemic, any future research on this topic would use a combination of approaches, such as culture, metagenomics, and qPCR. The issue with detecting genes of low abundance is a common feature

of metagenomic analyses of AMR genes, as resistant bacteria tend to be a subset of the total population (Gweon et al., 2019). A potential way of overcoming this issue would be to use culture-enriched metagenomics, allowing for a greater sequencing depth of AMR bacteria (Zhang, Zhang and Ju, 2022).

Another proposed goal of this work was to compare the isolates found in wastewater to those found in hospitals. So far, all CPE detected in UK wastewater have been found downstream of hospitals, and the MGEs they carry are closely related to those of clinical isolates in other countries. This suggests that wastewater isolates reflect those found in hospitals, and yet a clear link between these remains unproven. As we understand that the genetic epidemiology of CPE differs geographically, examining the bacteria that are isolated in a hospital and the receiving WWTP within a similar time period would be ideal.

CHAPTER 5: MOBILISATION OF IS*26*

5.1 Introduction

IS*26* has been shown to have played a critical role in the dissemination of AMR genes in Gram-negative bacteria, as it is associated with genes that confer resistance to many different classes of antibiotics, as well as other mobile genetic elements such as class 1 integrons (Harmer, Moran and Hall, 2014). IS*26* has been shown to form cointegrates with other DNA molecules, preferentially targeting those that contain another IS*26* element. This method of transposition is responsible for generating IS*26* arrays, where sections of DNA contain multiple copies of IS*26* in sequence, bracketing intervening sections of DNA (Harmer, Moran and Hall, 2014). Sections of these arrays, where DNA sequences are bounded by two directly oriented IS*26* elements, are known as pseudo compound transposons (PCTs), and these are able to form separate molecules of DNA, known as translocatable units (TUs), via homologous recombination (Harmer, Pong and Hall, 2020). These TUs are then able to form cointegrates with other DNA molecules and so transfer the intervening sections of DNA, which is a key mechanism in the spread of AMR genes. Previous bioinformatic analyses have shown that IS*26* is influential in the formation of MDR plasmids, and has specifically played a role in the dissemination of bla_{NDM}, especially in IncF plasmids found in *E. coli* (Acman et al., 2022). Experimental work has shown that artificially constructed TUs formed of an IS*26* and antimicrobial resistance genes, are able to form cointegrates with other DNA molecules containing IS*26*, and so transfer the resistance genes to these other DNA molecules (Harmer, Moran and Hall, 2014;

Harmer and Hall, 2016). Excision of a TU from an *E. coli* chromosome and its subsequent cointegration with a plasmid containing another IS*26* has also been described (Hubbard et al., 2020). However, no experimental work has been carried out to show that TUs containing multiple AMR genes that formed *in vivo* from wild-type MDR plasmids have been successfully transferred to another plasmid in the same cell. Though bioinformatic analysis strongly suggests this to have been the case, this is a gap in our knowledge that this work seeks to fill. A major reason for this gap is likely to be the difficulty in selecting for successful transfer of AMR genes between replicative DNA molecules. As TUs alone are not able to replicate, selection for the AMR genes contained within them in a susceptible recipient will result in the selection of only those that have successfully integrated somewhere within the host. However, integration between two plasmids is more difficult to detect, as selection for the relevant antibiotics will also result in the growth of bacteria where cointegration has not occurred.

To combat this, the donor plasmid will have to be selected against, but the usual methods of curing, such as heat or chemical stress, would also remove the recipient plasmid. Possible methods to resolve this issue include the use of the plasmid pCURE2, which uses anti-replication and anti-addiction systems to cure IncF plasmids (Hale et al., 2010); other potential plasmid-curing methods have used CRISPR-Cas based systems (Buckner, Ciusa and Piddock, 2018).

5.1.1 Incompatibility-based plasmid curing

The pCURE2 method of plasmid curing uses the mechanism of plasmid incompatibility to displace resident IncF plasmids. The plasmid pCURE2 contains sections of the FIA and FIB replicons, which contain DNA sequences responsible for blocking replication that are responsible for controlling the copy number of IncF plasmids (Womble and Rownd, 1988; Saul et al., 1989). It also contains the sequence for the antisense RNA, CopA, that indirectly blocks translation of the FII *repA* gene, again as part of regulation of plasmid copy number (Blomberg, Nordström and Wagner, 1992), as well as a kanamycin resistance gene. The combination of these sequences is used to block replication of other IncF plasmids, which often contain multiple replicons. Introduction of pCURE2 into a cell in combination with kanamycin selection can result in loss of IncF plasmids alongside maintenance of pCURE2 (Hale et al., 2010). Additionally, pCURE2 also contains the *sacB* gene used for sucrose counter selection. This encodes the levansucrase enzyme that converts sucrose to levans, which is harmful to the cell (Gay et al., 1985). When grown on media containing sucrose, any cells containing pCURE2 will produce this enzyme, resulting in cell death, and this can be used to select for plasmid-free cells.

Many IncF plasmids contain genes that ensure their propagation to daughter cells through the mechanism of **p**ost**s**egregational **k**illing (PSK). This mechanism involves the production of two genes, a short-lived antitoxin combined with a long-lived toxin, and is also known as a Toxin-Antitoxin (TA) system (Brendler, Reaves and Austin, 2004; Unterholzner, Poppenberger and Rozhon, 2013). The

first of these systems to be described, *ccdA*/*ccdB*, involves the production of two proteins. The first, CcdA, encodes an antitoxin, which binds to the toxin CcdB forming a protein-protein complex that results in toxin neutralisation. However, the toxin is stable in the cell, while the antitoxin is rapidly degraded by nucleases. This means that daughter cells will inherit the toxin from their parent, and only those which also contain the plasmid that encodes the antitoxin gene will survive (Unterholzner, Poppenberger and Rozhon, 2013). Many IncF plasmids contain one or more PSK systems, so successful curing of IncF plasmids will most often result in cell death unless the appropriate antitoxin is also present. For this reason, pCURE2 also contains the *flmB*, *ccdA*, *pemI* and *srnC* genes which encode for antitoxins from the most common PSK systems of IncF plasmids (Hale et al., 2010).

5.1.2 CRISPR-Cas9-based plasmid curing

While the previously described method of plasmid curing occurs using the indirect mechanism of incompatibility, others such as the CRISPR-Cas9-based method use a more direct approach. In this method, specific sequences of target plasmids are cleaved by the action of the Cas9 nuclease, directed to the target sequence by one or more designed single guide RNAs (sgRNA), alongside the CRISPR system. In some cases sgRNAs have been used to target specific plasmid replicons (He et al., 2021), while in other experiments, ARGs themselves have been used as targets (Kim et al., 2016; Buckner, Ciusa and Piddock, 2018; Walker-Sünderhauf et al., 2023). The plasmid pFREE (**Figure 2.1**)

contains a CRISPR-Cas9 system with sgRNAs designed to target the replicons of common laboratory cloning plasmids, including itself, in order to produce plasmid-free cells after complex cloning experiments (Lauritsen et al., 2017). This system is inducible, with the sgRNA array under the control of the PrhaBAD promoter, induced by the addition of rhamnose, while the Cas9 nuclease is controlled by the Ptet promoter, which can be induced by the addition of anhydrotetracycline (aTc). The plasmid also contains a kanamycin resistance gene for antibiotic selection.

5.1.3 Aims and Objectives

This chapter aims to show the transfer of *bla*$_{NDM}$ and other resistance genes, found in the environmental plasmids described in **Chapter 4**, to another plasmid via cointegration of IS*26* elements found on both plasmids, and a representation of hypothesised IS*26* mobilisation between plasmids is shown in **Figure 5.1**. To detect this, the donor plasmid will have to be cured from the cell, so that under antibiotic selection, only cells where mobilisation from one plasmid to another has occurred will survive. As the plasmids isolated in the previous chapter contain PSK systems, the recipient plasmid will also have to contain antitoxin genes to prevent cell death after plasmid curing. To promote the mobilisation of IS*26* between plasmids, the recipient plasmid will also need to contain an IS*26* gene. Overall, this will require construction of a recipient plasmid containing IS*26*, antitoxin genes, a selectable marker, as well as a system of plasmid curing. Following this, the constructed plasmid will need to

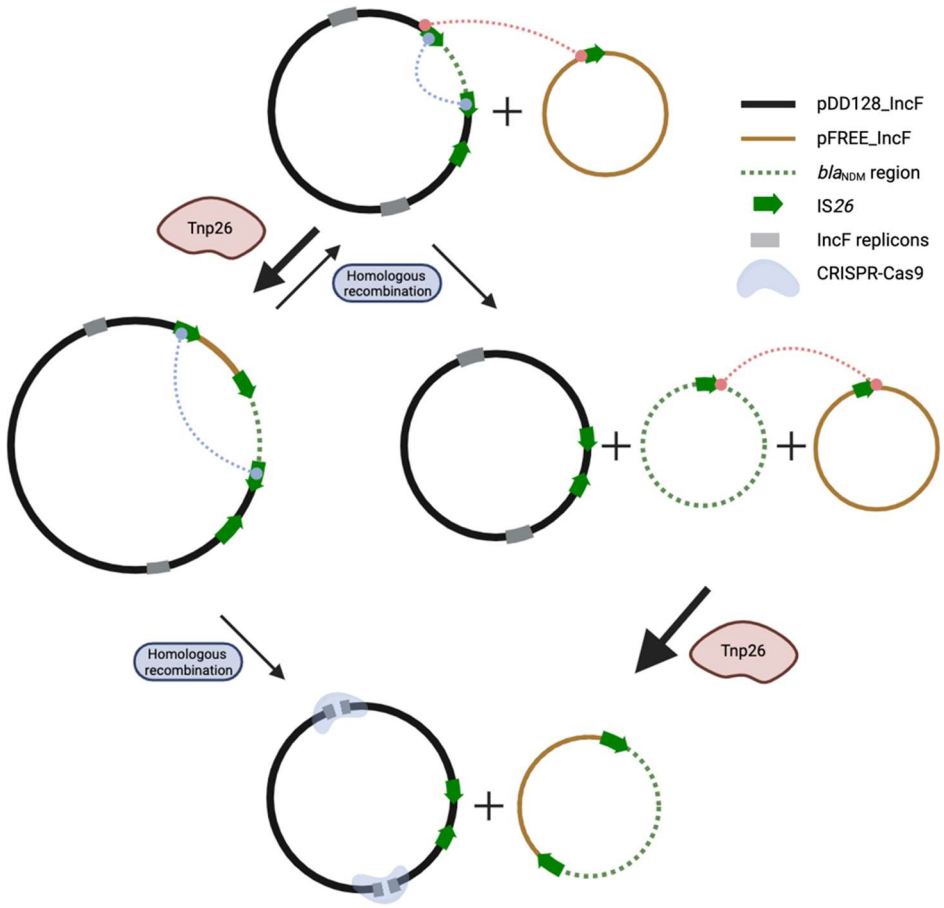

Figure 5.1. Predicted route of cointegration formation between recipient plasmid and bla_{NDM} region of DD128_IncF. Cointegrate will form between both plasmids (left), or by homologous recombination of the recipient plasmid and a translocatable unit formed from the bla_{NDM} region (right). Removal of pDD128_IncF (bottom) using a CRISPR-Cas9 system will result in recovery of cointegrates after antibiotic selection for bla_{NDM}. Arrows represent the relative frequencies of the homologous recombination-mediated and Tnp26-mediated reactions. Image created with BioRender.com.

be transformed into a cell containing the MDR environmental plasmid, followed by curing of the MDR plasmid and antibiotic selection. This chapter will investigate the feasibility of using both incompatibility-based and CRISPR-Cas-9-based plasmid curing for the recipient plasmid. Confirmation of plasmid curing and mobilisation of AMR genes via IS*26* cointegration will be performed by long-read sequencing using the ONT MinION platform.

5.2 Results

5.2.1 Conjugation of IncF plasmids into *E. coli* K-12 J53 Azi^R

As the potential recipient plasmids, pCURE2 and pFREE, use kanamycin as a selective marker, the environmental isolates to be used were tested for kanamycin susceptibility. The plasmid pDD128_IncF was chosen to be used as a donor for the IS*26* TU, as this plasmid had been detected in multiple isolates from different samples in **Chapter 4** and so possibly represented a dominant plasmid in this environment. A diagram of the genetic region containing *bla*$_{NDM}$ on this plasmid can be seen in **Figure 5.2**. Although ResFinder predicted that DD128 would be susceptible to kanamycin, experiments showed that it was able to grow on LB agar containing the antibiotic. Since DD128 contains multiple aminoglycoside resistance genes (**§4.2.5**), but only *aadA2* is found on pDD128_IncF, and this only confers resistance to streptomycin and spectinomycin (Ahmed and Shimamoto, 2004), it was hypothesised that a transconjugant of DD128 into a kanamycin susceptible recipient would remain kanamycin susceptible. Similarly, since pDD168_IncF also contains *aadA2* and

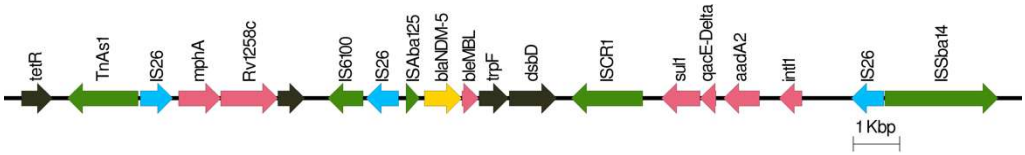

Figure 5.2. The genetic region of pDD128_IncF containing *bla*$_{NDM}$. Antimicrobial resistance genes (ARGs) are annotated in red, *bla*NDM is annotated in yellow, mobile genetic elements annotated in green and IS*26* genes annotated in blue. The two directly oriented IS*26* genes form a pseudo compound transposon (PCT) containing *bla*$_{NDM}$ and other ARGs. This PCT can excise from the plasmid and form a transposable unit (TU), which could be transferred to a recipient plasmid, as is the aim of this chapter.

no other aminoglycoside resistance genes, this was also used as a donor in a conjugation assay. Since kanamycin susceptibility was necessary to use either pCURE2 or pFREE, the kanamycin-resistant recipient CV601 used in previous conjugation experiments could not be used as a recipient strain. For this reason, the sodium azide-resistant *E. coli* J53 Azi^R was used instead (**Table 2.1**). Conjugation of pDD128_IncF into J53 Azi^R was performed (**§2.6.3**), however an accurate count of total transconjugants and therefore conjugation efficiency was not determined due to low numbers of recovered transconjugants. For pDD168_IncF, an average of 5.2×10^2 transconjugants were recovered which translates to an efficiency of conjugation of 1.9×10^{-7} transconjugants per donor cell. Ten colonies from each conjugation experiment were screened for the presence of the IncFII replicon (found on donor plasmids) and absence of either the IncI replicon (**§2.5.5**) (contained on another plasmid in donor DD128) or absence of $bla_{CTX\text{-}M}$ (**§2.5.2**) (found chromosomally in donor DD168). All colonies screened were positive for IncFII, negative for IncI or $bla_{CTX\text{-}M}$ respectively, and were unable to grow on LB agar containing kanamycin, and therefore identified as transconjugants.

5.2.2 Transformation of pCURE2 into transconjugants

Transformation into DD128J53 was carried out (**§2.7.2**) and colonies were patch plated (**§2.7.4**) onto LB agar containing sucrose, kanamycin and meropenem respectively. Since pCURE2 contains the *sacB* gene, sucrose counterselection can be used to determine successful transformation; colonies

containing pCURE2 should not be capable of growing on LB agar supplemented with sucrose. Colonies that contain pCURE2 where the IncF plasmid has been successfully cured should be susceptible to sucrose and meropenem, and resistant to kanamycin. Any recipient cells that do not contain pCURE2 should be susceptible to kanamycin but resistant to meropenem and sucrose. However, all 14 colonies tested were able to grow on all agars, while controls did not, suggesting that both pCURE2 and pDD128_IncF were present within the cells. PCR was performed on five transformants to detect the IncFIA (**§2.5.5**) and IncP *oriT* (**§2.5.8**) replicons of both pDD128_IncF and pCURE2, and all five were positive for both plasmid replicons.

Transformation experiments were repeated with DD168J53, and results from patch plating were the same: all transformants were able to grow on all agars, suggesting that both pCURE2 and the IncF plasmids were present within the cells. Bioinformatic analysis showed that the *copA* genes of both IncF plasmids have 100% homology with the corresponding gene in plasmid pEK499 (Woodford et al., 2009), which pCURE2 has been shown to be incapable of curing due to a lack of sequence similarity of their replicons, and this explains why pCURE2 was not able to cure the IncF plasmids in this study. Although a modified pCURE2 was shown to be able to cure pEK499 (Lazdins et al., 2020), lack of easy access to this plasmid led to the decision being made to modify a different plasmid, pFREE, for the mobilisation experiments.

5.2.3 Transformation of pFREE into transconjugant DD128J53

Transformation of pFREE into DD128J53 was carried out (**§2.7.2**) and five of the resulting colonies were determined by PCR to be positive for the presence of *colA*, the replicon found on pFREE (**§2.5.9**). One of these transformants was used to determine that the CRISPR-Cas9 system could successfully be induced by the addition of aTc and rhamnose (**§2.7.12**), and the results can be seen in **Figure 5.3**. This shows that the overall number of colonies were similar, but kanamycin-resistant colonies were reduced after CRISPR-Cas9 induction, which suggests that pFREE has been successfully cured from the majority of cells. Although, analysis of variance showed these results were not significant.

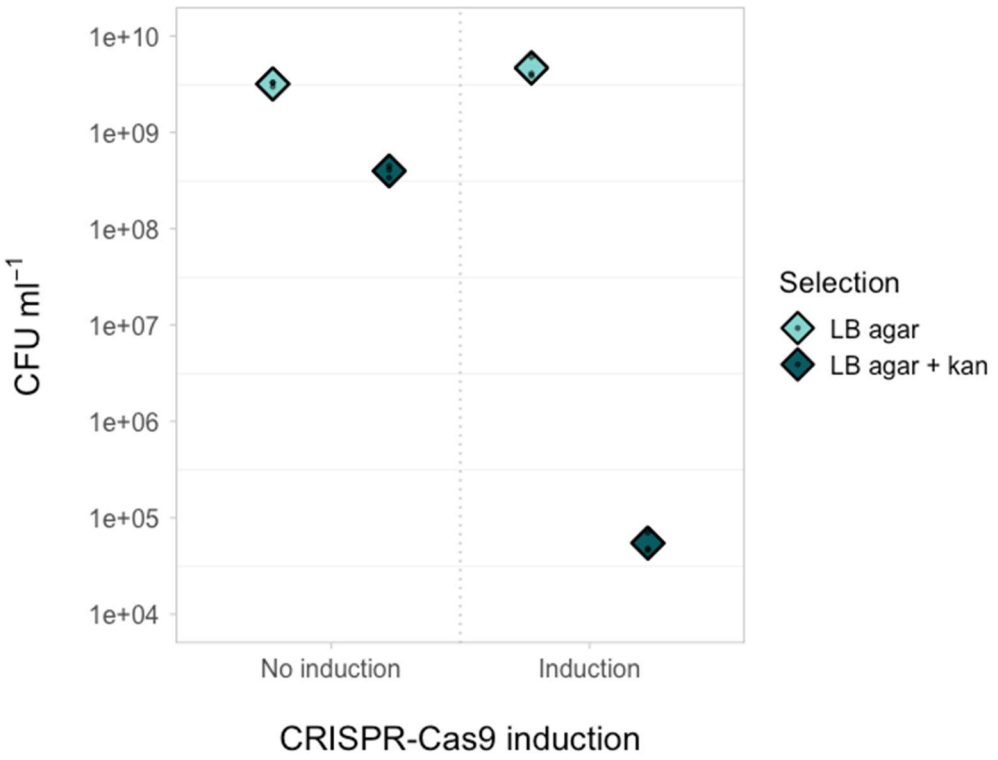

Figure 5.3. Growth of kanamycin-resistant colonies after CRISPR-Cas9 induction of cells containing pFREE, which contains a kanamycin resistance gene. The numbers of kanamycin-resistant colonies recovered on LB agar supplemented with kanamycin were reduced after induction of the CRISPR-Cas9 system when compared to a control with no induction. As the pFREE replicon is a target of its own CRISPR-Cas9 system, this reduction implies induction of the CRISPR-Cas9 system and replicon cleavage was successful. Analysis of variance showed the results were not significant**.**

5.2.4 Modification of pFREE to target IncF replicons

The sgRNAs contained on pFREE target the replicons of common laboratory plasmids. To use this plasmid to cure IncF plasmids, these sgRNAs would need to be changed to target IncF replicons. Similar to the design of pCURE2, the modified pFREE was designed to target FIA, FIB and FII replicons, so it would need three sgRNAs corresponding to these sequences. Although the precise sequences of the replicons in pDD128_IncF could have been used, the new sgRNAs were designed to target conserved regions of the IncF replicons, so this system could potentially be used with different IncF plasmids. To design sgRNA spacer sequences, the Custom Alt-R™ CRISPR-Cas9 guide RNA design tool was used (**§2.7.5.1**). A consensus sequence of each IncF replicon was generated, with ambiguous bases replaced with those found in pDD128_IncF for FIA and FII replicons, or pDD168_IncF for the FIB replicon. The FIA sgRNA sequence with the highest on-target score was 96, with 100% identity to 15/25 FIA replicons. However, it differed from 8/10 of the others by 3 or more base pairs. The sgRNA sequence that had 100% identity with the highest number of replicons, 16/25, had an on-target score of 82, while only differing from the remaining 9 replicons by 2 or fewer base pairs, as can be seen in **Figure 5.4**. This sequence is position 143-162 of the 384 bp FIA consensus sequence and was selected for use in the sgRNA array. The 2 sgRNA sequences with the highest on-target score for the FII replicon had a joint score of 70 but were only found with 100% identity in 14 and 16 of the 114 FII replicons respectively, so were not used.

Figure 5.4. Comparison of designed IncFIA gRNA to alignment of IncFIA replicons. Base pair differences are highlighted in white, with bases that match the consensus shaded in grey. The designed sgRNA is highlighted in blue. 16 replicons share 100% identity with the sgRNA sequence, while 5 differ by 2 bp, and the remaining 4 only 1 bp.

The sequence chosen to be used in the modified sgRNA array had the 3rd highest on-target score of 69 and was detected in 110 of 114 replicons at position 114-133 of the 158 bp IncFII consensus sequence. The sequence chosen for FIB, bases 259-278 of the 373 bp replicon, had the highest on-target score of 96, while also sharing 100% identity with 59/78 replicons, the highest of all potential sequences. The final sgRNA array can be seen in **Figure 5.5**.

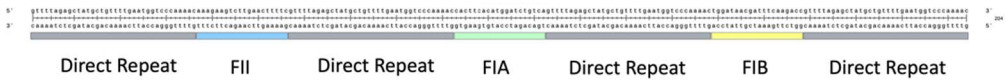

Figure 5.5. Single guide RNA spacer array in pFREE_IncF. Spacer sequences targeting the IncF replicons are labelled with coloured boxes. Each 20 bp spacer is bordered by direct repeats (DR).

5.2.5 Plasmid assembly and transformation into competent cells

NEB recommend a 1:1 ratio of DNA fragments in a 4+ fragment assembly, so the first 2 attempts to assemble the plasmid used a DNA fragment ratio of 1:1 and a total DNA concentration of 21.15 nM (**§2.7.7**). The third attempt used 33.35 nM and a 1:1.69 ratio of the largest fragment to all other fragments. However, none of these assembly mixtures generated any transformants. On the fourth attempt, using the same 1:169 ratio, a single transformant was recovered, but PCR results showed that the plasmid had not assembled properly (**§2.5.10.1**). PCR products spanning the Var and gRNA insertion region (**Figure 2.2**) individually were amplified, but no product was detected that encompassed both insertion regions. Due to this, an assembly mix was prepared using primers for pFREE_IncF_No_Ats, which was a version of pFREE_IncF that did not contain the two antitoxin genes (**§2.7.5**), as this would reduce the number of fragments in the assembly from six to four. This reaction used a 1:1 ratio and a total DNA concentration of 10.1 nM. Alongside this, another assembly mix for pFREE_IncF was prepared using a 1:1.69 ratio and 23.2 nM DNA, and the following day a single transformant was recovered from each of the assembly mixture transformations. Yet again, PCR showed that

pFREE_IncF had not assembled properly. However, PCR using pFREE_IncF_No_Ats as template did produce the products, though across one insertion region the product was around 1 kb shorter than expected. It was hypothesised that this was due to the assembled plasmid not containing the 912 bp IS*26* section.

5.2.6 Four-fragment assembly of pFREE_IncF

Since using a four-fragment assembly generated an assembled plasmid in pFREE_IncF_No_Ats, it was proposed that the number of DNA fragments needed to assemble pFREE_IncF be reduced. Since previous transformants had yielded a PCR product from primers either side of the three fragments encompassing the antitoxin and IS*26* regions, the previous assembly mix was used as a template to amplify these as a single fragment, using the *ccdA* Fw and IS*26* Rv primers, as can be seen in **Figure 5.6**, and this resulted in a 1606 bp DNA product (**Table 2.8**). When purified and used in a four-fragment assembly mixture in a 1:1 ratio with 12.5 nM total DNA, this resulted in the recovery of four transformants. One of these: G4, was shown to amplify products in all three PCR reactions used to check assembly, though not of the correct sizes, so was stored for later analysis. Finally, 3 assembly mixtures were set up concurrently, containing 1) a 1:3 ratio and 13.7 nM total DNA; 2) a 1:1 ratio and 12.5 nM total DNA; and 3) a 1:2 ratio of the 2 largest to 2 smallest fragments and 18.7 nM total DNA. These assembly mixtures resulted in 6, 5 and 8 transformants respectively, which all had their plasmids purified to check for

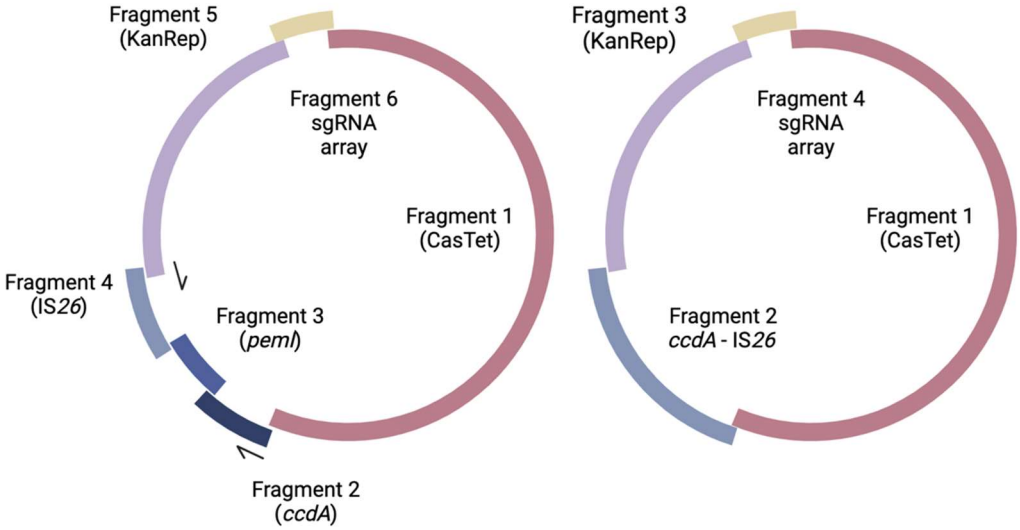

Figure 5.6. Representation of the original six-fragment Gibson assembly of pFREE_IncF (left) and the modified four-fragment assembly (right). Fragments 2-4 were amplified by PCR, using primers shown as arrows, from previous assembly mixtures where this region had been shown to assemble correctly by PCR. Image created with BioRender.com.

correct assembly by PCR. Seven amplified the correct product sizes across all the insertion regions, and one was sent for sequencing by Plasmidsaurus (**§2.7.10**), along with pFREE_IncF_No_Ats and one of the apparently incorrectly assembled plasmids, G4.

5.2.7 Sequencing of assembled plasmids

Plasmid sequencing by Plasmidsaurus generated a 9177 bp assembly of pFREE_IncF and a 4087 bp assembly of G4; while the results of pFREE_IncF_No_Ats were too low quality to generate a plasmid assembly. The relevant sequencing statistics can be found in **Table 5.1**. The 9177 bp assembly of pFREE_IncF differed from the designed 9176 bp by the insertion of a single

Table 5.1. Sequencing statistics of plasmids.

Sequence	Reference length	Reads	Mapped reads	Breadth of coverage	Mean depth of coverage
pFREE_IncF	9177	36	24	100%	7.92
G4	4087	572	560	100%	399.19
pFREE_IncF_No_Ats	8508*	23	5	16.77%	0.28

*Reference length refers to the generated assembly from Plasmidsaurus. * The reads of pFREE_IncF_No_Ats could not be assembled so were compared to the original designed sequence. Breadth and mean depth of coverage refer to the percentage of bases in the reference sequence present in the read files and mean number of times each base in the reference sequence is present in the read files, respectively.*

adenosine in the replicon. However, this insertion was between two other adenosine bases and only present in 4/10 of the read files that cover that region, and not present in 397/495 of G4 reads, so it is more likely that pFREE_IncF assembled as it was designed, and this is a sequencing error. The assembled sequence of G4 is missing the 5138 bp CasTet region, which explains its size, but since two of the primer sites used to check assembly are found in this region, it does not explain why amplified products were detected by PCR. Since the results showed pFREE_IncF had assembled correctly and could be used to test IS*26* mobilisaiton, G4 was not investigated further.

Although an assembly of pFREE_IncF_No_Ats was not generated, BLAST results showed that fragments of the CasTet and KanRep fragments were present in the mapped reads. The sequences of unmapped reads were found to be from other common cloning plasmids not used in this study, so presumed to be contamination from other DNA samples being sequenced at Plasmidsaurus.

5.2.8 Induction of the CRISPR-Cas9 system

After pFREE_IncF and pFREE_IncF_No_Ats were transformed into the transconjugant DD128J53 (**§2.7.11**), these were grown in various broths containing antibiotic supplements and aTc and rhamnose to induce the CRISPR-Cas9 system (**§2.7.12**). Each broth was diluted, and these dilutions spread onto selective and non-selective agar plates. Colonies were then counted and compared to controls without CRISPR-Cas9 induction.

Induction of the CRISPR-Cas9 system in pFREE_IncF_No_Ats resulted in an 8.9×10^5 reduction in CFU on LB agar containing kanamycin, when compared to pFREE_IncF and controls without induction, as shown in **Figure 5.7**. With no induction, a large proportion of cells remained kanamycin resistant, showing that they contain the kanamycin resistance gene found on pFREE_IncF_No_Ats. Whereas after induction, most cells are kanamycin sensitive, showing that the surviving bacteria do not contain pFREE_IncF_No_Ats. By comparison, most bacteria in the pFREE_IncF experiments are kanamycin resistant both with and without induction. This suggests that cells containing pFREE_IncF are better able to survive CRISPR-Cas9 induction than cells containing pFREE_IncF_No_Ats, which is expected as the latter does not contain the *pemI* or *ccdA* antitoxin genes that would prevent cell death due to the long-lived PemK and CcdB toxins produced by the IncF plasmid.

Cells where IS*26* had mobilised bla_{NDM} and the CRISPR-Cas9 system had also cured the IncF plasmid should be resistant to both kanamycin and meropenem,

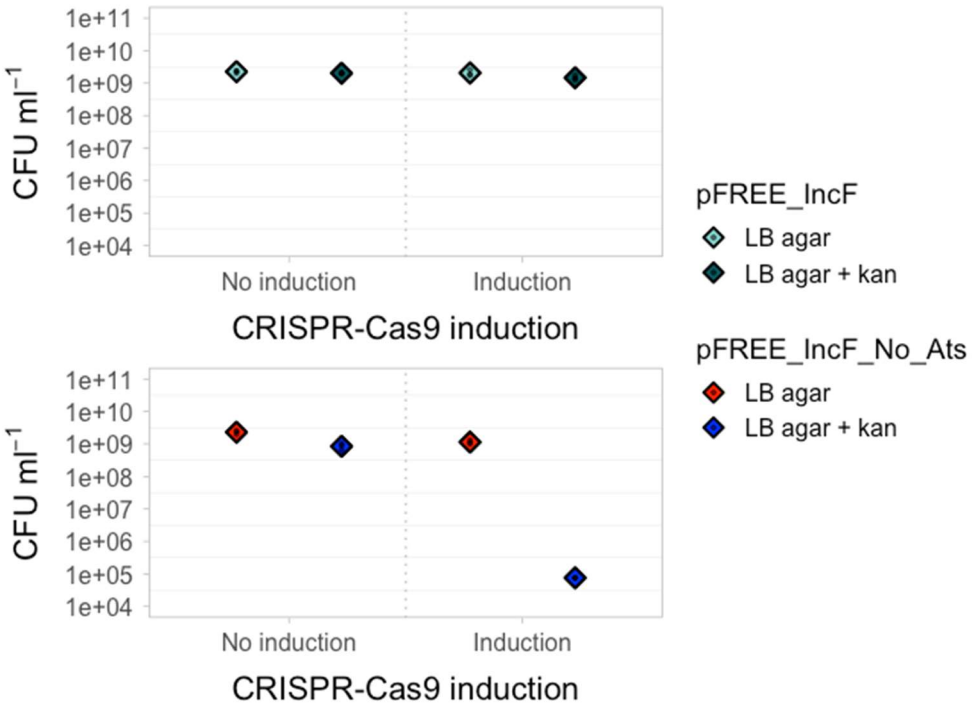

Figure 5.7. Growth of kanamycin-resistant colonies after CRISPR-Cas9 induction. The top panel shows the growth of transconjugants transformed with pFREE_IncF on LB agar and LB agar supplemented with kanamycin both after previous overnight incubation in LB broth with and without induction of the CRISPR-Cas9 system. The bottom panel shows transconjugants transformed with pFREE_IncF_No_Ats under the same conditions. After induction, a 4-log reduction in kanamycin-resistant colonies was observed from plates with pFREE_IncF_No_Ats compared to those in which no induction occurred. This suggests that induction of the CRISPR-Cas9 system results in the death of cells containing pFREE_IncF_No_Ats, but the same result is not seen for PFREE_IncF. However, analysis of variance found the results were not significant. not significant.

so cultures of the transconjugant transformant of pFREE_IncF and DD128J53, hereafter known as DD128J3p, were grown in broths both with and without the two antibiotics (**§2.7.12**). These were diluted and spread onto agar plates with and without the antibiotics. **Figure 5.8** shows there is little to no reduction in CFU between non-selective and kanamycin-selective agar both with and without induction for the two broths, suggesting that most cells still contain pFREE_IncF. However, there is a reduction in meropenem-resistant

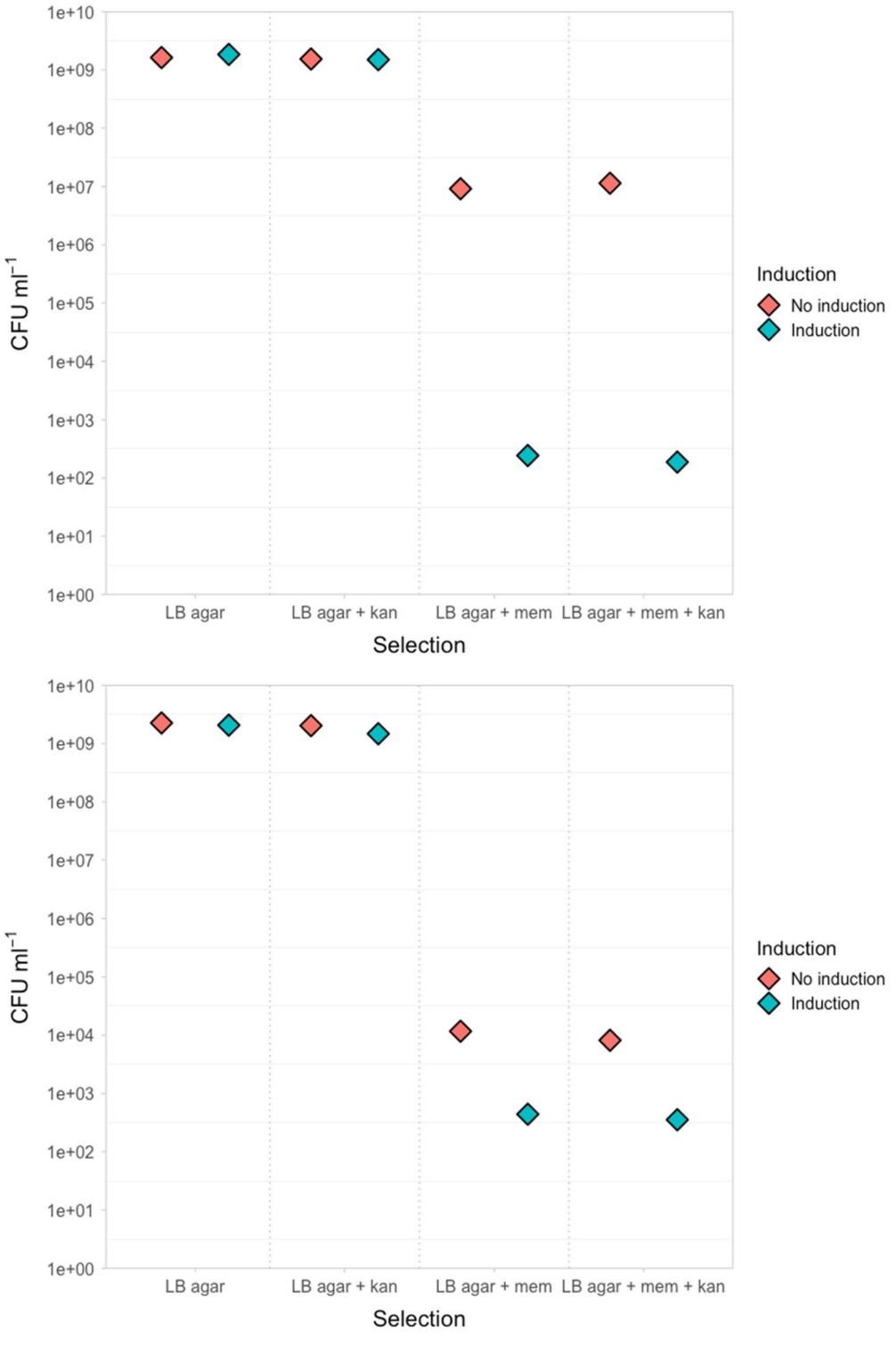

Figure 5.8. Growth of colonies on selective agar plates after CRISPR-Cas9 induction. Top panel shows CFU ml^{-1} after growth in non-selective broth. Bottom panel shows CFU ml^{-1} after growth in broth containing meropenem. Both panels show no reduction in kanamycin resistance, suggesting that all cells retain pFREE_IncF, but reductions in meropenem resistance. Growth in broth containing meropenem led to higher levels of meropenem resistance with no induction, but a similar level when induced. Analysis of variance showed these results were not significant.

plasmid. It is worth noting that most cells in the broth without antibiotics are not meropenem-resistant, which may be due to some cells losing the plasmid naturally and having a higher growth rate compared to those that retain it and its corresponding fitness cost in the absence of antibiotic selection. Overall, after induction in both broths, there is a reduction in meropenem-resistant colonies with little to no reduction in kanamycin-resistant colonies, which implies that a large proportion of cells contain pFREE_IncF but not the IncF plasmid. This suggests that the IncF plasmid was successfully cured but with no mobilisation of *bla*$_{NDM}$ via IS*26* in the majority of cells.

Colonies that were able to grow on agar containing kanamycin and meropenem were subcultured onto fresh agar plates to be used for PCR detection of the plasmid replicons ColA (**§2.5.9**), IncFIA and IncFII (**§2.5.5**), as well as *bla*$_{NDM}$ (**§2.5.4**). Ten colonies were taken from each set of plates diluted from broth containing no antibiotics, kanamycin only, and meropenem and kanamycin respectively for a total of thirty colonies. ColA and *bla*$_{NDM}$ were detected in all 30 colonies, while the IncF replicons were detected in 9/10 colonies from broth with no antibiotics, 8/10 from broth containing only kanamycin and 1/10 colonies from broth containing meropenem and kanamycin. It was noted that the colonies from which the IncF replicons were not detected were smaller than those in which they were detected. Therefore, DNA from ten of these small colonies was extracted and used in the same PCR reactions as previously, and the results can be seen in **Figure 5.9**. As ColA and *bla*$_{NDM}$ were both detected in all ten, while the IncF replicons were not, these isolates were presumed positive for IS*26* mobilisation of *bla*$_{NDM}$ and subjected to whole

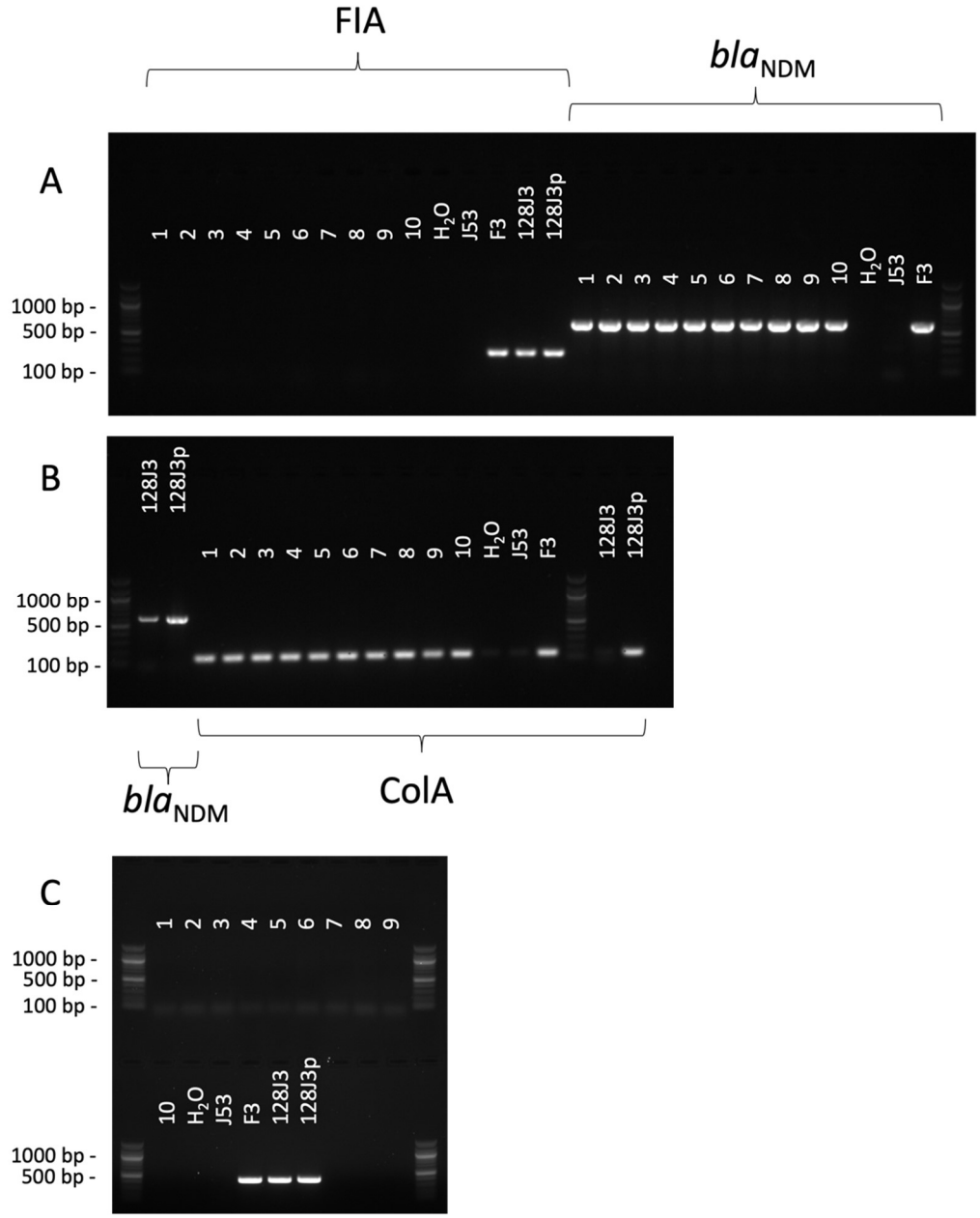

Figure 5.9. Gel images showing the PCR products generated using primers for A) FIA replicon and *bla*$_{NDM}$, B) *bla*$_{NDM}$ (controls) and ColA replicon of pFREE_IncF, and C) FII replicon. All 10 isolates were positive for *bla*$_{NDM}$ and ColA and negative for both IncF replicons, implying that *bla*$_{NDM}$ has been mobilised onto pFREE_IncF. Controls were H_2O, recipient strain J53, previous post-induction isolate F3, transconjugant DD128J53 and transconjugant transformant DD128J3p.

genome sequencing using the ONT MinION (**§2.8.2**). The original transconjugant DD128J53 and transformation transconjugant DD128J3p were

Table 5.2. Summary of transconjugants and transformants used in these experiments.

Donor	Recipient	Transconjugant	Transformed plasmid	Post-induction isolate	Name
DD128	J53 Azi^R	DD128J53	pFREE_IncF_ No_Ats	N/A	128J53pFree_ IncF_No_Ats*
DD128	J53 Azi^R	DD128J53	pFREE_IncF	N/A	G4*
DD128	J53 Azi^R	DD128J53	pFREE_IncF	N/A	128J3p
				1	128J3p1
				2	128J3p2
				3	128J3p3
				4	128J3p4
				5	128J3p5
				6	128J3p6
				7	128J3p7
				8	128J3p8
				9	128J3p9
				10	128J3p10

* indicates the plasmids were deemed to be assembled incorrectly in these strains.

also sequenced as controls, and a summary of these isolates can be seen in **Table 5.2**

5.2.9 Whole Genome Sequencing of isolates presumptive for IS*26* mobilisation

Assemblies were generated (**§2.9.1**) for all 12 isolates and the summary statistics can be seen in **Table 5.3**. The assembled genomes were between 4.5 and 4.8 Mbp in size with average coverage ranging from 15X to 161X. The assembled genomes were inputted into the Center for Genomic Epidemiology's cgMLSTFinder tool (**§2.9.2.3**) to check that each isolate had the same cgMLST and it was not the same as that of the original donor DD128, which was 141146. Eight isolates were found to belong to cgMLST 62585, as was the transconjugant DD128J53 and transconjugant transformant DD128J3p.

Table 5.3. Key statistics of read files and assemblies for isolates with presumptive IS*26* mobilisation, as well as the original transconjugant and transformation transconjugant as controls.

	Passed reads	Total length	Average read length	Assembly length	Average coverage	Contigs
1	193,276	185,971,302	962.2	4722640	39.38	2
2	174,492	168,466,363	965.5	4703570	35.82	2
3	129,581	107,654,524	830.8	4707025	22.87	28
4	205,799	760,779,419	3,696.70	4703157	161.76	4
5	47,803	70,949,050	1,484.20	4730912	15.00	16
6	323,324	387,133,367	1,197.40	4711327	82.17	4
7	268,824	722,277,687	2,686.80	4704551	153.53	3
8	202,750	292,698,179	1,443.60	4704014	62.22	2
9	255,434	189,118,098	740.4	4542234	41.64	77
10	227,122	194,751,531	857.5	4721955	41.24	4
128J53	326,510	728,821,741	2,232.20	4822982	151.11	3
128J3p	79,055	244,620,246	3,094.30	4762124	51.37	3

Strains 5 and 10 were identified as different sequence types, but as only 11.54% and 24.15% of the cgMLST alleles were present in those two assemblies, it could not be determined if these results were accurate.

5.2.9.1 Detection of the IncF plasmid sequence

The assemblies were screened for the presence of the conjugated IncF plasmid. The assembly of DD128J53 contained a 120,281 bp contig that shared 99.93% identity with the IncF plasmid of DD128, which combined with its cgMLST result confirms the IncF plasmid of DD128 was successfully conjugated into J53. The assembly of DD128J3p contained two smaller contigs, of 46 kbp (contig 2) and 30 kbp (contig 3) respectively that contained sections of the IncF plasmid. The 46 kbp contig shared 99% identity with a 46 kbp region of DD128_IncF. The 30 kbp contig was made up of two sections of DD128_IncF, bordering the

transformed plasmid pFREE_IncF, with IS*26* genes at the intersections, as can be seen in **Figure 5.10**. That a region of DD128_IncF between two IS*26* genes is missing from contig 3 suggests pFREE_IncF has not simply inserted between the sections of DD128_IncF but had formed a cointegrate with the plasmid on two separate occasions. Due to the nature of how read files are assembled, it was considered that this could be an error due to an assembly problem, as repetitive regions, such as IS*26* arrays, can lead to erroneous results. If pFREE_IncF had formed two separate cointegrates in different cells, A to B and B to C, then due to the nature of genome assembly algorithms contig 3 could have been assembled as A to C when that might not actually be the case. Therefore, the read files were aligned with the section of contig 3 that contains the sequence 2 kbp either side of pFREE_IncF, to find any reads that mapped across both potential cointegrate formations.

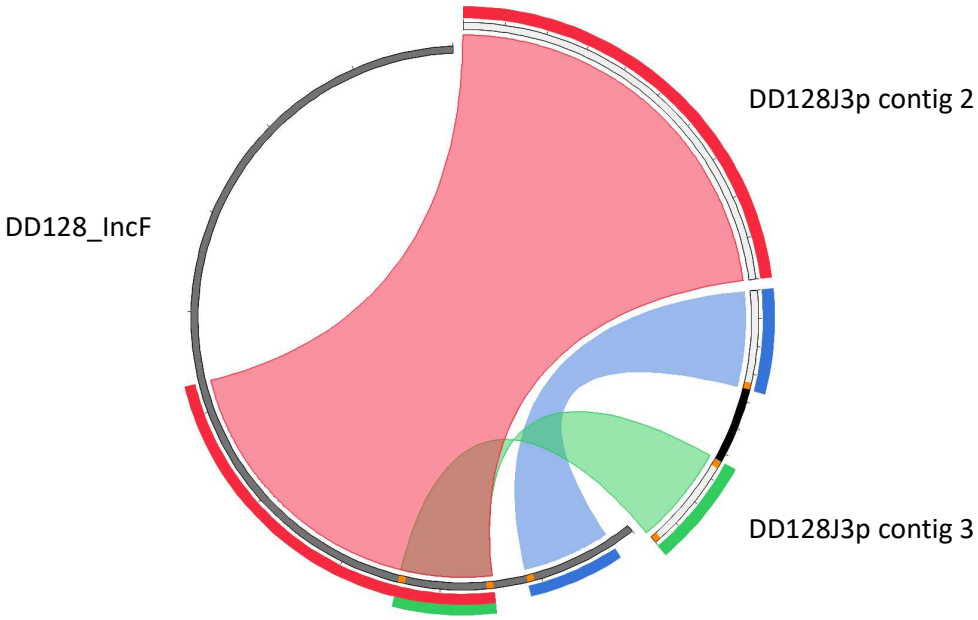

Figure 5.10. Map of BLAST alignments over 1000 bp of pDD128_IncF and the non-chromosomal contigs of the assembly of transconjugant transformant DD128J3p. Red, green and blue segments represent distinct alignments with over 99% identity. The black segment on contig 3 represents the sequence of pFREE_IncF, orange sections represent IS*26* elements. Contig 3 shows cointegrate formation of pFREE_IncF and pDD128_IncF.

Five reads were found that had an e-value of $<1e^{-20}$ and covered 90% of the sequence. These were aligned with the IncF plasmid DD128_IncF and pFREE_IncF and this can be seen in **Figure 5.11**. None of the reads show a similar structure to that found in contig 3, with pFREE_IncF found between two separate sections of DD128_IncF, so the structure of contig 3 is likely an error in assembly. The reads do show that pFREE_IncF has formed cointegrates with different IS26 elements within the IncF plasmid. **Figure 5.11A** and **Figure 5.11B** show cointegration at the 3' end of the leftmost IS*26*, while **Figure 5.11E** shows cointegration at the 5' end of the same element. **Figure 5.11C** and **Figure 5.11D** show that pFREE_IncF has formed a TU with the region containing bla_{NDM}, as the sections flanking pFREE_IncF are from either end of this region, showing this read must come from a circular section of DNA. These reads along with contig 2 also show that although the full sequence of DD128_IncF wasn't present in the assembly, at least large sections of the plasmid still exist in DD128J3p.

The assemblies of the 10 post-induction isolates were screened for the presence of the IncF plasmid, to check it was successfully cured by the CRISPR-Cas9 system. Since it was expected that some contigs would contain the bla_{NDM} region, they were aligned with the sequence of DD128_IncF with the IS*26* elements and intervening sequences removed. Furthermore, the read files of each assembly were also aligned to this sequence to check that the results of

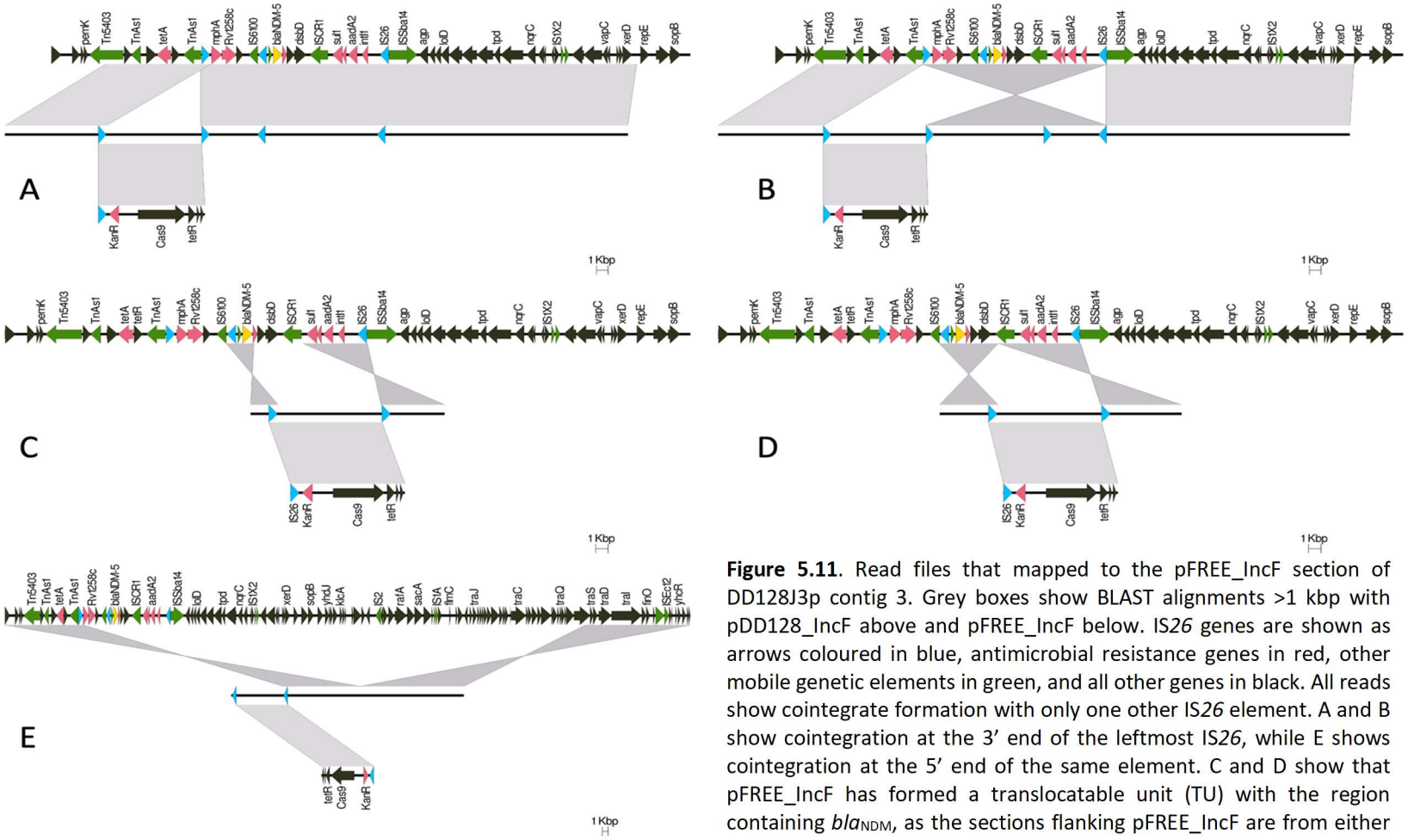

Figure 5.11. Read files that mapped to the pFREE_IncF section of DD128J3p contig 3. Grey boxes show BLAST alignments >1 kbp with pDD128_IncF above and pFREE_IncF below. IS*26* genes are shown as arrows coloured in blue, antimicrobial resistance genes in red, other mobile genetic elements in green, and all other genes in black. All reads show cointegrate formation with only one other IS*26* element. A and B show cointegration at the 3' end of the leftmost IS*26*, while E shows cointegration at the 5' end of the same element. C and D show that pFREE_IncF has formed a translocatable unit (TU) with the region containing *bla*$_{NDM}$, as the sections flanking pFREE_IncF are from either end of this region.

the previous alignment were not due to incorrect assembly. 9/10 of the assemblies did not contain any contigs with regions >1 kbp from the plasmid and contained between only 1 and 7 reads that aligned with the plasmid sequence. In contrast, the two controls DD128J53 and DD128J3p, contained 500 and 277 reads respectively that aligned to the plasmid sequence. However, the last remaining assembly did contain a 19 kbp contig that aligned with pDD128_IncF, as well as 349 reads that also aligned with this sequence, which suggests the IncF plasmid was not successfully cured in this isolate.

5.2.9.2 Detection of IS*26* mobilisation of *bla*$_{NDM}$

Having confirmed that 9/10 of the isolates had been effectively cured of the IncF plasmid, they were screened for the presence of the predicted cointegrate of pFREE_IncF and the *bla*$_{NDM}$ region. The assemblies were varied; some of them included these sequences as two individual contigs, and some as a single contig, but all nine contained both sequences in some form. Overall, 3 assemblies contained a 19.6 kbp contig that shared 99% identity with the expected 19.6 kbp TU formed from pFREE_IncF and the *bla*$_{NDM}$ region of pDD128_IncF. A further 3 assemblies contained both sections on separate contigs, while the remaining 3 assemblies contained contigs larger than 19.6 kbp with multiple copies of each section. Two of these were 39.2 kbp, and the last was 78.5 kbp, and these contained 2 and 4 copies of each section respectively, and these results can be seen in **Figure 5.12**.

It was again presumed that the assemblies may not be accurate due to the repetitive nature of the TU. Therefore, the read files of each assembly were

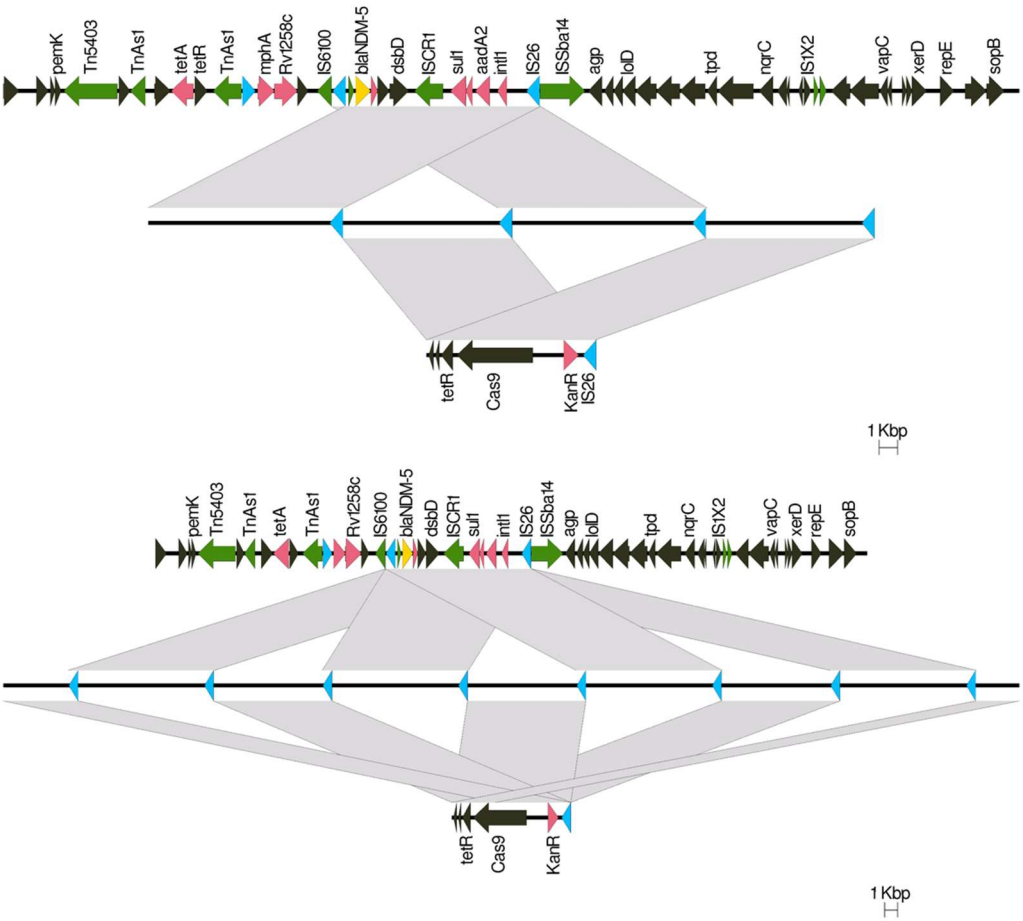

Figure 5.12. Contigs of two post-induction isolates that contain multiple copies of pFREE_IncF. Grey boxes show BLAST alignments >1 kbp with pDD128_IncF above and pFREE_IncF below. IS*26* genes are shown as arrows coloured in blue, antimicrobial resistance genes in red, other mobile genetic elements in green, and all other genes in black. Both contigs show the expected cointegration of pFREE_IncF with the *bla*$_{NDM}$ region of DD128_IncF, but this is replicated multiple times.

aligned with the pFREE_IncF_NDM sequence and those that aligned over 90% of the sequence were recorded. The 9 sequence files each had between 3 and 105 reads that aligned to the predicted 19.6 kbp pFREE_IncF_NDM sequence, with a combined total of 278 aligned reads. The average length of these reads was 34.3 kbp with 6 over 100 kbp in length. The longest was 138,792 bp in length and contained 8 copies of pFREE_IncF and can be seen **Figure 5.13**. The 5 longest reads of each sequence file (or all if less than 5) were aligned to pFREE_IncF and DD128_IncF separately to determine their structure and each

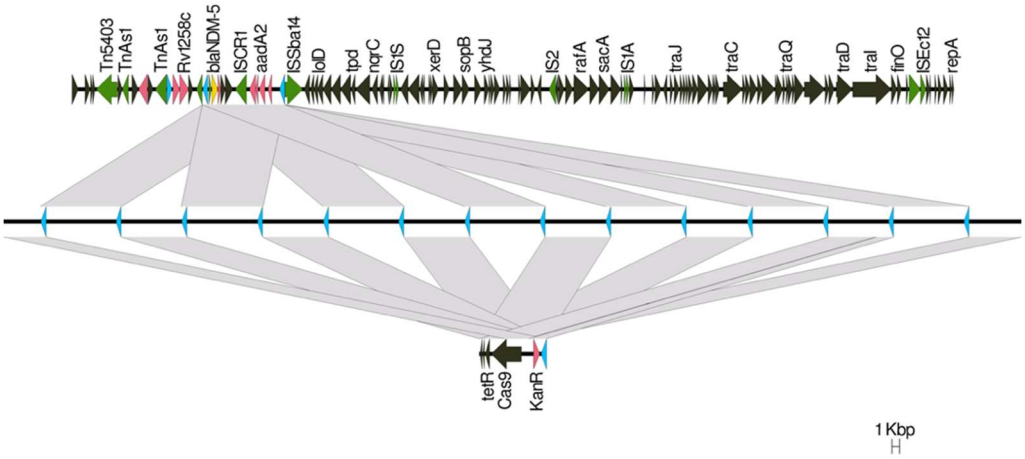

Figure 5.13. Longest read file containing pFREE_IncF and the *bla*$_{NDM}$ region of DD128_IncF. Grey boxes show BLAST alignments >1 kbp with pDD128_IncF above and pFREE_IncF below. IS*26* genes are shown as arrows coloured in blue, antimicrobial resistance genes in red, other mobile genetic elements in green, and all other genes in black. This read contains 7 copies of the DD128_IncF region and 8 copies of pFREE_IncF in a cyclical pattern, presumably formed by multiple cointegrations of smaller translocatable units.

shared the same cyclical pattern of pFREE_IncF – IS*26* – *bla*$_{NDM}$ region – IS*26* as shown in **Figure 5.12** and **Figure 5.13**.

5.2.9.3 Verifying the rhamnose induction of the CRISPR-Cas9 system

Due to an oversight in plasmid design, the induction of the CRISPR sgRNAs may have been affected by disruption of the pRhaBAD inducible promoter. The location of the promoter is not labelled on the publicly available sequence from addgene.com, and so the design of fragments used in Gibson assembly did not

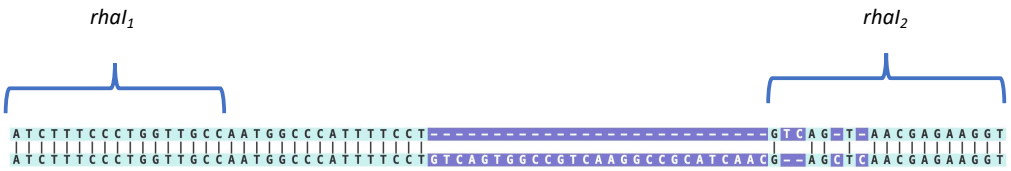

Figure 5.14. Alignment of the RhaS binding sites *rhaI*$_1$ and *rhaI*$_2$ of pFREE (above) and pFREE_IncF (below). The alignment shows that *rhaI*$_1$ is intact but *rhaI*$_2$ has been disrupted in pFREE_IncF, and binding sites are much further apart than in pFREE.

take this into account. The location of the RhaS binding sites in the original unaltered pFREE and in pFREE_IncF can be seen in **Figure 14**. The changes to the *rhaI* sites could have meant that RhaS did not bind to the DNA and therefore pRhaBAD was not induced and the sgRNAs were not transcribed. To test whether this likely influenced the CRISPR-Cas9 system, the host of unaltered pFREE was grown in broth with aTc and rhamnose as well as aTc alone and compared to controls. The results can be seen in **Figure 5.15**. There is still a reduction in kanamycin-resistant colonies without the addition of rhamnose, suggesting that the sgRNAs are transcribed, though analysis of variance showed the results were not statistically significant when compared to aTc and rhamnose or no induction.

Figure 5.15. Detecting the effect of the pRhaBAD promoter of pFREE on induction of the CRISPR_Cas9 system. Growth of kanamycin-resistant colonies after induction using anhydrotetracycline (aTc) and rhamnose, or anhydrotetracycline alone. Less colonies are recovered after induction with both substances, though the results were not significant.

5.3 Discussion

5.3.1 Use of transconjugant as recipient

The idea of these experiments was to show evidence of IS*26* mobilisation of AMR genes between plasmids in environmental isolates of clinical relevance, mimicking the proposed conditions that occur in the spread of AMR in nature. The qualities of these environmental isolates that make them so worthy of study is that they are highly resistant to a range of antibiotics, which unfortunately complicates experimental designs using antibiotic selection mechanisms. For this reason, it was necessary to perform the experiments in a strain that was susceptible to the antibiotic selection of the plasmids used, which required transferring the wild-type plasmids via conjugation into a kanamycin-susceptible recipient strain. This does not fundamentally change the outcome of the experiments, with the added benefit of not creating an even more resistant environmental isolate by the addition of further resistance mechanisms.

5.3.2 Design of pFREE_IncF

The intention of using pFREE_IncF was to create a plasmid that would be able to cure IncF plasmids while preventing cell death from plasmid PSK systems. This led to the incorporation of antitoxin genes into the sequence, as this method is used by the plasmid pCURE2, which was originally tried in this study, to achieve that goal. As the IncF plasmids used in this study contain the *pemIK*

and *ccdAB* PSK systems, the antitoxin of each system was added to pFREE_IncF. The reduction in the number of kanamycin-resistant colonies when using pFREE_IncF_No_Ats, which did not contain these antitoxin genes, suggests that these genes are functional in pFREE_IncF, and required to prevent PSK after plasmid curing.

The sgRNAs used in the CRISPR_Cas9 system were designed to be as conserved across IncF replicons as possible, so that this plasmid could easily be used to cure other IncF plasmids, such as others found in previous chapters. For this reason, the consensus sequences of the IncF replicons were used as inputs in the design tool.

5.3.3 Detection of plasmid curing

The enumeration of meropenem-resistant colonies showed that there was a reduction in CFU after induction of the CRISPR-Cas9 system, though these results were not statistically significant. Previous studies have used CRISPR-Cas9 systems to cure AMR plasmids either by targeting the plasmid replicons, or specific AMR genes. Bacteriophage have been used for delivering a CRISPR-Cas9 system into *E. coli* that targeted $bla_{\text{NDM-1}}$ and $bla_{\text{CTX-M-15}}$ genes (Yosef et al., 2015). Another system used the conserved region of bla_{TEM} and bla_{SHV} genes as sgRNA to cure the ESBL plasmid of a clinical isolate with a 1×10^{-3} reduction in resistant colonies (Kim et al., 2016). He et al. (2021) used IS*26* to transpose a CRISR-Cas9 system targeting both IncX and IncH plasmids as well as AMR genes into an *E. coli* chromosome. This was able to show 80% curing efficiency of

plasmids containing *mcr*-1 after 12 hours and 100% after 24 hours. More recently, a plasmid targeting the kanamycin resistance gene *aacC1* was conjugated into resistant strains and showed around 50% reduction in plasmid carriage (Walker-Sünderhauf et al., 2023). This shows a range of curing efficiencies present in the literature, and this study showing a 2.65 x 10^{-5} reduction in meropenem resistant colonies after meropenem selection is higher than in some other experiments.

PCR detection of plasmid replicon genes did show that the majority of surviving colonies tested retained the IncF plasmid, confirming that the CRISPR-Cas9 system was not effective in these cells. It is possible that the sgRNAs could be further optimised, and other studies have shown that optimisation can improve the efficiency (Dang et al., 2015). In particular, one study using an aTc inducible CRISPR-Cas9 system to target *Mycobacterium tuberculosis* genes was able to improve from 10-50% efficiency to 80-90% efficiency by modifying the sgRNA used (Singh et al., 2016).

However, PCR results did show that a subset of colonies did not contain IncF replicons while still containing the bla_{NDM} gene and pFREE_IncF replicon. This was confirmed by long-read sequencing which showed that there were colonies where the IncF plasmid had been successfully cured, as sections of it were only detected in a total of 35 out of 1.98 x 10^6 reads across 9 isolates.

5.3.4 IS*26* cointegrate formation

The sequencing results show that where the IncF plasmid had been successfully cured, cointegrate formation of the IS*26* elements on pFREE_IncF and the MDR region containing bla_{NDM} has occurred. Even in the assemblies where these were found on separate contigs, analysis of the read files showed that cointegrate formation had occurred. Regions of DNA found between two directly oriented IS*26* elements can move as pseudo composite transposons, as the IS*26* genes can undergo homologous recombination resulting in the formation of a translocatable unit (TU). For the circular DNA sequence of pFREE_IncF – IS*26* – MDR region – IS*26* to have been formed, one of two pathways must have been used. Either the MDR region must have formed a TU and then cointegrate formation catalysed by the IS*26* transposase occurred; or vice versa in that cointegration of both molecules happened while the MDR region is still found on the IncF plasmid, followed by homologous recombination of the IS*26* genes at either end of the entire 19.6 kbp section. It is not possible to know which of these has happened from these data, but either way it shows IS*26*-mediated mobilisation of the MDR region.

Multiple copies of this cointegrate were found on the same DNA molecule in individual reads from every post-induction isolate. This is likely because pFREE_IncF is a medium-copy number plasmid so there would be many IS*26* genes available within the cell with which to form cointegrates. The numbers of pFREE_IncF regions found on these reads were in multiples of 2, which suggests that these are forming from cointegrate formation, followed by

replication, followed by another cointegrate formation of these replicants. Otherwise, if multiple cointegrations between smaller plasmids were occurring it would be expected to find an uneven number of pFREE_IncF regions on a DNA fragment. However, it is very possible that these exist and were not detected by the bioinformatic methods used. These formations were detected in reads up to 138 kbp, and it is quite possible that this is due to the limitation of read lengths, as the longest read file in all isolates was only 249 kbp.

These findings are similar to those discovered when a constructed PCT containing *bla*$_{KPC}$ flanked by two IS*26* genes on the plasmid pUC57 was introduced into a recipient strain (Wei et al., 2022). After antibiotic selection and subsequent sequencing, the PCT was detected across multiple reads where it formed tandem arrays of itself. The fact that the colonies in this study that had been cured of their IncF plasmids were very small, coupled with the fact that they contained these large arrays of IS*26* cointegrates, suggested that they may be incurring a fitness cost due to the increased burden of these cointegrates.

5.3.5 Conclusion

The aim of this work was to show that AMR genes, including those conferring resistance to critical antibiotics such as *bla*$_{NDM}$, can be shown to transfer as pseudo compound transposons from one replicative plasmid to another, via cointegrate formation of IS*26* elements. This aim was achieved as bioinformatic analysis from post-induction isolates shows the MDR region of DD128_IncF has

formed a cointegrate with pFREE_IncF, transferring the resistance genes to that plasmid. The use of CRISPR-Cas9 to cure the IncF plasmid by targeting its replication genes allows selection and detection of these cointegrates. This study is the first to use this method of curing IncF plasmids by using CRISPR-Cas9 cleavage of plasmid replicons, and this adds to our knowledge of methods to remove MDR plasmids. Finally, this work also shows that care should be taken when interpreting whole genome assemblies from isolates containing IS*26*, as its ability to form TUs and cointegrates with other IS*26* genes can mean that different cells can have different IS*26* formations within the same culture, leading to mismatching reads. Analysis of these assembled regions of DNA containing multiple IS*26* genes requires checking the read files to have confidence of the assembly results.

5.3.6 Future work

To optimize the construction of pFREE_IncF, the DNA fragments used in Gibson assembly should first be modified to include the correct *rhaI* sites, aiming for better induction of the sgRNA array. Additionally, when combined with experiments targeting other sequences within the IncF replicons, this modification could potentially achieve a more efficient level of plasmid curing. The DNA fragments adjacent to the sgRNA array were designed to reintroduce the SfiI restriction sites so that this could more easily be achieved once a new array was synthesised. Alongside this, more replicates of these and the previous experiments measuring the CFU mL^{-1} of antibiotic resistant isolates

would be performed to better resolve whether the reductions are statistically significant.

Other donors would be used to show that pFREE_IncF also works with other IncF plasmids, including those that contain the FIB replicon that was designed and added to the sgRNA array for this purpose. The plasmid pDD168_IncF was successfully conjugated into J53 and would have been used in similar experiments if more time was available. A donor plasmid that contains more than two directly oriented IS*26* elements, such as pDD158_IncF, could be used to detect the formation and cointegration of differently sized TUs from the same plasmid, depending on which pair of IS*26* elements form the TU.

Finally, this method could be used to analyse the rate of mobilisation of IS*26* in the presence of different compounds or stressors. Wei et al. (2022) showed through qPCR that the copy number of IS*26* increased in the presence of antibiotic stress. Similarly, ARGs found on IS*26* PCTs have been showed through qPCR to be increased in expression in the presence of antibiotic stress (Hubbard et al., 2020). This system could potentially be used to test whether the levels of meropenem-resistant colonies are increased, i.e., more cointegrates have formed, when cells are grown in the presence of sublethal amounts of oxidative stressors or antimicrobials.

CHAPTER 6:

GENERAL DISCUSSION AND CONCLUDING REMARKS

6.1 Discussion

The aims of this research, described in Chapter 1 were:

i. Isolation and phenotypic characterisation via disc diffusion assay of cephalosporin and carbapenem resistant enterobacteria from raw and treated sewage and receiving waters.
ii. Genotypic characterisation of relevant AMR genes through PCR and whole genome sequencing.
iii. Characterisation of the MGEs of carbapenem resistant isolates, including conjugation assays to determine mobility of MGEs and associated ARGs.
iv. Investigation of genetic relatedness of isolates across a range of time points: are similarities in phenotypic and PCR results due to clonality or the spread of related MGEs?
v. Determination of sequence similarity of MGEs from collected wastewater isolates with other published MGE sequences from the UK.
vi. Investigation into the intracellular mobility of MGEs containing carbapenemase genes.

6.1.1 Isolation and characterisation of cephalosporin and carbapenem resistant bacteria

Chapter 3 showed that cephalosporin and carbapenem resistant enterobacteria can be isolated from raw and treated sewage from wastewater treatment plants in the East Midlands region of the UK. This is the first report of CPE identified in wastewater from this region, and only the third time CPE have been isolated from UK municipal wastewater (Ludden et al., 2017; Gibbon et al., 2021). This is also the first report of *C. portucalensis* in the UK, although it is worth noting that 16S sequencing first identified this as *C. freundii,* so previous studies which also used 16S identification will have described this species as *C. freundii.*

Antimicrobial resistance gene characterisation revealed that cephalosporin resistance patterns broadly aligned with the trends observed in prior studies of ESBL-producing enterobacteria in the UK. Specifically, CTX-M enzymes were found to be the most prevalent, with the *bla*$_{\text{CTX-M-15}}$ genotype being the most frequently detected, while TEM enzymes followed as the next most common (Day et al., 2019; Raven et al., 2019; Ibrahim et al., 2023). However, the patterns of CPE resistance were unlike those seen both regionally and nationally within the UK, where OXA-48-like enzymes and *K. pneumoniae* are most common, compared to the predominantly NDM-producing *E. coli* detected in this study. It was considered that the use of selective isolation media may have skewed the results of this study, but analysis showed no significant associations between the use of specific agar and the genera isolated on that media. Additionally, strains isolated from carbapenem-selective agar had a greater number of resistances to different classes of antimicrobials than those from cephalosporin-selective agar, and this seems to be driven by isolates harbouring *bla*$_{\text{NDM}}$, as this gene was associated with the most phenotypic resistance patterns. Whole genome sequencing showed this association is most likely because the majority of NDM-producing isolates contained MDR encoding regions surrounding the *bla*$_{\text{NDM}}$ gene, facilitated by the formation of pseudo compound transposons by the insertion sequence IS*26*. As *bla*$_{\text{NDM}}$ is itself heavily associated with IS*26* in *E. coli* (Acman et al., 2022), the association found in **Chapter 3** between *bla*$_{\text{NDM}}$ and phenotypic resistances is likely a proxy for the association of IS*26* with MDR phenotypes, due to its targeted method of transposition.

6.1.2 Characterisation by whole genome sequencing

The use of WGS enabled the full characterisation of the resistome of these isolates, from which the genotypes of the various beta-lactamase genes could be identified. This showed that all but one of the NDM-producing isolates in this study contained the *bla*$_{\text{NDM-5}}$ gene, while the remaining isolate that harboured *bla*$_{\text{NDM-4}}$ was of the same core genome multi locus sequence type as an isolate with *bla*$_{\text{NDM-5}}$ collected two weeks later. There were only two SNPs between these isolates, and this suggests that the NDM gene in this isolate has mutated from *bla*$_{\text{NDM-4}}$ to *bla*$_{\text{NDM-5}}$ in the intervening period. Combined with the overall high abundance of *bla*$_{\text{NDM-5}}$ found in this study, this evidence matches the recent UK and EU data that *bla*$_{\text{NDM-5}}$ is increasing in prevalence, and is now the most common genotype found in *E. coli* in this region, which matches the pattern previously found in Asia (Wu et al., 2019; Turton et al., 2022; ECDC, 2023b).

The use of long-read sequencing was key to resolving the plasmid sequences to enable characterisation of the MGEs responsible for dissemination of ARGs in these isolates. Short-read sequencing was used to confirm clonality of isolates found on different sample dates, and from those assemblies, none of the sequences of plasmids carrying ARGs could be fully resolved. However, the hybrid sequencing results using both long and short reads, were able to resolve most plasmids in this study, which enabled their phylogenetic analysis. This showed there were several distinct isolates that shared the same AMR plasmids. The ST361 group and ST405 isolate DD128 harboured *bla*$_{\text{NDM-5}}$ genes

on IncF plasmids that shared a recent common ancestor, and these closely related plasmids were isolated in multiple influent and effluent samples over a three-week period. The ST2851 isolates and ST205 isolate DD130 also contained very closely related IncF plasmids, which were detected in separate samples collected a week apart. Finally, the *K. quasipneumoniae* isolate DD112 and *E. coli* DD186 both harboured an almost identical (1 SNP difference) IncX3 plasmid containing $bla_{\text{NDM-5}}$. These isolates were detected from untreated wastewater samples collected 47 days apart. Analysis of plasmid sequences also explained why conjugation experiments for isolates DD129, DD130 and DD153 were unsuccessful, as they do not contain the complete *tra* operon responsible for plasmid transfer.

In the isolates where bla_{NDM} was found either on IncF plasmids or chromosomally encoded, the region around bla_{NDM} was very highly conserved. This region also had high levels of similarity with sequence data from $bla_{\text{NDM-5}}$-containing strains isolated from wastewater, clinical, and veterinary samples in the UK. The genetic environment of the $bla_{\text{NDM-5}}$ sequence found on IncX3 plasmids shared less sequence similarity, with only the region containing three downstream genes being found in other isolates. This was also the case with the downstream region of the *K. pneumoniae* clinical isolate (CP034201) that was used as comparison to the wastewater isolates in this study. That this IncX3 plasmid was found in a *Klebsiella* isolate, and this was distinctly different to sequences found in *E. coli*, supports the analysis performed by Acman et al. (2022) that there are distinct lineages of the genetic regions around bla_{NDM} that have formed and proliferated in different species. The regions surrounding

bla$_{NDM}$ in the majority of *E. coli* isolates contained multiple IS*26* genes, more so than for any other MGE, which matches previous analyses that this gene is heavily associated with *bla*$_{NDM}$, as well as ARGs more broadly (Leekitcharoenphon et al., 2021; Acman et al., 2022).

The AMR genes found in CPE in this study appeared to be spread via the transfer of similar plasmids between isolates of the same and different species, but also by clonal dissemination. Overall, there were three core genome sequence types that were detected in multiple different samples, in all cases these were detected from samples taken a week apart. This included the ST361 isolates, which were collected in untreated wastewater on 3rd and 10th March 2020 as well as treated wastewater on 10th March. Whether an ancestor of this IncF plasmid spread to DD128 because of the clonal spread of these isolates, or whether their dissemination is in part driven by the acquisition of this plasmid, or perhaps another explanation, it is not possible to determine this from the current data.

To compare these strains and their respective plasmids to those of clinical isolates in the local region, CPE from the hospital served by WWTP B were obtained and subject to whole genome sequencing. Unfortunately, there was not time to analyse the generated data before submission of this work.

6.1.3 Mobilisation of IS*26*

Chapter 5 showed that the MDR genetic region containing *bla*$_{NDM}$ and associated ARGs could be mobilised by the activity of IS*26*, via formation of a

translocatable unit (TU) and transposition through the targeted conservative route. This mechanism has previously been experimentally demonstrated to occur between TUs and plasmids (Harmer, Moran and Hall, 2014), as well as bacterial chromosomes and plasmids (Oliva et al., 2018; Hubbard et al., 2020), while plasmid fusion has been demonstrated to occur between plasmids both containing IS*26* (Wang et al., 2019). **Chapter 5** showed that TUs can transfer ARGs between plasmids, and this resulted in repetition of the MDR region due to formation of multiple IS*26* arrays, presumably due to repeated TU excision and transposition between the medium copy number plasmid vector. Previous studies have shown that these kinds of arrays can reduce susceptibility to antibiotics due to hyperproduction of ARGs found within them (Hubbard et al., 2020; Wei et al., 2022).

The answer to the question of whether hyperproduction of ARGs confers a fitness cost is not quite clear. Some previous studies have shown that hyperproduction of ARGs due to IS*26* arrays does incur a fitness cost (Adler et al., 2014; Hansen et al., 2019; Wei et al., 2022), while Hubbard et al. (2020) found no evidence of a fitness cost for the hyperproduction of bla_{TEM}. This may be due to the number and/or length of arrays generated by IS*26* as the hyperproduction of bla_{TEM} in the study by Hubbard et al. (2020) was caused by duplication of a 10.9 kbp region. In contrast, hyperproduction of bla_{TEM} described by Hansen et al. (2019) was caused by an array of IS*26* - bla_{TEM} - IS*26* where bla_{TEM} was detected 114 times in a single read. This would have resulted in over 218 kbp of additional DNA and subsequent RNA/protein produced by the cell, which is a possible reason why this was found to incur a fitness cost.

In this study, the largest repeat array of IS*26*-flanked regions detected was 138 kbp in length, containing 7 copies of the intervening gene sequence. The bacterial colonies that were found to have these multiple IS*26* arrays were seen to be smaller than colonies that had not been cured of their IncF plasmids. However, as the latter colonies were not sequenced, it is not possible to be sure that they did not also possess these multiple arrays.

Studies have shown that where these repeated arrays are discovered during antibiotic selection, the number of arrays is reduced once the antibiotic selection is removed (Adler et al., 2014; Hansen et al., 2019). Further evidence of gene loss through the excision of IS*26* PCTs has also been shown by bioinformatic analyses of plasmid sequence data where, when compared to ancestral sequences, large plasmid regions were no longer present (Wyrsch et al., 2019; Luo et al., 2022). This suggests that IS*26* PCTs play a role in genome evolution by enabling the excision of genomic sections that are no longer necessary or useful to the cell, and those that lose them may have an evolutionary advantage. However, that IS*26* arrays are responsible for the proliferation of AMR genes in Gram-negative bacteria by the formation of multiple ARG arrays, and these persist even in the absence of antibiotic selection, raises the question of why these large genomic sections with multiple PCTs are not lost over time. This same question has often been asked in the past about large plasmids, and, in addition to the plasmid PSK systems described previously, many studies have also shown that compensatory mutations in host cells are capable of overcoming the initial fitness costs of plasmid acquisition (Hall et al., 2020, 2021; Bird et al., 2023). It seems clear that

if there is no fitness cost to harbouring these plasmids (or that there is a cost associated with losing them), the presence of the AMR genes they carry can only be a net positive. Regarding IS*26,* perhaps in the absence of antibiotic selection and resulting hyperexpression, the multiple IS*26* arrays found within MDR plasmids are simply too small to impose a fitness cost on the cell and are not an evolutionary disadvantage.

6.1.4 The potential future of NDM carbapenemases

The recent history of ESBLs serves as a warning for the future spread of carbapenemases in the UK and worldwide. Initially identified in the UK in nosocomial pathogens, the spread of ESBLs outside hospitals in the wider UK community was first described in 2004 (Woodford et al., 2004; Pitout et al., 2005). Years later, Woerther et al. (2013) showed that rates of ESBL carriage in the community were increasing globally, especially in Asia. In 2017, it was once again shown that the global rate of ESBL carriage in the community was further increasing, and it was suggested that the spread of ESBLs to IncF plasmids mediated by IS*26* in *E. coli* was a contributing factor (Johnson et al., 2016; Bevan, Jones and Hawkey, 2017). A recent meta-analysis showed that this increase is still ongoing, and that globally, 17.6% of healthy individuals carry ESBL-producing *E. coli* in their intestine (Bezabih et al., 2022). As was the case with previous studies, this number is driven largely by studies from South-East Asia, where community prevalence was 35.1%, compared to 32.9% of hospital in-patients. In Europe, this number was much lower, as community carriage

was measured at 6.0% compared to hospital carriage at 13.8%. In the UK in 2014, the rate of carriage of CTX-M outside hospital settings was estimated to be 7.3%, and was significantly higher for those who were born in or recently travelled to South Asia (McNulty et al., 2018). This level of community carriage is reflected in the detection of human-associated ESBL-producing *E. coli* in multiple WWTPs in the UK (Bashawri, 2019; Day et al., 2019), including those that do not receive hospital wastewater (Raven et al., 2019), as well as the small rural WWTP A described in this and a previous study (Pritchard, 2022).

The spread of bla_{NDM} mirrors the rise of $bla_{CTX\text{-}M}$ in many ways. Both were discovered in Europe but found to be prominent in Asia, where community carriage is significantly higher than elsewhere. Both are associated with transposition events, including mobilisation by IS*26* and IncF plasmids. Also, they have both spread faster than some previously detected ESBLs or carbapenemases, such as bla_{TEM} and bla_{SHV} in the case of $bla_{CTX\text{-}M}$ and bla_{IMP} and bla_{VIM} for bla_{NDM}. The CTX-M enzymes became the globally dominant ESBL, which is not yet the case for NDM. However, between 2020 and 2021, the proportion of NDM among carbapenemase families isolated in the UK identified by the UKHSA was 25%, behind OXA-48-like enzymes at 41% (UKHSA, 2021). Between 2022 and 2023, the proportion of NDM amongst the carbapenemases had increased to 31.7% while OXA-48-like enzymes were reduced to 35.3% (UKHSA, 2023). This suggests the prevalence of NDM may be increasing in the UK. Another similarity between the CTX-M and NDM enzymes is the increased prevalence of a particularly successful genotype. Recently in the UK and Europe, $bla_{NDM\text{-}5}$ has become the dominant genotype in *E. coli*

(Turton et al., 2022; ECDC, 2023b), and perhaps this may be similar to the rise of *bla*$_{\text{CTX-M-15}}$ as the most dominant ESBL genotype (Cantón, González-Alba and Galán, 2012; Bevan, Jones and Hawkey, 2017).

According to UKHSA, the current burden of carbapenemase-producing bacteria in the UK is 2.12 positive samples per 100,000 population (UKHSA, 2023). This is measured by the number of positive samples from hospital patients, the majority of which are screening samples taken for the prevention of the spread of carbapenemase-producing organisms (CPO) within hospitals, compared against the local population of the NHS Trust. This shows that the current burden of CPO is lower than that of ESBL-producing organisms, and this may explain why to date the only CPOs isolated from UK wastewater have come from downstream of hospitals, as the community burden is not yet high enough for these to be detected elsewhere. If the spread of NDM does carry on in its similarity to the spread of the CTX-M enzymes, then at some point this will change, and NDM-producing bacteria will be found in wastewater that is not downstream of a hospital. Absent widespread community screening, wastewater-based epidemiology is the most viable tool to track this potential community spread and will enable more cost-effective surveillance of CPO outside of hospitals. More studies will be required like this one, but ideally those which attempt to isolate CPO from multiple WWTPs of similar sizes, so that the comparisons between wastewater in receipt of hospital effluent can be made.

6.1.5 Wastewater treatment and AMR: A One Health perspective

This study has focused on the surveillance of wastewater influent as a proxy for surveillance of AMR within the local clinical and/or community populations, but as CPO were also discovered in the treated effluent discharged from the WWTP, the impact of this on the environmental resistome needs further discussion. It is clear that the contamination of environmental water sources through discharge of untreated wastewater plays a key role in the spread of AMR in LMICs. It is estimated that 80% of the world's wastewater flows into the environment without being treated (UNESCO, 2017), and as a result, at least 2 billion people drink water from a source that is contaminated with human faeces (UNESCO, 2023). A report by the World Economic Forum (WEF) stated that "[i]n countries lacking universal wastewater treatment and access to clean water and sanitation, water is a primary vector in the spread of AMR and AMR diseases. Water access and pollution control can have a pivotal effect on AMR development and outcomes" (WEF, 2021). Similarly, the WHO identified improvements in water sanitation and hygiene (WASH) to be critical to reducing the spread of AMR in its Global Action Plan (WHO, 2020). A global study of wastewater by Hendriksen et al. (2019) found that although antimicrobial usage was correlated with AMR across countries, a much stronger correlation was seen between AMR and sanitation and health via the human development index. This problem is further exacerbated by the amounts of antibiotic residues detected in treated wastewater from LMICs. In one study, ciprofloxacin was detected at concentrations of 31 µg mL^{-1} (Larsson,

de Pedro and Paxeus, 2007), which is 31 times higher than the clinical breakpoint for resistance, and over 480,000 times higher than the predicted no effect environmental concentrations (PNEC) (Bengtsson-Palme and Larsson, 2016). Altogether, this evidence suggests that the spread of AMR through water sources in LMICs impacts the dissemination of AMR between human populations, which highlights the importance of wastewater treatment processes in those countries.

However, the impact of wastewater on the spread of AMR in high income countries is less well understood. Many studies have shown that antibiotic resistant bacteria are present in the effluent of wastewater treatment plants in the UK (Amos, Hawkey, et al., 2014; Amos, Zhang, et al., 2014; Amos et al., 2015; Ludden et al., 2017, 2020; Bashawri, 2019; Gouliouris et al., 2019; Raven et al., 2019; Pritchard, 2022; Matlock et al., 2023), but there are few studies showing that this poses a significant risk of transmission back into the human population. One study in Finland found that drinking water contaminated by wastewater effluent resulted in an outbreak of gastroenteritis (Lienemann et al., 2011), while surfers in the UK and open water swimmers in the Netherlands have been found to harbour ESBL-producing *E. coli* at significantly higher rates than the general population (Leonard et al., 2018; Blaak et al., 2019). A modelling study of intestinal carriage of ESBL and plasmid-mediated-AmpC-producing *E. coli* in the Netherlands estimated that swimming in surface freshwater was responsible for 2.3% of community acquisition (Mughini-Gras et al., 2019), and another modelling study from Italy estimated that 0.21% of clinical *Klebsiella* isolates originated in the environment (Thorpe et al., 2021).

It has also been suggested that wastewater possibly contributes to the spread of AMR through transmission of bacteria into the environment that spreads to food-producing animals and then into humans (Gholizadeh et al., 2023). Studies that have analysed the contribution of AMR in animal reservoirs to clinical infections in the UK have found that these environments for the most part contain distinct lineages. Multiple studies have shown that human clinical ESBL-producing *E. coli* isolates are dominated by ST131 and $bla_{\text{CTX-M-15}}$, while livestock isolates harboured ST10, ST602 and $bla_{\text{CTX-M-1}}$ (Day et al., 2019; Raven et al., 2019). Other studies have shown that UK livestock is not associated with clinical *K. pneumoniae* isolates (Ludden et al., 2020), and that ESBL-producing *E. coli* isolated from retail chicken meat is again associated with $bla_{\text{CTX-M-1}}$ (Randall et al., 2017). A systematic review in 2015 of the transmission of ESBL-producing *E. coli* between food-producing animals and humans found that 6 studies showed evidence of bacterial transmission between these environments, 13 showed evidence of HGT, while 17 studies did not demonstrate bacterial transmission, 2 did not demonstrate HGT, and of 4 observation epidemiological studies, 3 supported the hypothesis of animal to human transmission of ESBL-producing *E. coli* (Lazarus et al., 2015). The case of *mcr-1* is clear evidence that the spread of AMR from animals to humans has had a major effect on the resistome of human clinical isolates (Poirel and Nordmann, 2016; Wang et al., 2018), but precisely how much interaction there is between different environmental niches remains uncertain, especially in high income countries. Many papers have highlighted the fate of AMR in the environment as still being a vast knowledge gap (McCubbin et al., 2021;

Niegowska et al., 2021; Bengtsson-Palme et al., 2023; Gholizadeh et al., 2023), and so the impact of the release of CPO into UK rivers through treated wastewater is still unclear.

6.2 Conclusion

The surveillance of AMR in WWTPs gives an insight into the presence of AMR in a local population. Tracking the spread of specific AMR genes, and crucially their wider genetic environment such as the MGEs and plasmids on which they are found, is of major public interest given the rapid dissemination and dominance of specific resistance genes around the globe. This study shows that CPE showing high levels of multidrug resistance can regularly be isolated from a major UK WWTP that is downstream of a hospital in the East Midlands. The CPE isolated belonged to sequence types that have been associated with clinical infections around the globe, and the plasmids they carried were often mobilisable and highly similar to plasmids isolated from previously identified clinical isolates. Genetic characterisation of isolated CPE showed higher levels of bla_{NDM}-containing *E. coli* in this area than have been found previously in this and other parts of the country, and this is important for tracking the spread of the next major evolution in UK antimicrobial resistance.

This study adds to our knowledge on the impact of IS*26* in the spread of AMR, as bioinformatic analysis showed that this insertion sequence was heavily involved in the construction of MDR regions within the majority of carbapenem-resistance plasmids detected here. Experiments showed that IS*26*

was responsible for the transfer of the genetic region containing *bla*$_{NDM}$ along with a class 1 integron containing multiple ARGs, and this region could be transferred from one plasmid to another by the activity of IS*26.*

6.3 Future direction of work

Wastewater based epidemiology (WBE) is increasingly being used to monitor the spread of AMR in various communities and locations around the world (Chau et al., 2022). As stated in recent reviews, standardisation of WBE methods would greatly improve the ability of researchers to compare results and to track the AMR burden across different parts of the globe (Chau et al., 2022; Tiwari et al., 2022). Chau et al. (2022) also called for the use of composite sampling over longitudinal timeframes (>12 months) to generate more robust data on the presence of AMR in the sampled area. The original timeframe for this study was intended to be much longer to get a broader picture of AMR from the sampled WWTPs, rather than the "snapshot in time" that is captured from shorter sampling periods, but this had to be curtailed due to the COVID-19 pandemic. Future work in this area would involve longer sampling periods, and had that been the case in this study, it may have helped to answer the question of whether the nearly identical bacteria and plasmids that were detected were found due to temporal variations or truly represent a consistent spread of these genotypes. Chau et al. (2022) also pointed out that genomic approaches such as metagenomic sequencing enable a more unbiased approach to the surveillance of AMR. This is useful for comparing the overall

burden of AMR across studies, but with regards to the spread of certain clinically relevant bacteria such as CPE, bias may be warranted. If we are interested in the spread of the most clinically important genes, then unbiased metagenomics may not be the most appropriate tool as even a very high sequencing depth cannot entirely capture the total diversity of AMR in a sample (Gweon et al., 2019). For this reason, so-called culture-enriched metagenomics has been used to investigate the cystic fibrosis lung microbiota (Whelan et al., 2020), the resistome of *Enterobacteriaceae* in wild owls (Miller et al., 2020), as well as the presence of carbapenem-resistant bacteria from WWTPs (Zhang, Zhang and Ju, 2022; Acosta et al., 2023). This involves culture-based enrichment for a particular subset of bacteria; in the latter case, selection by culturing on agar containing carbapenems and/or other antimicrobials, followed by metagenomic sequencing. It combines the advantages of culture-based techniques, that clinically important bacteria can be selected for, with the advantages of metagenomics, in that all the bacteria within the enriched sample will be sequenced. For ARG detection, the use of this technique has so far been limited to short-read metagenomic sequencing. In this study, the use of long-read technology was crucial to understanding the role MGEs and plasmids have played in the spread of AMR, by enabling the circular assembly of plasmid sequences and identification of the MGEs upstream and downstream of their MDR regions. For this reason, culture enriched metagenomics using a hybrid approach of long and short-read sequencing could be an important method in the future of WBE. So far, only one study has used culture-enrichment combined with long-read

metagenomics, which was used to generate nearly complete microbial genomes from the microbiota of oceanic sediment (Wang et al., 2021). It seems only a matter of time before this method is used to investigate the clinically relevant fraction of the wastewater resistome, and ideally, future work would use this to better understand the spread of CPE in UK wastewater.

The experiments in this work using CRISPR-Cas9-based curing of an IncF plasmid to facilitate detection of IS*26* mobilisation raised the question of the potential fitness costs of large numbers of repetitive IS*26* regions. To further understand the transfer of IS*26* between plasmids, experiments to measure any fitness costs of the transconjugant transformants described in **Chapter 5** could be performed. It was also hypothesised that the repetitive sections of multiple bla_{NDM} regions were caused by cointegration of multiple IS*26* molecules followed by plasmid replication followed by further cointegration events. If this did produce a fitness cost, then this would suggest IS*26* transposition to medium or high-copy number plasmids would be detrimental to the cell, and this could perhaps be related to the fact that MDR plasmids that are commonly associated with IS*26* are all low-copy number (Rozwandowicz et al., 2018). As many studies have previously shown, IS*26* plays an important role in the evolution of AMR, and its preferred mechanism of transposition leads to the formation of increasingly drug-resistant bacteria. Here we present that there is more knowledge required to fully understand its magnificence.

CHAPTER 7: REFERENCES

7.1 Reference list

Aarestrup, F.M. and Woolhouse, M.E.J. (2020) 'Using sewage for surveillance of antimicrobial resistance', *Science*, 367(6478), pp. 630–632. Available at: https://doi.org/10.1126/science.aba3432.

Abraham, E.P. and Chain, E. (1940) 'An Enzyme from Bacteria able to destroy Penicillin', *Nature*, 146, p. 837.

Abraham, E.P. and Newton, G.G.F. (1961) 'The structure of cephalosporin C', *Biochemical Journal*, 79(2), pp. 377–393. Available at: https://doi.org/10.1042/bj0790377.

Acman, M., Wang, R., van Dorp, L., Shaw, L.P., Wang, Q., Luhmann, N., Yin, Y., Sun, S., Chen, H., Wang, H. and Balloux, F. (2022) 'Role of mobile genetic elements in the global dissemination of the carbapenem resistance gene blaNDM', *Nature Communications*, 13(1), p. 1131. Available at: https://doi.org/10.1038/s41467-022-28819-2.

Acosta, N., Lee, J., Bautista, M.A., Bhatnagar, S., Waddell, B.J., Au, E., Pradhan, P., Clark, R.G., Meddings, J., Ruecker, N., Achari, G., Pitout, J.D., Conly, J., Frankowski, K., Hubert, C.R.J. and Parkins, M.D. (2023) 'Metagenomic analysis after selective culture enrichment of wastewater demonstrates increased burden of antibiotic resistant genes in hospitals relative to the community'. medRxiv, p. 2023.03.07.23286790. Available at: https://doi.org/10.1101/2023.03.07.23286790.

Adler, M., Anjum, M., Berg, O.G., Andersson, D.I. and Sandegren, L. (2014) 'High Fitness Costs and Instability of Gene Duplications Reduce Rates of Evolution of New Genes by Duplication-Divergence Mechanisms', *Molecular Biology and Evolution*, 31(6), pp. 1526–1535. Available at: https://doi.org/10.1093/molbev/msu111.

Adrian, P.V., du Plessis, M., Klugman, K.P. and Amyes, S.G.B. (1998) 'New Trimethoprim-Resistant Dihydrofolate Reductase Cassette, dfrXV, Inserted in a Class 1 Integron', *Antimicrobial Agents and Chemotherapy*, 42(9), pp. 2221–2224.

Ahmed, A.M. and Shimamoto, T. (2004) 'A plasmid-encoded class 1 integron carrying sat, a putative phosphoserine phosphatase gene and aadA2 from enterotoxigenic Escherichia coli O159 isolated in Japan', *FEMS Microbiology Letters*, 235(2), pp. 243–248. Available at: https://doi.org/10.1111/j.1574-6968.2004.tb09595.x.

Ahn, K., Hwang, G.Y., Kim, Y.K., Kim, H.Y., Jeong, H.R., Hong, J.S. and Uh, Y. (2019) 'Nosocomial Outbreak Caused by NDM-5 and OXA-181 Carbapenemase

Co-producing Escherichia coli', *Infection & Chemotherapy*, 51(2), pp. 177–182. Available at: https://doi.org/10.3947/ic.2019.51.2.177.

Aires-De-Sousa, M., Ortiz De La Rosa, J.M., Goncalves, M.L., Costa, A., Nordmann, P. and Poirel, L. (2020) 'Occurrence of NDM-1-producing Morganella morganii and Proteus mirabilis in a single patient in Portugal: probable in vivo transfer by conjugation', *The Journal of antimicrobial chemotherapy*, 75(4), pp. 903–906. Available at: https://doi.org/10.1093/JAC/DKZ542.

Alcock, B.P., Raphenya, A.R., Lau, T.T.Y., Tsang, K.K., Bouchard, M., Edalatmand, A., Huynh, W., Nguyen, A.L.V., Cheng, A.A., Liu, S., Min, S.Y., Miroshnichenko, A., Tran, H.K., Werfalli, R.E., Nasir, J.A., Oloni, M., Speicher, D.J., Florescu, A., Singh, B., Faltyn, M., Hernandez-Koutoucheva, A., Sharma, A.N., Bordeleau, E., Pawlowski, A.C., Zubyk, H.L., Dooley, D., Griffiths, E., Maguire, F., Winsor, G.L., Beiko, R.G., Brinkman, F.S.L., Hsiao, W.W.L., Domselaar, G.V. and McArthur, A.G. (2020) 'CARD 2020: Antibiotic resistome surveillance with the comprehensive antibiotic resistance database', *Nucleic Acids Research*, 48(D1), pp. D517–D525. Available at: https://doi.org/10.1093/nar/gkz935.

Alexander, J., Bollmann, A., Seitz, W. and Schwartz, T. (2015) 'Microbiological characterization of aquatic microbiomes targeting taxonomical marker genes and antibiotic resistance genes of opportunistic bacteria', *Science of the Total Environment*, 512–513, pp. 316–325. Available at: https://doi.org/10.1016/j.scitotenv.2015.01.046.

Alexander, J., Hembach, N. and Schwartz, T. (2020) 'Evaluation of antibiotic resistance dissemination by wastewater treatment plant effluents with different catchment areas in Germany', *Scientific Reports*, 10(1). Available at: https://doi.org/10.1038/s41598-020-65635-4.

Alikhan, N.-F., Petty, N.K., Ben Zakour, N.L. and Beatson, S.A. (2011) 'BLAST Ring Image Generator (BRIG): simple prokaryote genome comparisons', *BMC Genomics*, 12(1), p. 402. Available at: https://doi.org/10.1186/1471-2164-12-402.

Alm, R.A., Johnstone, M.R. and Lahiri, S.D. (2015) 'Characterization of Escherichia coli NDM isolates with decreased susceptibility to aztreonam/avibactam: role of a novel insertion in PBP3', *Journal of Antimicrobial Chemotherapy*, 70(5), pp. 1420–1428. Available at: https://doi.org/10.1093/JAC/DKU568.

Altschul, S.F., Gish, W., Miller, W., Myers, E.W. and Lipman, D.J. (1990) 'Basic local alignment search tool', *Journal of Molecular Biology*, 215(3), pp. 403–410. Available at: https://doi.org/10.1016/S0022-2836(05)80360-2.

Amador, P.P., Fernandes, R.M., Prudêncio, M.C., Barreto, M.P. and Duarte, I.M. (2015) 'Antibiotic resistance in wastewater: Occurrence and fate of Enterobacteriaceae producers of Class A and Class C β-lactamases', *Journal of*

Environmental Science and Health - Part A Toxic/Hazardous Substances and Environmental Engineering, 50(1), pp. 26–39. Available at: https://doi.org/10.1080/10934529.2015.964602.

Ambler, R.P. (1980) 'The Structure of beta-Lactamases', *Philosophical Transactions of the Royal Society B: Biological Sciences*, 289(1036), pp. 321–331. Available at: https://doi.org/10.1098/rstb.1980.0049.

Aminov, R.I. (2010) 'A brief history of the antibiotic era: lessons learned and challenges for the future.', *Frontiers in microbiology*, 1, p. 134. Available at: https://doi.org/10.3389/fmicb.2010.00134.

Amos, G.C.A., Gozzard, E., Carter, C.E., Mead, A., Bowes, M.J., Hawkey, P.M., Zhang, L., Singer, A.C., Gaze, W.H. and Wellington, E.M.H. (2015) 'Validated predictive modelling of the environmental resistome', *The ISME Journal*, 9(6), pp. 1467–1476. Available at: https://doi.org/10.1038/ismej.2014.237.

Amos, G.C.A., Hawkey, P.M., Gaze, W.H. and Wellington, E.M. (2014) 'Waste water effluent contributes to the dissemination of CTX-M-15 in the natural environment', *Journal of Antimicrobial Chemotherapy*, 69(7), p. 1785. Available at: https://doi.org/10.1093/JAC/DKU079.

Amos, G.C.A., Zhang, L., Hawkey, P.M., Gaze, W.H. and Wellington, E.M. (2014) 'Functional metagenomic analysis reveals rivers are a reservoir for diverse antibiotic resistance genes', *Veterinary Microbiology*, 171(3–4), pp. 441–447. Available at: https://doi.org/10.1016/j.vetmic.2014.02.017.

Andersen, J.B., Sternberg, C., Poulsen, L.K., Bjørn, S.P., Givskov, M. and Molin, S. (1998) 'New Unstable Variants of Green Fluorescent Protein for Studies of Transient Gene Expression in Bacteria', *Applied and Environmental Microbiology*, 64(6), p. 2240. Available at: https://doi.org/10.1128/AEM.64.6.2240-2246.1998.

Andrews, S. (2010) *FastQC A Quality Control tool for High Throughput Sequence Data*. Available at: https://www.bioinformatics.babraham.ac.uk/projects/fastqc/ (Accessed: 25 April 2023).

Arakawa, Y., Murakami, M., Suzuki, K., Ito, H., Wacharotayankun, R., Ohsuka, S., Kato, N. and Ohta, M. (1995) 'A novel integron-like element carrying the metallo-beta-lactamase gene blaIMP', *Antimicrobial Agents and Chemotherapy*, 39(7), pp. 1612–1615. Available at: https://doi.org/10.1128/AAC.39.7.1612.

Arredondo-Alonso, S., Willems, R.J., van Schaik, W. and Schürch, A.C. (2017) 'On the (im)possibility of reconstructing plasmids from whole-genome short-read sequencing data', *Microbial Genomics*, 3(10), p. e000128. Available at: https://doi.org/10.1099/mgen.0.000128.

Ayukekbong, J.A., Ntemgwa, M. and Atabe, A.N. (2017) 'The threat of antimicrobial resistance in developing countries: causes and control strategies', *Antimicrobial Resistance & Infection Control*, 6(1), p. 47. Available at: https://doi.org/10.1186/s13756-017-0208-x.

Bahr, G., Vitor-Horen, L., Bethel, C.R., Bonomo, R.A., González, L.J. and Vila, A.J. (2017) 'Clinical Evolution of New Delhi Metallo-β-Lactamase (NDM) Optimizes Resistance under Zn(II) Deprivation', *Antimicrobial Agents and Chemotherapy*, 62(1), pp. e01849-17. Available at: https://doi.org/10.1128/AAC.01849-17.

Balcazar, J.L. (2014) 'Bacteriophages as Vehicles for Antibiotic Resistance Genes in the Environment', *PLoS Pathogens*, 10(7), p. e1004219. Available at: https://doi.org/10.1371/journal.ppat.1004219.

Ball, P.R., Shales, S.W. and Chopra, I. (1980) 'Plasmid-mediated tetracycline resistance in escherichia coli involves increased efflux of the antibiotic', *Biochemical and Biophysical Research Communications*, 93(1), pp. 74–81. Available at: https://doi.org/10.1016/S0006-291X(80)80247-6.

Bankevich, A., Nurk, S., Antipov, D., Gurevich, A.A., Dvorkin, M., Kulikov, A.S., Lesin, V.M., Nikolenko, S.I., Pham, S., Prjibelski, A.D., Pyshkin, A.V., Sirotkin, A.V., Vyahhi, N., Tesler, G., Alekseyev, M.A. and Pevzner, P.A. (2012) 'SPAdes: A new genome assembly algorithm and its applications to single-cell sequencing', *Journal of Computational Biology*, 19(5), pp. 455–477. Available at: https://doi.org/10.1089/cmb.2012.0021.

Baraniak, A., Grabowska, A., Izdebski, R., Fiett, J., Herda, M., Bojarska, K., Zabicka, D., Kania-Pudło, M., Młynarczyk, G., Zak-Puławska, Z., Hryniewicz, W., Gniadkowski, M., Cieplińska, T., Czekalska, E., Filczak, K., Guzek, A., Iskra, E., Jędrzejewska, A., Kociszewska, D., Naumiuk, Łopaciuk, U., Pawlik, K., Połowniak-Pracka, H., Sodo, A., Sulikowska, A., Szymanek, K. and Witman, D. (2011) 'Molecular characteristics of KPC-producing Enterobacteriaceae at the early stage of their dissemination in Poland, 2008-2009', *Antimicrobial Agents and Chemotherapy*, 55(12), pp. 5493–5499. Available at: https://doi.org/10.1128/AAC.05118-11.

Barcellos, D.S., Barquilha, C.E.R., Oliveira, P.E., Prokopiuk, M. and Etchepare, R.G. (2023) 'How has the COVID-19 pandemic impacted wastewater-based epidemiology?', *The Science of the Total Environment*, 892, p. 164561. Available at: https://doi.org/10.1016/J.SCITOTENV.2023.164561.

Barlow, M. and Hall, B.G. (2002) 'Phylogenetic Analysis Shows That the OXA b-Lactamase Genes Have Been on Plasmids for Millions of Years', *Journal of Molecular Evolution*, 55(3), pp. 314–321. Available at: https://doi.org/10.1007/s00239-002-2328-y.

Barnich, N., Bringer, M.A., Claret, L. and Daffeuille-Michaud, A. (2004) 'Involvement of lipoprotein NlpI in the virulence of adherent invasive Escherichia coli strain LF82 isolated from a patient with Crohn's disease',

Infection and immunity, 72(5), pp. 2484–2493. Available at: https://doi.org/10.1128/IAI.72.5.2484-2493.2004.

Barutcu, A.R., Fritz, A.J., Zaidi, S.K., van Wijnen, A.J., Lian, J.B., Stein, J.L., Nickerson, J.A., Imbalzano, A.N. and Stein, G.S. (2016) 'C-ing the Genome: A Compendium of Chromosome Conformation Capture Methods to Study Higher-Order Chromatin Organization', *Journal of Cellular Physiology*, 231(1), pp. 31–35. Available at: https://doi.org/10.1002/jcp.25062.

Bashawri, Y.M.A. (2019) *Understanding the Role of Wastewater in the Spread of Antibiotic Resistant Bacteria*. Bangor University.

Bauernfeind, A., Stemplinger, I., Jungwirth, R., Ernst, S. and Casellas, J.M. (1996) Sequences of-Lactamase Genes Encoding CTX-M-1 (MEN-1) and CTX-M-2 and Relationship of Their Amino Acid Sequences with Those of Other-Lactamases', *Antimicrobial Agents and Chemotherapy*, 40(2), pp. 509–513. Available at: http://aac.asm.org/

Bayer, A.S., Schneider, T. and Sahl, H.G. (2013) 'Mechanisms of daptomycin resistance in Staphylococcus aureus: role of the cell membrane and cell wall'. *Annals of the New York Academy of Sciences*, 1277(1), pp. 139-58. Available at: https://doi.org/10.1111/j.1749-6632.2012.06819.x

Bengtsson-Palme, J., Abramova, A., Berendonk, T.U., Coelho, L.P., Forslund, S.K., Gschwind, R., Heikinheimo, A., Jarquín-Díaz, V.H., Khan, A.A., Klümper, U., Löber, U., Nekoro, M., Osińska, A.D., Ugarcina Perovic, S., Pitkänen, T., Rødland, E.K., Ruppé, E., Wasteson, Y., Wester, A.L. and Zahra, R. (2023) 'Towards monitoring of antimicrobial resistance in the environment: For what reasons, how to implement it, and what are the data needs?', *Environment International*, 178, p. 108089. Available at: https://doi.org/10.1016/j.envint.2023.108089.

Bengtsson-Palme, J., Hammarén, R., Pal, C., Östman, M., Björlenius, B., Flach, C.-F., Fick, J., Kristiansson, E., Tysklind, M. and Larsson, D.G.J. (2016) 'Elucidating selection processes for antibiotic resistance in sewage treatment plants using metagenomics', *Science of The Total Environment*, 572, pp. 697–712. Available at: https://doi.org/10.1016/j.scitotenv.2016.06.228.

Bengtsson-Palme, J. and Larsson, D.G.J. (2016) 'Concentrations of antibiotics predicted to select for resistant bacteria: Proposed limits for environmental regulation', *Environment International*, 86, pp. 140–149. Available at: https://doi.org/10.1016/j.envint.2015.10.015.

Bengtsson-Palme, J., Milakovic, M., Švecová, H., Ganjto, M., Jonsson, V., Grabic, R. and Udikovic-Kolic, N. (2019) 'Industrial wastewater treatment plant enriches antibiotic resistance genes and alters the structure of microbial communities', *Water Research*, 162, pp. 437–445. Available at: https://doi.org/10.1016/j.watres.2019.06.073.

Bennett, P.M. (2004) 'Genome Plasticity', in N. Woodford and A.P. Johnson (eds) *Genomics, Proteomics, and Clinical Bacteriology: Methods and Reviews*. Totowa, NJ: Humana Press (Methods in Molecular Biology™), pp. 71–113. Available at: https://doi.org/10.1385/1-59259-763-7:071.

Bennett, P.M. (2008) 'Plasmid encoded antibiotic resistance: acquisition and transfer of antibiotic resistance genes in bacteria', *British Journal of Pharmacology*, 153(Suppl 1), pp. S347–S357. Available at: https://doi.org/10.1038/sj.bjp.0707607.

Berbers, B., Vanneste, K., Roosens, N.H.C.J., Marchal, K., Ceyssens, P.J. and De Keersmaecker, S.C.J. (2023) 'Using a combination of short- and long-read sequencing to investigate the diversity in plasmid- and chromosomally encoded extended-spectrum beta-lactamases (ESBLs) in clinical Shigella and Salmonella isolates in Belgium', *Microbial genomics*, 9(1). Available at: https://doi.org/10.1099/MGEN.0.000925.

Berg, D.E., Davies, J., Allet, B. and Rochaix, J.D. (1975) 'Transposition of R factor genes to bacteriophage lambda', *Proceedings of the National Academy of Sciences of the United States of America*, 72(9), pp. 3628–3632. Available at: https://doi.org/10.1073/pnas.72.9.3628.

Bevan, E.R., Jones, A.M. and Hawkey, P.M. (2017) 'Global epidemiology of CTX-M β-lactamases: temporal and geographical shifts in genotype', *Journal of Antimicrobial Chemotherapy*, 72(8), pp. 2145–2155. Available at: https://doi.org/10.1093/jac/dkx146.

Bezabih, Y.M., Bezabih, A., Dion, M., Batard, E., Teka, S., Obole, A., Dessalegn, N., Enyew, A., Roujeinikova, A., Alamneh, E., Mirkazemi, C., Peterson, G.M. and Bezabhe, W.M. (2022) 'Comparison of the global prevalence and trend of human intestinal carriage of ESBL-producing Escherichia coli between healthcare and community settings: a systematic review and meta-analysis', *JAC-Antimicrobial Resistance*, 4(3), p. dlac048. Available at: https://doi.org/10.1093/jacamr/dlac048.

Bhullar, K., Waglechner, N., Pawlowski, A., Koteva, K., Banks, E.D., Johnston, M.D., Barton, H.A. and Wright, G.D. (2012) 'Antibiotic Resistance Is Prevalent in an Isolated Cave Microbiome', *PLOS ONE*, 7(4), p. e34953. Available at: https://doi.org/10.1371/journal.pone.0034953.

Bird, S.M., Ford, S., Thompson, C.M.A., Little, R., Hall, J.P.J., Jackson, R.W., Malone, J., Harrison, E. and Brockhurst, M.A. (2023) 'Compensatory mutations reducing the fitness cost of plasmid carriage occur in plant rhizosphere communities', *FEMS Microbiology Ecology*, 99(4), p. fiad027. Available at: https://doi.org/10.1093/femsec/fiad027.

Blaak, H., Kemper, M.A., Pijnacker, R., Mughini Gras, L., de Roda Husman, A.M., Schets, C. and Schmitt, H. (2019) *Resistente darmbacteriën bij open water zwemmers*. Report. Rijksinstituut voor Volksgezondheid en Milieu RIVM.

Available at: https://rivm.openrepository.com/handle/10029/623618 (Accessed: 18 December 2023).

Blanco, P., Hernando-Amado, S., Reales-Calderon, J.A., Corona, F., Lira, F., Alcalde-Rico, M., Bernardini, A., Sanchez, M.B. and Martinez, J.L. (2016) 'Bacterial Multidrug Efflux Pumps: Much More Than Antibiotic Resistance Determinants', *Microorganisms*, 4(1), p. 14. Available at: https://doi.org/10.3390/microorganisms4010014.

Blomberg, P., Nordström, K. and Wagner, E.G. (1992) 'Replication control of plasmid R1: RepA synthesis is regulated by CopA RNA through inhibition of leader peptide translation.', *The EMBO Journal*, 11(7), pp. 2675–2683.

Bolger, A.M., Lohse, M. and Usadel, B. (2014) 'Trimmomatic: A flexible trimmer for Illumina sequence data', *Bioinformatics*, 30(15), pp. 2114–2120. Available at: https://doi.org/10.1093/bioinformatics/btu170.

Boll, E.J., Frimodt-Møller, J., Olesen, B., Krogfelt, K.A. and Struve, C. (2016) 'Heat resistance in extended-spectrum beta-lactamase-producing Escherichia coli may favor environmental survival in a hospital setting', *Research in microbiology*, 167(5), pp. 345–349. Available at: https://doi.org/10.1016/J.RESMIC.2016.02.002.

Bontron, S., Nordmann, P. and Poirel, L. (2016) 'Transposition of Tn125 Encoding the NDM-1 Carbapenemase in Acinetobacter baumannii', *Antimicrobial Agents and Chemotherapy*, 60(12), pp. 7245–7251. Available at: https://doi.org/10.1128/aac.01755-16.

Bortolaia, V., Kaas, R.S., Ruppe, E., Roberts, M.C., Schwarz, S., Cattoir, V., Philippon, A., Allesoe, R.L., Rebelo, A.R., Florensa, A.F., Fagelhauer, L., Chakraborty, T., Neumann, B., Werner, G., Bender, J.K., Stingl, K., Nguyen, M., Coppens, J., Xavier, B.B., Malhotra-Kumar, S., Westh, H., Pinholt, M., Anjum, M.F., Duggett, N.A., Kempf, I., Nykäsenoja, S., Olkkola, S., Wieczorek, K., Amaro, A., Clemente, L., Mossong, J., Losch, S., Ragimbeau, C., Lund, O. and Aarestrup, F.M. (2020) 'ResFinder 4.0 for predictions of phenotypes from genotypes', *Journal of Antimicrobial Chemotherapy*, 75(12), pp. 3491–3500. Available at: https://doi.org/10.1093/jac/dkaa345.

Bosch, F. and Rosich, L. (2008) 'The contributions of Paul Ehrlich to pharmacology: a tribute on the occasion of the centenary of his Nobel Prize.', *Pharmacology*, 82(3), pp. 171–9. Available at: https://doi.org/10.1159/000149583.

Bouki, C., Venieri, D. and Diamadopoulos, E. (2013) 'Detection and fate of antibiotic resistant bacteria in wastewater treatment plants: A review', *Ecotoxicology and Environmental Safety*, 91, pp. 1–9. Available at: https://doi.org/10.1016/j.ecoenv.2013.01.016.

Bowers, J.R., Kitchel, B., Driebe, E.M., MacCannell, D.R., Roe, C., Lemmer, D., Man, T. de, Rasheed, J.K., Engelthaler, D.M., Keim, P. and Limbago, B.M. (2015) 'Genomic Analysis of the Emergence and Rapid Global Dissemination of the Clonal Group 258 Klebsiella pneumoniae Pandemic', *PLOS ONE*, 10(7), p. e0133727. Available at: https://doi.org/10.1371/journal.pone.0133727.

Bradford, P.A. (2001) 'Extended-spectrum beta-lactamases in the 21st century: characterization, epidemiology, and detection of this important resistance threat.', *Clinical microbiology reviews*, 14(4), pp. 933–51, table of contents. Available at: https://doi.org/10.1128/CMR.14.4.933-951.2001.

Bréchet, C., Plantin, J., Sauget, M., Thouverez, M., Talon, D., Cholley, P., Guyeux, C., Hocquet, D. and Bertrand, X. (2014) 'Wastewater Treatment Plants Release Large Amounts of Extended-Spectrum β-Lactamase–Producing Escherichia coli Into the Environment', *Clinical Infectious Diseases*, 58(12), pp. 1658–1665. Available at: https://doi.org/10.1093/cid/ciu190.

Brendler, T., Reaves, L. and Austin, S. (2004) 'Interplay between Plasmid Partition and Postsegregational Killing Systems', *Journal of Bacteriology*, 186(8), pp. 2504–2507. Available at: https://doi.org/10.1128/JB.186.8.2504-2507.2004.

Brown, A.G., Butterworth, D., Cole, M., Hanscomb, G., Hood, J.D., Reading, C. and Rolinson, G.N. (1976) 'Naturally-occurring beta-lactamase inhibitors with antibacterial activity.', *The Journal of antibiotics*, 29(6), pp. 668–9.

Brown, M.G. and Balkwill, D.L. (2009) 'Antibiotic Resistance in Bacteria Isolated from the Deep Terrestrial Subsurface', *Microbial Ecology*, 57(3), pp. 484–493. Available at: https://doi.org/10.1007/s00248-008-9431-6.

Browne, A.J., Chipeta, M.G., Haines-Woodhouse, G., Kumaran, E.P.A., Hamadani, B.H.K., Zaraa, S., Henry, N.J., Deshpande, A., Reiner, R.C., Day, N.P.J., Lopez, A.D., Dunachie, S., Moore, C.E., Stergachis, A., Hay, S.I. and Dolecek, C. (2021) 'Global antibiotic consumption and usage in humans, 2000–18: a spatial modelling study', *The Lancet Planetary Health*, 5(12), pp. e893–e904. Available at: https://doi.org/10.1016/S2542-5196(21)00280-1.

Buckner, M.M.C., Ciusa, M.L. and Piddock, L.J.V. (2018) 'Strategies to combat antimicrobial resistance: anti-plasmid and plasmid curing', *FEMS Microbiology Reviews*, 42(6), p. 781. Available at: https://doi.org/10.1093/FEMSRE/FUY031.

Bush, K. (2018) 'Past and Present Perspectives on β-Lactamases.', *Antimicrobial agents and chemotherapy*, 62(10), pp. e01076-18. Available at: https://doi.org/10.1128/AAC.01076-18.

Bush, K. and Bradford, P.A. (2016) 'β-Lactams and β-Lactamase Inhibitors: An Overview.', *Cold Spring Harbor perspectives in medicine*, 6(8), p. a025247. Available at: https://doi.org/10.1101/cshperspect.a025247.

Bush, K. and Jacoby, G.A. (2010) 'Updated functional classification of beta-lactamases.', *Antimicrobial agents and chemotherapy*, 54(3), pp. 969–76. Available at: https://doi.org/10.1128/AAC.01009-09.

Cabot, G., Ocampo-Sosa, A.A., Tubau, F., Macia, M.D., Rodríguez, C., Moya, B., Zamorano, L., Suárez, C., Peña, C., Martínez-Martínez, L. and Oliver, A. (2011) 'Overexpression of AmpC and Efflux Pumps in Pseudomonas aeruginosa Isolates from Bloodstream Infections: Prevalence and Impact on Resistance in a Spanish Multicenter Study ▿ ', *Antimicrobial Agents and Chemotherapy*, 55(5), pp. 1906–1911. Available at: https://doi.org/10.1128/AAC.01645-10.

Cacace, D., Fatta-Kassinos, D., Manaia, C.M., Cytryn, E., Kreuzinger, N., Rizzo, L., Karaolia, P., Schwartz, T., Alexander, J., Merlin, C., Garelick, H., Schmitt, H., de Vries, D., Schwermer, C.U., Meric, S., Ozkal, C.B., Pons, M.N., Kneis, D. and Berendonk, T.U. (2019) 'Antibiotic resistance genes in treated wastewater and in the receiving water bodies: A pan-European survey of urban settings', *Water Research*, 162, pp. 320–330. Available at: https://doi.org/10.1016/j.watres.2019.06.039.

Cahill, N., O'Connor, L., Mahon, B., Varley, Á., McGrath, E., Ryan, P., Cormican, M., Brehony, C., Jolley, K.A., Maiden, M.C., Brisse, S. and Morris, D. (2019) 'Hospital effluent: A reservoir for carbapenemase-producing Enterobacterales?', *Science of the Total Environment*, 672, pp. 618–624. Available at: https://doi.org/10.1016/j.scitotenv.2019.03.428.

Camacho, C., Coulouris, G., Avagyan, V., Ma, N., Papadopoulos, J., Bealer, K. and Madden, T.L. (2009) 'BLAST+: Architecture and applications', *BMC Bioinformatics*, 10(1), pp. 1–9. Available at: https://doi.org/10.1186/1471-2105-10-421/FIGURES/4.

Cantón, R., González-Alba, J.M. and Galán, J.C. (2012) 'CTX-M Enzymes: Origin and Diffusion.', *Frontiers in microbiology*, 3, p. 110. Available at: https://doi.org/10.3389/fmicb.2012.00110.

Cantón, R., Gottlieb, T., Coombs, G.W., Woo, P.C.Y., Korman, T.M., Garcia-Castillo, M., Daley, D., Bauer, K.A., Wong, M., Wolf, D.J., Siddiqui, F. and Motyl, M. (2023) 'Antimicrobial surveillance: A 20-year history of the SMART approach to addressing global antimicrobial resistance into the future', *International Journal of Antimicrobial Agents*, 62(6), p. 107014. Available at: https://doi.org/10.1016/j.ijantimicag.2023.107014.

Cao, X., Xie, H., Huang, D., Zhou, W., Liu, Y., Shen, H. and Zhou, K. (2021) 'Detection of a clinical carbapenem-resistant Citrobacter portucalensis strain and the dissemination of C. portucalensis in clinical settings', *Journal of Global Antimicrobial Resistance*, 27, pp. 79–81. Available at: https://doi.org/10.1016/j.jgar.2021.04.027.

Carattoli, A. (2011) 'Plasmids in Gram negatives: Molecular typing of resistance plasmids', *International Journal of Medical Microbiology*, 301(8), pp. 654–658. Available at: https://doi.org/10.1016/j.ijmm.2011.09.003.

Carattoli, A. (2013) 'Plasmids and the spread of resistance', *International Journal of Medical Microbiology*, 303(6–7), pp. 298–304. Available at: https://doi.org/10.1016/j.ijmm.2013.02.001.

Carattoli, A., Bertini, A., Villa, L., Falbo, V., Hopkins, K.L. and Threlfall, E.J. (2005) 'Identification of plasmids by PCR-based replicon typing', *Journal of Microbiological Methods*, 63(3), pp. 219–228. Available at: https://doi.org/10.1016/j.mimet.2005.03.018.

Carattoli, A., Zankari, E., Garciá-Fernández, A., Larsen, M.V., Lund, O., Villa, L., Aarestrup, F.M. and Hasman, H. (2014) 'In Silico detection and typing of plasmids using plasmidfinder and plasmid multilocus sequence typing', *Antimicrobial Agents and Chemotherapy*, 58(7), pp. 3895–3903. Available at: https://doi.org/10.1128/AAC.02412-14.

Carfi, A., Pares, S., Duée, E., Galleni, M., Duez, C., Frère, J.M. and Dideberg, O. (1995) 'The 3-D structure of a zinc metallo-beta-lactamase from Bacillus cereus reveals a new type of protein fold', *The EMBO journal*, 14(20), pp. 4914–4921. Available at: https://doi.org/10.1002/j.1460-2075.1995.tb00174.x.

Castañeda-Barba, S., Top, E.M. and Stalder, T. (2023) 'Plasmids, a molecular cornerstone of antimicrobial resistance in the One Health era', *Nature Reviews Microbiology*, pp. 1–15. Available at: https://doi.org/10.1038/s41579-023-00926-x.

Castanheira, M., Deshpande, L.M., Mathai, D., Bell, J.M., Jones, R.N. and Mendes, R.E. (2011) 'Early Dissemination of NDM-1- and OXA-181-Producing Enterobacteriaceae in Indian Hospitals: Report from the SENTRY Antimicrobial Surveillance Program, 2006-2007', *Antimicrobial Agents and Chemotherapy*, 55(3), pp. 1274–1278. Available at: https://doi.org/10.1128/AAC.01497-10.

Castanheira, M., Simner, P.J. and Bradford, P.A. (2021) 'Extended-spectrum β-lactamases: an update on their characteristics, epidemiology and detection', *JAC-Antimicrobial Resistance*, 3(3), p. dlab092. Available at: https://doi.org/10.1093/jacamr/dlab092.

Chain, E., Florey, H.W., Gardner, A.D., Heatley, N.G., Jennings, M.A., Orr-Ewing, J., Sanders, A.G. and Peltier, L.F. (2005) 'THE CLASSIC: Penicillin as a Chemotherapeutic Agent', *Clinical Orthopaedics and Related Research*, 439(NA;), pp. 23–26. Available at: https://doi.org/10.1097/01.blo.0000183429.83168.07.

Chakraborty, T., Sadek, M., Yao, Y., Imirzalioglu, C., Stephan, R., Poirel, L. and Nordmann, P. (2021) 'Cross-Border Emergence of Escherichia coli Producing

the Carbapenemase NDM-5 in Switzerland and Germany', *Journal of Clinical Microbiology*, 59(3). Available at: https://doi.org/10.1128/JCM.02238-20.

Chandler, M., de la Cruz, F., Dyda, F., Hickman, A.B., Moncalian, G. and Ton-Hoang, B. (2013) 'Breaking and joining single-stranded DNA: the HUH endonuclease superfamily', *Nature reviews. Microbiology*, 11(8), pp. 525–538. Available at: https://doi.org/10.1038/nrmicro3067.

Chandler, M. and Siguier, P. (2013) 'Insertion Sequences', in *Brenner's Encyclopedia of Genetics: Second Edition*. Elsevier Inc., pp. 86–94. Available at: https://doi.org/10.1016/B978-0-12-374984-0.00799-3.

Chapman, J.S. (2003) 'Disinfectant resistance mechanisms, cross-resistance, and co-resistance', *International Biodeterioration & Biodegradation*, 51(4), pp. 271–276. Available at: https://doi.org/10.1016/S0964-8305(03)00044-1.

Chau, K.K., Barker, L., Budgell, E.P., Vihta, K.D., Sims, N., Kasprzyk-Hordern, B., Harriss, E., Crook, D.W., Read, D.S., Walker, A.S. and Stoesser, N. (2022) 'Systematic review of wastewater surveillance of antimicrobial resistance in human populations', *Environment International*, 162, p. 107171. Available at: https://doi.org/10.1016/j.envint.2022.107171.

Chau, K.K., Goodall, T., Bowes, M., Easterbrook, K., Brett, H., Hughes, J., Crook, D.W., Read, D.S., Walker, A.S. and Stoesser, N. (2023) 'High-resolution characterization of short-term temporal variability in the taxonomic and resistome composition of wastewater influent', *Microbial Genomics*, 9(5), p. mgen000983. Available at: https://doi.org/10.1099/mgen.0.000983.

Chen, J., Quiles-Puchalt, N., Chiang, Y.N., Bacigalupe, R., Fillol-Salom, A., Chee, M.S.J., Fitzgerald, J.R. and Penadés, J.R. (2018) 'Genome hypermobility by lateral transduction', *Science (New York, N.Y.)*, 362(6411), pp. 207–212. Available at: https://doi.org/10.1126/science.aat5867.

Chen, L., Mathema, B., Chavda, K.D., DeLeo, F.R., Bonomo, R.A. and Kreiswirth, B.N. (2014) 'Carbapenemase-producing Klebsiella pneumoniae: Molecular and genetic decoding', *Trends in Microbiology*, 22(12), pp. 686–696. Available at: https://doi.org/10.1016/j.tim.2014.09.003.

Chiang, Y.N., Penadés, J.R. and Chen, J. (2019) 'Genetic transduction by phages and chromosomal islands: The new and noncanonical', *PLoS Pathogens*, 15(8), p. e1007878. Available at: https://doi.org/10.1371/journal.ppat.1007878.

Choi, P.M., Tscharke, B.J., Donner, E., O'Brien, J.W., Grant, S.C., Kaserzon, S.L., Mackie, R., O'Malley, E., Crosbie, N.D., Thomas, K.V. and Mueller, J.F. (2018) 'Wastewater-based epidemiology biomarkers: Past, present and future', *TrAC Trends in Analytical Chemistry*, 105, pp. 453–469. Available at: https://doi.org/10.1016/j.trac.2018.06.004.

Chopra, I. and Roberts, M. (2001) 'Tetracycline antibiotics: mode of action, applications, molecular biology, and epidemiology of bacterial resistance', *Microbiology and Molecular Biology Reviews*, 65(2), pp. 232-60. Available at: https://doi.org/10.1128/MMBR.65.2.232-260.2001

Chudejova, K., Kraftova, L., Mattioni Marchetti, V., Hrabak, J., Papagiannitsis, C.C. and Bitar, I. (2021) 'Genetic Plurality of OXA/NDM-Encoding Features Characterized From Enterobacterales Recovered From Czech Hospitals', *Frontiers in Microbiology*, 12, p. 178. Available at: https://doi.org/10.3389/fmicb.2021.641415.

Ciofu, O., Moser, C., Jensen, P.Ø. and Høiby, N. (2022) 'Tolerance and resistance of microbial biofilms', *Nature Reviews Microbiology*, 20(10), pp. 621–635. Available at: https://doi.org/10.1038/s41579-022-00682-4.

Clardy, J., Fischbach, M. and Currie, C. (2009) 'The natural history of antibiotics', *Current biology : CB*, 19(11), pp. R437–R441. Available at: https://doi.org/10.1016/j.cub.2009.04.001.

Clausen, P.T.L.C., Aarestrup, F.M. and Lund, O. (2018) 'Rapid and precise alignment of raw reads against redundant databases with KMA', *BMC Bioinformatics*, 19(1), pp. 1–8. Available at: https://doi.org/10.1186/s12859-018-2336-6.

CLSI (2012) *Performance Standards for Antimicrobial Disk Susceptibility Tests; Approved Standard. M02-A11.* Sixth Edition. Clinical and Laboratory Standards Institute.

CLSI (2016) *Methods for Antimicrobial Dilution and Disk Susceptibility Testing of Infrequently Isolated or Fastidious Bacteria. M45*. Third Edition. Clinical and Laboratory Standards Institute.

CLSI (2019) *Performance standards for antimicrobial susceptibility testing. M100.* 29th Edition. Clinical and Laboratory Standards Institute.

Codjoe, F.S. and Donkor, E.S. (2017) 'Carbapenem Resistance: A Review.', *Medical sciences (Basel, Switzerland)*, 6(1). Available at: https://doi.org/10.3390/medsci6010001.

Colomer-Lluch, M., Jofre, J. and Muniesa, M. (2011) 'Antibiotic Resistance Genes in the Bacteriophage DNA Fraction of Environmental Samples', *PLoS ONE*, 6(3), p. e17549. Available at: https://doi.org/10.1371/journal.pone.0017549.

Colomer-Lluch, M., Jofre, J. and Muniesa, M. (2014) 'Quinolone resistance genes (qnrA and qnrS) in bacteriophage particles from wastewater samples and the effect of inducing agents on packaged antibiotic resistance genes', *Journal of Antimicrobial Chemotherapy*, 69(5), pp. 1265–1274. Available at: https://doi.org/10.1093/jac/dkt528.

Connell, S.R., Tracz, D.M., Nierhaus, K.H. and Taylor, D.E. (2003) 'Ribosomal protection proteins and their mechanism of tetracycline resistance', *Antimicrobial Agents and Chemotherapy*, 47(12), pp. 3675–3681. Available at: https://doi.org/10.1128/AAC.47.12.3675-3681.2003.

Coque, T.M., Novais, Â., Carattoli, A., Poirel, L., Pitout, J., Peixe, L., Baquero, F., Cantón, R. and Nordmann, P. (2008) 'Dissemination of Clonally Related Escherichia coli Strains Expressing Extended-Spectrum β-Lactamase CTX-M-15', *Emerging Infectious Diseases*, 14(2), p. 195. Available at: https://doi.org/10.3201/EID1402.070350.

Cornaglia, G., Giamarellou, H. and Rossolini, G.M. (2011) 'Metallo-β-lactamases: a last frontier for β-lactams?', *The Lancet. Infectious Diseases*, 11(5), pp. 381–393. Available at: https://doi.org/10.1016/S1473-3099(11)70056-1.

Cornaglia, G., Riccio, M., Mazzariol, A., Lauretti, L., Fontana, R. and Rossolini, G. (1999) 'Appearance of IMP-1 metallo-β-lactamase in Europe', *The Lancet*, 353(9156), pp. 899–900. Available at: https://doi.org/10.1016/S0140-6736(98)05954-6.

Correia, S., Poeta, P., Hébraud, M., Capelo, J.L. and Igrejas, G. (2017) 'Mechanisms of quinolone action and resistance: where do we stand?', *Journal of Medical Microbiology*, 66(5), pp. 551–559. Available at: https://doi.org/10.1099/jmm.0.000475.

Cosentino, S., Voldby Larsen, M., Møller Aarestrup, F. and Lund, O. (2013) 'PathogenFinder - Distinguishing Friend from Foe Using Bacterial Whole Genome Sequence Data', *PLoS ONE*, 8(10), p. 77302. Available at: https://doi.org/10.1371/journal.pone.0077302.

Cox, G. and Wright, G.D. (2013) 'Intrinsic antibiotic resistance: Mechanisms, origins, challenges and solutions', *International Journal of Medical Microbiology*, 303(6), pp. 287–292. Available at: https://doi.org/10.1016/j.ijmm.2013.02.009.

Dadashi, M., Yaslianifard, S., Hajikhani, B., Kabir, K., Owlia, P., Goudarzi, M., Hakemivala, M. and Darban-Sarokhalil, D. (2019) 'Frequency distribution, genotypes and prevalent sequence types of New Delhi metallo-β-lactamase-producing Escherichia coli among clinical isolates around the world: A review', *Journal of Global Antimicrobial Resistance*, 19, pp. 284–293. Available at: https://doi.org/10.1016/J.JGAR.2019.06.008.

Dam, S., Pagès, J.M. and Masi, M. (2017) 'Dual Regulation of the Small RNA MicC and the Quiescent Porin OmpN in Response to Antibiotic Stress in Escherichia coli', *Antibiotics (Basel)*, 6(4): p. 33. Available at: https://doi.org/10.3390/antibiotics6040033.

Dang, Y., Jia, G., Choi, J., Ma, H., Anaya, E., Ye, C., Shankar, P. and Wu, H. (2015) 'Optimizing sgRNA structure to improve CRISPR-Cas9 knockout efficiency', *Genome Biology*, 16(1), pp. 1–10. Available at: https://doi.org/10.1186/S13059-015-0846-3/FIGURES/7.

Darby, E.M., Trampari, E., Siasat, P., Solsona Gaya, M., Alav, I., Webber, M.A. and Blair, J. M.A. (2023) 'Molecular mechanisms of antibiotic resistance revisited', *Nature Reviews. Microbiology,* 21, pp. 280–295. Available at: https://doi.org/10.1038/s41579-022-00820-y

Davidson, A.R. (2018) 'A common trick for transferring bacterial DNA', *Science*, 362(6411), pp. 152–153. Available at: https://doi.org/10.1126/science.aav1723.

Davies, R.B. (1975) 'Comparison of beta-lactamase II from Bacillus cereus 569/H/9 with a beta-lactamase from Bacillus cereus 5/B/6.', *Biochemical Journal*, 145(2), pp. 409–411.

Davies, R.B., Abraham, E.P. and Melling, J. (1974) 'Separation, purification and properties of β-lactamase I and β-lactamase II from Bacillus cereus 569/H/9', *Biochemical Journal*, 143(1), pp. 115–127.

Day, M.J., Hopkins, K.L., Wareham, D.W., Toleman, M.A., Elviss, N., Randall, L., Teale, C., Cleary, P., Wiuff, C., Doumith, M., Ellington, M.J., Woodford, N. and Livermore, D.M. (2019) 'Extended-spectrum β-lactamase-producing Escherichia coli in human-derived and foodchain-derived samples from England, Wales, and Scotland: an epidemiological surveillance and typing study', *The Lancet Infectious Diseases*, 19(12), pp. 1325–1335. Available at: https://doi.org/10.1016/S1473-3099(19)30273-7.

D'Costa, V.M., King, C.E., Kalan, L., Morar, M., Sung, W.W.L., Schwarz, C., Froese, D., Zazula, G., Calmels, F., Debruyne, R., Golding, G.B., Poinar, H.N. and Wright, G.D. (2011) 'Antibiotic resistance is ancient', *Nature*, 477(7365), pp. 457–461. Available at: https://doi.org/10.1038/nature10388.

Delcour, A.H. (2009) 'Outer Membrane Permeability and Antibiotic Resistance', *Biochimica et biophysica acta*, 1794(5), pp. 808–816. Available at: https://doi.org/10.1016/j.bbapap.2008.11.005.

Deng, Y., Bao, X., Ji, L., Chen, L., Liu, J., Miao, J., Chen, D., Bian, H., Li, Y. and Yu, G. (2015) 'Resistance integrons: class 1, 2 and 3 integrons', *Annals of Clinical Microbiology and Antimicrobials*, 14(1), p. 45. Available at: https://doi.org/10.1186/S12941-015-0100-6.

Di Conza, J., Ayala, J.A., Power, P., Mollerach, M. and Gutkind, G. (2002) 'Novel class 1 integron (InS21) carrying blaCTX-M-2 in Salmonella enterica serovar infantis', *Antimicrobial Agents and Chemotherapy*, 46(7), pp. 2257–2261. Available at: https://doi.org/10.1128/AAC.46.7.2257-2261.2002.

Diaz, R., Rech, J. and Bouet, J.-Y. (2015) 'Imaging centromere-based incompatibilities: Insights into the mechanism of incompatibility mediated by low-copy number plasmids', *Plasmid*, 80, pp. 54–62. Available at: https://doi.org/10.1016/j.plasmid.2015.03.007.

Dinos, G.P. (2017) 'The macrolide antibiotic renaissance', *British Journal of Pharmacology*, 174(18), pp. 2967–2983. Available at: https://doi.org/10.1111/bph.13936.

Domingues, S., Harms, K., Fricke, W.F., Johnsen, P.J., da Silva, G.J. and Nielsen, K.M. (2012) 'Natural Transformation Facilitates Transfer of Transposons, Integrons and Gene Cassettes between Bacterial Species', *PLoS Pathogens*, 8(8), p. e1002837. Available at: https://doi.org/10.1371/journal.ppat.1002837.

Domingues, S., da Silva, G.J. and Nielsen, K.M. (2012) 'Integrons', *Mobile Genetic Elements*, 2(5), pp. 211–223. Available at: https://doi.org/10.4161/mge.22967.

Dookie, N., Rambaran, S., Padayatchi, N., Mahomed, S. and Naidoo, K. (2018) 'Evolution of drug resistance in Mycobacterium tuberculosis: a review on the molecular determinants of resistance and implications for personalized care', *Journal of Antimicrobial Chemotherapy*, 73(5), pp. 1138–1151. Available at: https://doi.org/10.1093/jac/dkx506.

Drawz, S.M. and Bonomo, R.A. (2010) 'Three Decades of Beta-Lactamase Inhibitors', *Clinical Microbiology Reviews*, 23(1), pp. 160–201. Available at: https://doi.org/10.1128/CMR.00037-09.

Ebomah, K.E. and Okoh, A.I. (2020) 'Detection of carbapenem-resistance genes in Klebsiella species recovered from selected environmental niches in the Eastern Cape Province, South Africa', *Antibiotics*, 9(7), pp. 1–12. Available at: https://doi.org/10.3390/antibiotics9070425.

ECDC (2023a) *European Antimicrobial Resistance Surveillance Network (EARS-Net)*. Available at: https://www.ecdc.europa.eu/en/about-us/networks/disease-networks-and-laboratory-networks/ears-net-data (Accessed: 23 December 2023).

ECDC (2023b) 'Increase in Escherichia coli isolates carrying blaNDM-5 in the European Union/European Economic Area, 2012–2022.'

Eden, P.A., Schmidt, T.M., Blakemore, R.P. and Pace, N.R. (1991) 'Phylogenetic analysis of Aquaspirillum magnetotacticum using polymerase chain reaction-amplified 16S rRNA-specific DNA', *International Journal of Systematic Bacteriology*, 41(2), pp. 324–325. Available at: https://doi.org/10.1099/00207713-41-2-324/CITE/REFWORKS.

Edgar, R.C. (2004) 'MUSCLE: multiple sequence alignment with high accuracy and high throughput', *Nucleic Acids Research*, 32(5), p. 1792. Available at: https://doi.org/10.1093/NAR/GKH340.

EUCAST (2019) *Breakpoint tables for interpretation of MICs and zone diameters.* Available at: http://www.eucast.org. (Accessed: 26 May 2019).

European Commission (2022) *Proposal for a revised Urban Wastewater Treatment Directive - European Commission*. Available at: https://environment.ec.europa.eu/publications/proposal-revised-urban-wastewater-treatment-directive_en (Accessed: 23 December 2023).

Evans, B.A. and Amyes, S.G.B. (2014) 'OXA β-Lactamases', *Clinical Microbiology Reviews*, 27(2), pp. 241–263. Available at: https://doi.org/10.1128/CMR.00117-13.

Fahrenfeld, N. and J. Bisceglia, K. (2016) 'Emerging investigators series: sewer surveillance for monitoring antibiotic use and prevalence of antibiotic resistance: urban sewer epidemiology', *Environmental Science: Water Research & Technology*, 2(5), pp. 788–799. Available at: https://doi.org/10.1039/C6EW00158K.

Findlay, J., Hopkins, K.L., Alvarez-Buylla, A., Meunier, D., Mustafa, N., Hill, R., Pike, R., McCrae, L.-X., Hawkey, P.M. and Woodford, N. (2017) 'Characterization of carbapenemase-producing Enterobacteriaceae in the West Midlands region of England: 2007–14 | Journal of Antimicrobial Chemotherapy | Oxford Academic', *Journal of Antimicrobial Chemotherapy*, 72(4), pp. 1054–1062.

Fitzpatrick, D. and Walsh, F. (2016) *Antibiotic resistance genes across a wide variety of metagenomes*. Available at: https://academic.oup.com/femsec/article/92/2/fiv168/2484737 (Accessed: 26 June 2020).

Flach, C.-F., Hutinel, M., Razavi, M., Åhrén, C. and Larsson, D.G.J. (2021) 'Monitoring of hospital sewage shows both promise and limitations as an early-warning system for carbapenemase-producing Enterobacterales in a low-prevalence setting', *Water Research*, 200, p. 117261. Available at: https://doi.org/10.1016/j.watres.2021.117261.

Fleming, A. (1929) 'On the Antibacterial Action of the Cultures of a Penicillium, with Special References to their use in the Isolation of B. influenzae', *British Journal of Experimental Pathology*, 10(3), pp. 226–236.

Flerlage, T., Brazelton de Cardenas, J.N., Garner, C.D., Hasan, N.A., Karathia, H., Qudeimat, A., Maron, G. and Hayden, R. (2020) 'Multiple NDM-5-Expressing Escherichia Coli Isolates From an Immunocompromised Pediatric Host', *Open Forum Infectious Diseases*, 7(2). Available at: https://doi.org/10.1093/OFID/OFAA018.

Forghani, F., Li, S., Zhang, S., Mann, D.A., Deng, X., den Bakker, H.C. and Diez-Gonzalez, F. (2020) 'Detection and Serotyping of Salmonella and Escherichia coli in Wheat Flour by a Quasimetagenomic Approach Assisted by Magnetic Capture, Multiple Displacement Amplification and Real-Time Sequencing', *Applied and Environmental Microbiology*, 86(13). Available at: https://doi.org/10.1128/aem.00097-20.

Freitag, C., Michael, G., Kadlec, K., Hassel, M. and S, S. (2017) 'Detection of plasmid-borne extended-spectrum β-lactamase (ESBL) genes in Escherichia coli isolates from bovine mastitis', *Veterinary microbiology*, 200, pp. 151–156. Available at: https://doi.org/10.1016/J.VETMIC.2016.08.010.

Gabashvili, E., Osepashvili, M., Koulouris, S., Ujmajuridze, L., Tskhitishvili, Z. and Kotetishvili, M. (2020) 'Phage Transduction is Involved in the Intergeneric Spread of Antibiotic Resistance-Associated blaCTX-M, mel, and tetM Loci in Natural Populations of Some Human and Animal Bacterial Pathogens', *Current Microbiology*, 77(2), pp. 185-193. Available at: https://doi.org/10.1007/s00284-019-01817-2.

Galata, V., Fehlmann, T., Backes, C. and Keller, A. (2019) 'PLSDB: A resource of complete bacterial plasmids', *Nucleic Acids Research*, 47(D1), pp. D195–D202. Available at: https://doi.org/10.1093/nar/gky1050.

Garneau-Tsodikova, S. and Labby, K.J. (2016) 'Mechanisms of Resistance to Aminoglycoside Antibiotics: Overview and Perspectives', *MedChemComm*, 7(1), pp. 11–27. Available at: https://doi.org/10.1039/C5MD00344J.

Gay, P., Le Coq, D., Steinmetz, M., Berkelman, T. and Kado, C.I. (1985) 'Positive selection procedure for entrapment of insertion sequence elements in gram-negative bacteria.', *Journal of Bacteriology*, 164(2), pp. 918–921.

Gaynes, R. (2017) 'The Discovery of Penicillin—New Insights After More Than 75 Years of Clinical Use', *Emerging Infectious Diseases*, 23(5), pp. 849–853. Available at: https://doi.org/10.3201/eid2305.161556.

George, M.P., Masur, H., Norris, K.A., Palmer, S.M., Clancy, C.J. and McDyer, J.F. (2014) 'Infections in the immunosuppressed host.', *Annals of the American Thoracic Society*, 11 Suppl 4(Suppl 4), pp. S211-20. Available at: https://doi.org/10.1513/AnnalsATS.201401-038PL.

Getino, M. and de la Cruz, F. (2018) 'Natural and Artificial Strategies To Control the Conjugative Transmission of Plasmids', *Microbiology Spectrum*, 6(1). Available at: https://doi.org/10.1128/microbiolspec.mtbp-0015-2016.

Gholizadeh, A., Khiadani, M., Foroughi, M., Alizade Siuki, H. and Mehrfar, H. (2023) 'Wastewater treatment plants: The missing link in global One-Health surveillance and management of antibiotic resistance', *Journal of Infection and Public Health*, 16, pp. 217–224. Available at: https://doi.org/10.1016/j.jiph.2023.09.017.

Gibbon, M.J., Couto, N., David, S., Barden, R., Standerwick, R., Jagadeesan, K., Birkwood, H., Dulyayangkul, P., Avison, M.B., Kannan, A., Kibbey, D., Craft, T., Habib, S., Thorpe, H.A., Corander, J., Kasprzyk-Hordern, B. and Feil, E.J. (2021) 'A high prevalence of bla OXA-48 in Klebsiella (Raoultella) ornithinolytica and related species in hospital wastewater in South West England', *Microbial Genomics*, 7(3), pp. 1848–55. Available at: https://doi.org/10.1099/MGEN.0.000509.

Gibson, D.G., Young, L., Chuang, R.-Y., Venter, J.C., Hutchison, C.A. and Smith, H.O. (2009) 'Enzymatic assembly of DNA molecules up to several hundred kilobases', *Nature Methods*, 6(5), pp. 343–345. Available at: https://doi.org/10.1038/nmeth.1318.

Gillings, M.R., Gaze, W.H., Pruden, A., Smalla, K., Tiedje, J.M. and Zhu, Y.-G. (2015) 'Using the class 1 integron-integrase gene as a proxy for anthropogenic pollution', *The ISME Journal*, 9(6), pp. 1269–1279. Available at: https://doi.org/10.1038/ismej.2014.226.

Gleckman, R., Blagg, N. and Joubert, D.W. (1981) 'Trimethoprim: mechanisms of action, antimicrobial activity, bacterial resistance, pharmacokinetics, adverse reactions, and therapeutic indications', *Pharmacotherapy*, 1(1), pp. 14–20. Available at: https://doi.org/10.1002/j.1875-9114.1981.tb03548.x.

Götz, A., Pukall, R., Smit, E., Tietze, E., Prager, R., Tschäpe, H., Van Elsas, J.D. and Smalla, K. (1996) 'Detection and characterization of broad-host-range plasmids in environmental bacteria by PCR', *Applied and environmental microbiology*, 62(7), pp. 2621–2628. Available at: https://doi.org/10.1128/AEM.62.7.2621-2628.1996.

Gould, K. (2016) 'Antibiotics: from prehistory to the present day', *Journal of Antimicrobial Chemotherapy*, 71(3), pp. 572–575. Available at: https://doi.org/10.1093/jac/dkv484.

Gouliouris, T., Raven, K.E., Moradigaravand, D., Ludden, C., Coll, F., Blane, B., Naydenova, P., Horner, C., Brown, N.M., Corander, J., Limmathurotsakul, D., Parkhill, J. and Peacock, S.J. (2019) 'Detection of vancomycin-resistant Enterococcus faecium hospital-adapted lineages in municipal wastewater treatment plants indicates widespread distribution and release into the environment', *Genome Research*, 29(4), pp. 626–634. Available at: https://doi.org/10.1101/gr.232629.117.

Grabow, W.O. and Prozesky, O.W. (1973) 'Drug resistance of coliform bacteria in hospital and city sewage.', *Antimicrobial agents and chemotherapy*, 3(2), pp. 175–80. Available at: https://doi.org/10.1128/aac.3.2.175.

Graf, F.E., Goodman, R.N., Gallichan, S., Forrest, S., Picton-Barlow, E., Fraser, A.J., Phan, M.D., Mphasa, M., Hubbard, A.T.M., Musicha, P., Schembri, M.A., Roberts, A.P., Edwards, T., Lewis, J.M. and Feasey, N.A. (2024) 'Molecular mechanisms of re-emerging chloramphenicol susceptibility in extended-

spectrum beta-lactamase-producing Enterobacterales', *Nature Communications*, 15(1): 9019. Available at: https://doi.org/10.1038/s41467-024-53391-2.

Grossman, T.H. (2016) 'Tetracycline Antibiotics and Resistance', *Cold Spring Harbor Perspectives in Medicine*, 6(4), p. a025387. Available at: https://doi.org/10.1101/cshperspect.a025387.

Gurevich, A., Saveliev, V., Vyahhi, N. and Tesler, G. (2013) 'QUAST: quality assessment tool for genome assemblies', *Bioinformatics (Oxford, England)*, 29(8), pp. 1072–1075. Available at: https://doi.org/10.1093/BIOINFORMATICS/BTT086.

Gweon, H. Soon, Shaw, Liam P., Swann, Jeremy, De Maio, Nicola, AbuOun, M., Niehus, R., Hubbard, Alasdair T. M., Bowes, Mike J., Bailey, Mark J., Peto, Tim E. A., Hoosdally, S.J., Walker, A. Sarah, Sebra, R.P., Crook, Derrick W., Anjum, M.F., Read, Daniel S., Stoesser, N., Abuoun, M., Anjum, M., Bailey, M. J., Barker, L., Brett, H., Bowes, M. J., Chau, K., Crook, D. W., De Maio, N., Gilson, D., Gweon, H. S., Hubbard, A. T. M., Hoosdally, S., Kavanagh, J., Jones, H., Peto, T. E. A., Read, D. S., Sebra, R., Shaw, L. P., Sheppard, A.E., Smith, R., Stubberfield, E., Swann, J., Walker, A. S., Woodford, N., and on behalf of the REHAB consortium (2019) 'The impact of sequencing depth on the inferred taxonomic composition and AMR gene content of metagenomic samples', *Environmental Microbiome*, 14(1), p. 7. Available at: https://doi.org/10.1186/s40793-019-0347-1.

Haenni, M. and Moreillon (2006) 'Effects of Amino Acid Alterations in Penicillin-Binding Proteins (PBPs) 1a, 2b, and 2x on PBP Affinities of Penicillin, Ampicillin, Amoxicillin, Cefditoren, Cefuroxime, Cefprozil, and Cefaclor in 18 Clinical Isolates of Penicillin-Susceptible, -Intermediate, and -Resistant Pneumococci - PMC'. Available at: https://www.ncbi.nlm.nih.gov/pmc/articles/PMC127189/ (Accessed: 19 November 2023).

Halat, D.H. and Moubareck, C.A. (2020) 'The Current Burden of Carbapenemases: Review of Significant Properties and Dissemination among Gram-Negative Bacteria', *Antibiotics*, 9(4), p. 186. Available at: https://doi.org/10.3390/antibiotics9040186.

Halawa, E.M., Fadel, M., Al-Rabia, M.W., Behairy, A., Nouh, N.A., Abdo, M., Olga, R., Fericean, L., Atwa, A.M., El-Nablaway, M. and Abdeen, A. (2024) 'Antibiotic action and resistance: updated review of mechanisms, spread, influencing factors, and alternative approaches for combating resistance', *Frontiers in Pharmacology*, 14:1305294. Available at: https://doi.org/10.3389/fphar.2023.1305294.

Hale, L., Lazos, O., Haines, A.S. and Thomas, C.M. (2010) 'An efficient stress-free strategy to displace stable bacterial plasmids', *BioTechniques*, 48(3), pp. 223–228. Available at: https://doi.org/10.2144/000113366.

Hall, B. and Barlow, M. (2005) 'Revised Ambler classification of β-lactamases', *Journal of Antimicrobial Chemotherapy* [Preprint]. Available at: https://academic.oup.com/jac/article/55/6/1050/725573 (Accessed: 24 June 2020).

Hall, B.G. and Barlow, M. (2004) 'Evolution of the serine β-lactamases: past, present and future', *Drug Resistance Updates*, 7(2), pp. 111–123. Available at: https://doi.org/10.1016/J.DRUP.2004.02.003.

Hall, J.P.J., Wright, R.C.T., Guymer, D., Harrison, E. and Brockhurst, M.A. (2020) 'Extremely fast amelioration of plasmid fitness costs by multiple functionally diverse pathways', *Microbiology*, 166(1), pp. 56–62. Available at: https://doi.org/10.1099/mic.0.000862.

Hall, J.P.J., Wright, R.C.T., Harrison, E., Muddiman, K.J., Wood, A.J., Paterson, S. and Brockhurst, M.A. (2021) 'Plasmid fitness costs are caused by specific genetic conflicts enabling resolution by compensatory mutation', *PLoS Biology*, 19(10), p. e3001225. Available at: https://doi.org/10.1371/journal.pbio.3001225.

Hall, R.M. (2022) 'Comment on "the IS6 family, a clinically important group of insertion sequences including IS26" by Varani and co-authors', *Mobile DNA*, 13(1), p. 1. Available at: https://doi.org/10.1186/s13100-021-00257-9.

Hammerum, A.M., Porsbo, L.J., Hansen, F., Roer, L., Kaya, H., Henius, A., Lauenborg Møller, K., Justesen, U.S., Søes, L., Røder, B.L., Thomsen, P.K., Wang, W., Søndergaard, T.S., Holzknecht, B.J., Østergaard, C., Kjerulf, A., Kristensen, B. and Hasman, H. (2020) 'Surveillance of OXA-244-producing Escherichia coli and epidemiologic investigation of cases, Denmark, January 2016 to August 2019', *Euro surveillance : bulletin Europeen sur les maladies transmissibles = European communicable disease bulletin*, 25(18), pp. 1–9. Available at: https://doi.org/10.2807/1560-7917.ES.2020.25.18.1900742.

Hancock, R.E. and Bellido, F. (1996) 'Antibacterial in vitro activity of fourth generation cephalosporins', *Journal of Chemotherapy (Florence, Italy)*, 8 Suppl 2, pp. 31–36.

Haniford, D.B. and Ellis, M.J. (2015) 'Transposons Tn10 and Tn5', *Microbiology spectrum*, 3(1). Available at: https://doi.org/10.1128/MICROBIOLSPEC.MDNA3-0002-2014.

Hansen, G.T. (2021) 'Continuous Evolution: Perspective on the Epidemiology of Carbapenemase Resistance Among Enterobacterales and Other Gram-Negative Bacteria', *Infectious Diseases and Therapy*, 10(1), pp. 75–92. Available at: https://doi.org/10.1007/s40121-020-00395-2.

Hansen, K.H., Andreasen, M.R., Pedersen, M.S., Westh, H., Jelsbak, L. and Schønning, K. (2019) 'Resistance to piperacillin/tazobactam in Escherichia coli resulting from extensive IS26-associated gene amplification of blaTEM-1',

Journal of Antimicrobial Chemotherapy, 74(11), pp. 3179–3183. Available at: https://doi.org/10.1093/jac/dkz349.

Harmer, C.J. and Hall, R.M. (2016) 'IS 26 -Mediated Formation of Transposons Carrying Antibiotic Resistance Genes', *mSphere*, 1(2). Available at: https://doi.org/10.1128/MSPHERE.00038-16.

Harmer, C.J. and Hall, R.M. (2019) 'An analysis of the IS6/IS26 family of insertion sequences: is it a single family?', *Microbial Genomics*, 5(9). Available at: https://doi.org/10.1099/MGEN.0.000291.

Harmer, C.J. and Hall, R.M. (2020) 'IS26 Family Members IS257 and IS1216 Also Form Cointegrates by Copy-In and Targeted Conservative Routes', *mSphere*, 5(1), p. 10.1128/msphere.00811-19. Available at: https://doi.org/10.1128/msphere.00811-19.

Harmer, C.J., Moran, R.A. and Hall, R.M. (2014) 'Movement of IS26-Associated Antibiotic Resistance Genes Occurs via a Translocatable Unit That Includes a Single IS26 and Preferentially Inserts Adjacent to Another IS26', *mBio*, 5(5). Available at: https://doi.org/10.1128/mBio.01801-14.

Harmer, C.J., Pong, C.H. and Hall, R.M. (2020) 'Structures bounded by directly-oriented members of the IS26 family are pseudo-compound transposons.', *Plasmid*, 111, p. 102530. Available at: https://doi.org/10.1016/J.PLASMID.2020.102530.

Hasman, H., Mevius, D., Veldman, K., Olesen, I. and Aarestrup, F.M. (2005) 'β-Lactamases among extended-spectrum β-lactamase (ESBL)-resistant Salmonella from poultry, poultry products and human patients in The Netherlands', *Journal of Antimicrobial Chemotherapy*, 56(1), pp. 115–121. Available at: https://doi.org/10.1093/JAC/DKI190.

Hawker, J.I., Smith, S., Smith, G.E., Morbey, R., Johnson, A.P., Fleming, D.M., Shallcross, L. and Hayward, A.C. (2014) 'Trends in antibiotic prescribing in primary care for clinical syndromes subject to national recommendations to reduce antibiotic resistance, UK 1995–2011: analysis of a large database of primary care consultations', *Journal of Antimicrobial Chemotherapy*, 69(12), pp. 3423–3430. Available at: https://doi.org/10.1093/jac/dku291.

He, S., Hickman, A.B., Varani, A.M., Siguier, P., Chandler, M., Dekker, J.P. and Dyda, F. (2015) 'Insertion Sequence IS26 Reorganizes Plasmids in Clinically Isolated Multidrug-Resistant Bacteria by Replicative Transposition', *mBio*, 6(3), pp. e00762-15. Available at: https://doi.org/10.1128/mBio.00762-15.

He, Y.Z., Kuang, X., Long, T.F., Li, G., Ren, H., He, B., Yan, J.R., Liao, X.P., Liu, Y.H., Chen, L. and Sun, J. (2021) 'Re-engineering a mobile-CRISPR/Cas9 system for antimicrobial resistance gene curing and immunization in Escherichia coli', *Journal of Antimicrobial Chemotherapy*, 77(1), pp. 74–82. Available at: https://doi.org/10.1093/JAC/DKAB368.

Hendriksen, R.S., Munk, P., Njage, P., van Bunnik, B., McNally, L., Lukjancenko, O., Röder, T., Nieuwenhuijse, D., Pedersen, S.K., Kjeldgaard, J., Kaas, R.S., Clausen, P.T.L.C., Vogt, J.K., Leekitcharoenphon, P., van de Schans, M.G.M., Zuidema, T., de Roda Husman, A.M., Rasmussen, S., Petersen, B., Global Sewage Surveillance project consortium, T.G.S.S. project, Amid, C., Cochrane, G., Sicheritz-Ponten, T., Schmitt, H., Alvarez, J.R.M., Aidara-Kane, A., Pamp, S.J., Lund, O., Hald, T., Woolhouse, M., Koopmans, M.P., Vigre, H., Petersen, T.N. and Aarestrup, F.M. (2019) 'Global monitoring of antimicrobial resistance based on metagenomics analyses of urban sewage.', *Nature communications*, 10(1), p. 1124. Available at: https://doi.org/10.1038/s41467-019-08853-3.

Hernández-Allés, S., Benedí, V.J., Martínez-Martínez, L., Pascual, Á., Aguilar, A., Tomás, J.M. and Albertí, S. (1999) 'Development of Resistance during Antimicrobial Therapy Caused by Insertion Sequence Interruption of Porin Genes', *Antimicrobial Agents and Chemotherapy*, 43(4), pp. 937–939.

Hickman, A.B. and Dyda, F. (2015) 'Mechanisms of DNA Transposition', *Microbiology spectrum*, 3(2). Available at: https://doi.org/10.1128/microbiolspec.MDNA3-0034-2014.

Hiller, C.X., Hübner, U., Fajnorova, S., Schwartz, T. and Drewes, J.E. (2019) 'Antibiotic microbial resistance (AMR) removal efficiencies by conventional and advanced wastewater treatment processes: A review', *Science of the Total Environment*, 685, pp. 596–608. Available at: https://doi.org/10.1016/j.scitotenv.2019.05.315.

Ho, S.E., Subramaniam, G., Palasubramaniam, S. and Navaratnam, P. (2002) 'Carbapenem-resistant Pseudomonas aeruginosa in malaysia producing IMP-7 beta-lactamase', *Antimicrobial Agents and Chemotherapy*, 46(10), pp. 3286–3287. Available at: https://doi.org/10.1128/AAC.46.10.3286-3287.2002.

Hobman, J.L. (2017) 'Antimicrobial metal ion resistance and its impact on co-selection of antibiotic resistance', *Culture*, 37(1).

Hobman, J.L. and Crossman, L.C. (2015) 'Bacterial antimicrobial metal ion resistance', *Journal of Medical Microbiology*, 64(Pt 5), pp. 471–497. Available at: https://doi.org/10.1099/jmm.0.023036-0.

Hoelle, J., Johnson, J.R., Johnston, B.D., Kinkle, B., Boczek, L., Ryu, H. and Hayes, S. (2019) 'Survey of US wastewater for carbapenem-resistant Enterobacteriaceae', *Journal of Water and Health*, 17(2), pp. 219–226. Available at: https://doi.org/10.2166/wh.2019.165.

Honoré, N., Nicolas, M.H. and Cole, S.T. (1986) 'Inducible cephalosporinase production in clinical isolates of Enterobacter cloacae is controlled by a regulatory gene that has been deleted from Escherichia coli', *The EMBO journal*, 5(13), pp. 3709–3714. Available at: https://doi.org/10.1002/j.1460-2075.1986.tb04704.x.

Hooper, D.C. (2000) 'Mechanisms of Action and Resistance of Older and Newer Fluoroquinolones', *Clinical Infectious Diseases*, 31(Supplement_2), pp. S24–S28. Available at: https://doi.org/10.1086/314056.

Hooper, D.C. and Jacoby, G.A. (2016) 'Topoisomerase Inhibitors: Fluoroquinolone Mechanisms of Action and Resistance', *Cold Spring Harbor Perspectives in Medicine*, 6(9), a025320. Available at: https://doi.org/10.1101/cshperspect.a025320

Hopkins, K.L., Ellaby, N., Ellington, M.J., Doumith, M., Mustafa, N., Meunier, D. and Woodford, N. (2022) 'Diversity of carbapenemase-producing Enterobacterales in England as revealed by whole-genome sequencing of isolates referred to a national reference laboratory over a 30-month period', *Journal of Medical Microbiology*, 71(5), p. 001518. Available at: https://doi.org/10.1099/jmm.0.001518.

Hornsey, M., Phee, L. and Wareham, D.W. (2011) 'A novel variant, NDM-5, of the New Delhi metallo-β-lactamase in a multidrug-resistant Escherichia coli ST648 isolate recovered from a patient in the United Kingdom', *Antimicrobial Agents and Chemotherapy*, 55(12), pp. 5952–5954. Available at: https://doi.org/10.1128/AAC.05108-11.

Hossain, M., Tabassum, T., Rahman, A., Hossain, A., Afroze, T., Momen, A.M.I., Sadique, A., Sarker, M., Shams, F., Ishtiaque, A., Khaleque, A., Alam, M., Huq, A., Ahsan, G.U. and Colwell, R.R. (2020) 'Genotype–phenotype correlation of β-lactamase-producing uropathogenic Escherichia coli (UPEC) strains from Bangladesh', *Scientific Reports*, 10(1). Available at: https://doi.org/10.1038/S41598-020-71213-5.

Hu, B., Khara, P. and Christie, P.J. (2019) 'Structural bases for F plasmid conjugation and F pilus biogenesis in Escherichia coli', *Proceedings of the National Academy of Sciences*, 116(28), pp. 14222–14227. Available at: https://doi.org/10.1073/pnas.1904428116.

Hua, X., Zhang, L., Moran, R.A., Xu, Q., Sun, L., van Schaik, W. and Yu, Y. (2020) 'Cointegration as a mechanism for the evolution of a KPC-producing multidrug resistance plasmid in Proteus mirabilis', *Emerging Microbes & Infections*, 9(1), pp. 1206–1218. Available at: https://doi.org/10.1080/22221751.2020.1773322.

Hubbard, A.T.M., Mason, J., Roberts, P., Parry, C.M., Corless, C., van Aartsen, J., Howard, A., Bulgasim, I., Fraser, A.J., Adams, E.R., Roberts, A.P. and Edwards, T. (2020) 'Piperacillin/tazobactam resistance in a clinical isolate of Escherichia coli due to IS26-mediated amplification of blaTEM-1B', *Nature Communications*, 11(1). Available at: https://doi.org/10.1038/S41467-020-18668-2.

Hultman, J., Tamminen, M., Pärnänen, K., Cairns, J., Karkman, A. and Virta, M. (2018) 'Host range of antibiotic resistance genes in wastewater treatment plant

influent and effluent', *FEMS Microbiology Ecology*, 94(4). Available at: https://doi.org/10.1093/FEMSEC/FIY038.

Hyeon, J.Y., Li, S., Mann, D.A., Zhang, S., Li, Z., Chen, Y. and Deng, X. (2018) 'Quasimetagenomics-based and real-time-sequencing-aided detection and subtyping of Salmonella enterica from food samples', *Applied and Environmental Microbiology*, 84(4). Available at: https://doi.org/10.1128/AEM.02340-17.

Hyeon, J.Y., Mann, D.A., Townsend, A.M. and Deng, X. (2018) 'Quasi-metagenomic Analysis of Salmonella from Food and Environmental Samples', *Journal of visualized experiments : JoVE* [Preprint], (140). Available at: https://doi.org/10.3791/58612.

Iaconis, J.P. and Sanders, C.C. (1990) 'Purification and characterization of inducible beta-lactamases in Aeromonas spp', *Antimicrobial Agents and Chemotherapy*, 34(1), pp. 44–51. Available at: https://doi.org/10.1128/AAC.34.1.44.

Ibrahim, D.R., Dodd, C.E.R., Stekel, D.J., Meshioye, R.T., Diggle, M., Lister, M. and Hobman, J.L. (2023) 'Multidrug-Resistant ESBL-Producing E. coli in Clinical Samples from the UK', *Antibiotics*, 12(1), p. 169. Available at: https://doi.org/10.3390/antibiotics12010169.

Iida, S., Meyer, J., Linder, P., Goto, N., Nakaya, R., Reif, H.J. and Arber, W. (1982) 'The kanamycin resistance transposon Tn2680 derived from the R plasmid Rts1 and carried by phage P1Km has flanking 0.8-kb-long direct repeats', *Plasmid*, 8(2), pp. 187–198. Available at: https://doi.org/10.1016/0147-619x(82)90056-7.

Iida, S., Mollet, B., Meyer, J. and Arber, W. (1984) 'Functional characterization of the prokaryotic mobile genetic element IS26', *Molecular & general genetics: MGG*, 198(2), pp. 84–89. Available at: https://doi.org/10.1007/BF00328705.

Illumina (2023) *Introduction to Microbial Whole-Genome Sequencing*. Available at: https://emea.illumina.com/areas-of-interest/microbiology/microbial-sequencing-methods/microbial-whole-genome-sequencing.html#:~:text=Microbial%20whole%2Dgenome%20sequencing%20is,comparing%20genomes%20across%20multiple%20samples. (Accessed: 26 December 2023).

Ilyina, T.S. (2012) 'Mobile ISCR elements: Structure, functions, and role in emergence, increase, and spread of blocks of bacterial multiple antibiotic resistance genes', *Molecular Genetics, Microbiology and Virology 2012 27:4*, 27(4), pp. 135–146. Available at: https://doi.org/10.3103/S0891416812040040.

Integrated DNA Technologies (no date) *Custom Alt-R™ CRISPR-Cas9 guide RNA*. Available at:

https://eu.idtdna.com/site/order/designtool/index/CRISPR_CUSTOM (Accessed: 24 April 2023).

Iwata, S., Tada, T., Hishinuma, T., Tohya, M., Oshiro, S., Kuwahara-Arai, K., Ogawa, M., Shimojima, M. and Kirikae, T. (2020) 'Emergence of Carbapenem-Resistant Providencia rettgeri and Providencia stuartii Producing IMP-Type Metallo-β-Lactamase in Japan', *Antimicrobial Agents and Chemotherapy*, 64(11), pp. e00382-20. Available at: https://doi.org/10.1128/AAC.00382-20.

Jain, A., Hopkins, K.L., Turton, J., Doumith, M., Hill, R., Loy, R., Meunier, D., Pike, R., Livermore, D.M. and Woodford, N. (2014) 'NDM carbapenemases in the United Kingdom: an analysis of the first 250 cases | Journal of Antimicrobial Chemotherapy | Oxford Academic', *Journal of Antimicrobial Chemotherapy*, 69(7), pp. 1777–1784.

Jana, S. and Deb, J.K. (2006) 'Molecular understanding of aminoglycoside action and resistance', *Applied Microbiology and Biotechnology*, 70, pp. 140–150. https://doi.org/10.1007/s00253-005-0279-0

Janda, J.M. and Abbott, S.L. (2010) 'The Genus Aeromonas: Taxonomy, Pathogenicity, and Infection', *Clinical Microbiology Reviews*, 23(1), p. 35. Available at: https://doi.org/10.1128/CMR.00039-09.

Jaureguy, F., Landraud, L., Passet, V., Diancourt, L., Frapy, E., Guigon, G., Carbonnelle, E., Lortholary, O., Clermont, O., Denamur, E., Picard, B., Nassif, X. and Brisse, S. (2008) 'Phylogenetic and genomic diversity of human bacteremic Escherichia coli strains', *BMC genomics*, 9. Available at: https://doi.org/10.1186/1471-2164-9-560.

Jellen-Ritter, A.S. and Kern, W.V. (2001) 'Enhanced expression of the multidrug efflux pumps AcrAB and AcrEF associated with insertion element transposition in Escherichia coli mutants Selected with a fluoroquinolone', *Antimicrobial Agents and Chemotherapy*, 45(5), pp. 1467–1472. Available at: https://doi.org/10.1128/AAC.45.5.1467-1472.2001.

Jeon, J.H., Lee, J.H., Lee, J.J., Park, K.S., Karim, A.M., Lee, C.R., Jeong, B.C. and Lee, S.H. (2015) 'Structural basis for carbapenem-hydrolyzing mechanisms of carbapenemases conferring antibiotic resistance', International Journal of Molecular Sciences, 16(5), pp. 9654-92. Available at: https://doi.org/10.3390/ijms16059654.

Joensen, K.G., Scheutz, F., Lund, O., Hasman, H., Kaas, R.S., Nielsen, E.M. and Aarestrup, F.M. (2014) 'Real-time whole-genome sequencing for routine typing, surveillance, and outbreak detection of verotoxigenic Escherichia coli', *Journal of Clinical Microbiology*, 52(5), pp. 1501–1510. Available at: https://doi.org/10.1128/JCM.03617-13.

Johnson, A.P. and Woodford, N. (2013) 'Global spread of antibiotic resistance: the example of New Delhi metallo-β-lactamase (NDM)-mediated carbapenem

resistance', *Journal of Medical Microbiology*, 62(4), pp. 499–513. Available at: https://doi.org/10.1099/jmm.0.052555-0.

Johnson, T.J., Bielak, E.M., Fortini, D., Hansen, L.H., Hasman, H., Debroy, C., Nolan, L.K. and Carattoli, A. (2012) 'Expansion of the IncX plasmid family for improved identification and typing of novel plasmids in drug-resistant Enterobacteriaceae', *Plasmid*, 68(1), pp. 43–50. Available at: https://doi.org/10.1016/J.PLASMID.2012.03.001.

Johnson, T.J., Danzeisen, J.L., Youmans, B., Case, K., Llop, K., Munoz-Aguayo, J., Flores-Figueroa, C., Aziz, M., Stoesser, N., Sokurenko, E., Price, L.B. and Johnson, J.R. (2016) 'Separate F-Type Plasmids Have Shaped the Evolution of the H30 Subclone of Escherichia coli Sequence Type 131', *mSphere*, 1(4), p. 10.1128/msphere.00121-16. Available at: https://doi.org/10.1128/msphere.00121-16.

Jolley, K.A., Bray, J.E. and Maiden, M.C.J. (2018) 'Open-access bacterial population genomics: BIGSdb software, the PubMLST.org website and their applications', *Wellcome open research*, 3. Available at: https://doi.org/10.12688/WELLCOMEOPENRES.14826.1.

Jones, L.S., Toleman, M.A., Weeks, J.L., Howe, R.A., Walsh, T.R. and Kumarasamy, K.K. (2014) 'Plasmid carriage of blaNDM-1 in clinical Acinetobacter baumannii isolates from India', *Antimicrobial Agents and Chemotherapy*, 58(7), pp. 4211-3. Available at: https://doi.org/10.1128/AAC.02500-14.

Joseph, S.M., Battaglia, T., Maritz, J.M., Carlton, J.M. and Blaser, M.J. (2019) 'Longitudinal Comparison of Bacterial Diversity and Antibiotic Resistance Genes in New York City Sewage.', *mSystems*, 4(4). Available at: https://doi.org/10.1128/mSystems.00327-19.

Jutkina, J., Marathe, N.P., Flach, C.F. and Larsson, D.G.J. (2018) 'Antibiotics and common antibacterial biocides stimulate horizontal transfer of resistance at low concentrations', *Science of the Total Environment*, 616–617, pp. 172–178. Available at: https://doi.org/10.1016/j.scitotenv.2017.10.312.

Jutkina, J., Rutgersson, C., Flach, C.F. and Joakim Larsson, D.G. (2016) 'An assay for determining minimal concentrations of antibiotics that drive horizontal transfer of resistance', *Science of the Total Environment*, 548–549, pp. 131–138. Available at: https://doi.org/10.1016/j.scitotenv.2016.01.044.

Kahan, F.M., Kropp, H., Sundelof, J.G. and Birnbaum, J. (1983) 'Thienamycin: development of imipenen-cilastatin.', *The Journal of antimicrobial chemotherapy*, 12 Suppl D, pp. 1–35. Available at: https://doi.org/10.1093/jac/12.suppl_d.1.

Kahan, J.S., Kahan, F.M., Goegelman, R., Currie, S.A., Jackson, M., Stapley, E.O., Miller, T.W., Miller, A.K., Hendlin, D., Mochales, S., Hernandez, S., Woodruff,

H.B. and Birnbaum, J. (1979) 'Thienamycin, a new beta-lactam antibiotic. I. Discovery, taxonomy, isolation and physical properties.', *The Journal of antibiotics*, 32(1), pp. 1–12.

Kapoor, G., Saigal, S. and Elongavan, A. (2017) 'Action and resistance mechanisms of antibiotics: A guide for clinicians', *Journal of Anaesthesiology, Clinical Pharmacology*, 33(3), pp. 300–305. Available at: https://doi.org/10.4103/joacp.JOACP_349_15.

Karkman, A., Do, T.T., Walsh, F. and Virta, M.P.J. (2018) 'Antibiotic-Resistance Genes in Waste Water', *Trends in Microbiology*, 26(3), pp. 220–228. Available at: https://doi.org/10.1016/j.tim.2017.09.005.

Karkman, A., Johnson, T.A., Lyra, C., Stedtfeld, R.D., Tamminen, M., Tiedje, J.M. and Virta, M. (2016) 'High-throughput quantification of antibiotic resistance genes from an urban wastewater treatment plant', *FEMS Microbiology Ecology*. Edited by E. Topp, 92(3), p. fiw014. Available at: https://doi.org/10.1093/femsec/fiw014.

Katz, L., Griswold, T., Morrison, S., Caravas, J., Zhang, S., Bakker, H., Deng, X. and Carleton, H. (2019) 'Mashtree: a rapid comparison of whole genome sequence files', *Journal of Open Source Software*, 4(44), p. 1762. Available at: https://doi.org/10.21105/joss.01762.

Kazama, H., Hamashima, H., Sasatsu, M. and Arai, T. (1998) 'Distribution of the antiseptic-resistance genes qacE and qacEΔ1 in Gram-negative bacteria', *FEMS Microbiology Letters*, 159(2), pp. 173–178. Available at: https://doi.org/10.1111/j.1574-6968.1998.tb12857.x.

Khan, A.U., Maryam, L. and Zarrilli, R. (2017) 'Structure, Genetics and Worldwide Spread of New Delhi Metallo-β-lactamase (NDM): a threat to public health', *BMC Microbiology*, 17(1), p. 101. Available at: https://doi.org/10.1186/s12866-017-1012-8.

Kim, J.S., Cho, D.H., Park, M., Chung, W.J., Shin, D., Ko, K.S. and Kweon, D.H. (2016) 'CRISPR/Cas9-Mediated Re-Sensitization of Antibiotic-Resistant Escherichia coli Harboring Extended-Spectrum β-Lactamases', *J. Microbiol. Biotechnol.*, 26(2), pp. 394–401. Available at: https://doi.org/10.4014/JMB.1508.08080.

Kitchel, B., Rasheed, J.K., Patel, J.B., Srinivasan, A., Navon-Venezia, S., Carmeli, Y., Brolund, A. and Giske, C.G. (2009) 'Molecular epidemiology of KPC-producing Klebsiella pneumoniae isolates in the United States: Clonal expansion of multilocus sequence type 258', *Antimicrobial Agents and Chemotherapy*, 53(8), pp. 3365–3370. Available at: https://doi.org/10.1128/AAC.00126-09.

Klein, E.Y., Van Boeckel, T.P., Martinez, E.M., Pant, S., Gandra, S., Levin, S.A., Goossens, H. and Laxminarayan, R. (2018) 'Global increase and geographic

convergence in antibiotic consumption between 2000 and 2015', *Proceedings of the National Academy of Sciences*, 115(15), pp. E3463–E3470. Available at: https://doi.org/10.1073/pnas.1717295115.

Kneis, D., Berendonk, T.U. and Heß, S. (2019) 'High prevalence of colistin resistance genes in German municipal wastewater', *Science of the Total Environment*, 694. Available at: https://doi.org/10.1016/j.scitotenv.2019.07.260.

Kobylka, J., Kuth, M.S., Müller, R.T., Geertsma, E.R. and Pos, K.M. (2020) 'AcrB: a mean, keen, drug efflux machine', *Annals of the New York Academy of Sciences*, 1459(1), pp. 38–68. Available at: https://doi.org/10.1111/nyas.14239.

Kolmogorov, M., Yuan, J., Lin, Y. and Pevzner, P.A. (2019) 'Assembly of long, error-prone reads using repeat graphs', *Nature biotechnology*, 37(5), pp. 540–546. Available at: https://doi.org/10.1038/S41587-019-0072-8.

Kong, K.-F., Schneper, L. and Mathee, K. (2010) 'Beta-lactam Antibiotics: From Antibiosis to Resistance and Bacteriology', *APMIS : acta pathologica, microbiologica, et immunologica Scandinavica*, 118(1), p. 1. Available at: https://doi.org/10.1111/J.1600-0463.2009.02563.X.

Kormutakova, R., Klucar, L. and Turna, J. (2000) 'DNA sequence analysis of the tellurite-resistance determinant from clinical strain of Escherichia coli and identification of essential genes', *BioMetals*, 13(2), pp. 135–139. Available at: https://doi.org/10.1023/A:1009272122989/METRICS.

Korzeniewska, E. and Harnisz, M. (2013) 'Extended-spectrum beta-lactamase (ESBL)-positive Enterobacteriaceae in municipal sewage and their emission to the environment', *Journal of Environmental Management*, 128, pp. 904–911. Available at: https://doi.org/10.1016/J.JENVMAN.2013.06.051.

Kotra, L.P., Haddad, J. and Mobashery, S. (2000) 'Aminoglycosides: Perspectives on Mechanisms of Action and Resistance and Strategies to Counter Resistance', *Antimicrobial Agents and Chemotherapy*, 44(12), pp. 3249–3256.

de Kraker, M.E.A., Stewardson, A.J. and Harbarth, S. (2016) 'Will 10 Million People Die a Year due to Antimicrobial Resistance by 2050?', *PLOS Medicine*, 13(11), p. e1002184. Available at: https://doi.org/10.1371/journal.pmed.1002184.

Krause, K.M., Serio, A.W., Kane, T.R. and Connolly, L.E. (2016) 'Aminoglycosides: An Overview', *Cold Spring Harbor Perspectives in Medicine*, 6(6), p. a027029. Available at: https://doi.org/10.1101/cshperspect.a027029.

Krier, J.B., Kalia, S.S. and Green, R.C. (2016) 'Genomic sequencing in clinical practice: applications, challenges, and opportunities', *Dialogues in Clinical Neuroscience*, 18(3), pp. 299–312.

Kropp, H., Sundelof, J.G., Hajdu, R. and Khan, F.M. (1982) 'Metabolism of thienamycin and related carbapenem antibiotics by the renal dipeptidase, dehydropeptidase-I', *Antimicrobial Agents and Chemotherapy*, 22(1), pp. 62–70. Available at: https://doi.org/10.1128/AAC.22.1.62.

Kuwabara, S. (1970) 'Purification and properties of two extracellular beta-lactamases from Bacillus cereus 569-H', *The Biochemical journal*, 118(3), pp. 457–465. Available at: https://doi.org/10.1042/bj1180457.

Kwak, Y.-K., Colque, P., Byfors, S., Giske, C.G., Möllby, R. and Kühn, I. (2015) 'Surveillance of antimicrobial resistance among Escherichia coli in wastewater in Stockholm during 1 year: does it reflect the resistance trends in the society?', *International Journal of Antimicrobial Agents*, 45(1), pp. 25–32. Available at: https://doi.org/10.1016/J.IJANTIMICAG.2014.09.016.

Lamba, M., Gupta, S., Shukla, R., Graham, D.W., Sreekrishnan, T.R. and Ahammad, S.Z. (2018) 'Carbapenem resistance exposures via wastewaters across New Delhi', *Environment International*, 119, pp. 302–308. Available at: https://doi.org/10.1016/j.envint.2018.07.004.

Lan, F., Demaree, B., Ahmed, N. and Abate, A.R. (2017) 'Single-cell genome sequencing at ultra-high-throughput with microfluidic droplet barcoding', *Nature Biotechnology*, 35(7), pp. 640–646. Available at: https://doi.org/10.1038/nbt.3880.

Landgraf, T.N., Berlese, A., Fernandes, F.F., Milanezi, M.L., Martinez, R. and Panunto-Castelo, A. (2012) 'The ferric aerobactin receptor IutA, a protein isolated on agarose column, is not essential for uropathogenic Escherichia coli infection', *Revista latino-americana de enfermagem*, 20(2), pp. 340–345. Available at: https://doi.org/10.1590/S0104-11692012000200017.

Langstraat, J., Bohse, M. and Clegg, S. (2001) 'Type 3 fimbrial shaft (MrkA) of Klebsiella pneumoniae, but not the fimbrial adhesin (MrkD), facilitates biofilm formation', *Infection and immunity*, 69(9), pp. 5805–5812. Available at: https://doi.org/10.1128/IAI.69.9.5805-5812.2001.

Larsen, M.V., Cosentino, S., Rasmussen, S., Friis, C., Hasman, H., Marvig, R.L., Jelsbak, L., Sicheritz-Pontén, T., Ussery, D.W., Aarestrup, F.M. and Lund, O. (2012) 'Multilocus sequence typing of total-genome-sequenced bacteria', *Journal of Clinical Microbiology*, 50(4), pp. 1355–1361. Available at: https://doi.org/10.1128/JCM.06094-11.

Larsson, D.G.J., Flach, C.-F. and Laxminarayan, R. (2023) 'Sewage surveillance of antibiotic resistance holds both opportunities and challenges', *Nature*

Reviews Microbiology, 21(4), pp. 213–214. Available at: https://doi.org/10.1038/s41579-022-00835-5.

Larsson, D.G.J., de Pedro, C. and Paxeus, N. (2007) 'Effluent from drug manufactures contains extremely high levels of pharmaceuticals', *Journal of Hazardous Materials*, 148(3), pp. 751–755. Available at: https://doi.org/10.1016/j.jhazmat.2007.07.008.

Lauritsen, I., Porse, A., Sommer, M.O.A. and Nørholm, M.H.H. (2017) 'A versatile one-step CRISPR-Cas9 based approach to plasmid-curing', *Microbial Cell Factories*, 16(1), p. 135. Available at: https://doi.org/10.1186/S12934-017-0748-Z.

Lazarus, B., Paterson, D.L., Mollinger, J.L. and Rogers, B.A. (2015) 'Do Human Extraintestinal Escherichia coli Infections Resistant to Expanded-Spectrum Cephalosporins Originate From Food-Producing Animals? A Systematic Review', *Clinical Infectious Diseases*, 60(3), pp. 439–452. Available at: https://doi.org/10.1093/cid/ciu785.

Lazdins, A., Maurya, A.P., Miller, C.E., Kamruzzaman, M., Liu, S., Stephens, E.R., Lloyd, G.S., Haratianfar, M., Chamberlain, M., Haines, A.S., Kreft, J.U., Webber, M.A., Iredell, J. and Thomas, C.M. (2020) 'Potentiation of curing by a broad-host-range self-transmissible vector for displacing resistance plasmids to tackle AMR', *PLOS ONE*, 15(1), p. e0225202. Available at: https://doi.org/10.1371/JOURNAL.PONE.0225202.

Leclercq, R. (2002) 'Mechanisms of Resistance to Macrolides and Lincosamides: Nature of the Resistance Elements and Their Clinical Implications', *Clinical Infectious Diseases*, 34(4), pp. 482–492. Available at: https://doi.org/10.1086/324626.

Lederberg, J. and Tatum, E.L. (1946) 'Gene recombination in Escherichia coli', *Nature*, 158(4016), p. 558. Available at: https://doi.org/10.1038/158558a0.

Lee, C.-H., Chu, C., Liu, J.-W., Chen, Y.-S., Chiu, C.-J. and Su, L.-H. (2007) 'Collateral damage of flomoxef therapy: in vivo development of porin deficiency and acquisition of blaDHA-1 leading to ertapenem resistance in a clinical isolate of Klebsiella pneumoniae producing CTX-M-3 and SHV-5 beta-lactamases', *The Journal of Antimicrobial Chemotherapy*, 60(2), pp. 410–413. Available at: https://doi.org/10.1093/jac/dkm215.

Leekitcharoenphon, P., Johansson, M.H.K., Munk, P., Malorny, B., Skarżyńska, M., Wadepohl, K., Moyano, G., Hesp, A., Veldman, K.T., Bossers, A., Zając, M., Wasyl, D., Sanders, P., Gonzalez-Zorn, B., Brouwer, M.S.M., Wagenaar, J.A., Heederik, D.J.J., Mevius, D. and Aarestrup, F.M. (2021) 'Genomic evolution of antimicrobial resistance in Escherichia coli', *Scientific Reports*, 11(1), p. 15108. Available at: https://doi.org/10.1038/s41598-021-93970-7.

Leonard, A.F.C., Zhang, L., Balfour, A.J., Garside, R., Hawkey, P.M., Murray, A.K., Ukoumunne, O.C. and Gaze, W.H. (2018) 'Exposure to and colonisation by antibiotic-resistant E. coli in UK coastal water users: Environmental surveillance, exposure assessment, and epidemiological study (Beach Bum Survey)', *Environment International*, 114, pp. 326–333. Available at: https://doi.org/10.1016/j.envint.2017.11.003.

Li, H., Luo, Y.-F., Williams, B.J., Blackwell, T.S. and Xie, C.-M. (2012) 'Structure and function of OprD protein in Pseudomonas aeruginosa: From antibiotic resistance to novel therapies', *International journal of medical microbiology : IJMM*, 302(2), p. 10.1016/j.ijmm.2011.10.001. Available at: https://doi.org/10.1016/j.ijmm.2011.10.001.

Li, H., Sun, L., Qiao, H., Sun, Z., Wang, P., Xie, C., Hu, X., Nie, T., Yang, X., Li, G., Zhang, Y., Wang, X., Li, Z., Jiang, J., Li, C. and You, X. (2023) 'Polymyxin resistance caused by large-scale genomic inversion due to IS26 intramolecular translocation in Klebsiella pneumoniae', *Acta Pharmaceutica Sinica. B*, 13(9), pp. 3678–3693. Available at: https://doi.org/10.1016/j.apsb.2023.06.003.

Liakopoulos, A., Mevius, D. and Ceccarelli, D. (2016) 'A review of SHV extended-spectrum β-lactamases: Neglected yet ubiquitous', *Frontiers in Microbiology*, 7(SEP). Available at: https://doi.org/10.3389/fmicb.2016.01374.

Liebert, C.A., Hall, R.M. and Summers, A.O. (1999) 'Transposon Tn21, flagship of the floating genome', *Microbiology and molecular biology reviews: MMBR*, 63(3), pp. 507–522. Available at: https://doi.org/10.1128/MMBR.63.3.507-522.1999.

Lienemann, T., Pitkänen, T., Antikainen, J., Mölsä, E., Miettinen, I., Haukka, K., Vaara, M. and Siitonen, A. (2011) 'Shiga Toxin-Producing Escherichia coli O100:H–: stx 2e in Drinking Water Contaminated by Waste Water in Finland'. Available at: https://link.springer.com/article/10.1007/s00284-010-9832-x (Accessed: 18 December 2023).

Lima, L.M., Silva, B.N.M.D., Barbosa, G. and Barreiro, E.J. (2020) 'β-lactam antibiotics: An overview from a medicinal chemistry perspective', *European Journal of Medicinal Chemistry*, 208, 112829. Available at: https://doi.org/10.1016/j.ejmech.2020.112829.

Linton, K., Richmond, M., Bevan, R. and Gillespie, W. (1974) 'Antibiotic resistance and R factors in coliform bacilli isolated from hospital and domestic sewage', *J. Med Microbiol*, 7.

Liu, Y. and Breukink, E. (2016) 'The Membrane Steps of Bacterial Cell Wall Synthesis as Antibiotic Targets', *Antibiotics*, *5*(3), p. 28. Available at: https://doi.org/10.3390/antibiotics5030028

Liu, Y.-Y., Wang, Y., Walsh, T.R., Yi, L.-X., Zhang, R., Spencer, J., Doi, Y., Tian, G., Dong, B., Huang, X., Yu, L.-F., Gu, D., Ren, H., Chen, X., Lv, L., He, D., Zhou, H.,

Liang, Z., Liu, J.-H. and Shen, J. (2016) 'Emergence of plasmid-mediated colistin resistance mechanism MCR-1 in animals and human beings in China: a microbiological and molecular biological study', *The Lancet. Infectious Diseases*, 16(2), pp. 161–168. Available at: https://doi.org/10.1016/S1473-3099(15)00424-7.

Liu, Z., Xiao, X., Li, Y., Liu, Y., Li, R. and Wang, Z. (2019) 'Emergence of IncX3 Plasmid-Harboring blaNDM–5 Dominated by Escherichia coli ST48 in a Goose Farm in Jiangsu, China', *Frontiers in Microbiology*, 10, pp. 2002–2002. Available at: https://doi.org/10.3389/FMICB.2019.02002/PDF.

Livermore, D.M. (2012) 'Fourteen years in resistance', *International Journal of Antimicrobial Agents*, 39(4), pp. 283–294. Available at: https://doi.org/10.1016/j.ijantimicag.2011.12.012.

Lobanovska, M. and Pilla, G. (2017) 'Penicillin's Discovery and Antibiotic Resistance: Lessons for the Future?', *The Yale journal of biology and medicine*, 90(1), pp. 135–145.

Lorusso, A.B., Carrara, J.A., Barroso, C.D.N., Tuon, F.F. and Faoro, H. (2022) 'Role of Efflux Pumps on Antimicrobial Resistance in Pseudomonas aeruginosa', *International Journal of Molecular Sciences*, 23(24), p. 15779. Available at: https://doi.org/10.3390/ijms232415779.

Lowy, F.D. (2003) 'Antimicrobial resistance: the example of Staphylococcus aureus.', *The Journal of clinical investigation*, 111(9), pp. 1265–73. Available at: https://doi.org/10.1172/JCI18535.

Lucena Baeza, L., Pfennigwerth, N., Greissl, C., G € Ottig, S., Saleh, A., Stelzer, Y., Gatermann, S.G., Hamprecht, A. and Allerberger, F. (2019) 'Comparison of five methods for detection of carbapenemases in Enterobacterales with proposal of a new algorithm', *Clinical Microbiology and Infection*, 25, p. 1286.e9-1286.e15. Available at: https://doi.org/10.1016/j.cmi.2019.03.003.

Ludden, C., Moradigaravand, D., Jamrozy, D., Gouliouris, T., Blane, B., Naydenova, P., Hernandez-Garcia, J., Wood, P., Hadjirin, N., Radakovic, M., Crawley, C., Brown, N.M., Holmes, M., Parkhill, J. and Peacock, S.J. (2020) 'A One Health Study of the Genetic Relatedness of Klebsiella pneumoniae and Their Mobile Elements in the East of England', *Clinical Infectious Diseases: An Official Publication of the Infectious Diseases Society of America*, 70(2), pp. 219–226. Available at: https://doi.org/10.1093/cid/ciz174.

Ludden, C., Reuter, S., Judge, K., Gouliouris, T., Blane, B., Coll, F., Naydenova, P., Hunt, M., Tracey, A., Hopkins, K.L., Brown, N.M., Woodford, N., Parkhill, J. and Peacock, S.J. (2017) 'Sharing of carbapenemase-encoding plasmids between Enterobacteriaceae in UK sewage uncovered by MinION sequencing.', *Microbial genomics*, 3(7), p. e000114. Available at: https://doi.org/10.1099/mgen.0.000114.

Luo, T.L., Corey, B.W., Snesrud, E., Iovleva, A., McElheny, C.L., Preston, L.N., Kwak, Y.I., Bennett, J.W., Doi, Y., McGann, P.T. and Lebreton, F. (2022) 'IS26-mediated plasmid reshuffling results in convergence of toxin–antitoxin systems but loss of resistance genes in XDR Klebsiella pneumoniae from a chronic infection', *Microbial Genomics*, 8(9), p. 000892. Available at: https://doi.org/10.1099/mgen.0.000892.

Luo, X., Yu, L., Feng, J., Zhang, J., Zheng, C., Hu, D., Dai, P., Xu, M., Li, P., Lin, R. and Mu, K. (2022) 'Emergence of Extensively Drug-Resistant ST170 Citrobacter portucalensis with Plasmids pK218-KPC, pK218-NDM, and pK218-SHV from a Tertiary Hospital, China', *Microbiology Spectrum*, 10(5), pp. e02510-22. Available at: https://doi.org/10.1128/spectrum.02510-22.

Magiorakos, A.-P., Srinivasan, A., Carey, R.B., Carmeli, Y., Falagas, M.E., Giske, C.G., Harbarth, S., Hindler, J.F., Kahlmeter, G., Olsson-Liljequist, B., Peterson, D.L., Rice, L.B., Stelling, J., Struelens, M.J., Vatopoulos, A., Weber, JT. and Monnet, D.L. (2012) 'Multidrug-resistant, extensively drug-resistant and pandrug-resistant bacteria: an international expert proposal for interim standard definitions for acquired resistance', *Clinical Microbiology and Infection,* 18(3), pp. 268-281. Available at: https://doi.org/10.1111/j.1469-0691.2011.03570.x

Mairi, A., Pantel, A., Sotto, A., Lavigne, J.-P. and Touati, A. (2018) 'OXA-48-like carbapenemases producing Enterobacteriaceae in different niches', *European Journal of Clinical Microbiology & Infectious Diseases*, 37(4), pp. 587–604. Available at: https://doi.org/10.1007/s10096-017-3112-7.

Mak, S., Xu, Y. and Nodwell, J.R. (2014) 'The expression of antibiotic resistance genes in antibiotic-producing bacteria', *Molecular Microbiology*, 93(3), pp. 391–402. Available at: https://doi.org/10.1111/mmi.12689.

Makowska, N., Philips, A., Dabert, M., Nowis, K., Trzebny, A., Koczura, R. and Mokracka, J. (2020) 'Metagenomic analysis of β-lactamase and carbapenemase genes in the wastewater resistome', *Water Research*, 170, p. 115277. Available at: https://doi.org/10.1016/j.watres.2019.115277.

Mammeri, H., Nordmann, P., Berkani, A. and Eb, F. (2008) 'Contribution of extended-spectrum AmpC (ESAC) β-lactamases to carbapenem resistance in Escherichia coli', *FEMS Microbiology Letters*, 282(2), pp. 238–240. Available at: https://doi.org/10.1111/j.1574-6968.2008.01126.x.

Mammeri, H., Poirel, L. and Nordmann, P. (2007) 'Extension of the hydrolysis spectrum of AmpC beta-lactamase of Escherichia coli due to amino acid insertion in the H-10 helix', *The Journal of Antimicrobial Chemotherapy*, 60(3), pp. 490–494. Available at: https://doi.org/10.1093/jac/dkm227.

Mantilla-Calderon, D., Jumat, M.R., Wang, T., Ganesan, P., Al-Jassim, N. and Hong, P.Y. (2016) 'Isolation and characterization of NDM-positive Escherichia coli from municipal wastewater in Jeddah, Saudi Arabia', *Antimicrobial Agents*

and Chemotherapy, 60(9), pp. 5223–5231. Available at: https://doi.org/10.1128/AAC.00236-16.

Markley, J.L. and Wencewicz, T.A. (2018) 'Tetracycline-Inactivating Enzymes', *Frontiers in Microbiology*, 9, 1058. Available at: https://doi.org/10.3389/fmicb.2018.01058

Marti, E., Variatza, E. and Balcazar, J.L. (2014) 'The role of aquatic ecosystems as reservoirs of antibiotic resistance', *Trends in Microbiology*, 22(1), pp. 36-41. Available at: https://doi.org/ 10.1016/j.tim.2013.11.001.

Masuda, N., Sakagawa, E., Ohya, S., Gotoh, N., Tsujimoto, H. and Nishino, T. (2000) 'Substrate Specificities of MexAB-OprM, MexCD-OprJ, and MexXY-OprM Efflux Pumps in Pseudomonas aeruginosa', *Antimicrobial Agents and Chemotherapy*, 44(12), pp. 3322–3327.

Mathers, A. (2016) 'Mobilization of Carbapenemase-Mediated Resistance in Enterobacteriaceae', *Microbiology Spectrum*, 4(3), p. 10.1128/microbiolspec.ei10-0010–2015. Available at: https://doi.org/10.1128/microbiolspec.ei10-0010-2015.

Matlock, W., Lipworth, S., Chau, K.K., AbuOun, M., Barker, L., Kavanagh, J., Andersson, M., Oakley, S., Morgan, M., Crook, D.W., Read, D.S., Anjum, M., Shaw, L.P., Stoesser, N., and REHAB Consortium (2023) 'Enterobacterales plasmid sharing amongst human bloodstream infections, livestock, wastewater, and waterway niches in Oxfordshire, UK', *eLife*, 12, p. e85302. Available at: https://doi.org/10.7554/eLife.85302.

Mazel, D. (2006) 'Integrons: agents of bacterial evolution', *Nature Reviews Microbiology*, 4(8), pp. 608–620. Available at: https://doi.org/10.1038/nrmicro1462.

McCarthy, K.L., Jennison, A., Wailan, A.M. and Paterson, D.L. (2017) 'Draft Genome Sequence of an IMP-7-Producing Pseudomonas aeruginosa Bloodstream Infection Isolate from Australia', *Genome Announcements*, 5(27), pp. e00596-17. Available at: https://doi.org/10.1128/genomeA.00596-17.

McConnell, M.M., Truelstrup Hansen, L., Jamieson, R.C., Neudorf, K.D., Yost, C.K. and Tong, A. (2018) 'Removal of antibiotic resistance genes in two tertiary level municipal wastewater treatment plants', *Science of the Total Environment*, 643, pp. 292–300. Available at: https://doi.org/10.1016/j.scitotenv.2018.06.212.

McCubbin, K.D., Anholt, R.M., de Jong, E., Ida, J.A., Nóbrega, D.B., Kastelic, J.P., Conly, J.M., Götte, M., McAllister, T.A., Orsel, K., Lewis, I., Jackson, L., Plastow, G., Wieden, H.-J., McCoy, K., Leslie, M., Robinson, J.L., Hardcastle, L., Hollis, A., Ashbolt, N.J., Checkley, S., Tyrrell, G.J., Buret, A.G., Rennert-May, E., Goddard, E., Otto, S.J.G. and Barkema, H.W. (2021) 'Knowledge Gaps in the Understanding of Antimicrobial Resistance in Canada', *Frontiers in Public*

Health, 9, p. 726484. Available at: https://doi.org/10.3389/fpubh.2021.726484.

McLaughlin, M., Advincula, M.R., Malczynski, M., Qi, C., Bolon, M. and Scheetz, M.H. (2013) 'Correlations of antibiotic use and carbapenem resistance in enterobacteriaceae.', *Antimicrobial agents and chemotherapy*, 57(10), pp. 5131–3. Available at: https://doi.org/10.1128/AAC.00607-13.

McNulty, C.A.M., Lecky, D.M., Xu-McCrae, L., Nakiboneka-Ssenabulya, D., Chung, K.-T., Nichols, T., Thomas, H.L., Thomas, M., Alvarez-Buylla, A., Turner, K., Shabir, S., Manzoor, S., Smith, S., Crocker, L. and Hawkey, P.M. (2018) 'CTX-M ESBL-producing Enterobacteriaceae: estimated prevalence in adults in England in 2014', *Journal of Antimicrobial Chemotherapy*, 73(5), pp. 1368–1388. Available at: https://doi.org/10.1093/jac/dky007.

Meletis, G. (2016) 'Carbapenem resistance: overview of the problem and future perspectives', *Therapeutic Advances in Infectious Disease*, 3(1), pp. 15–21. Available at: https://doi.org/10.1177/2049936115621709.

MicrobesNG (2021) *Genome Sequencing Service Methods v20210419*. Available at: https://microbesng.com/documents/39/Genome_Sequencing_Methods_V20231206.pdf (Accessed: 11 June 2021).

Miller, E.A., Ponder, J.B., Willette, M., Johnson, T.J. and VanderWaal, K.L. (2020) 'Merging Metagenomics and Spatial Epidemiology To Understand the Distribution of Antimicrobial Resistance Genes from Enterobacteriaceae in Wild Owls', *Applied and Environmental Microbiology*, 86(20), pp. e00571-20. Available at: https://doi.org/10.1128/AEM.00571-20.

Miller, S.I. (2016) 'Antibiotic Resistance and Regulation of the Gram-Negative Bacterial Outer Membrane Barrier by Host Innate Immune Molecules', *mBio*, 7(5), pp. e01541-16. Available at: https://doi.org/10.1128/mBio.01541-16.

Miriagou, V., Carattoli, A., Tzelepi, E., Villa, L. and Tzouvelekis, L.S. (2005) 'IS26-Associated In4-Type Integrons Forming Multiresistance Loci in Enterobacterial Plasmids', *Antimicrobial Agents and Chemotherapy*, 49(8), p. 3541. Available at: https://doi.org/10.1128/AAC.49.8.3541-3543.2005.

Mohapatra, S.S., Dwibedy, S.K. and Padhy, I. (2021) 'Polymyxins, the last-resort antibiotics: Mode of action, resistance emergence, and potential solutions', *Journal of Biosciences*, 46(3), p. 85. Available at: https://doi.org/10.1007/s12038-021-00209-8.

Mollet, B., Clerget, M., Meyer, J. and Iida, S. (1985) 'Organization of the Tn6-related kanamycin resistance transposon Tn2680 carrying two copies of IS26 and an IS903 variant, IS903. B.', *Journal of Bacteriology*, 163(1), pp. 55–60.

Mollet, B., Iida, S. and Arber, W. (1985) 'Gene organization and target specificity of the prokaryotic mobile genetic element IS26', *Molecular and General Genetics MGG*, 201(2), pp. 198–203. Available at: https://doi.org/10.1007/BF00425660.

Morgan, D.J., Okeke, I.N., Laxminarayan, R., Perencevich, E.N. and Weisenberg, S. (2011) 'Non-prescription antimicrobial use worldwide: a systematic review.', *The Lancet. Infectious diseases*, 11(9), pp. 692–701. Available at: https://doi.org/10.1016/S1473-3099(11)70054-8.

Morse, M.L., Lederberg, E.M. and Lederberg, J. (1956) 'Transduction in Escherichia Coli K-12', *Genetics*, 41(1), pp. 142–156.

Mughini-Gras, L., Dorado-García, A., van Duijkeren, E., van den Bunt, G., Dierikx, C.M., Bonten, M.J.M., Bootsma, M.C.J., Schmitt, H., Hald, T., Evers, E.G., de Koeijer, A., van Pelt, W., Franz, E., Mevius, D.J. and Heederik, D.J.J. (2019) 'Attributable sources of community-acquired carriage of Escherichia coli containing β-lactam antibiotic resistance genes: a population-based modelling study', *The Lancet Planetary Health*, 3(8), pp. e357–e369. Available at: https://doi.org/10.1016/S2542-5196(19)30130-5.

Mugnier, P.D., Poirel, L., Naas, T. and Nordmann, P. (2010) 'Worldwide Dissemination of the blaOXA-23 Carbapenemase Gene of Acinetobacter baumannii1', *Emerging Infectious Diseases*, 16(1), pp. 35–40. Available at: https://doi.org/10.3201/eid1601.090852.

Mühlberg, E., Umstätter, F., Kleist, C., Domhan, C., Mier, W. and Uhl, P. (2020) 'Renaissance of vancomycin: approaches for breaking antibiotic resistance in multidrug-resistant bacteria', *Canadian Journal of Microbiology*, 66(1), pp. 11–16. Available at: https://doi.org/10.1139/cjm-2019-0309.

Mulchandani, R., Wang, Y., Gilbert, M. and Boeckel, T.P.V. (2023) 'Global trends in antimicrobial use in food-producing animals: 2020 to 2030', *PLOS Global Public Health*, 3(2), p. e0001305. Available at: https://doi.org/10.1371/journal.pgph.0001305.

Muller, H., Sib, E., Gajdiss, M., Klanke, U., Lenz-Plet, F., Barabasch, V., Albert, C., Schallenberg, A., Timm, C., Zacharias, N., Schmithaused, R.M., Engelhart, S., Exner, M., Parcina, M., Schreiber, C. and Bierbaum, G. (2018) 'Dissemination of multi-resistant Gram-negative bacteria into German wastewater and surface waters', *FEMS Microbiology Ecology*, 94.

Munita, J.M. and Arias, C.A. (2016) 'Mechanisms of Antibiotic Resistance', *Microbiology spectrum*, 4(2), p. 10.1128/microbiolspec.VMBF-0016–2015. Available at: https://doi.org/10.1128/microbiolspec.VMBF-0016-2015.

Munoz-Price, L.S., Poirel, L., Bonomo, R.A., Schwaber, M.J., Daikos, G.L., Cormican, M., Cornaglia, G., Garau, J., Gniadkowski, M., Hayden, M.K., Kumarasamy, K., Livermore, D.M., Maya, J.J., Nordmann, P., Patel, J.B.,

Paterson, D.L., Pitout, J., Villegas, M.V., Wang, H., Woodford, N. and Quinn, J.P. (2013) 'Clinical epidemiology of the global expansion of Klebsiella pneumoniae carbapenemases', *The Lancet Infectious Diseases*, 13(9), pp. 785–796. Available at: https://doi.org/10.1016/S1473-3099(13)70190-7.

Murray, C.J.L., Ikuta, K.S., Sharara, F., Swetschinski, L., Aguilar, G.R., Gray, A., Han, C., Bisignano, C., Rao, P., Wool, E., Johnson, S.C., Browne, A.J., Chipeta, M.G., Fell, F., Hackett, S., Haines-Woodhouse, G., Hamadani, B.H.K., Kumaran, E.A.P., McManigal, B., Agarwal, R., Akech, S., Albertson, S., Amuasi, J., Andrews, J., Aravkin, A., Ashley, E., Bailey, F., Baker, S., Basnyat, B., Bekker, A., Bender, R., Bethou, A., Bielicki, J., Boonkasidecha, S., Bukosia, J., Carvalheiro, C., Castañeda-Orjuela, C., Chansamouth, V., Chaurasia, S., Chiurchiù, S., Chowdhury, F., Cook, A.J., Cooper, B., Cressey, T.R., Criollo-Mora, E., Cunningham, M., Darboe, S., Day, N.P.J., De Luca, M., Dokova, K., Dramowski, A., Dunachie, S.J., Eckmanns, T., Eibach, D., Emami, A., Feasey, N., Fisher-Pearson, N., Forrest, K., Garrett, D., Gastmeier, P., Giref, A.Z., Greer, R.C., Gupta, V., Haller, S., Haselbeck, A., Hay, S.I., Holm, M., Hopkins, S., Iregbu, K.C., Jacobs, J., Jarovsky, D., Javanmardi, F., Khorana, M., Kissoon, N., Kobeissi, E., Kostyanev, T., Krapp, F., Krumkamp, R., Kumar, A., Kyu, H.H., Lim, C., Limmathurotsakul, D., Loftus, M.J., Lunn, M., Ma, J., Mturi, N., Munera-Huertas, T., Musicha, P., Mussi-Pinhata, M.M., Nakamura, T., Nanavati, R., Nangia, S., Newton, P., Ngoun, C., Novotney, A., Nwakanma, D., Obiero, C.W., Olivas-Martinez, A., Olliaro, P., Ooko, E., Ortiz-Brizuela, E., Peleg, A.Y., Perrone, C., Plakkal, N., Ponce-de-Leon, A., Raad, M., Ramdin, T., Riddell, A., Roberts, T., Robotham, J.V., Roca, A., Rudd, K.E., Russell, N., Schnall, J., Scott, J.A.G., Shivamallappa, M., Sifuentes-Osornio, J., Steenkeste, N., Stewardson, A.J., Stoeva, T., Tasak, N., Thaiprakong, A., Thwaites, G., Turner, C., Turner, P., van Doorn, H.R., Velaphi, S., Vongpradith, A., Vu, H., Walsh, T., Waner, S., Wangrangsimakul, T., Wozniak, T., Zheng, P., Sartorius, B., Lopez, A.D., Stergachis, A., Moore, C., Dolecek, C., and Naghavi, M. (2022) 'Global burden of bacterial antimicrobial resistance in 2019: a systematic analysis', *Lancet,* 399(10325), pp. 629-655. Available at: https://doi.org/10.1016/S0140-6736(21)02724-0.

Naas, T., Oueslati, S., Bonnin, R.A., Dabos, M.L., Zavala, A., Dortet, L., Retailleau, P. and Iorga, B.I. (2017) 'Beta-lactamase database (BLDB)–structure and function', *Journal of Enzyme Inhibition and Medicinal Chemistry*, 32(1), pp. 917–919. Available at: https://doi.org/10.1080/14756366.2017.1344235.

Nesmelova, I.V. and Hackett, P.B. (2010) 'DDE Transposases: Structural Similarity and Diversity', *Advanced drug delivery reviews*, 62(12), pp. 1187–1195. Available at: https://doi.org/10.1016/j.addr.2010.06.006.

Newton, R.J., McLellan, S.L., Dila, D.K., Vineis, J.H., Morrison, H.G., Eren, A.M. and Sogin, M.L. (2015) 'Sewage Reflects the Microbiomes of Human Populations', *mBio*, 6(2), pp. e02574-14. Available at: https://doi.org/10.1128/mBio.02574-14.

Nicolas, E., Lambin, M., Dandoy, D., Galloy, C., Nguyen, N., Oger, C.A. and Hallet, B. (2015) 'The Tn3-family of Replicative Transposons', *Microbiology Spectrum*, 3(4), p. 10.1128/microbiolspec.mdna3-0060–2014. Available at: https://doi.org/10.1128/microbiolspec.mdna3-0060-2014.

Niegowska, M., Sanseverino, I., Navarro, A. and Lettieri, T. (2021) 'Knowledge gaps in the assessment of antimicrobial resistance in surface waters', *FEMS Microbiology Ecology*, 97(11), p. fiab140. Available at: https://doi.org/10.1093/femsec/fiab140.

Nikaido, H. (2003) 'Molecular Basis of Bacterial Outer Membrane Permeability Revisited', *Microbiology and Molecular Biology Reviews*, 67(4), pp. 593–656. Available at: https://doi.org/10.1128/mmbr.67.4.593-656.2003.

Nixon, M.R., Saionz, K.W., Koo, M.S., Szymonifka, M.J., Jung, H., Roberts, J.P., Nandakumar, M., Kumar, A., Liao, R., Rustad, T., Sacchettini, J.C., Rhee, K.Y., Freundlich, J.S. and Sherman, D.R. (2014) 'Folate pathway disruption leads to critical disruption of methionine derivatives in Mycobacterium tuberculosis', *Chemistry and Biology*, 21(7), pp. 819-30. Available at: https://doi.org/10.1016/j.chembiol.2014.04.009

Nordmann, P., Naas, T. and Poirel, L. (2011) 'Global Spread of Carbapenemase-producing Enterobacteriaceae', *Emerging Infectious Diseases*, 17(10), pp. 1791–1798. Available at: https://doi.org/10.3201/eid1710.110655.

Nordmann, P., Yao, Y., Falgenhauer, L., Sadek, M., Imirzalioglu, C. and Chakraborty, T. (2021) 'Recent Emergence of Aztreonam-Avibactam Resistance in NDM and OXA-48 Carbapenemase-Producing Escherichia coli in Germany', *Antimicrobial agents and chemotherapy*, 65(11). Available at: https://doi.org/10.1128/AAC.01090-21.

Norrby, S.R., Alestig, K., Bjornegard, B., Burman, L.A., Ferber, F., Huber, J.L., Jones, K.H., Kahan, F.M., Kahan, J.S., Kropp, H., Meisinger, M.A. and Sundelof, J.G. (1983) 'Urinary recovery of N-formimidoyl thienamycin (MK0787) as affected by coadministration of N-formimidoyl thienamycin dehydropeptidase inhibitors', *Antimicrobial Agents and Chemotherapy*, 23(2), pp. 300–307. Available at: https://doi.org/10.1128/AAC.23.2.300.

Nothias, L.-F., Knight, R. and Dorrestein, P.C. (2016) 'Antibiotic discovery is a walk in the park', *Proceedings of the National Academy of Sciences*, 113(51), pp. 14477–14479. Available at: https://doi.org/10.1073/pnas.1618221114.

Novick, R.P. (1987) 'Plasmid incompatibility', *Microbiological Reviews*, 51(4), pp. 381–395. Available at: https://doi.org/10.1128/mr.51.4.381-395.1987.

Oliva, M., Monno, R., Addabbo, P., Pesole, G., Scrascia, M., Calia, C., Dionisi, A.M., Chiara, M., Horner, D.S., Manzari, C. and Pazzani, C. (2018) 'IS26 mediated antimicrobial resistance gene shuffling from the chromosome to a

mosaic conjugative FII plasmid', *Plasmid*, 100, pp. 22–30. Available at: https://doi.org/10.1016/j.plasmid.2018.10.001.

Olliver, A., Vallé, M., Chaslus-Dancla, E. and Cloeckaert, A. (2005) 'Overexpression of the Multidrug Efflux Operon acrEF by Insertional Activation with IS1 or IS10 Elements in Salmonella enterica Serovar Typhimurium DT204 acrB Mutants Selected with Fluoroquinolones', *Antimicrobial Agents and Chemotherapy*, 49(1), pp. 289–301. Available at: https://doi.org/10.1128/AAC.49.1.289-301.2005.

Olson, A.B., Silverman, M., Boyd, D.A., McGeer, A., Willey, B.M., Pong-Porter, V., Daneman, N. and Mulvey, M.R. (2005) 'Identification of a progenitor of the CTX-M-9 group of extended-spectrum β-lactamases from Kluyvera georgiana isolated in Guyana', *Antimicrobial Agents and Chemotherapy*, 49(5), pp. 2112–2115. Available at: https://doi.org/10.1128/AAC.49.5.2112-2115.2005.

Ondov, B.D., Treangen, T.J., Melsted, P., Mallonee, A.B., Bergman, N.H., Koren, S. and Phillippy, A.M. (2016) 'Mash: Fast genome and metagenome distance estimation using MinHash', *Genome Biology*, 17(1), pp. 1–14. Available at: https://doi.org/10.1186/s13059-016-0997-x.

O'Neill, J. (2014) *Antimicrobial Resistance: Tackling a crisis for the health and wealth of nations*. The Review on Antimicrobial Resistance.

O'Neill, J. (2016) *Tackling Drug-Resistant Infections Globally: Final Report and Recommendations*. The Review on Antimicrobial Resistance.

Oxford Nanopore Technologies (no date) *nanoporetech/medaka: Sequence correction provided by ONT Research*. Available at: https://github.com/nanoporetech/medaka (Accessed: 25 April 2023).

Page, A.J., Cummins, C.A., Hunt, M., Wong, V.K., Reuter, S., Holden, M.T.G., Fookes, M., Falush, D., Keane, J.A. and Parkhill, J. (2015) 'Roary: Rapid large-scale prokaryote pan genome analysis', *Bioinformatics*, 31(22), pp. 3691–3693. Available at: https://doi.org/10.1093/bioinformatics/btv421.

Pagès, J.-M., James, C.E. and Winterhalter, M. (2008) 'The porin and the permeating antibiotic: a selective diffusion barrier in Gram-negative bacteria', *Nature Reviews Microbiology*, 6(12), pp. 893–903. Available at: https://doi.org/10.1038/nrmicro1994.

Pal, C., Asiani, K., Arya, S., Rensing, C., Stekel, D.J., Larsson, D.G.J. and Hobman, J.L. (2017) 'Chapter Seven - Metal Resistance and Its Association With Antibiotic Resistance', in R.K. Poole (ed.) *Advances in Microbial Physiology*. Academic Press (Microbiology of Metal Ions), pp. 261–313. Available at: https://doi.org/10.1016/bs.ampbs.2017.02.001.

Pal, C., Bengtsson-Palme, J., Kristiansson, E. and Larsson, D.G.J. (2015) 'Co-occurrence of resistance genes to antibiotics, biocides and metals reveals novel

insights into their co-selection potential', *BMC Genomics*, 16(1), p. 964. Available at: https://doi.org/10.1186/s12864-015-2153-5.

Palzkill, T. (2013) 'Metallo-β-lactamase structure and function', *Annals of the New York Academy of Sciences*, 1277, pp. 91–104. Available at: https://doi.org/10.1111/j.1749-6632.2012.06796.x.

Papp-Wallace, K.M., Endimiani, A., Taracila, M.A. and Bonomo, R.A. (2011) 'Carbapenems: Past, Present, and Future', *Antimicrobial Agents and Chemotherapy*, 55(11), pp. 4943–4960. Available at: https://doi.org/10.1128/AAC.00296-11.

Park, Y., Choi, Q., Kwon, G.C. and Koo, S.H. (2020) 'Emergence and transmission of New Delhi metallo-beta-lactamase-5-producing Escherichia coli Sequence Type 361 in a Tertiary Hospital in South Korea', *Journal of Clinical Laboratory Analysis*, 34(2). Available at: https://doi.org/10.1002/JCLA.23041.

Pärnänen, K., Karkman, A., Tamminen, M., Lyra, C., Hultman, J., Paulin, L. and Virta, M. (2016) 'Evaluating the mobility potential of antibiotic resistance genes in environmental resistomes without metagenomics', *Scientific Reports*, 6(1), pp. 1–9. Available at: https://doi.org/10.1038/srep35790.

Partridge, S.R. and Hall, R.M. (2005) 'Evolution of Transposons Containing blaTEM Genes', *Antimicrobial Agents and Chemotherapy*, 49(3), p. 1267. Available at: https://doi.org/10.1128/AAC.49.3.1267-1268.2005.

Partridge, S.R. and Iredell, J.R. (2012) 'Genetic Contexts of blaNDM-1', *Antimicrobial Agents and Chemotherapy*, 56(11), p. 6065. Available at: https://doi.org/10.1128/AAC.00117-12.

Partridge, S.R., Kwong, S.M., Firth, N. and Jensen, S.O. (2018) 'Mobile Genetic Elements Associated with Antimicrobial Resistance.', *Clinical microbiology reviews*, 31(4). Available at: https://doi.org/10.1128/CMR.00088-17.

Partridge, S.R., Tsafnat, G., Coiera, E. and Iredell, J.R. (2009) 'Gene cassettes and cassette arrays in mobile resistance integrons', *FEMS Microbiology Reviews*, 33(4), pp. 757–784. Available at: https://doi.org/10.1111/j.1574-6976.2009.00175.x.

Pazda, M., Kumirska, J., Stepnowski, P. and Mulkiewicz, E. (2019) 'Antibiotic resistance genes identified in wastewater treatment plant systems – A review', *Science of the Total Environment*, 697, p. 134023. Available at: https://doi.org/10.1016/j.scitotenv.2019.134023.

Peirano, G., Chen, L., Nobrega, D., Finn, T.J., Kreiswirth, B.N., DeVinney, R. and Pitout, J.D.D. (2022) 'Genomic Epidemiology of Global Carbapenemase-Producing Escherichia coli, 2015–2017', *Emerging Infectious Diseases*, 28(5), pp. 924–931. Available at: https://doi.org/10.3201/eid2805.212535.

Pham, T.D.M., Ziora, Z.M. and Blaskovich, M.A.T. (2019) 'Quinolone antibiotics', *MedChemComm*, 10(10), pp. 1719–1739. Available at: https://doi.org/10.1039/c9md00120d.

Pightling, A.W., Pettengill, J.B., Luo, Y., Baugher, J.D., Rand, H. and Strain, E. (2018) 'Interpreting Whole-Genome Sequence Analyses of Foodborne Bacteria for Regulatory Applications and Outbreak Investigations', *Frontiers in Microbiology*, 9:1482. Avaiable at: https://doi.org/10.3389/fmicb.2018.01482.

Pitout, J.D.D. and Chen, L. (2023) 'The Significance of Epidemic Plasmids in the Success of Multidrug-Resistant Drug Pandemic Extraintestinal Pathogenic Escherichia coli', *Infectious Diseases and Therapy*, 12(4), pp. 1029–1041. Available at: https://doi.org/10.1007/s40121-023-00791-4.

Pitout, J.D.D., Nordmann, P., Laupland, K.B. and Poirel, L. (2005) 'Emergence of Enterobacteriaceae producing extended-spectrum β-lactamases (ESBLs) in the community', *Journal of Antimicrobial Chemotherapy*, 56(1), pp. 52–59. Available at: https://doi.org/10.1093/jac/dki166.

Pitout, J.D.D., Peirano, G., Kock, M.M., Strydom, K.-A. and Matsumura, Y. (2019) 'The Global Ascendency of OXA-48-Type Carbapenemases', *Clinical Microbiology Reviews*, 33(1), p. 10.1128/cmr.00102-19. Available at: https://doi.org/10.1128/cmr.00102-19.

Plasterk, R.H.A. (1996) 'The Tc1/mariner Transposon Family', in H. Saedler and A. Gierl (eds) *Transposable Elements*. Berlin, Heidelberg: Springer (Current Topics in Microbiology and Immunology), pp. 125–143. Available at: https://doi.org/10.1007/978-3-642-79795-8_6.

Poirel, L., Bonnin, R.A., Boulanger, A., Schrenzel, J., Kaase, M. and Nordmann, P. (2012) 'Tn125-Related Acquisition of blaNDM-Like Genes in Acinetobacter baumannii', *Antimicrobial Agents and Chemotherapy*, 56(2), p. 1087. Available at: https://doi.org/10.1128/AAC.05620-11.

Poirel, L., Bonnin, R.A. and Nordmann, P. (2011a) 'Analysis of the Resistome of a Multidrug-Resistant NDM-1-Producing Escherichia coli Strain by High-Throughput Genome Sequencing', *Antimicrobial Agents and Chemotherapy*, 55(9), p. 4224. Available at: https://doi.org/10.1128/AAC.00165-11.

Poirel, L., Bonnin, R.A. and Nordmann, P. (2011b) 'Genetic basis of antibiotic resistance in pathogenic Acinetobacter species', *IUBMB Life*, 63(12), pp. 1061–1067. Available at: https://doi.org/10.1002/iub.532.

Poirel, L., Decousser, J.-W. and Nordmann, P. (2003) 'Insertion sequence ISEcp1B is involved in expression and mobilization of a bla(CTX-M) beta-lactamase gene.', *Antimicrobial agents and chemotherapy*, 47(9), pp. 2938–45. Available at: https://doi.org/10.1128/aac.47.9.2938-2945.2003.

Poirel, L., Héritier, C., Tolün, V. and Nordmann, P. (2004) 'Emergence of Oxacillinase-Mediated Resistance to Imipenem in Klebsiella pneumoniae', *Antimicrobial Agents and Chemotherapy*, 48(1), pp. 15–22. Available at: https://doi.org/10.1128/AAC.48.1.15-22.2004.

Poirel, L., Naas, T., Le Thomas, I., Karim, A., Bingen, E. and Nordmann, P. (2001) 'CTX-M-type extended-spectrum β-lactamase that hydrolyzes ceftazidime through a single amino acid substitution in the omega loop', *Antimicrobial Agents and Chemotherapy*, 45(12), pp. 3355–3361. Available at: https://doi.org/10.1128/AAC.45.12.3355-3361.2001.

Poirel, L. and Nordmann, P. (2016) 'Emerging plasmid-encoded colistin resistance: the animal world as the culprit?', *Journal of Antimicrobial Chemotherapy*, 71(8), pp. 2326–2327. Available at: https://doi.org/10.1093/jac/dkw074.

Poirel, L., Walsh, T.R., Cuvillier, V. and Nordmann, P. (2011) 'Multiplex PCR for detection of acquired carbapenemase genes', *Diagnostic Microbiology and Infectious Disease*, 70(1), pp. 119–123. Available at: https://doi.org/10.1016/j.diagmicrobio.2010.12.002.

Pong, C.H., Harmer, C.J., Flores, J.K., Ataide, S.F. and Hall, R.M. (2021) 'Characterization of the specific DNA-binding properties of Tnp26, the transposase of insertion sequence IS26', *Journal of Biological Chemistry*, 297(4), p. 101165. Available at: https://doi.org/10.1016/j.jbc.2021.101165.

Poole, N.M., Green, S.I., Rajan, A., Vela, L.E., Zeng, X.L., Estes, M.K. and Maresso, A.W. (2017) 'Role for FimH in extraintestinal pathogenic Escherichia coli invasion and translocation through the intestinal epithelium', *Infection and Immunity*, 85(11). Available at: https://doi.org/10.1128/IAI.00581-17/SUPPL_FILE/ZII999092195S1.PDF.

Potron, A., Poirel, L. and Nordmann, P. (2011) 'Origin of OXA-181, an Emerging Carbapenem-Hydrolyzing Oxacillinase, as a Chromosomal Gene in Shewanella xiamenensis ▿', *Antimicrobial Agents and Chemotherapy*, 55(9), pp. 4405–4407. Available at: https://doi.org/10.1128/AAC.00681-11.

Pritchard, A.C.W. (2022) *Mobile mercury resistance transposons: surveillance and resistance gene cassette variation in wastewater.* University of Nottingham.

Proia, L., Anzil, A., Borrego, C., Farrè, M., Llorca, M., Sanchis, J., Bogaerts, P., Balcázar, J.L. and Servais, P. (2018) 'Occurrence and persistence of carbapenemases genes in hospital and wastewater treatment plants and propagation in the receiving river', *Journal of Hazardous Materials*, 358, pp. 33–43. Available at: https://doi.org/10.1016/j.jhazmat.2018.06.058.

Queenan, A.M. and Bush, K. (2007) 'Carbapenemases: the Versatile β-Lactamases', *Clinical Microbiology Reviews*, 20(3), pp. 440–458. Available at: https://doi.org/10.1128/CMR.00001-07.

Rammelkamp, C. and Maxon, T. (1942) 'Resistance of Staphylococcus aureus to the Action of Penicillin', *Exp Biol Med.*, 51(3), pp. 386–389.

Randall, L.P., Lodge, M.P., Elviss, N.C., Lemma, F.L., Hopkins, K.L., Teale, C.J. and Woodford, N. (2017) 'Evaluation of meat, fruit and vegetables from retail stores in five United Kingdom regions as sources of extended-spectrum beta-lactamase (ESBL)-producing and carbapenem-resistant Escherichia coli', *International Journal of Food Microbiology*, 241, pp. 283–290. Available at: https://doi.org/10.1016/j.ijfoodmicro.2016.10.036.

Rasmussen, B.A., Bush, K., Keeney, D., Yang, Y., Hare, R., O'Gara, C. and Medeiros, A.A. (1996) 'Characterization of IMI-1 beta-lactamase, a class A carbapenem-hydrolyzing enzyme from Enterobacter cloacae.', *Antimicrobial Agents and Chemotherapy*, 40(9), pp. 2080–2086.

Raven, K.E., Ludden, C., Gouliouris, T., Blane, B., Naydenova, P., Brown, N.M., Parkhill, J. and Peacock, S.J. (2019) 'Genomic surveillance of Escherichia coli in municipal wastewater treatment plants as an indicator of clinically relevant pathogens and their resistance genes', *Microbial Genomics*, 5(5). Available at: https://doi.org/10.1099/mgen.0.000267.

Reardon, S. (2014) 'WHO warns against "post-antibiotic" era', *Nature* [Preprint]. Available at: https://doi.org/10.1038/nature.2014.15135.

Redgrave, L.S., Sutton, S.B., Webber, M.A. and Piddock, L.J.V. (2014) 'Fluoroquinolone resistance: mechanisms, impact on bacteria, and role in evolutionary success', *Trends in Microbiology*, 22(8), pp. 438–445. Available at: https://doi.org/10.1016/j.tim.2014.04.007.

Reinthaler, F.F., Galler, H., Feierl, G., Haas, D., Leitner, E., Mascher, F., Melkes, A., Posch, J., Pertschy, B., Winter, I., Himmel, W., Marth, E. and Zarfel, G. (2013) 'Resistance patterns of Escherichia coli isolated from sewage sludge in comparison with those isolated from human patients in 2000 and 2009', *Journal of Water and Health*, 11(1), pp. 13–20. Available at: https://doi.org/10.2166/wh.2012.207.

Reynolds, M.E., Phan, H.T.T., George, S., Hubbard, A.T.M., Stoesser, N., Maciuca, I.E., Crook, D.W. and Timofte, D. (2019) 'Occurrence and characterization of Escherichia coli ST410 co-harbouring blaNDM-5, blaCMY-42 and blaTEM-190 in a dog from the UK', *The Journal of antimicrobial chemotherapy*, 74(5), pp. 1207–1211. Available at: https://doi.org/10.1093/JAC/DKZ017.

Ribeiro, T.G., Gonçalves, B.R., da Silva, M.S., Novais, Â., Machado, E., Carriço, J.A. and Peixe, L. (2017) 'Citrobacter portucalensis sp. nov., isolated from an

aquatic sample', *International Journal of Systematic and Evolutionary Microbiology*, 67(9), pp. 3513–3517. Available at: https://doi.org/10.1099/ijsem.0.002154.

Ross, K., Varani, A.M., Snesrud, E., Huang, H., Alvarenga, D.O., Zhang, J., Wu, C., McGann, P. and Chandler, M. (2021) 'TnCentral: a Prokaryotic Transposable Element Database and Web Portal for Transposon Analysis', *mBio*, 12(5). Available at: https://doi.org/10.1128/mBio.02060-21.

Rizzo, L., Manaia, C., Merlin, C., Schwartz, T., Dagot, C., Ploy, M.C., Michael, I. and Fatta-Kassinos, D. (2013) 'Urban wastewater treatment plants as hotspots for antibiotic resistant bacteria and genes spread into the environment: A review', *Science of the Total Environment*, 447, pp. 345–360. Available at: https://doi.org/10.1016/j.scitotenv.2013.01.032.

Rozwandowicz, M., Brouwer, M.S.M., Fischer, J., Wagenaar, J.A., Gonzalez-Zorn, B., Guerra, B., Mevius, D.J. and Hordijk, J. (2018) 'Plasmids carrying antimicrobial resistance genes in Enterobacteriaceae', *Journal of Antimicrobial Chemotherapy*, 73(5), pp. 1121–1137. Available at: https://doi.org/10.1093/jac/dkx488.

Sadek, M., Juhas, M., Poirel, L. and Nordmann, P. (2020) 'Genetic Features Leading to Reduced Susceptibility to Aztreonam-Avibactam among Metallo-β-Lactamase-Producing Escherichia coli Isolates', *Antimicrobial Agents and Chemotherapy*, 64(12). Available at: https://doi.org/10.1128/AAC.01659-20.

Saino, Y., Kobayashi, F., Inoue, M. and Mitsuhashi, S. (1982) 'Purification and properties of inducible penicillin beta-lactamase isolated from Pseudomonas maltophilia', *Antimicrobial Agents and Chemotherapy*, 22(4), pp. 564–570. Available at: https://doi.org/10.1128/AAC.22.4.564.

Sandegren, L. (2014) 'Selection of antibiotic resistance at very low antibiotic concentrations', *Upsala Journal of Medical Sciences*, 119(2), pp. 103–107. Available at: https://doi.org/10.3109/03009734.2014.904457.

Sanders, C.C., Bradford, P.A., Ehrhardt, A.F., Bush, K., Young, K.D., Henderson, T.A. and Sanders, W.E. (1997) 'Penicillin-binding proteins and induction of AmpC beta-lactamase', *Antimicrobial Agents and Chemotherapy*, 41(9), pp. 2013–2015. Available at: https://doi.org/10.1128/AAC.41.9.2013.

Santos, A.C.M., Silva, R.M., Valiatti, T.B., Santos, F.F., Santos-Neto, J.F., Cayô, R., Streling, A.P., Nodari, C.S., Gales, A.C., Nishiyama-Jr, M.Y., Carvalho, E. and Gomes, T.A.T. (2020) 'Virulence Potential of a Multidrug-Resistant Escherichia coli Strain Belonging to the Emerging Clonal Group ST101-B1 Isolated from Bloodstream Infection', *Microorganisms*, 8(6), p. 827. Available at: https://doi.org/10.3390/MICROORGANISMS8060827.

Sarkar, A., Pazhani, G.P., Chowdhury, G., Ghosh, A. and Ramamurthy, T. (2015) 'Attributes of carbapenemase encoding conjugative plasmid pNDM-SAL from

an extensively drug-resistant Salmonella enterica Serovar Senftenberg', *Frontiers in microbiology*, 6(SEP). Available at: https://doi.org/10.3389/FMICB.2015.00969.

Saul, D., Spiers, A.J., McAnulty, J., Gibbs, M.G., Bergquist, P.L. and Hill, D.F. (1989) 'Nucleotide sequence and replication characteristics of RepFIB, a basic replicon of IncF plasmids', *Journal of Bacteriology*, 171(5), pp. 2697–2707. Available at: https://doi.org/10.1128/jb.171.5.2697-2707.1989.

Sauvage, E., Kerff, F., Terrak, M., Ayala, J.A. and Charlier, P. (2008) 'The penicillin-binding proteins: structure and role in peptidoglycan biosynthesis', *FEMS Microbiology Reviews*, 32(2), pp. 234–258. Available at: https://doi.org/10.1111/j.1574-6976.2008.00105.x.

Schmartz, G.P., Hartung, A., Hirsch, P., Kern, F., Fehlmann, T., Müller, R. and Keller, A. (2022) 'PLSDB: advancing a comprehensive database of bacterial plasmids', *Nucleic Acids Research*, 50(D1), pp. D273–D278. Available at: https://doi.org/10.1093/NAR/GKAB1111.

Schultsz, C. and Geerlings, S. (2012) 'Plasmid-mediated resistance in enterobacteriaceae: Changing landscape and implications for therapy', *Drugs*, 72(1), pp. 1–16. Available at: https://doi.org/10.2165/11597960-000000000-00000.

Schumacher, M.A. (2012) 'Bacterial plasmid partition machinery: a minimalist approach to survival', *Current opinion in structural biology*, 22(1), pp. 72–79. Available at: https://doi.org/10.1016/j.sbi.2011.11.001.

Schwarz, S., Shen, J., Kadlec, K., Wang, Y., Brenner Michael, G., Feßler, A.T. and Vester, B. (2016) 'Lincosamides, Streptogramins, Phenicols, and Pleuromutilins: Mode of Action and Mechanisms of Resistance', *Cold Spring Harbor Perspectives in Medicine*, 6(11), p. a027037. Available at: https://doi.org/10.1101/cshperspect.a027037.

Seemann, T. (2014) 'Prokka: Rapid prokaryotic genome annotation', *Bioinformatics*, 30(14), pp. 2068–2069. Available at: https://doi.org/10.1093/bioinformatics/btu153.

Seeman, T. (2015) 'Snippy: fast bacterial variant calling from NGS reads'. Available at: https://github.com/tseemann/snippy

Sekizuka, T., Inamine, Y., Segawa, T. and Kuroda, M. (2019) 'Characterization of NDM-5-and CTX-M-55-coproducing Escherichia coli GSH8M-2 isolated from the effluent of a wastewater treatment plant in Tokyo Bay', *Infection and Drug Resistance*, 12, pp. 2243–2249. Available at: https://doi.org/10.2147/IDR.S215273.

Senda, K., Arakawa, Y., Ichiyama, S., Nakashima, K., Ito, H., Ohsuka, S., Shimokata, K., Kato, N. and Ohta, M. (1996) 'PCR detection of metallo-beta-

lactamase gene (blaIMP) in gram-negative rods resistant to broad-spectrum beta-lactams.', *Journal of Clinical Microbiology*, 34(12), pp. 2909–2913.

Serio, A.W., Keepers, T., Andrews, L. and Krause, K.M. (2018) 'Aminoglycoside Revival: Review of a Historically Important Class of Antimicrobials Undergoing Rejuvenation', *EcoSal Plus*, 8:1. Available at: https://doi.org/10.1128/ecosalplus.esp-0002-2018

Sheppard, A.E., Stoesser, N., Wilson, D.J., Sebra, R., Kasarskis, A., Anson, L.W., Giess, A., Pankhurst, L.J., Vaughan, A., Grim, C.J., Cox, H.L., Yeh, A.J., the Modernising Medical Microbiology (MMM) Informatics Group, Sifri, C.D., Walker, A.S., Peto, T.E., Crook, D.W. and Mathers, A.J. (2016) 'Nested Russian Doll-Like Genetic Mobility Drives Rapid Dissemination of the Carbapenem Resistance Gene blaKPC', *Antimicrobial Agents and Chemotherapy*, 60(6), pp. 3767–3778. Available at: https://doi.org/10.1128/aac.00464-16.

Sherchan, J.B., Tada, T., Shrestha, S., Uchida, H., Hishinuma, T., Morioka, S., Shahi, R.K., Bhandari, S., Twi, R.T., Kirikae, T. and Sherchand, J.B. (2020) 'Emergence of clinical isolates of highly carbapenem-resistant Klebsiella pneumoniae co-harboring blaNDM-5 and blaOXA-181 or -232 in Nepal', *International Journal of Infectious Diseases*, 92, pp. 247–252. Available at: https://doi.org/10.1016/j.ijid.2020.01.040.

Shnaiderman-Torban, Navon-Venezia S, R, D., Z, D., M, T., Y, P., N, E. and A, S. (2020) 'CTX-M-15 Producing Escherichia coli Sequence Type 361 and Sequence Type 38 Causing Bacteremia and Umbilical Infection in a Neonate Foal', *Journal of equine veterinary science*, 85. Available at: https://doi.org/10.1016/J.JEVS.2019.102881.

Shree, P., Singh, C.K., Sodhi, K.K., Surya, J.N. and Singh, D.K. (2023) 'Biofilms: Understanding the structure and contribution towards bacterial resistance in antibiotics', *Medicine in Microecology*, 16, p. 100084. Available at: https://doi.org/10.1016/j.medmic.2023.100084.

Shrestha, B., Tada, T., Shimada, K., Shrestha, S., Ohara, H., Pokhrel, B.M., Sherchand, J.B. and Kirikae, T. (2017) 'Emergence of Various NDM-Type-Metallo-β-Lactamase-Producing Escherichia coli Clinical Isolates in Nepal', *Antimicrobial Agents and Chemotherapy*, 61(12). Available at: https://doi.org/10.1128/AAC.01425-17.

Siguier, P., Gagnevin, L. and Chandler, M. (2009) 'The new IS1595 family, its relation to IS1 and the frontier between insertion sequences and transposons', *Research in Microbiology*, 160(3), pp. 232–241. Available at: https://doi.org/10.1016/j.resmic.2009.02.003.

Siguier, P., Gourbeyre, E., Varani, A., Ton-Hoang, B. and Chandler, M. (2015) 'Everyman's Guide to Bacterial Insertion Sequences', *Microbiology Spectrum*, 3(2), p. 10.1128/microbiolspec.mdna3-0030–2014. Available at: https://doi.org/10.1128/microbiolspec.mdna3-0030-2014.

Siguier, P., Perochon, J., Lestrade, L., Mahillon, J. and Chandler, M. (2006) 'ISfinder: the reference centre for bacterial insertion sequences', *Nucleic Acids Research*, 34(Database issue), pp. D32-36. Available at: https://doi.org/10.1093/nar/gkj014.

Singh, A.K., Carette, X., Potluri, L.P., Sharp, J.D., Xu, R., Prisic, S. and Husson, R.N. (2016) 'Investigating essential gene function in Mycobacterium tuberculosis using an efficient CRISPR interference system', *Nucleic Acids Research*, 44(18), p. e143. Available at: https://doi.org/10.1093/NAR/GKW625.

Sköld, O. (2000) 'Sulfonamide resistance: mechanisms and trends', *Drug Resistance Updates*, 3(3), pp. 155–160. Available at: https://doi.org/10.1054/drup.2000.0146.

Smalla, K., Heuer, H., Gotz, A., Niemeyer, D., Krogerrecklenfort, E. and Tietze, E. (2000) 'Exogenous Isolation of Antibiotic Resistance Plasmids from Piggery Manure Slurries Reveals a High Prevalence and Diversity of IncQ-Like Plasmids', *Applied and Environmental Microbiology*, 66(11), p. 4854. Available at: https://doi.org/10.1128/AEM.66.11.4854-4862.2000.

Sneader, W. (2001) 'History of Sulfonamides', in *Encyclopedia of Life Sciences*. Chichester: John Wiley & Sons, Ltd. Available at: https://doi.org/10.1038/npg.els.0003625.

Solovyev, V. and Salamov, A. (2011) 'Automatic Annotation of Microbial Genomes and Metagenomic Sequences', in R.W. Li (ed.) *Metagenomics and its Applications in Agriculture, Biomedicine and Environmental Studies*. Nova Science Publishers.

Sougakoff, W., Goussard, S. and Courvalin, P. (1988) 'The TEM-3 Î²-lactamase, which hydrolyzes broad-spectrum cephalosporins, is derived from the TEM-2 penicillinase by two amino acid substitutions', *FEMS Microbiology Letters*, 56(3), pp. 343–348. Available at: https://doi.org/10.1111/j.1574-6968.1988.tb03204.x.

Spencer, S.J., Tamminen, M.V., Preheim, S.P., Guo, M.T., Briggs, A.W., Brito, I.L., A Weitz, D., Pitkänen, L.K., Vigneault, F., Virta, M.P. and Alm, E.J. (2016) 'Massively parallel sequencing of single cells by epicPCR links functional genes with phylogenetic markers', *ISME Journal*, 10(2), pp. 427–436. Available at: https://doi.org/10.1038/ismej.2015.124.

Spížek, J. and Řezanka, T. (2017) 'Lincosamides: Chemical structure, biosynthesis, mechanism of action, resistance, and applications', *Biochemical Pharmacology,* 133, pp. 20-28. Available at: https://doi.org/10.1016/j.bcp.2016.12.001

Spratt, B.G. (1975) 'Distinct penicillin binding proteins involved in the division, elongation, and shape of Escherichia coli K12.', *Proceedings of the National*

Academy of Sciences of the United States of America, 72(8), pp. 2999–3003. Available at: https://doi.org/10.1073/pnas.72.8.2999.

Spratt, B.G. (1977) 'Properties of the Penicillin-Binding Proteins of Escherichia coli K12', *European Journal of Biochemistry*, 72(2), pp. 341–352. Available at: https://doi.org/10.1111/j.1432-1033.1977.tb11258.x.

Stalder, T., Press, M.O., Sullivan, S., Liachko, I. and Top, E.M. (2019) 'Linking the resistome and plasmidome to the microbiome', *ISME Journal*, 13(10), pp. 2437–2446. Available at: https://doi.org/10.1038/s41396-019-0446-4.

Stapleton, P.D. and Taylor, P.W. (2002) 'Methicillin resistance in Staphylococcus aureus: mechanisms and modulation', *Science Progress*, 85(Pt 1), pp. 57-72. Available at: https://doi.org/10.3184/003685002783238870

Stoesser, N., Sheppard, A.E., Pankhurst, L., De Maio, N., Moore, C.E., Sebra, R., Turner, P., Anson, L.W., Kasarskis, A., Batty, E.M., Kos, V., Wilson, D.J., Phetsouvanh, R., Wyllie, D., Sokurenko, E., Manges, A.R., Johnson, T.J., Price, L.B., Peto, T.E.A., Johnson, J.R., Didelot, X., Walker, A.S., Crook, D.W. and Modernizing Medical Microbiology Informatics Group (MMMIG), M.M.M.I.G. (2016) 'Evolutionary History of the Global Emergence of the Escherichia coli Epidemic Clone ST131.', *mBio*, 7(2), p. e02162. Available at: https://doi.org/10.1128/mBio.02162-15.

Strebhardt, K. and Ullrich, A. (2008) 'Paul Ehrlich's magic bullet concept: 100 years of progress', *Nature Reviews Cancer*, 8(6), pp. 473–480. Available at: https://doi.org/10.1038/nrc2394.

Su, J.Q., An, X.L., Li, B., Chen, Q.L., Gillings, M.R., Chen, H., Zhang, T. and Zhu, Y.G. (2017) 'Metagenomics of urban sewage identifies an extensively shared antibiotic resistome in China', *Microbiome*, 5(1), pp. 1–15. Available at: https://doi.org/10.1186/S40168-017-0298-Y/FIGURES/7.

Subirats, J., Royo, E., Balcázar, J.L. and Borrego, C.M. (2017) 'Real-time PCR assays for the detection and quantification of carbapenemase genes (bla KPC, bla NDM, and bla OXA-48) in environmental samples', *Environmental Science and Pollution Research*, 24(7), pp. 6710–6714. Available at: https://doi.org/10.1007/s11356-017-8426-6.

Sugawara, Y., Akeda, Y., Sakamoto, N., Takeuchi, D., Motooka, D., Nakamura, S., Hagiya, H., Yamamoto, N., Nishi, I., Yoshida, H., Okada, K., Zin, K.N., Aye, M.M., Tonomo, K. and Hamada, S. (2017) 'Genetic characterization of blaNDM-harboring plasmids in carbapenem-resistant Escherichia coli from Myanmar', *PLoS ONE*, 12(9), p. e0184720. Available at: https://doi.org/10.1371/journal.pone.0184720.

Sullivan, M.J., Petty, N.K. and Beatson, S.A. (2011) 'Easyfig: a genome comparison visualizer', *Bioinformatics*, 27(7), p. 1009. Available at: https://doi.org/10.1093/BIOINFORMATICS/BTR039.

Sun, L., Xu, J. and He, F. (2019) 'Genomic characterisation of a Proteus mirabilis clinical isolate from China carrying blaNDM-5 on an IncX3 plasmid', *Journal of global antimicrobial resistance*, 19, pp. 317–319. Available at: https://doi.org/10.1016/J.JGAR.2019.10.025.

Tamma, P.D., Doi, Y., Bonomo, R.A., Johnson, J.K., Simner, P.J., and Antibacterial Resistance Leadership Group (2019) 'A Primer on AmpC β-Lactamases: Necessary Knowledge for an Increasingly Multidrug-resistant World', *Clinical Infectious Diseases*, 69(8), pp. 1446–1455. Available at: https://doi.org/10.1093/cid/ciz173.

Tao, G., Tan, H. and Chen, Q. (2023) 'The First Report of *Escherichia coli* and *Klebsiella pneumoniae* Strains That Produce Both NDM-5 and OXA-181 in Jiangsu Province, China', *Infection and drug resistance*, 16, pp. 3245–3255. Available at: https://doi.org/10.2147/idr.s412678.

Tenson, T., Lovmar, M. and Ehrenberg, M. (2003) 'The Mechanism of Action of Macrolides, Lincosamides and Streptogramin B Reveals the Nascent Peptide Exit Path in the Ribosome', *Journal of Molecular Biology,* 330 (5), pp. 1005-1014. Available at: https://doi.org/10.1016/S0022-2836(03)00662-4

Tetzschner, A.M.M., Johnson, J.R., Johnston, B.D., Lund, O. and Scheutz, F. (2020) 'In Silico genotyping of Escherichia coli isolates for extraintestinal virulence genes by use of whole-genome sequencing data', *Journal of Clinical Microbiology*, 58(10). Available at: https://doi.org/10.1128/JCM.01269-20.

Thanassi, D.G., Cheng, L.W. and Nikaido, H. (1997) 'Active efflux of bile salts by Escherichia coli', *Journal of Bacteriology*, 179(8), pp. 2512–2518. Available at: https://doi.org/10.1128/jb.179.8.2512-2518.1997.

The Galaxy Community (2024) 'The Galaxy platform for accessible, reproducible, and collaborative data analyses: 2024 update', *Nucleic Acids Research*, 52(W1), pp. W83–W94. Available at: https://doi.org/10.1093/nar/gkae410Thorpe, H., Booton, R., Kallonen, T., Gibbon, M.J., Couto, N., Passet, V., Fernandez, J.S.L., Rodrigues, C., Matthews, L., Mitchell, S., Reeve, R., David, S., Merla, C., Corbella, M., Ferrari, C., Comandatore, F., Marone, P., Brisse, S., Sassera, D., Corander, J. and Feil, E.J. (2021) 'One Health or Three? Transmission modelling of Klebsiella isolates reveals ecological barriers to transmission between humans, animals and the environment'. bioRxiv, p. 2021.08.05.455249. Available at: https://doi.org/10.1101/2021.08.05.455249.

Tian, C., Shi, Y., Ren, L., Huang, D., Wang, S., Zhao, Y., Fu, L., Bai, Y., Xia, D. and Fan, X. (2023) 'Emergence of IS26-mediated pLVPK-like virulence and NDM-1 conjugative fusion plasmid in hypervirulent carbapenem-resistant Klebsiella pneumoniae', *Infection, Genetics and Evolution*, 113, p. 105471. Available at: https://doi.org/10.1016/j.meegid.2023.105471.

Tiwari, A., Kurittu, P., Al-Mustapha, A.I., Heljanko, V., Johansson, V., Thakali, O., Mishra, S.K., Lehto, K.-M., Lipponen, A., Oikarinen, S., Pitkänen, T., WastPan Study Group, Heikinheimo, A., Länsivaara, A., Hyder, R., Janhonen, E., Hokajärvi, A.-M., Sarekoski, A., Kolehmainen, A., Blomqvist, S., Räisänen, K., Kopra, C.S., Möttönen, T., Luomala, O., Juutinen, A., Thakali, O. and Mishra, S.K. (2022) 'Wastewater surveillance of antibiotic-resistant bacterial pathogens: A systematic review', *Frontiers in Microbiology*, 13. Available at: https://www.frontiersin.org/articles/10.3389/fmicb.2022.977106 (Accessed: 19 December 2023).

Toleman, M.A., Bennett, P.M. and Walsh, T.R. (2006a) 'Common regions e.g. orf513 and antibiotic resistance: IS91-like elements evolving complex class 1 integrons', *Journal of Antimicrobial Chemotherapy*, 58(1), pp. 1–6. Available at: https://doi.org/10.1093/jac/dkl204.

Toleman, M.A., Bennett, P.M. and Walsh, T.R. (2006b) 'ISCR Elements: Novel Gene-Capturing Systems of the 21st Century?', *Microbiology and Molecular Biology Reviews*, 70(2), pp. 296–316. Available at: https://doi.org/10.1128/MMBR.00048-05.

Toleman, M.A., Spencer, J., Jones, L. and Walsh, T.R. (2012) 'blaNDM-1 Is a Chimera Likely Constructed in Acinetobacter baumannii', *Antimicrobial Agents and Chemotherapy*, 56(5), p. 2773. Available at: https://doi.org/10.1128/AAC.06297-11.

Traglia, G.M., Place, K., Dotto, C., Fernandez, J.S., Montaña, S., Bahiense, C. dos S., Soler-Bistue, A., Iriarte, A., Perez, F., Tolmasky, M.E., Bonomo, R.A., Melano, R.G. and Ramírez, M.S. (2019) 'Interspecies DNA acquisition by a naturally competent Acinetobacter baumannii strain', *International Journal of Antimicrobial Agents*, 53(4), pp. 483–490. Available at: https://doi.org/10.1016/j.ijantimicag.2018.12.013.

Tran, T.T., Munita, J.M. and Arias, C.A. (2015) 'Mechanisms of drug resistance: daptomycin resistance', *Annals of the New York Academy of Sciences*,1354, pp. 32-53. Available at: https://doi.org/10.1111/nyas.12948.

Trimble, M.J., Mlynárčik, P., Kolář, M. and Hancock, R.E.W. (2016) 'Polymyxin: Alternative Mechanisms of Action and Resistance', *Cold Spring Harbor Perspectives in Medicine*, 6(10), p. a025288. Available at: https://doi.org/10.1101/cshperspect.a025288.

Turton, Jane, Davies, F., Turton, Jack, Perry, C., Payne, Z. and Pike, R. (2019) 'Hybrid Resistance and Virulence Plasmids in "High-Risk" Clones of Klebsiella pneumoniae, Including Those Carrying blaNDM-5', *Microorganisms*, 7(9). Available at: https://doi.org/10.3390/MICROORGANISMS7090326.

Turton, J.F., Pike, R., Perry, C., Jenkins, C., Turton, J.A., Meunier, D. and Hopkins, K.L. (2022) 'Wide distribution of Escherichia coli carrying IncF plasmids containing bla NDM-5 and rmtB resistance genes from hospitalized patients in

England', *Journal of medical microbiology*, 71(8). Available at: https://doi.org/10.1099/JMM.0.001569.

Tymoszewska, A., Szylińska, M. and Aleksandrzak-Piekarczyk, T. (2023) 'The LiaFSR-LiaX System Mediates Resistance of Enterococcus faecium to Peptide Antibiotics and to Aureocin A53- and Enterocin L50-Like Bacteriocins', *Microbiology Spectrum*, 11(3), pp. e00343-23. Available at: https://doi.org/10.1128/spectrum.00343-23.

Typas, A., Banzhaf, M., Gross, C. and Vollmer, W. (2012) 'From the regulation of peptidoglycan synthesis to bacterial growth and morphology', *Nature Reviews Microbiology,* 10, pp. 123–136. Available at: https://doi.org/10.1038/nrmicro2677

UKHSA (2020) 'Framework of actions to contain carbapenemase-producing Enterobacterales'. Available at: https://www.gov.uk/government/publications/actions-to-contain-carbapenemase-producing-enterobacterales-cpe (Accessed: 8 September 2021).

UKHSA (2021) *Acquired carbapenemase-producing Gram-negative bacteria in England: October 2020 to September 2021*. Available at: https://www.gov.uk/government/publications/carbapenemase-producing-gram-negative-bacteria-laboratory-surveillance.

UKHSA (2023) *Acquired carbapenemase-producing Gram-negative bacteria in England: October 2020 to March 2023*, *Health Protection Report*. Available at: https://www.gov.uk/government/publications/carbapenemase-producing-gram-negative-bacteria-laboratory-surveillance.

UKWIR (2022) 'The National Chemical Investigations Programme, 2020-2022, Volume 1, Investigations into Changes to Antimicrobial Resistance through Wastewater and Sludge Treatment Processes'.

UN News (2018) *Antimicrobial resistance a 'global health emergency,' UN, ahead of awareness week | UN News*. Available at: https://news.un.org/en/node/1025511/antimicrobial-resistance-a-global-health-emergency-un-ahead-of-awareness-week-2 (Accessed: 29 July 2019).

UNESCO (2017) *The United Nations world water development report, 2017: Wastewater: the untapped resource*. Available at: https://unesdoc.unesco.org/ark:/48223/pf0000247153?posInSet=1&queryId=719a7c03-6247-4548-801c-218d5ff430ab (Accessed: 18 December 2023).

UNESCO (2023) *The United Nations World Water Development Report 2023: Partnerships and cooperation for water*. Available at: https://unesdoc.unesco.org/ark:/48223/pf0000384655 (Accessed: 18 December 2023).

Unterholzner, S.J., Poppenberger, B. and Rozhon, W. (2013) 'Toxin–antitoxin systems', *Mobile Genetic Elements*, 3(5), p. e26219. Available at: https://doi.org/10.4161/mge.26219.

Varani, A., He, S., Siguier, P., Ross, K. and Chandler, M. (2021) 'The IS6 family, a clinically important group of insertion sequences including IS26', *Mobile DNA*, 12(1). Available at: https://doi.org/10.1186/S13100-021-00239-X.

Varani, A., He, S., Siguier, P., Ross, K. and Chandler, M. (2022) 'Response from Varani et al. to "Comment on 'the IS6 family, a clinically important group of insertion sequences including IS26' by Ruth M. Hall"', *Mobile DNA*, 13(1), p. 2. Available at: https://doi.org/10.1186/s13100-021-00258-8.

Vázquez-Laslop, N. and Mankin, A.S. (2018) 'How macrolide antibiotics work', *Trends in biochemical sciences*, 43(9), pp. 668–684. Available at: https://doi.org/10.1016/j.tibs.2018.06.011.

Veening, J.-W. and Blokesch, M. (2017) 'Interbacterial predation as a strategy for DNA acquisition in naturally competent bacteria', *Nature Reviews Microbiology*, 15(10), pp. 621–629. Available at: https://doi.org/10.1038/nrmicro.2017.66.

Ventola, C.L. (2015) 'The Antibiotic Resistance Crisis', *Pharmacy and Therapeutics*, 40(4), pp. 277–283.

Vetting, M.W., Park, C.H., Hegde, S.S., Jacoby, G.A., Hooper, D.C. and Blanchard, J.S. (2008) 'Mechanistic and Structural Analysis of Aminoglycoside N-Acetyltransferase AAC(6')-Ib and Its Bifunctional, Fluoroquinolone-Active AAC(6')-Ib-cr Variant', *Biochemistry*, 47(37), pp. 9825–9835. Available at: https://doi.org/10.1021/bi800664x.

Villa, L., García-Fernández, A., Fortini, D. and Carattoli, A. (2010) 'Replicon sequence typing of IncF plasmids carrying virulence and resistance determinants', *Journal of Antimicrobial Chemotherapy*, 65(12), pp. 2518–2529. Available at: https://doi.org/10.1093/jac/dkq347.

Virolle, C., Goldlust, K., Djermoun, S., Bigot, S. and Lesterlin, C. (2020) 'Plasmid Transfer by Conjugation in Gram-Negative Bacteria: From the Cellular to the Community Level', *Genes*, 11(11), p. 1239. Available at: https://doi.org/10.3390/genes11111239.

Vollmer, W., Blanot, D. and De Pedro, M.A. (2008) 'Peptidoglycan structure and architecture', *FEMS Microbiology Reviews*, 32, pp. 149-167. Available at: https://doi.org/10.1111/j.1574-6976.2007.00094.x

Wachino, J., Yamane, K., Kimura, K., Shibata, N., Suzuki, S., Ike, Y. and Arakawa, Y. (2006) 'Mode of transposition and expression of 16S rRNA methyltransferase gene rmtC accompanied by ISEcp1', *Antimicrobial Agents and Chemotherapy*, 50(9), pp. 3212–3215. Available at: https://doi.org/10.1128/AAC.00550-06.

Walker-Sünderhauf, D., Klümper, U., Pursey, E., Westra, E.R., Gaze, W.H. and van Houte, S. (2023) 'Removal of AMR plasmids using a mobile, broad host-range CRISPR-Cas9 delivery tool', *Microbiology (Reading, England)*, 169(5), p. 001334. Available at: https://doi.org/10.1099/MIC.0.001334/CITE/REFWORKS.

Wallden, K., Rivera-Calzada, A. and Waksman, G. (2010) 'Type IV secretion systems: versatility and diversity in function', *Cellular Microbiology*, 12(9), pp. 1203–1212. Available at: https://doi.org/10.1111/j.1462-5822.2010.01499.x.

Wallinga, D., Smit, L.A.M., Davis, M.F., Casey, J.A. and Nachman, K.E. (2022) 'A Review of the Effectiveness of Current US Policies on Antimicrobial Use in Meat and Poultry Production', *Current Environmental Health Reports*, 9(2), pp. 339–354. Available at: https://doi.org/10.1007/s40572-022-00351-x.

Walsh, F. and Duffy, B. (2013) 'The Culturable Soil Antibiotic Resistome: A Community of Multi-Drug Resistant Bacteria', *PLoS ONE*. Edited by A.M. Ibekwe, 8(6), p. e65567. Available at: https://doi.org/10.1371/journal.pone.0065567.

Walsh, T.R. (2010) 'Emerging carbapenemases: a global perspective', *International Journal of Antimicrobial Agents*, 36, pp. S8–S14. Available at: https://doi.org/10.1016/S0924-8579(10)70004-2.

Walsh, T.R., Toleman, M.A., Poirel, L. and Nordmann, P. (2005) 'Metallo-β-Lactamases: the Quiet before the Storm?', *Clinical Microbiology Reviews*, 18(2), pp. 306–325. Available at: https://doi.org/10.1128/CMR.18.2.306-325.2005.

Walsh, T.R., Weeks, J., Livermore, D.M. and Toleman, M.A. (2011) 'Dissemination of NDM-1 positive bacteria in the New Delhi environment and its implications for human health: an environmental point prevalence study', *The Lancet. Infectious Diseases*, 11(5), pp. 355–362. Available at: https://doi.org/10.1016/S1473-3099(11)70059-7.

Wang, H., Wang, M., Fan, S., Lu, J., Lan, Y., Li, M., Li, J., Liu, R., Sun, J., Fang, J., Qian, P.-Y., Zhang, Y.-Z. and Zhang, W. (2021) 'Culture Enrichment Combined With Long-Read Sequencing Facilitates Genomic Understanding of Hadal Sediment Microbes', *Frontiers in Marine Science*, 8. Available at: https://www.frontiersin.org/articles/10.3389/fmars.2021.754332 (Accessed: 19 December 2023).

Wang, R., van Dorp, L., Shaw, L.P., Bradley, P., Wang, Q., Wang, X., Jin, L., Zhang, Q., Liu, Y., Rieux, A., Dorai-Schneiders, T., Weinert, L.A., Iqbal, Z., Didelot, X., Wang, H. and Balloux, F. (2018) 'The global distribution and spread of the mobilized colistin resistance gene mcr-1', *Nature Communications*, 9(1), p. 1179. Available at: https://doi.org/10.1038/s41467-018-03205-z.

Wang, X.-C., Lei, C.-W., Kang, Z.-Z., Zhang, Y. and Wang, H.-N. (2019) 'IS26-Mediated Genetic Rearrangements in Salmonella Genomic Island 1 of Proteus

mirabilis', *Frontiers in Microbiology*, 10, p. 2245. Available at: https://doi.org/10.3389/fmicb.2019.02245.

Wang, Y.L., Liu, S., Yu, Z.J., Lei, Y., Huang, M.Y., Yan, Y.H., Ma, Q., Zheng, Y., Deng, H., Sun, Y., Wu, C., Yu, Y., Chen, Q., Wang, Z., Wu, Y. and Li, G.B. (2019) 'Structure-Based Development of (1-(3'-Mercaptopropanamido)methyl)boronic Acid Derived Broad-Spectrum, Dual-Action Inhibitors of Metallo- and Serine-β-lactamases', *Journal of Medicinal Chemistry*, 62(15), pp. 7160-7184. Available ati: https://doi.org/10.1021/acs.jmedchem.9b00735.

Watanabe, M., Iyobe, S., Inoue, M. and Mitsuhashi, S. (1991) 'Transferable imipenem resistance in Pseudomonas aeruginosa.', *Antimicrobial agents and chemotherapy*, 35(1), pp. 147–51. Available at: https://doi.org/10.1128/aac.35.1.147.

Watanabe, M., Nakano, R., Tanouchi, A., Nakano, A., Suzuki, Y., Saito, K., Sakata, R., Ogawa, M. and Yano, H. (2022) 'Emergence and Evolution of Unique Plasmids Harboring blaIMP-70 and blaCTX-M-253 in Multidrug-Resistant Providencia rettgeri', *Microbiology Spectrum*, 10(4), pp. e01204-22. Available at: https://doi.org/10.1128/spectrum.01204-22.

Watve, M., Tickoo, R., Jog, M. and Bhole, B. (2001) 'How many antibiotics are produced by the genus Streptomyces ?', *Archives of Microbiology*, 176(5), pp. 386–390. Available at: https://doi.org/10.1007/s002030100345.

WEF (2021) *Antimicrobial Resistance and Water: The risks and costs for economies and societies*. World Economic Forum. Available at: https://www3.weforum.org/docs/WEF_Antimicrobial_Resistance_and_Water_2021.pdf (Accessed: 23 October 2023).

Wei, D.W., Wong, N.K., Song, Y., Zhang, G., Wang, C., Li, J. and Feng, J. (2022) 'IS26 Veers Genomic Plasticity and Genetic Rearrangement toward Carbapenem Hyperresistance under Sublethal Antibiotics', *mBio*, 13(1). Available at: https://doi.org/10.1128/MBIO.03340-21.

Weill, F.X., Demartin, M., Tandé, D., Espié, E., Rakotoarivony, I. and Grimont, P.A.D. (2004) 'SHV-12-Like Extended-Spectrum-β-Lactamase-Producing Strains of Salmonella enterica Serotypes Babelsberg and Enteritidis Isolated in France among Infants Adopted from Mali', *Journal of Clinical Microbiology*, 42(6), p. 2432. Available at: https://doi.org/10.1128/JCM.42.6.2432-2437.2004.

Weisburg, W.G., Barns, S.M., Pelletier, D.A. and Lane, D.J. (1991) '16S Ribosomal DNA Amplification for Phylogenetic Study', *Journal of Bacteriology*, 173(2), pp. 697–703.

Whelan, F.J., Waddell, B., Syed, S.A., Shekarriz, S., Rabin, H.R., Parkins, M.D. and Surette, M.G. (2020) 'Culture-enriched metagenomic sequencing enables

in-depth profiling of the cystic fibrosis lung microbiota', *Nature Microbiology*, 5(2), pp. 379–390. Available at: https://doi.org/10.1038/s41564-019-0643-y.

White, L., Hopkins, K.L., Meunier, D., Perry, C.L., Pike, R., Wilkinson, P., Pickup, R.W., Cheesbrough, J. and Woodford, N. (2016) 'Carbapenemase-producing Enterobacteriaceae in hospital wastewater: a reservoir that may be unrelated to clinical isolates', *Journal of Hospital Infection*, 93(2), pp. 145–151. Available at: https://doi.org/10.1016/j.jhin.2016.03.007.

WHO (2016) *WHO Director-General briefs UN on antimicrobial resistance*. World Health Organization. Available at: https://www.who.int/dg/speeches/2016/antimicrobial-resistance-un/en/ (Accessed: 29 July 2019).

WHO (2017) *WHO publishes list of bacteria for which new antibiotics are urgently needed*. Available at: https://www.who.int/news-room/detail/27-02-2017-who-publishes-list-of-bacteria-for-which-new-antibiotics-are-urgently-needed (Accessed: 29 July 2019).

WHO (2020) *Technical brief on water, sanitation, hygiene (WASH) and wastewater management to prevent infections and reduce the spread of antimicrobial resistance (AMR)*. Available at: https://www.who.int/publications-detail-redirect/9789240006416 (Accessed: 18 December 2023).

WHO (2021) *Antimicrobial resistance*. Available at: https://www.who.int/news-room/fact-sheets/detail/antimicrobial-resistance (Accessed: 19 November 2023).

WHO (2023) *Global Antimicrobial Resistance and Use Surveillance System (GLASS)*. Available at: https://www.who.int/initiatives/glass (Accessed: 23 December 2023).

Wick, R.R., Judd, L.M., Gorrie, C.L. and Holt, K.E. (2017a) 'Completing bacterial genome assemblies with multiplex MinION sequencing', *Microbial genomics*, 3(10). Available at: https://doi.org/10.1099/MGEN.0.000132.

Wick, R.R., Judd, L.M., Gorrie, C.L. and Holt, K.E. (2017b) 'Unicycler: Resolving bacterial genome assemblies from short and long sequencing reads', *PLoS Computational Biology*, 13(6). Available at: https://doi.org/10.1371/journal.pcbi.1005595.

Wiegand, I., Hilpert, K. and Hancock, R.E.W. (2008) 'Agar and broth dilution methods to determine the minimal inhibitory concentration (MIC) of antimicrobial substances', *Nature Protocols 2008 3:2*, 3(2), pp. 163–175. Available at: https://doi.org/10.1038/nprot.2007.521.

Wilson, D.N. (2014) 'Ribosome-targeting antibiotics and mechanisms of bacterial resistance', *Nature Reviews Microbiology*, 12(1), pp. 35–48. Available at: https://doi.org/10.1038/nrmicro3155.

Wilson, D.N., Hauryliuk, V., Atkinson, G.C. and O'Neill, A.J. (2020) 'Target protection as a key antibiotic resistance mechanism', *Nature Reviews Microbiology*, 18(11), pp. 637–648. Available at: https://doi.org/10.1038/s41579-020-0386-z.

Winau, F., Westphal, O. and Winau, R. (2004) 'Paul Ehrlich — in search of the magic bullet', *Microbes and Infection*, 6(8), pp. 786–789. Available at: https://doi.org/10.1016/J.MICINF.2004.04.003.

Winter, M., Buckling, A., Harms, K., Johnsen, P.J. and Vos, M. (2021) 'Antimicrobial resistance acquisition via natural transformation: context is everything', *Current Opinion in Microbiology*, 64, pp. 133–138. Available at: https://doi.org/10.1016/j.mib.2021.09.009.

Wirth, T., Falush, D., Lan, R., Colles, F., Mensa, P., Wieler, L.H., Karch, H., Reeves, P.R., Maiden, M.C.J., Ochman, H. and Achtman, M. (2006) 'Sex and virulence in Escherichia coli: an evolutionary perspective', *Molecular microbiology*, 60(5), pp. 1136–1151. Available at: https://doi.org/10.1111/J.1365-2958.2006.05172.X.

Womble, D.D. and Rownd, R.H. (1988) 'Genetic and Physical Map of Plasmid NR1: Comparison with Other IncFII Antibiotic Resistance Plasmids', *Microbiological Reviews*, 52(4), pp. 433–451.

Wong, M.H., Chan, E.W. and Chen, S. (2017) 'IS26-mediated formation of a virulence and resistance plasmid in Salmonella Enteritidis', *Journal of Antimicrobial Chemotherapy*, 72(10), pp. 2750–2754. Available at: https://doi.org/10.1093/jac/dkx238.

Woodford, N., Carattoli, A., Karisik, E., Underwood, A., Ellington, M.J. and Livermore, D.M. (2009) 'Complete nucleotide sequences of plasmids pEK204, pEK499, and pEK516, encoding CTX-M enzymes in three major Escherichia coli lineages from the United Kingdom, all belonging to the international O25:H4-ST131 clone', *Antimicrobial agents and chemotherapy*, 53(10), pp. 4472–4482. Available at: https://doi.org/10.1128/AAC.00688-09.

Woodford, N. and Ellington, M.J. (2007) 'The emergence of antibiotic resistance by mutation', *Clinical Microbiology and Infection*, 13(1), pp. 5–18. Available at: https://doi.org/10.1111/j.1469-0691.2006.01492.x.

Woodford, N., Ward, M.E., Kaufmann, M.E., Turton, J., Fagan, E.J., James, D., Johnson, A.P., Pike, R., Warner, M., Cheasty, T., Pearson, A., Harry, S., Leach, J.B., Loughrey, A., Lowes, J.A., Warren, R.E. and Livermore, D.M. (2004) 'Community and hospital spread of Escherichia coli producing CTX-M extended-spectrum β-lactamases in the UK', *Journal of Antimicrobial*

Chemotherapy, 54(4), pp. 735–743. Available at: https://doi.org/10.1093/jac/dkh424.

Wu, W., Feng, Y., Tang, G., Qiao, F., McNally, A. and Zong, Z. (2019) 'NDM Metallo-β-Lactamases and Their Bacterial Producers in Health Care Settings', *Clinical Microbiology Reviews*, 32(2). Available at: https://doi.org/10.1128/CMR.00115-18.

Wyrsch, E.R., Hawkey, J., Judd, L.M., Haites, R., Holt, K.E., Djordjevic, S.P. and Billman-Jacobe, H. (2019) 'Z/I1 Hybrid Virulence Plasmids Carrying Antimicrobial Resistance genes in S. Typhimurium from Australian Food Animal Production', *Microorganisms*, 7(9), p. 299. Available at: https://doi.org/10.3390/microorganisms7090299.

Yang, F., Mao, D., Zhou, H. and Luo, Y. (2016) 'Prevalence and fate of carbapenemase genes in a wastewater treatment plant in northern China', *PLoS ONE*, 11(5). Available at: https://doi.org/10.1371/journal.pone.0156383.

Yang, Y.J., Wu, P.J. and Livermore, D.M. (1990) 'Biochemical characterization of a beta-lactamase that hydrolyzes penems and carbapenems from two Serratia marcescens isolates.', *Antimicrobial Agents and Chemotherapy*, 34(5), pp. 755–758.

Yi, H., Cho, Y.J., Yong, D. and Chun, J. (2012) 'Genome Sequence of Escherichia coli J53, a Reference Strain for Genetic Studies', *Journal of Bacteriology*, 194(14), p. 3742. Available at: https://doi.org/10.1128/JB.00641-12.

Yigit, H., Queenan, A.M., Anderson, G.J., Domenech-Sanchez, A., Biddle, J.W., Steward, C.D., Alberti, S., Bush, K. and Tenover, F.C. (2001) 'Novel carbapenem-hydrolyzing β-lactamase, KPC-1, from a carbapenem-resistant strain of Klebsiella pneumoniae', *Antimicrobial Agents and Chemotherapy*, 45(4), pp. 1151–1161. Available at: https://doi.org/10.1128/AAC.45.4.1151-1161.2001.

Yong, D., Toleman, M.A., Giske, C.G., Cho, H.S., Sundman, K., Lee, K. and Walsh, T.R. (2009) 'Characterization of a New Metallo- -Lactamase Gene, blaNDM-1, and a Novel Erythromycin Esterase Gene Carried on a Unique Genetic Structure in Klebsiella pneumoniae Sequence Type 14 from India', *Antimicrobial Agents and Chemotherapy*, 53(12), pp. 5046–5054. Available at: https://doi.org/10.1128/AAC.00774-09.

Yosef, I., Manor, M., Kiro, R. and Qimron, U. (2015) 'Temperate and lytic bacteriophages programmed to sensitize and kill antibiotic-resistant bacteria', *Proceedings of the National Academy of Sciences of the United States of America*, 112(23), pp. 7267–7272. Available at: https://doi.org/10.1073/PNAS.1500107112/-/DCSUPPLEMENTAL.

Yu, Z., Zhang, Z., Shi, L., Hua, S., Luan, T., Lin, Q., Zheng, Z., Feng, X., Liu, M. and Li, X. (2022) 'In silico characterization of IncX3 plasmids carrying blaOXA-181 in Enterobacterales', *Frontiers in Cellular and Infection Microbiology*, 12.

Available at: https://www.frontiersin.org/articles/10.3389/fcimb.2022.988236 (Accessed: 4 November 2023).

Zaid Alkilani, A., Hamed, R., Musleh, B., Sharaire, Z. 'Breaking boundaries: the advancements in transdermal delivery of antibiotics', *Drug Delivery*, 31(1), 2304251. Available at: https://doi.org/10.1080/10717544.2024.2304251.

Zaniani, F.R., Meshkat, Z., Nasab, M.N., Khaje-Karamadini, M., Ghazvini, K., Rezaee, A., Esmaily, H., Nabavinia, M.S. and Hoseini, M.D. (2012) 'The Prevalence of TEM and SHV Genes among Extended-Spectrum Beta-Lactamases Producing Escherichia Coli and Klebsiella Pneumoniae', *Iranian Journal of Basic Medical Sciences*, 15(1), p. 654.

Zankari, E., Allesøe, R., Joensen, K.G., Cavaco, L.M., Lund, O. and Aarestrup, F.M. (2017) 'PointFinder: A novel web tool for WGS-based detection of antimicrobial resistance associated with chromosomal point mutations in bacterial pathogens', *Journal of Antimicrobial Chemotherapy*, 72(10), pp. 2764–2768. Available at: https://doi.org/10.1093/jac/dkx217.

Zhanel, G.G., Simor, A. E., Vercaigne, L., and Mandell, L. (1998) 'Imipenem and Meropenem: Comparison of in Vitro Activity, Pharmacokinetics, Clinical Trials and Adverse Effects', *The Canadian journal of infectious diseases = Journal canadien des maladies infectieuses*, 9(4). Available at: https://doi.org/10.1155/1998/831425.

Zhanel, G.G., Wiebe, R., Dilay, L., Thomson, K., Rubinstein, E., Hoban, D.J., Noreddin, A.M. and Karlowsky, J.A. (2007) 'Comparative review of the carbapenems', *Drugs*, 67(7), pp. 1027–1052. Available at: https://doi.org/10.2165/00003495-200767070-00006.

Zhang, B., Yu, Q., Yan, G., Zhu, H., Xu, X.Y. and Zhu, L. (2018) 'Seasonal bacterial community succession in four typical wastewater treatment plants: correlations between core microbes and process performance', *Scientific Reports 2018 8:1*, 8(1), pp. 1–11. Available at: https://doi.org/10.1038/s41598-018-22683-1.

Zhang, Y., Zhang, N., Wang, M., Luo, M., Peng, Y., Li, Z., Xu, J., Ou, M., Kan, B., Li, X. and Lu, X. (2023) 'The prevalence and distribution of aminoglycoside resistance genes', *Biosafety and Health*, 5(1), pp. 14–20. Available at: https://doi.org/10.1016/j.bsheal.2023.01.001.

Zhang, Z., Zhang, G. and Ju, F. (2022) 'Using Culture-Enriched Phenotypic Metagenomics for Targeted High-Throughput Monitoring of the Clinically Important Fraction of the β-Lactam Resistome', *Environmental Science & Technology*, 56(16), pp. 11429–11439. Available at: https://doi.org/10.1021/acs.est.2c03627.

Zhou, Z., Alikhan, N.F., Mohamed, K., Fan, Y. and Achtman, M. (2020) 'The EnteroBase user's guide, with case studies on Salmonella transmissions, Yersinia pestis phylogeny, and Escherichia core genomic diversity', *Genome Research*, 30(1), pp. 138–152. Available at: https://doi.org/10.1101/gr.251678.119.

Zinder, N.D. and Lederberg, J. (1952) 'GENETIC EXCHANGE IN SALMONELLA1', *Journal of Bacteriology*, 64(5), pp. 679–699.

Zogg, A.L., Zurfluh, K., Schmitt, S., Nüesch-Inderbinen, M. and Stephan, R. (2018) 'Antimicrobial resistance, multilocus sequence types and virulence profiles of ESBL producing and non-ESBL producing uropathogenic Escherichia coli isolated from cats and dogs in Switzerland', *Veterinary Microbiology*, 216, pp. 79–84. Available at: https://doi.org/10.1016/J.VETMIC.2018.02.011.

Zurfluh, K., Bagutti, C., Brodmann, P., Alt, M., Schulze, J., Fanning, S., Stephan, R. and Nüesch-Inderbinen, M. (2017) 'Wastewater is a reservoir for clinically relevant carbapenemase- and 16s rRNA methylase-producing Enterobacteriaceae', *International Journal of Antimicrobial Agents*, 50(3), pp. 436–440. Available at: https://doi.org/10.1016/j.ijantimicag.2017.04.017.

CHAPTER 8: APPENDIX

Table 8.1. Antibiotic sensitivity results for strains isolated on agar supplemented with cefotaxime.

Isolate	Species/Genus	Sample Date	Sample Point	AMP	AMC	FOX	CTX	CPD	ATM	MEM	S10	OT	CIP	NA	SXT	C	F	AZM
77	*E. coli*	01/10/2019	Inf A	0	0	0	0	0	16	25	15	0	0	0	0	30	25	0
78	*E. coli*	01/10/2019	Inf A	0	8	13	0	0	13	31	8	0	0	0	28	30	0	18
79	*K. pneumoniae*	01/10/2019	Inf A	0	23	25	0	13	11	30	0	7	23	21	0	0	15	8
80	*E. coli*	01/10/2019	Inf A	0	8	18	0	0	11	30	14	0	29	14	25	29	22	19
81	*Pseudomonas*	01/10/2019	Inf A	0	9	0	0	17	16	34	25	31	35	12	0	22	0	9
82	*Pseudomonas*	01/10/2019	Inf A	0	13	0	0	15	14	30	17	28	30	13	0	24	0	0
83	*E. coli*	01/10/2019	Inf A	0	0	0	0	0	15	25	15	0	0	0	0	31	23	0
84	*K. pneumoniae*	01/10/2019	Inf A	0	22	23	0	11	16	28	0	0	21	20	0	0	16	10
85	*E. coli*	01/10/2019	Inf A	0	20	18	0	0	14	27	14	0	21	24	10	28	20	14
86	*K. pneumoniae*	01/10/2019	Inf A	0	24	25	0	12	17	30	0	0	23	21	0	0	16	9
87	*Escherichia*	01/10/2019	Inf A	0	0	8	0	0	0	27	15	0	0	0	0	30	24	0
88	*K. pneumoniae*	01/10/2019	Inf A	0	22	21	0	0	18	28	0	8	23	19	0	0	16	9
89	*Escherichia*	01/10/2019	Inf A	0	0	24	0	0	0	30	15	28	28	15	28	30	21	19
90	*Escherichia*	01/10/2019	Inf A	0	23	23	0	8	15	32	0	28	21	0	0	32	23	19
91	*Escherichia*	01/10/2019	Inf A	0	0	0	0	0	13	25	14	0	0	0	29	30	23	0
92	*Escherichia*	01/10/2019	Inf A	0	21	23	0	8	16	27	0	8	21	20	0	0	12	10
93	*E. coli*	01/10/2019	Inf A	0	0	22	0	0	14	29	0	23	28	13	11	30	20	17
94	*E. coli*	01/10/2019	Inf A	0	0	25	0	8	13	34	9	0	23	21	0	31	21	0
95	*E. coli*	01/10/2019	Inf A	0	0	23	0	0	10	30	15	26	30	15	29	31	21	0

96	*K. pneumoniae*	01/10/2019	Inf A	0	9	23	0	11	18	29	0	0	22	21	0	0	16	9
97	*Pseudomonas*	01/10/2019	Inf A	0	0	0	0	12	17	32	24	28	33	14	0	21	0	11
98	*E. coli*	01/10/2019	Inf A	0	0	0	0	0	18	26	16	27	0	0	30	30	25	0
99	*E. coli*	01/10/2019	Inf A	0	0	0	0	0	12	24	14	26	0	0	26	30	23	0
100	*Escherichia*	01/10/2019	Inf A	0	0	24	0	0	20	31	15	0	0	0	0	33	21	0
101	*Pseudomonas*	01/10/2019	Inf A	0	0	0	0	10	13	33	15	24	35	12	0	12	0	0
102	*Escherichia coli*	01/10/2019	Inf A	0	0	0	0	0	16	25	11	26	0	0	29	29	24	0
103	*Pseudomonas*	01/10/2019	Inf A	0	9	0	0	9	22	31	19	29	34	12	0	25	0	0
104	*E. coli*	01/10/2019	Inf A	0	0	16	0	8	14	33	15	24	29	25	28	30	22	15
105	*Escherichia*	01/10/2019	Inf A	0	0	22	0	11	12	29	0	7	23	21	0	0	14	9
106	*Pseudomonas*	01/10/2019	Inf A	0	0	0	0	14	9	31	19	25	28	8	0	15	0	0
107	*E. coli*	01/10/2019	Inf A	0	0	20	0	0	0	26	13	25	26	12	25	27	20	15
108	*K. pneumoniae*	01/10/2019	Inf A	0	7	23	0	10	13	29	0	0	22	20	0	0	18	9
109	*Pseudomonas*	01/10/2019	Inf A	0	8	0	0	14	9	33	23	30	32	16	0	22	0	8
244	*Aeromonas*	12.05.22	U	6	17	6	17	6	33	34	16	22	24	6	16	32	22	22
245	*Enterobacter*	12.05.22	D1	6	6	6	6	6	20	30	17	26	30	25	25	27	14	14
246	*Aeromonas*	12.05.22	Eff B	6	10	6	17	6	34	34	15	34	20	7	18	32	27	20
247	*E. coli*	12.05.22	D1	6	14	23	6	6	12	34	16	16	26	6	6	27	21	10
248	*Escherichia*	12.05.22	D2	6	15	23	11	9	20	34	16	31	6	6	25	30	25	21
249	*Escherichia*	12.05.22	Eff B	6	15	20	6	6	14	35	16	17	24	24	24	29	23	19
250	*E. coli*	12.05.22	Eff B	6	16	28	13	6	20	38	18	32	6	8	28	30	21	21
251	*Escherichia*	12.05.22	D2	6	13	24	6	6	14	34	16	30	7	6	28	31	21	21

252	*Pseudomonas*	12.05.22	D2	6	6	6	15	6	11	33	26	32	32	13	6	16	6	14
253	*Pseudomonas*	12.05.22	D2	6	10	6	19	6	22	36	26	34	6	18	15	24	6	6
254	*Ae. media*	12.05.22	Eff B	6	15	6	16	6	28	32	19	20	15	7	18	26	26	20
255	*Ae. media*	12.05.22	Eff B	6	10	6	17	6	34	33	16	33	19	7	19	34	28	20
256	*Ae. media*	12.05.22	Eff B	6	20	11	25	6	32	33	20	20	19	9	11	32	27	19
257	*Escherichia*	12.05.22	Eff B	6	16	25	9	6	15	31	17	15	31	25	29	27	22	20
258	*Escherichia*	12.05.22	Eff B	6	19	25	11	6	18	32	16	30	6	22	26	28	22	20
259	*E. coli*	12.05.22	Eff B	11	20	24	12	6	20	33	15	27	30	27	25	29	18	21
260	*Sten. maltophilia*	12.05.22	Eff B	6	6	6	9	6	6	6	15	25	30	26	26	30	6	17
265	*Pseudomonas*	12.05.22	D1	6	6	6	17	6	15	18	15	25	32	11	6	12	6	6
267	*Escherichia*	05.07.22	D1	6	15	24	12	6	18	30	15	9	6	12	6	29	21	12
268	*E. coli*	05.07.22	D1	6	8	23	7	6	10	30	15	29	22	19	26	27	19	6
270	*Aeromonas*	05.07.22	D1	6	14	28	11	6	21	31	7	17	19	11	18	29	27	18
272	*Pseudomonas*	05.07.22	D2	6	9	6	26	6	31	29	28	36	32	11	6	32	6	15
276	*Ae. hydrophila*	05.07.22	Eff B	6	9	13	24	6	38	34	20	40	30	13	23	36	33	23
277	*Aeromonas*	05.07.22	Eff B	6	13	6	23	6	34	34	15	33	23	11	20	32	25	20
280	*E. coli*	05.07.22	Eff B	6	17	20	6	6	11	31	15	27	20	12	24	26	20	18
281	*E. coli*	05.07.22	Eff B	6	16	22	13	6	18	31	15	28	21	18	6	25	20	11
282	*E. coli*	05.07.22	Eff B	6	9	6	14	6	20	35	23	32	34	18	6	21	6	6
284	*E. coli*	05.07.22	Eff B	6	11	21	7	6	11	29	8	9	6	7	6	26	20	12

Table 8.2. Antibiotic sensitivity results for strains isolated on agar supplemented with carbapenems.

Isolate	Species/Genus	Sample Date	Sample Point	AMP	AMC	FOX	CTX	CPD	ATM	MEM	S10	OT	CIP	NA	SXT	C	F	AZM
112	*Klebsiella*	23.01.20	Inf B	0	0	0	0	0	19	11	10	25	21	14	12	25	18	20
119	*R. ornithinolytica*	18.02.20	Inf B	0	0	0	24	19	21	13	21	22	18	0	21	22	21	18
120	*Aeromonas*	18.02.20	Inf B	0	15	14	26	0	36	20	0	0	22	0	0	36	28	11
121	*Aeromonas*	18.02.20	Inf B	0	8	10	18	0	18	28	12	25	10	0	19	26	26	17
122	*Aeromonas*	18.02.20	Inf B	0	11	0	13	0	0	32	13	9	16	0	0	26	28	12
123	*Escherichia*	18.02.20	Inf B	0	0	0	0	0	0	27	15	0	0	0	0	22	21	0
124	*Aeromonas*	18.02.20	Inf B	0	12	0	16	0	26	27	8	0	11	0	0	9	22	8
125	*Aeromonas*	18.02.20	Inf B	0	11	0	22	15	25	17	10	23	14	22	20	28	21	16
126	*Aeromonas*	18.02.20	Inf B	0	10	0	11	0	22	24	16	27	14	10	22	30	24	19
127	*R. ornithinolytica*	18.02.20	Inf B	0	0	0	23	14	24	0	17	19	18	0	23	26	22	11
128	*E. coli*	18.02.20	Inf B	0	0	0	0	0	12	8	13	0	0	0	0	23	24	0
129	*E. coli*	18.02.20	Inf B	0	0	0	0	0	0	13	0	25	0	0	0	21	11	0
130	*E. coli*	18.02.20	Inf B	0	0	0	0	0	15	13	10	0	0	0	0	25	23	7
131	*Escherichia*	18.02.20	Inf B	0	12	16	0	0	8	30	15	0	0	0	0	25	22	10
132	*Aeromonas*	18.02.20	Inf B	0	0	17	21	16	26	27	11	25	11	0	16	27	22	16
133	*Aeromonas*	18.02.20	Inf B	0	10	15	22	15	22	29	13	25	9	0	18	26	21	15
134	*Raoultella*	18.02.20	Inf B	0	0	10	25	20	25	24	19	26	21	0	26	28	23	13
135	*K. aerogenes/Enterobacter*	18.02.20	Inf B	0	0	0	10	0	13	13	17	18	17	0	19	20	13	11
136	*C. freundii*	18.02.20	Inf B	0	0	0	8	0	13	10	11	0	7	0	0	26	22	0

137	*C. freundii*	18.02.20	Inf B	0	0	0	9	0	0	13	14	8	18	18	0	31	20	8
138	*Citrobacter*	18.02.20	Inf B	0	0	0	12	0	15	14	20	22	18	0	22	18	19	12
139	*Citrobacter*	18.02.20	Inf B	0	0	0	16	0	19	13	16	23	15	0	14	20	14	8
140	*Enterobacter*	18.02.20	Inf B	0	0	0	11	0	0	12	12	0	11	0	0	0	12	11
141	*Raoultella/Klebsiella*	18.02.20	Inf B	0	8	10	25	18	25	26	11	26	18	8	26	28	26	10
142	*Aeromonas*	18.02.20	Inf B	0	0	10	17	0	23	11	0	0	9	0	0	22	16	12
143	*C. freundii*	18.02.20	Inf B	0	0	0	12	0	18	0	14	0	11	0	0	24	25	0
144	*C. freundii*	18.02.20	Inf B	0	0	0	8	0	23	12	16	8	18	18	0	30	20	0
145	*K. aerogenes/Enterobacter*	18.02.20	Inf B	0	0	0	0	0	13	14	17	17	15	0	17	19	12	10
146	*K. aerogenes/Enterobacter*	18.02.20	Inf B	0	0	0	0	0	12	13	18	18	17	0	19	20	12	11
147	*K. aerogenes/Enterobacter*	18.02.20	Inf B	0	0	0	0	0	12	14	18	19	16	0	18	20	13	11
148	*K. aerogenes/Enterobacter*	18.02.20	Inf B	0	0	0	0	0	13	15	17	18	15	0	19	18	13	11
149	*Klebsiella*	0303.03.20	Eff B	0	0	0	13	0	32	20	19	26	20	13	0	28	20	13
150	*Escherichia*	03.03.20	Inf B	0	0	0	0	0	0	17	13	0	0	0	0	27	22	15
151	*E. coli*	03.03.20	Inf B	0	0	0	0	0	0	13	14	0	0	0	0	25	20	15
152	*E. coli*	03.03.20	Inf B	0	0	0	0	0	0	12	13	0	0	0	0	23	19	15
153	*E. coli*	03.03.20	Inf B	0	0	0	0	0	0	10	9	24	0	0	0	22	10	0
154	*E. coli*	03.03.20	Inf B	0	0	0	0	0	0	13	9	26	0	0	0	23	11	0
155	*E. coli*	03.03.20	Inf B	0	0	0	0	0	0	12	13	0	0	0	0	23	21	10
156	*Escherichia*	03.03.20	Inf B	0	0	0	0	0	0	16	13	0	0	0	0	27	23	16
157	*Escherichia*	03.03.20	Inf B	0	0	0	0	0	0	16	14	0	0	0	0	27	22	16
158	*E. coli*	03.03.20	Inf B	0	0	0	0	0	0	15	13	0	0	0	0	26	20	16

159	*Escherichia*	03.03.20	Inf B	0	0	0	0	0	0	16	13	0	0	0	0	27	22	15
160	*Escherichia*	03.03.20	Inf B	0	0	0	0	0	0	16	12	0	0	0	0	28	25	17
161	*Aeromonas*	03.03.20	Inf B	0	0	0	20	0	25	12	7	8	15	0	0	20	25	10
162	*E. coli*	03.03.20	Inf B	0	0	0	0	0	0	12	14	0	0	0	0	24	22	15
163	*Escherichia*	03.03.20	Inf B	0	0	0	0	0	0	14	12	0	0	0	0	24	23	15
164	*E. coli*	03.03.20	Eff B	0	0	0	0	0	0	10	15	0	0	0	0	24	16	11
165	*E. coli*	03.03.20	Eff B	0	0	0	0	0	0	16	16	0	0	0	0	25	18	13
166	*E. coli*	03.03.20	Eff B	0	0	0	0	0	0	18	16	0	0	0	0	26	20	12
167	*E. coli*	03.03.20	Eff B	0	0	0	0	0	0	20	17	0	0	0	0	27	21	11
168	*E. coli*	03.03.20	Eff B	0	0	0	0	0	0	14	15	0	0	0	0	27	17	11
169	*Escherichia*	03.03.20	Inf B	0	0	0	0	0	9	10	10	0	0	0	0	0	16	0
170	*Aeromonas*	03.03.20	Inf B	0	0	0	0	0	18	22	0	10	0	0	0	18	20	0
171	*E. coli*	03.03.20	Inf B	0	0	0	0	0	0	10	13	0	0	0	0	22	18	13
172	*E. coli*	03.03.20	Inf B	0	0	0	0	0	0	11	13	0	0	0	0	25	19	15
173	*Escherichia*	03.03.20	Inf B	0	0	0	0	0	9	10	10	0	0	0	0	0	15	0
174	*E. coli*	03.03.20	Inf B	0	0	0	0	0	11	9	9	0	0	0	0	0	16	0
175	*Pseudomonas*	03.03.20	Inf B	0	10	0	15	0	15	30	16	23	29	0	0	14	0	0
176	*E. coli*	03.03.20	Inf B	0	0	0	0	0	11	10	10	0	0	0	0	0	17	0
177	*E. coli*	03.03.20	Inf B	0	0	0	0	0	9	7	9	0	0	0	0	0	13	0
178	*E. coli*	03.03.20	Inf B	0	0	0	0	0	10	9	10	0	0	0	0	0	16	0
179	*Ae. media*	10.03.20	Inf B	0	0	0	12	0	22	17	15	10	10	8	19	21	28	10
180	*Escherichia*	10.03.20	Inf B	0	0	0	0	0	9	13	10	0	0	0	0	0	15	0

181	*E. coli*	10.03.20	Inf B	0	0	0	0	0	0	19	13	0	0	0	0	28	24	15
182	*Ae. media*	10.03.20	Inf B	0	0	0	9	0	23	15	16	8	11	9	17	22	30	10
183	*Escherichia*	10.03.20	Inf B	0	0	0	0	0	0	18	13	0	0	0	0	25	24	16
184	*Ae. media*	10.03.20	Inf B	0	0	0	15	0	27	19	17	10	13	10	20	23	31	12
185	*Aeromonas*	10.03.20	Inf B	0	0	0	22	15	30	18	17	8	17	0	18	34	26	21
186	*Escherichia*	10.03.20	Inf B	0	0	0	0	0	13	13	0	0	0	0	0	24	20	0
187	*E. coli*	10.03.20	Inf B	0	0	0	0	0	8	12	10	0	0	0	0	0	18	0
188	*Ae. media*	10.03.20	Inf B	0	0	0	12	0	25	17	15	10	11	9	18	21	30	11
189	*E. coli*	10.03.20	Inf B	0	0	0	0	0	10	12	10	0	0	0	0	0	18	0
190	*Escherichia*	10.03.20	Inf B	0	0	0	0	0	0	18	14	0	0	0	0	26	22	16
191	*E. coli*	10.03.20	Eff B	0	0	0	0	0	10	11	9	0	0	0	0	0	17	0
192	*Escherichia*	10.03.20	Eff B	0	0	0	0	0	10	13	10	0	0	0	0	0	18	0
193	*Ae. media*	10.03.20	Eff B	0	0	0	15	0	28	19	15	12	13	11	18	21	30	13
194	*Pseudomonas*	10.03.20	Inf B	0	0	0	9	0	11	33	16	20	24	0	0	0	0	25
195	*Enterobacter*	10.03.20	Inf B	0	0	0	12	0	0	9	7	29	12	0	0	31	20	0
196	*Pseudomonas*	10.03.20	Inf B	0	0	0	14	0	12	31	13	18	25	0	0	0	0	28
197	*Ae. media*	10.03.20	Inf B	0	0	0	12	0	24	17	16	9	10	7	17	20	26	10
198	*Ae. media*	10.03.20	Inf B	0	11	0	18	0	27	26	10	8	11	11	18	22	30	10
199	*Ae. media*	10.03.20	Inf B	0	0	0	15	0	24	18	16	12	14	11	20	24	32	13
200	*Ae. media*	10.03.20	Eff B	0	0	0	14	0	25	17	16	8	12	9	18	21	31	11
201	*Aeromonas*	10.03.20	Eff B	0	0	0	15	0	28	26	14	14	12	13	16	21	25	12
202	*P. aeruginosa*	10.03.20	Eff B	0	0	0	0	0	20	0	0	15	0	0	0	10	0	21

203	*Aeromonas*	10.03.20	Eff B	0	0	0	12	0	23	17	16	10	9	11	17	19	26	9
204	*Aeromonas*	10.03.20	Eff B	0	0	0	11	0	19	16	15	10	11	9	13	16	21	11
205	*Aeromonas*	10.03.20	Eff B	0	0	0	16	0	24	20	18	16	14	15	21	21	29	15
243	*Aeromonas*	12.05.20	Eff B	6	9	6	24	10	30	20	15	28	17	9	17	33	25	20
261	*Enterococcus*	12.05.20	Eff B	6	6	6	6	6	6	6	6	17	6	6	6	27	14	6
262	*Enterococcus*	12.05.20	Eff B	6	6	6	6	6	6	6	6	17	6	6	6	28	20	6
263	*Enterococcus*	12.05.20	Eff B	6	6	6	6	6	6	6	6	18	6	6	6	30	12	6
264	*Pseudomonas*	12.05.20	D1	6	6	6	16	6	17	20	17	27	34	12	6	16	6	6
266	*Pseudomonas*	12.05.22	D1	6	6	6	15	6	16	18	16	24	32	11	6	14	6	6
269	*Aeromonas*	05.07.22	D1	6	13	20	34	30	36	31	15	34	29	33	21	34	25	21
274	*Aeromonas*	05.07.22	Eff B	6	11	6	21	6	29	20	16	30	18	10	20	31	26	10
278	*Pseudomonas*	05.07.22	Eff B	6	9	6	13	6	17	23	33	30	29	12	6	11	6	21

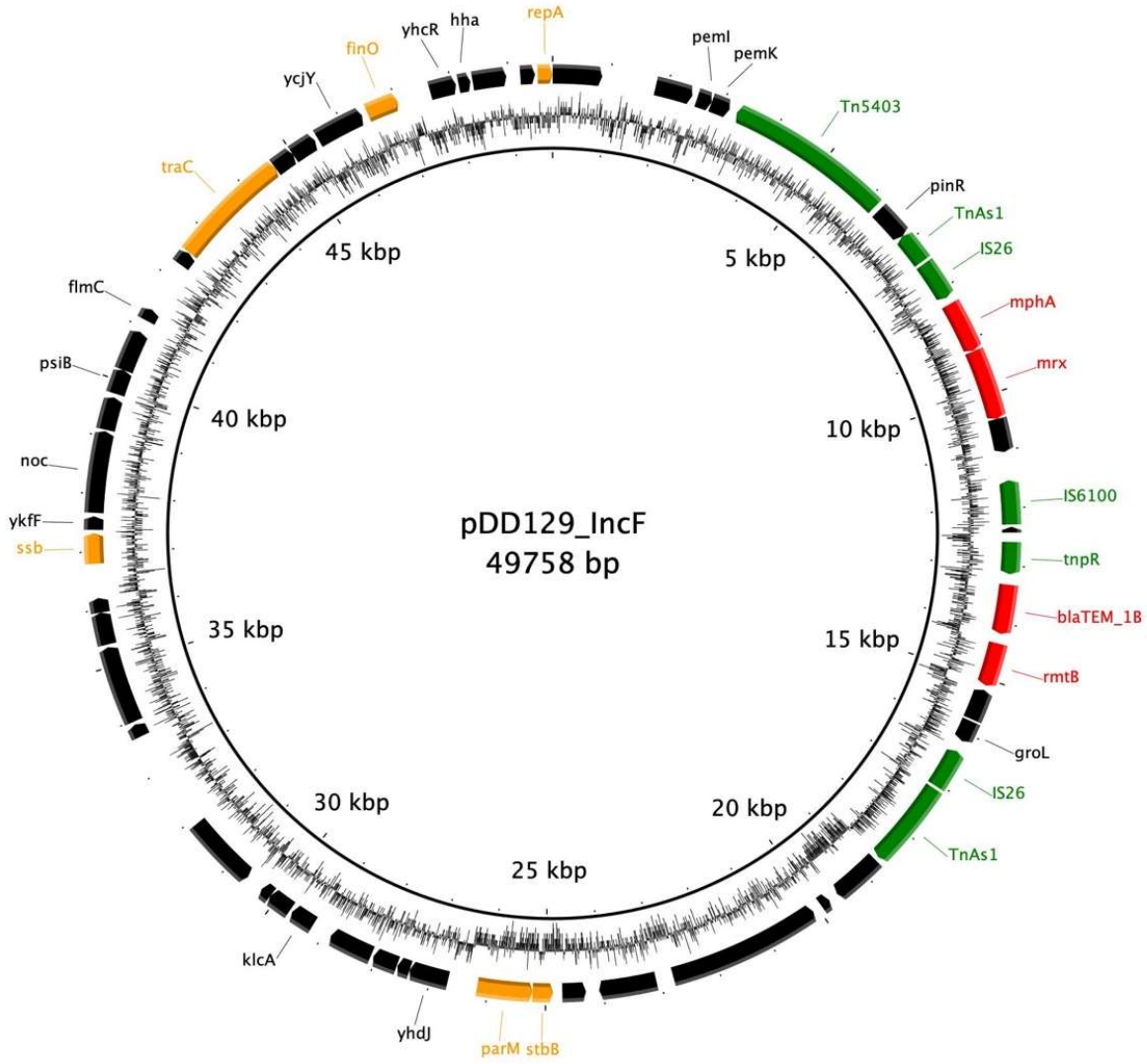

Figure 8.1. Plasmid map of pDD129_IncF. GC content is annotated on an inner ring and predicted coding sequences (CDS) on an outer ring. Resistance genes are annotated in red, mobile genetic elements annotated in green, and DNA replication/plasmid transfer in yellow.

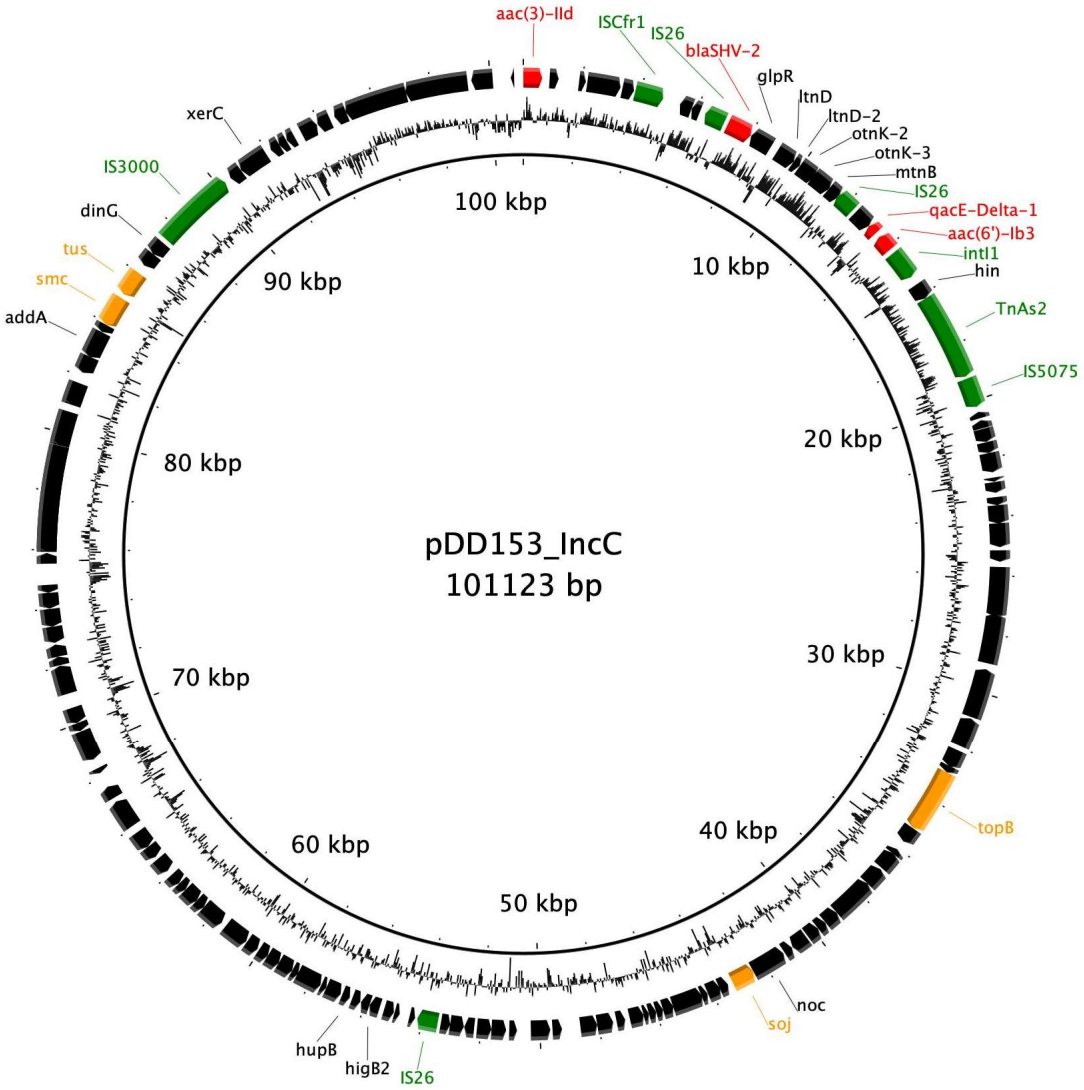

Figure 8.2. Plasmid map of pDD153_IncC. GC is content annotated on an inner ring and predicted coding sequences (CDS) on an outer ring. Resistance genes are annotated in red, mobile genetic elements annotated in green, and DNA replication/plasmid transfer in yellow.

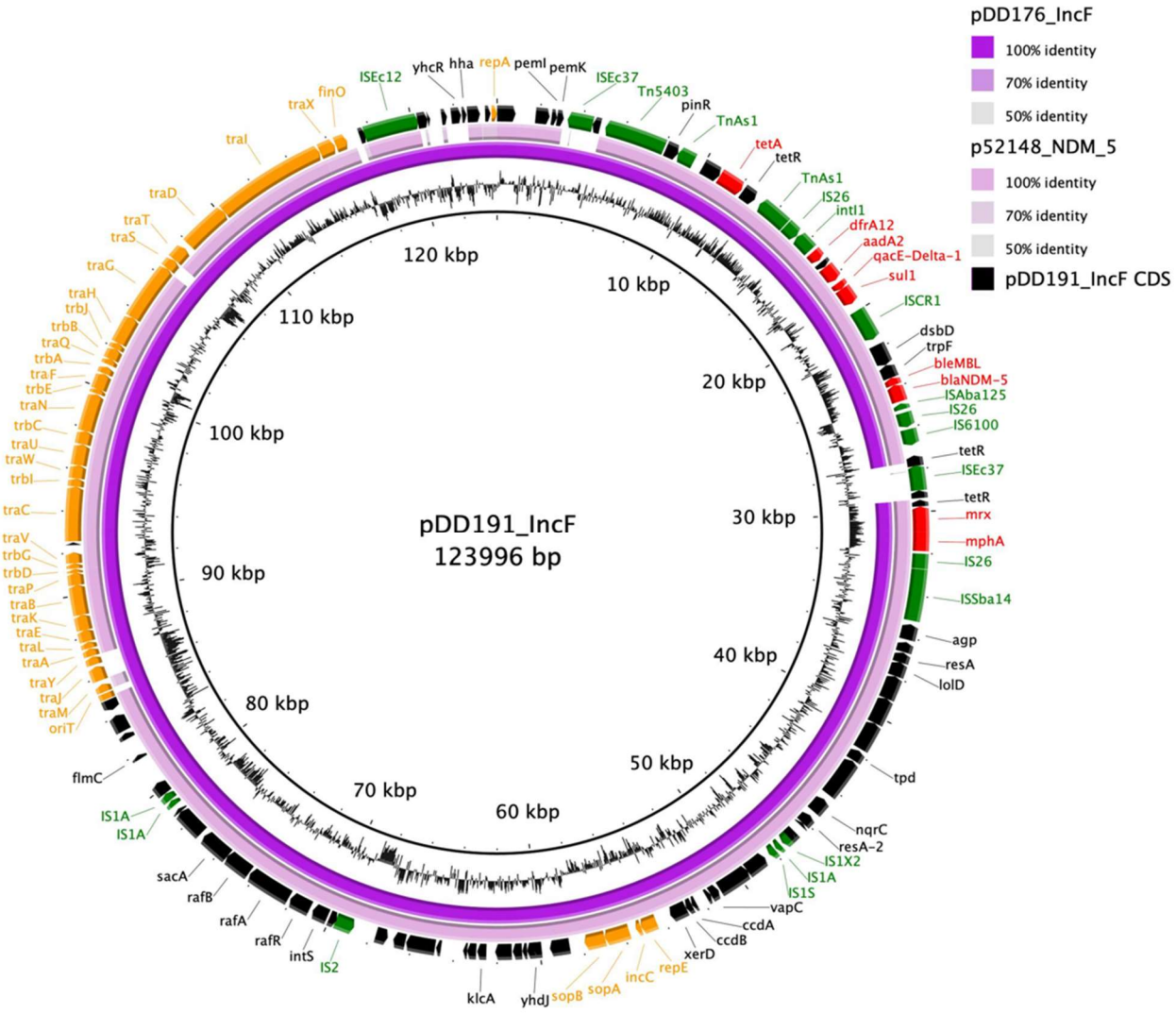

Figure 8.3. Plasmid comparison of pDD191_IncF compared via BLAST to the closest alignment in Genbank, p52148_NDM_5, and pDD176_IncF. The predicted coding sequences (CDS) of pDD191_IncF are annotated on an outer ring, with resistance genes in red, mobile genetic elements in green, and DNA replication/plasmid transfer in yellow. The aligned regions of the other plasmids are shown by coloured rings.

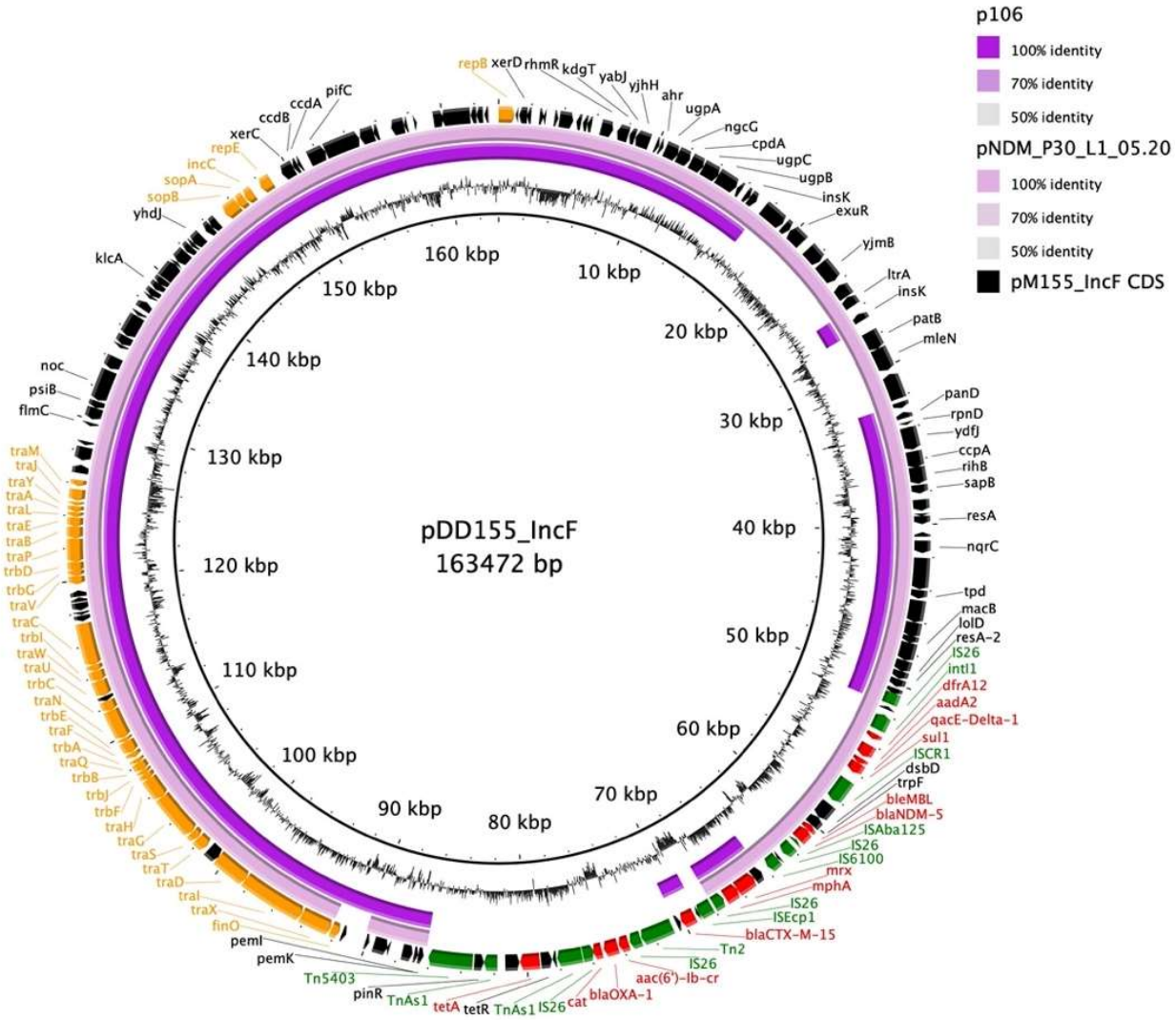

Figure 8.4. Plasmid comparison of pDD155_IncF compared via BLAST to the closest alignments in Genbank, p106, and pNDM_P30_L1_05.20. The predicted coding sequences (CDS) of pDD155_IncF are annotated on an outer ring, with resistance genes in red, mobile genetic elements in green, and DNA replication/plasmid transfer in yellow. The aligned regions of the other plasmids are shown by coloured rings.

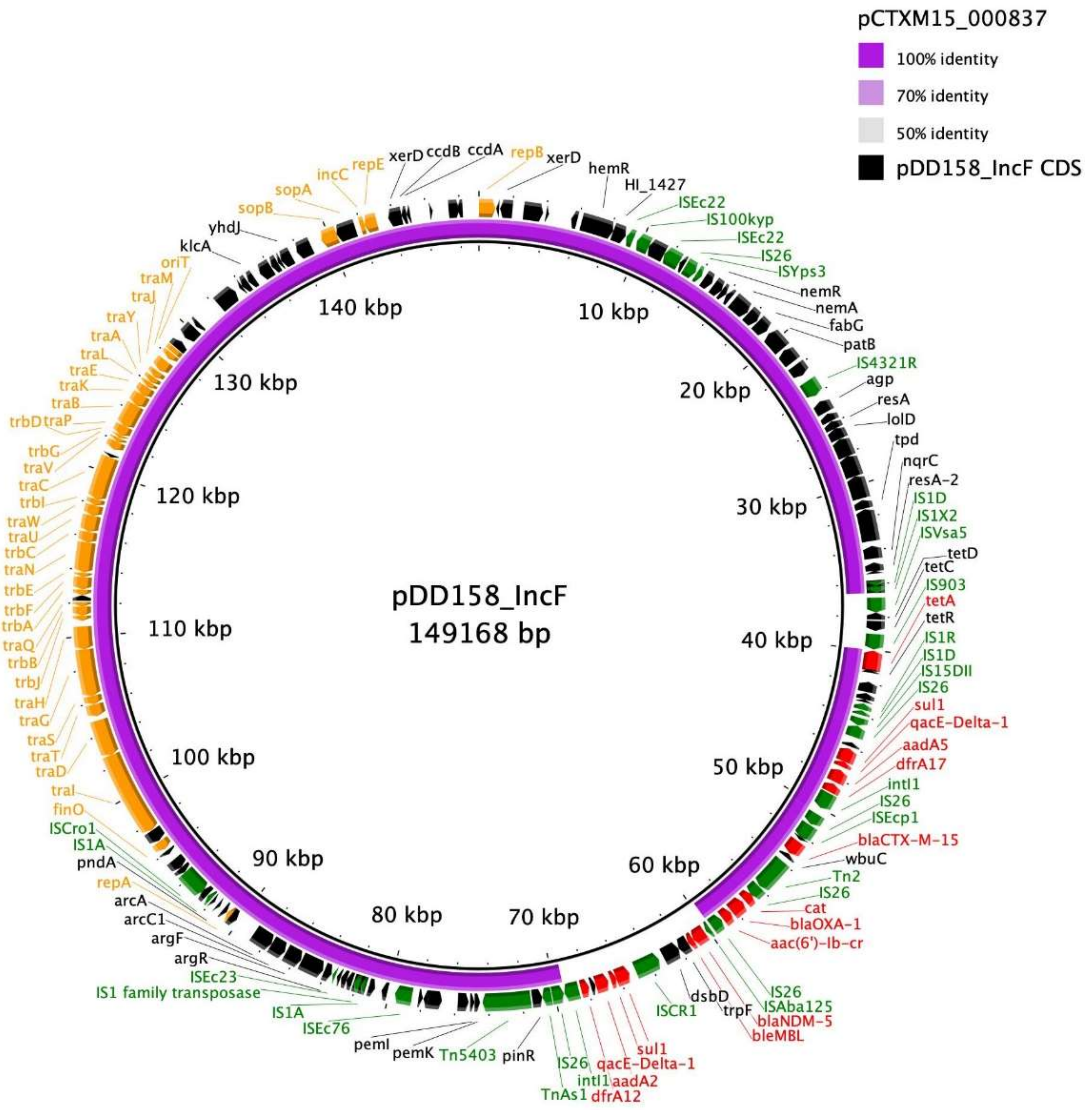

Figure 8.5. Plasmid comparison of pDD158_IncF compared via BLAST to the closest alignment in Genbank, pCTXM15_000837. The predicted coding sequences (CDS) of pDD158_IncF are annotated on an outer ring, with resistance genes in red, mobile genetic elements in green, and DNA replication/plasmid transfer in yellow. The aligned regions of the other plasmid are shown by a coloured ring.

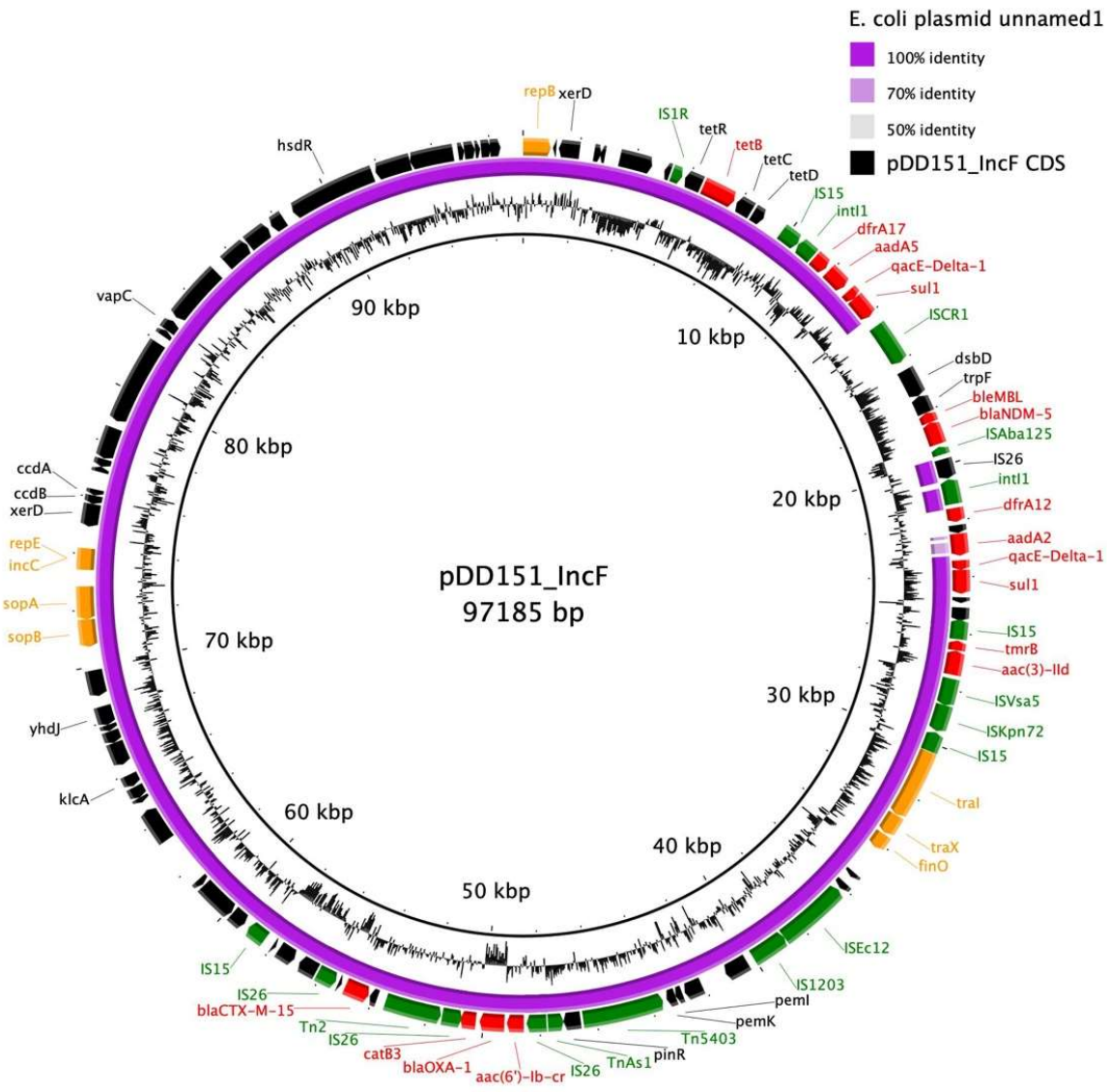

Figure 8.6. Plasmid comparison of pDD151_IncF compared via BLAST to the closest alignment in Genbank, an unnamed *E coli* plasmid. The predicted coding sequences (CDS) of pDD151_IncF are annotated on an outer ring, with resistance genes in red, mobile genetic elements in green, and DNA replication/plasmid transfer in yellow. The aligned regions of the other plasmid are shown by a coloured ring.

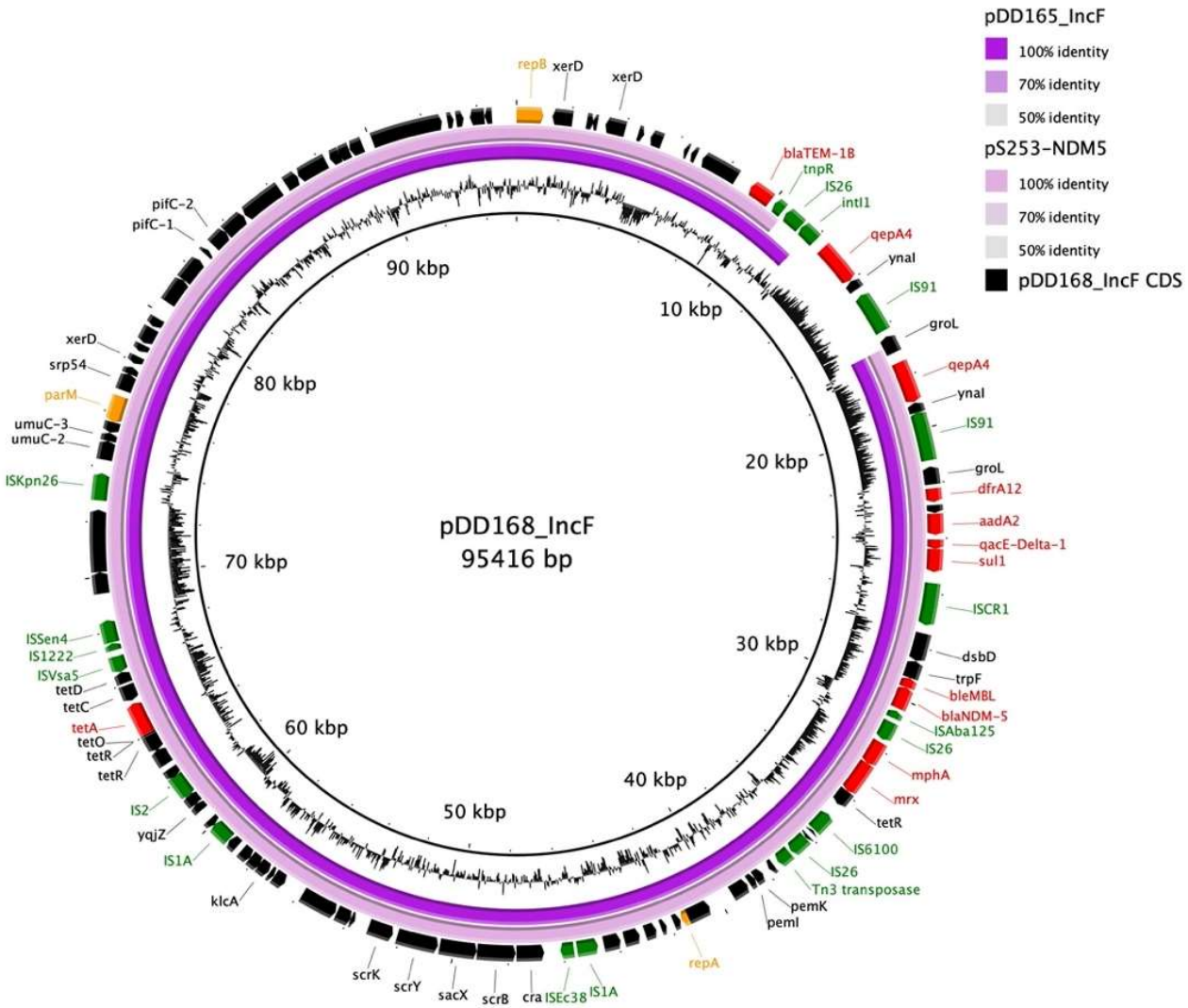

Figure 8.7. Plasmid comparison of pDD168_IncF compared via BLAST to the closest alignment in Genbank, pS253-NDM5, as well as pDD165_IncF. The predicted coding sequences (CDS) of pDD168_IncF are annotated on an outer ring, with resistance genes in red, mobile genetic elements in green, and DNA replication/plasmid transfer in yellow. The aligned regions of the other plasmids are shown by a coloured ring.

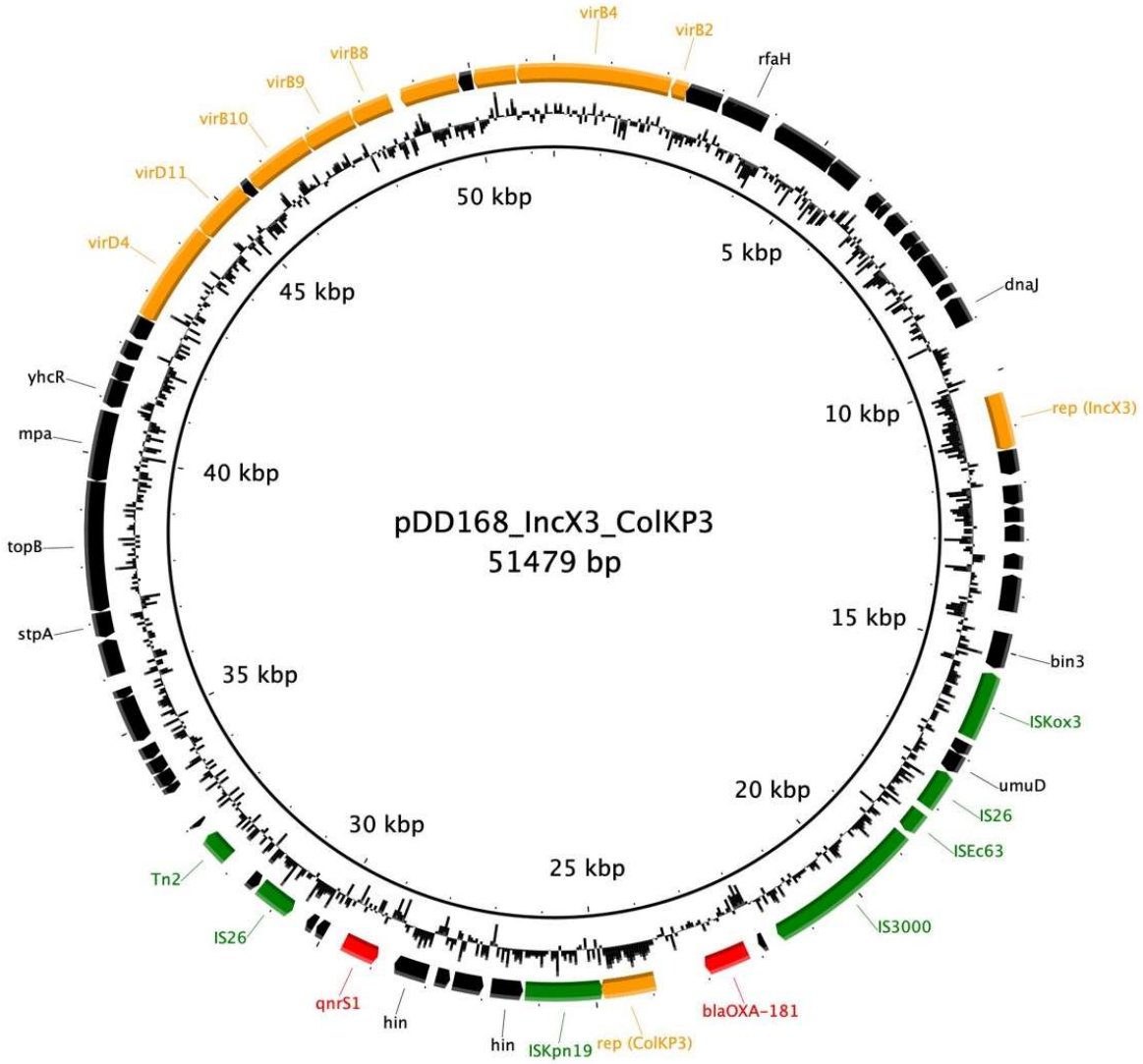

Figure 8.8. Plasmid map of pDD168_IncX3_ColKP3 containing *bla*$_{IMP}$. GC content is annotated on an inner ring and predicted coding sequences (CDS) on an outer ring. Resistance genes are annotated in red, mobile genetic elements annotated in green, and DNA replication/plasmid transfer in yellow.

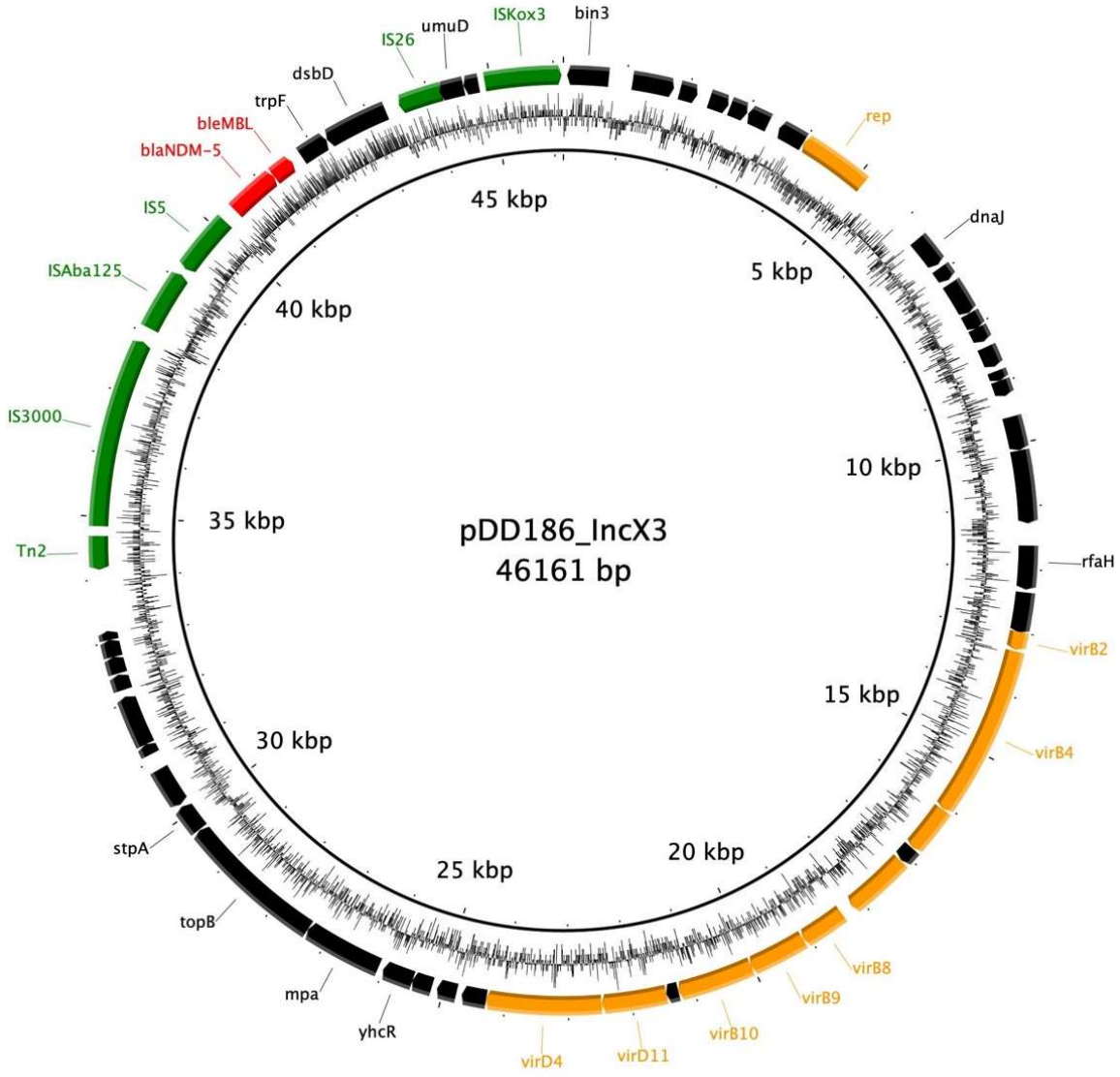

Figure 8.9. Plasmid map of pDD186_IncX3. GC content is annotated on an inner ring and predicted coding sequences (CDS) on an outer ring. Resistance genes are annotated in red, mobile genetic elements annotated in green, and DNA replication/plasmid transfer in yellow.

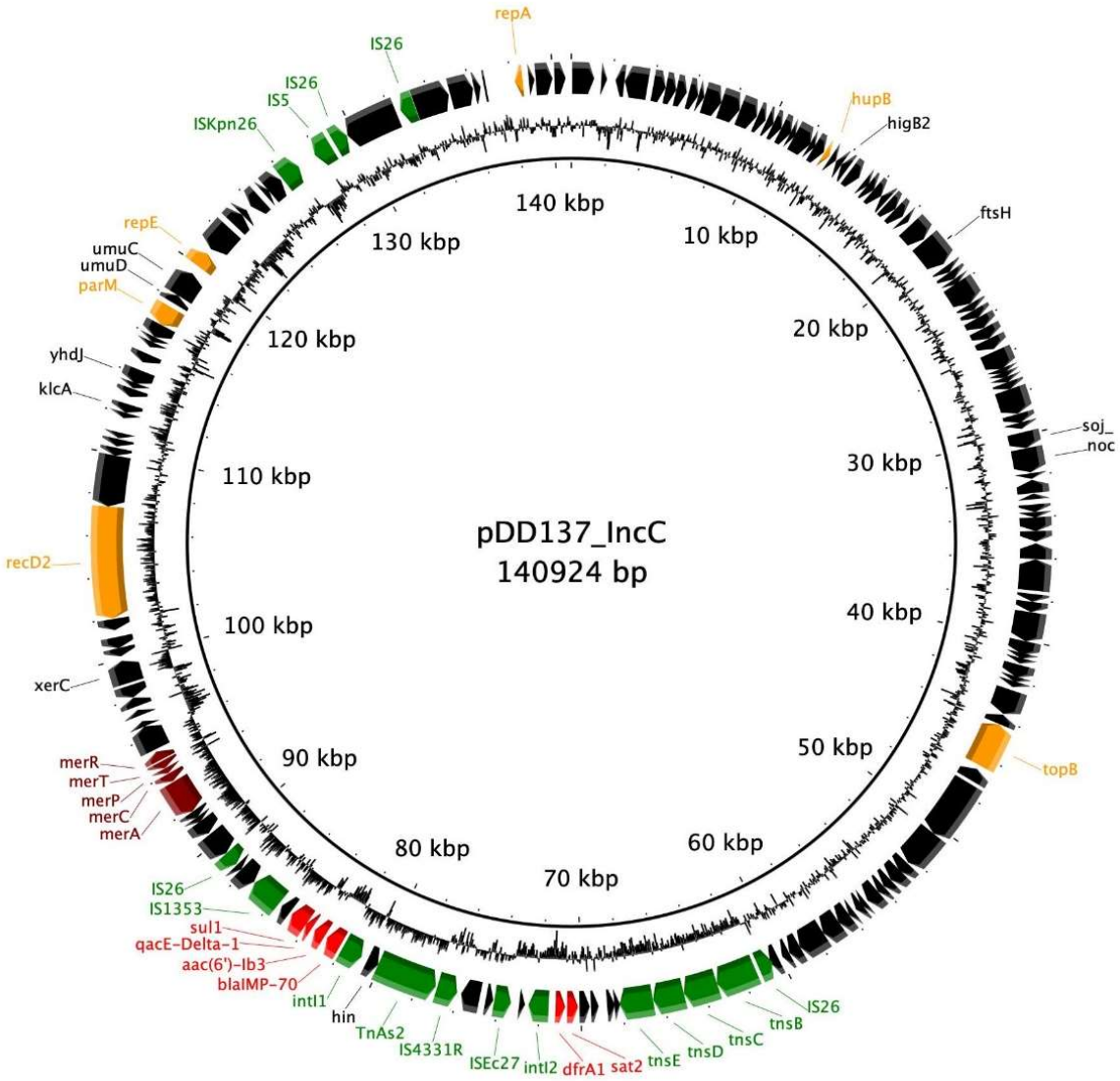

Figure 8.10. Plasmid map of pDD137_IncC. GC content is annotated on an inner ring and predicted coding sequences (CDS) on an outer ring. Resistance genes are annotated in red, mobile genetic elements annotated in green, metal resistance genes in maroon, and DNA replication/plasmid transfer in yellow.

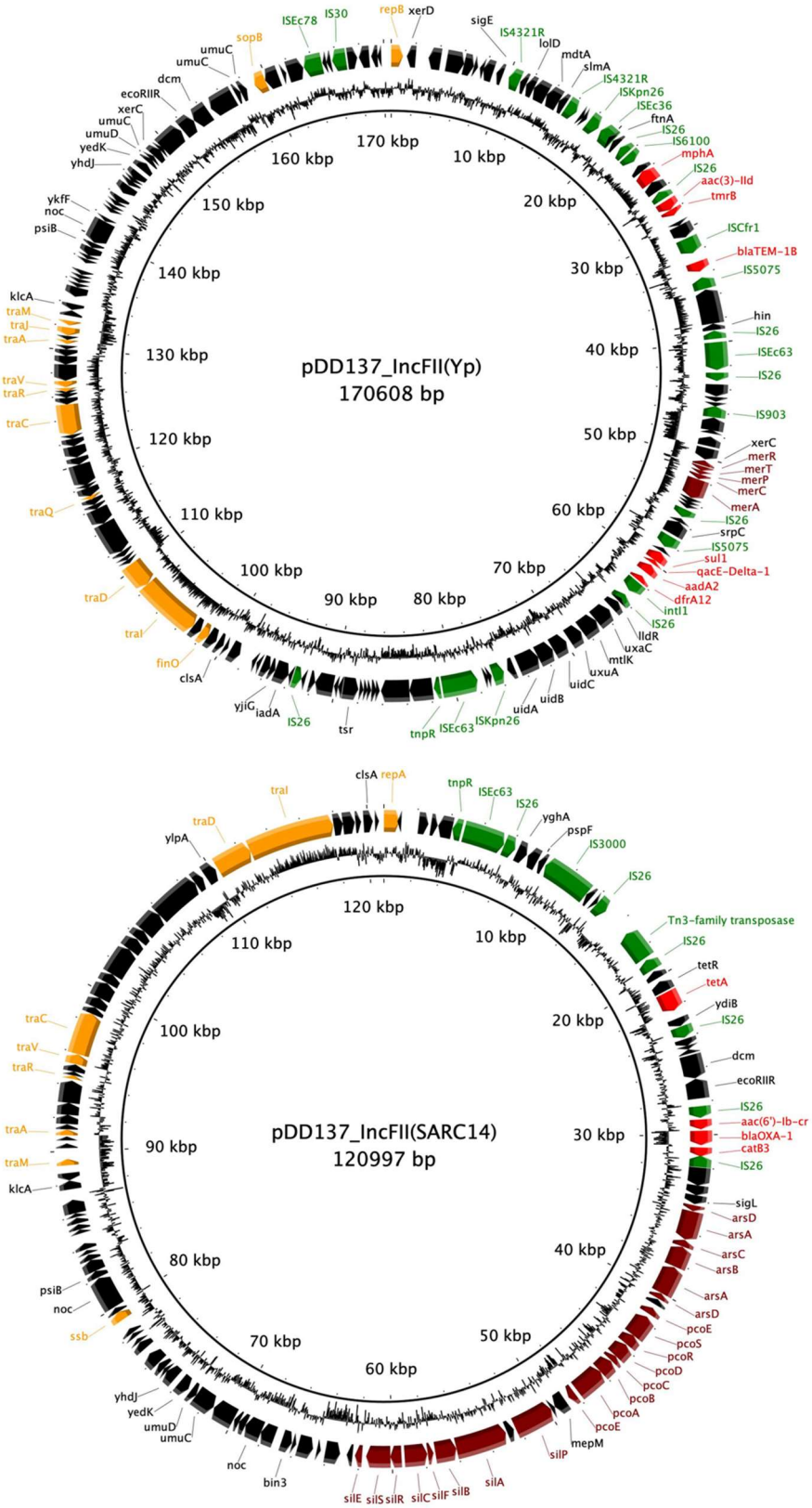

Figure 8.11. Plasmid maps of the two IncF plasmids of DD137. GC content is annotated on an inner ring and predicted coding sequences (CDS) on an outer ring. Resistance genes are annotated in red, mobile genetic elements annotated in green, metal resistance genes in maroon, and DNA replication/plasmid transfer in yellow.

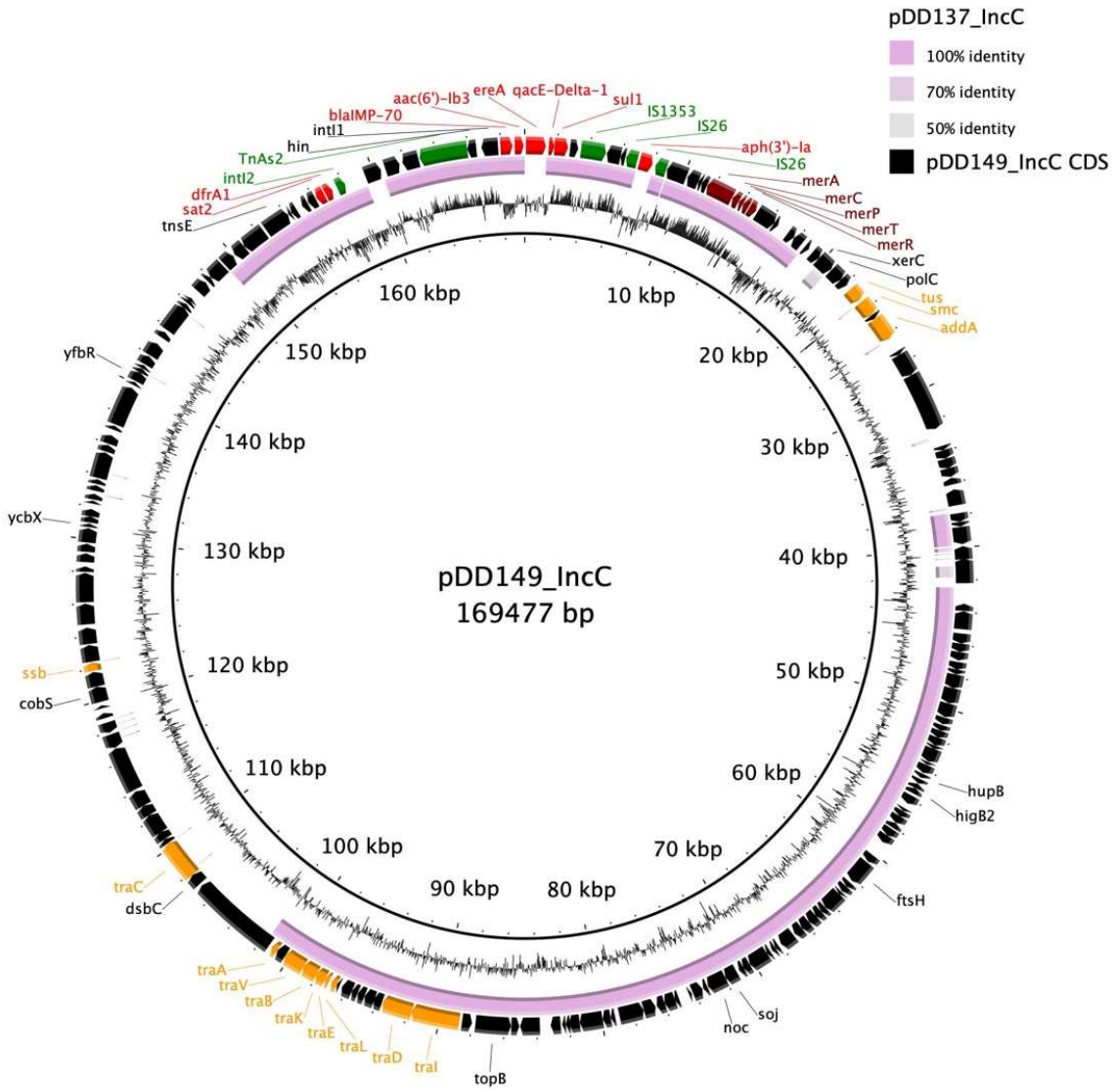

Figure 8.12. Plasmid comparison of pDD149_IncC compared via BLAST to the IncC plasmid of DD137, both containing *bla*$_{IMP-70}$. The predicted coding sequences (CDS) of pDD149_IncC are annotated on an outer ring, with resistance genes in red, mobile genetic elements in green, and DNA replication/plasmid transfer in yellow. The aligned regions of pDD137_IncC are shown by a coloured ring.